NASA TECHNICAL TRANSLATION

NASA TT F-91

C.1

NASA TT F-91

TECH LIBRARY KAFB, NM
0068614

VARIATIONS OF COSMIC RAYS AND SOLAR CORPUSCULAR STREAMS: COLLECTION OF ARTICLES

S. N. Vernov and L. I. Dorman, Editors

IGY Program, Section VII, No. 2,
USSR Academy of Sciences Press, Moscow, 1960

RECEIVED
21 OCT 1965
Technical Library
AF Weapons
Laboratory

NATIONAL AERONAUTICS AND SPACE ADMINISTRATION • WASHINGTON, D. C. • OCTOBER 1965

TECH LIBRARY KAFB, NM
0068614

NASA TT F-91

VARIATIONS OF COSMIC RAYS AND SOLAR CORPUSCULAR STREAMS:

COLLECTION OF ARTICLES

S. N. Vernov and L. I. Dorman, Editors

Translation of "Variatsii kosmicheskikh luchey i solnechnyye korpuskulyarnyye potoki. Sbornik statey."
IGY Program, Section VII, No. 2, USSR Academy of Sciences Press, Moscow, 1960.

NATIONAL AERONAUTICS AND SPACE ADMINISTRATION

For sale by the Clearinghouse for Federal Scientific and Technical Information
Springfield, Virginia 22151 – Price $5.00

TABLE OF CONTENTS

Ya. L. Blokh, L. I. Dorman, N. S. Kaminer. Individual Cases of the Influence of Magnetic Storms on Cosmic Rays and Their Interpretation 1

L. I. Dorman. Variations of Cosmic Ray Intensity during the Period when the Earth is Captured by Corpuscular Streams Carrying Homogeneous and Inhomogeneous Frozen Magnetic Fields 64

Ye. S. Glokova. Diurnal Variations of the Hard Component of Cosmic Rays near the Minimum of Solar Activity 82

T. M. Krupitskaya. Determination of the Energy Spectrum of the Primary Diurnal Variations of the Cosmic Ray Intensity . . 107

N. A. Zhukovskaya, A. I. Ol'. Changes in the Amplitude of the Diurnal Variation of Cosmic Ray Intensity as a Function of the Magnetic Activity 116

L. I. Dorman. Anisotropy of Cosmic Rays Caused by the Electric Field of a Corpuscular Stream 121

L. I. Dorman. Diurnal Variations of Cosmic Rays Caused by Anisotropic Scattering of Particles by Inhomogeneous Magnetic Fields of Corpuscular Streams 127

A. I. Ol'. Variation of Cosmic Ray Intensity during Magnetic Storms with Sudden and Gradual Beginnings 151

K. K. Fedchenko. Relationship of the Cosmic Ray Intensity to Solar Activity 158

A. I. Ol', M. I. Tyasto. Relationship of the Cosmic Ray Intensity to the Magnetic Activity and Radio Emission of the Sun 164

INDIVIDUAL CASES OF THE INFLUENCE OF MAGNETIC STORMS ON COSMIC RAYS AND THEIR INTERPRETATION*

Ya. L. Blokh, L. I. Dorman, N. S. Kaminer

1. INTRODUCTION

The effects of magnetic storms on the intensity of cosmic rays, or the so-called lowering effects of the Forbush type, have been studied for a long time. Many tens of works have been devoted to this problem. But none of them noted the fact that magnetic storms cause various effects. Practically no one concerned himself with an investigation of separate individual cases. This is explained by the fact that there were very few cosmic ray stations before the IGY, and the overwhelming majority of them were equipped with apparatus for recording only the hard component. In view of this, corrections for the temperature effect have to be carefully introduced in order to investigate individual cases. This presents great difficulties, both on account of the complexity of the temperature effects, and in view of the fact that aerological sounding of the atmosphere is conducted rather rarely and with insufficient accuracy. Hence it was risky to ascribe any sort of significance to individual fluctuations of the intensity, since they could be only accidental in nature, related to variations of atmospheric origin.

In view of this, the effects were averaged over many magnetic storms, and various statistical patterns were studied.

During the IGY a vast world network of cosmic ray stations was set up. This permitted an investigation of individual cases to be approached for the first time, since a comparison of the variation of cosmic rays at many stations makes it possible to see fluctuations as accidental or world-wide in character. We can attempt to interpret world-wide fluctuations and relate them to concrete geophysical or geomagnetic phenomena that accompany them. The first such investigation on the materials of the broad network of stations was performed in reference [1] on the storm of 29 August 1957. A report on it was made to

---

* A brief version of this article was read at the International Conference on Cosmic Rays in 1959.

the Fifth IGY Assembly. In this investigation the energy spectrum of the effect of the storm was found (i.e., the change in the spectrum of the primary particles, causing this effect), and it was shown that it is in rather good agreement with the modulations of primary cosmic rays by corpuscular streams, which carry regular magnetic fields, expected from the theory [2]. The parameters ε_δ and f, which determine this spectrum, were found. ε_δ denotes the quantity 300 $H_\delta l_\delta$, where H_δ is the field intensity in the corpuscular stream around the Earth (more accurately: a certain averaged quantity, if the field is not entirely homogeneous), and l_δ is the width of the stream around the Earth. The parameter f characterizes the fraction of particles subjected to this modulation. Even in the investigation of the storm of 29 August 1957, special attention was paid to the fact frequently noted previously that the drop in intensity occurs very rapidly, literally in several hours (5-10), while its reestablishment occurs slowly, during a period of many days [1]. At that time the theory was advanced that such a character of the change is related not so much to a specific corpuscular stream, as to a specific entry of the Earth into the corpuscular stream, i.e. that the corpuscular stream was moving at a great rate ($\sim 10^8$ cm/sec), capturing the Earth with its forward front. On account of the Sun's rotation, the stream itself has a tangential component.*

$$u_t = \frac{2\pi \cdot R_\delta}{27{,}3 \cdot 10^5 \cdot 0{,}86} = 4 \cdot 10^7 \text{ cm/sec} \qquad (1)$$

and the radial component of the rate of displacement of the forward front is u_r. Let us note that u_t is a quantity that is practically the same for all streams, while u_r can vary within broad limits (values of u_r from $2 \cdot 10^7$ to $3 \cdot 10^8$ cm/sec have been observed). In determining the relative motion of the Earth in the stream, we shall neglect the yearly revolution of the Earth around the Sun. Such a neglect changes the value of u_t by a total of $3 \cdot 10^6$ cm/sec. The tangent of the angle of inclination of the trajectory of the Earth in the stream to the axis of the stream is determined by the ratio u_t/u_r. Hence, the larger u_r, the smaller this angle. The scattering of particles by the stream can be determined by the shortest distance from the Earth to any edge of the stream. This will be the quantity l, which enters into the determination of ε_{min} [5]. In a first approximation, very rough, we can con-

---

* Here we support the theory of S. Chapman [3], according to whom the particles ejected from the Sun move radially. But inasmuch as each time the Sun rotates, new particles are ejected from it, the particles themselves do not have a tangential component of the velocity, but only the bending flux, which thus rotates around the Sun with the same angular frequency as the Sun itself.

sider that the effect of a decrease in the intensity of cosmic rays is proportional to this shortest distance. This allows us to calculate how the lowering effect varies as the Earth penetrates into the corpuscular stream. Such calculations have been performed in references [4, 5]. It is obvious that the greatest effect will be noted when the Earth passes through the axis of the stream. Reference [5, Fig. 2] shows the relative change of the shortest distance in the case when the Earth is captured by the side of the stream and passes through its axis during its subsequent motion.

If the Earth enters the side portion of the stream, the quantity u_r plays no role, since in this case the change in the shortest distance with time will be determined only by the value of u_t. It is evident from the Figure in reference [5] mentioned above that in this case we should expect a smooth drop in the intensity and the same smooth restoration. When the Earth passes at some distance from the axis of the stream during its subsequent motion, the change in the intensity of cosmic rays will be still smoother. If the Earth is captured only by the edge of the stream, then a very smooth change in the intensity will also be observed.

Reference [5, Figs. 3 and 4] shows the cases when the Earth is captured by the forward front of the stream under various assumptions on the velocity of the front u_r and on various distances between the Earth's position in the stream and the axis of the latter (only cases when the Earth intersects the axis of the stream during its further motion were considered). Of special interest here are the cases that arise at large velocities of the stream; a break is observed during the drop in intensity, i.e. first the rate of dropping is very great, and then it sharply decreases. In all these calculations we considered the stream as symmetrical.

Let us note that the restoration of the intensity should always occur smoothly, independent of the nature of the Earth's entry into the stream and the velocity of its forward front. In principle cases are possible when the stream is sharply broken off, and then the restoration can occur just as rapidly as the drop in intensity when the Earth is captured by the forward front.* The results cited above pertain, strictly speaking, not to the change in intensity, but to the change in the quantity ε_{min}, which characterizes the hardness of the primary variation. Hence we should expect a somewhat different variation of the intensity of cosmic rays for components sensitive to various ener-

---

* Such an abrupt restoration will be observed only in the case when the stream, interrupted at the Sun, will possess a sharp rear front. If the latter is essentially diffuse, the restoration will be smooth. There is apparently not one such case of restoration in the experimental data cited below. This shows that although cases with the presence of a rear front do occur, this front should be greatly smeared out.

gies of the primary particles. In view of this, the calculations were continued [5], considering the coupling constants and the primary variations of the energy spectrum. The time variation was calculated for the intensity of the hard component at sea level and the neutron component at sea level and in the mountains. The results of these calculations for values of ε^{δ} on the axis of the stream (i.e. $\varepsilon^{\delta} = 300\ H_{\delta} l_{\delta}$, where l_{δ} is the total width of the stream around the Earth) equal to 120, 100, 80, and 60 bev for various cases of entry of the Earth into the stream and for various velocities of the latter (from $3 \cdot 10^7$ to $2 \cdot 10^8$ cm/sec) are presented in references [5, 15]. It was assumed in these calculations that the fraction of particles subjected to modulation, f = 0.3. Similar calculations can be performed for any other component with a known coupling constant. The results of these calculations can be compared directly with the experimental data. From the indicated Figures [5, Figs. 3, 4], we can see that the effect of lowering on all the components begins somewhat later than the magnetic storm, i.e. somewhat after the Earth enters the stream. This is understandable, since even for a small lowering, some time is needed for ε_{min} to reach any sort of noticeable value. Related to this is the fact that the effect on the components sensitive to smaller primary energies should begin somewhat earlier than the effect on the components sensitive to higher energies. Thus, for example, we can see from these Figures that the lowering in the neutron component should begin somewhat earlier than that in the hard component.

Now we are investigating the changes in the intensity of the hard and neutron components of cosmic rays observed at the stations of the world network during various magnetic storms during the period from 1954 to 1959 (a total of about 40 cases).

For each case we find the corresponding profile of the change in intensity of cosmic rays and compare it with that expected theoretically under various assumptions on the velocities of the corpuscular streams that carry frozen magnetic fields, and under various assumptions on the nature of the capture of the Earth by the streams (side, forward front at various distances from the axis of the stream, etc.) and on the structure of the field. We are attempting to give an interpretation for each individual case by this method, we are determining the nature of the capture of the Earth by the streams, and finding their properties (dimensions, intensity, and distribution of the field in them). The results obtained are compared for each stream with the nature of the geomagnetic disturbances on the Earth and the properties of the active region on the Sun corresponding to them.

2. CLASSIFICATION OF PROFILES OF EFFECTS OF COSMIC RAYS DURING MAGNETIC STORMS AND GENERAL SCHEME OF INVESTIGATION OF VARIOUS INDIVIDUAL CASES

The following classification of the profiles of effects of cosmic rays during magnetic storms can be given according to [5, 6, 15].

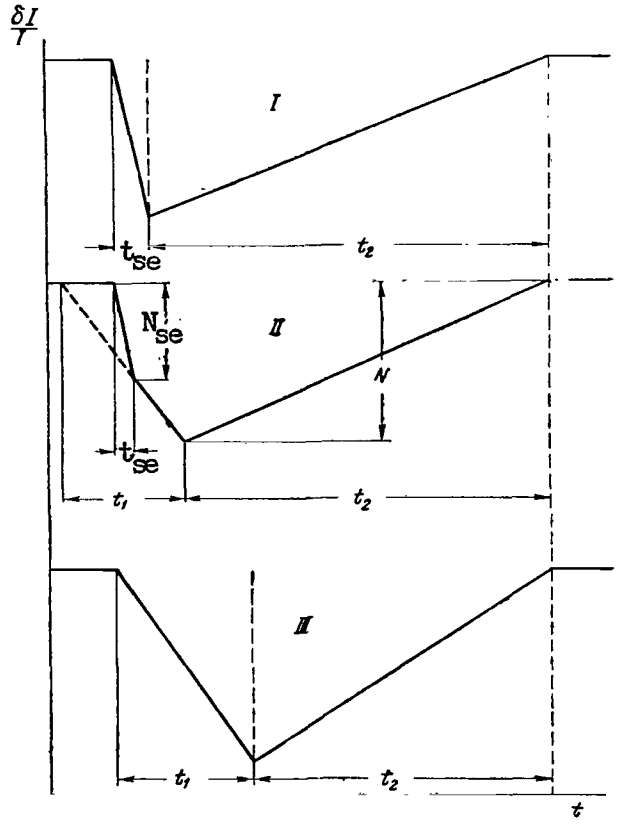

Fig. 1. Classification of profiles of the change in intensity of cosmic rays during magnetic storms (types I, II, and III).

Graphs of the variation of the intensity of cosmic rays during magnetic storms show three basic types of variations (Fig. 1). Variation of type I is characterized by an abrupt rapid drop for several hours and a gradual restoration over a period of several days. This type corresponds to capture of the Earth by the forward front of the stream, when the Earth does not intersect the axis (or the line with the least intensity in the case of an inhomogeneous magnetic field in the stream) during its further motion in the axial plane. The variation of type II exhibits a break in the branch of the curve of the drop in intensity: first the intensity falls almost as steeply as in case I, then the drop becomes less steep, after which a gradual smooth restoration occurs. This type also corresponds to capture of the Earth by the forward front, but the Earth intersects the axis of the stream (or the line of least intensity in the case of an inhomogeneous field) during its further motion in the axial plane. Type III is characterized by a smooth slow drop, almost the same as the restoration. This

type corresponds to capture of the Earth by the side edge of the stream. We should note that in certain cases, when the velocity of the front is small and is comparable to the tangential velocity of the motion of the bending stream, it is rather difficult to distinguish types I and II.* In this case data on the geomagnetic disturbances should also be enlisted. We believe that magnetic storms with sudden beginnings for the most part correspond to capture of the Earth by the forward front, while storms with gradual beginnings correspond to capture of the Earth, apparently by a rather diffuse side edge. Let us turn now to an investigation of the profiles of individual magnetic storms. In this case the most unambiguous interpretation can be given to storms of type II, when two parameters are determined at the same time according to the drop in intensity. They characterize the time of the rapid drop in the intensity of cosmic rays, i.e. the time of entry of the Earth into the forward portion of the stream until the side edge begins to exert its influence (t_{se}) and the time of leaving the forward side edge to the line of the least intensity (t_1) (Fig. 1). The third parameter (t_2) characterizes the time of restoration of intensity of the cosmic rays, i.e. the time of the Earth's passage from the line of least intensity to the rear edge of the stream. If more quantities, characterizing the amplitude of the effect in the neutron and hard components, are added to these three parameters, we can establish the entire picture of the phenomenon. The scheme of the investigation is the following.

Profiles of type II. Let us find ε_{min} with respect to the amplitudes of the total effect in the neutron (N) and in the hard (I) components of cosmic rays at sea level in the middle latitudes. For this purpose we calculated the values of the integrals

$$\int_{\varepsilon_{\lambda,\varphi}^{min}}^{\infty} \frac{\delta D}{D}(\varepsilon)\, W^{i}_{\lambda,\varphi}(\varepsilon, h_0)\, d\varepsilon \qquad (1)$$

for the neutron and hard components at various values of ε_{min} and $f = 0.3$ (Fig. 2) with the aid of the energy spectrum of the primary variation for the line of least intensity

---

* If the radial velocity of the stream is less than or equal to the tangential velocity, then in this case a variation of type II is impossible to detect; the nature of the variation will correspond to the profile of type III.

$$\frac{\delta D}{D}(\varepsilon) = f \begin{cases} -1, & \text{if } \varepsilon < \frac{\varepsilon_{min}}{4}, \\ -\frac{2}{\pi} \arcsin\left(\frac{\varepsilon_{min}}{2\varepsilon} - 1\right), & \text{if } \frac{\varepsilon_{min}}{4} < \varepsilon < \frac{\varepsilon_{min}}{2}, \\ 0, & \text{if } \varepsilon > \frac{\varepsilon_{min}}{2}, \end{cases} \tag{2}$$

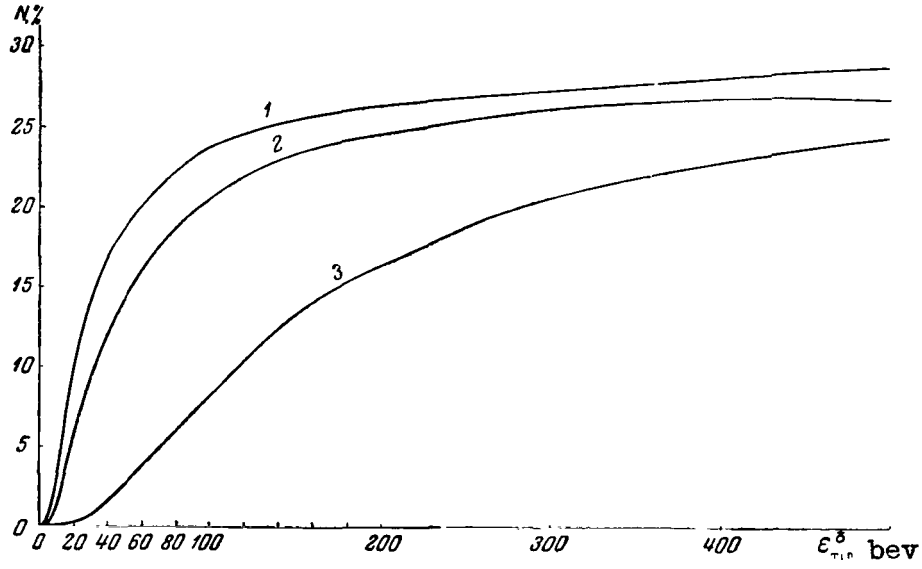

Fig. 2. Values of $\int_{\varepsilon_{\lambda,\varphi}}^{\infty} \frac{\delta D}{D}(\varepsilon)\, W^{i}_{\lambda,\varphi}(\varepsilon, h_0)\, d\varepsilon$ for $\frac{\delta D}{D}(\varepsilon)$, determined by expression (2) when f = 0.3 for the neutron component at mountain level (1), at sea level (2), and for the hard component at sea level (3) in the region of the middle latitudes as a function of the value of ε_{min} in formula (2).

and the coupling constants $W^{i}_{\lambda,\varphi}(\varepsilon, h_0)$ for the hard and neutron components. Fig. 3 presents the dependence of the ratio of the amplitudes of the effects N/I as a function of ε_{min}, calculated by the same method. By means of this graph, the value of ε_{min} can be found without difficulty according to the experimentally found ratio of the amplitudes of the effects N/I. Then, according to the known value of the effect in the neutron component N and the value of ε_{min} found, we

find the value of f -- the fraction of cosmic radiation subjected to modulation, by means of the graph depicted in Fig. 2.

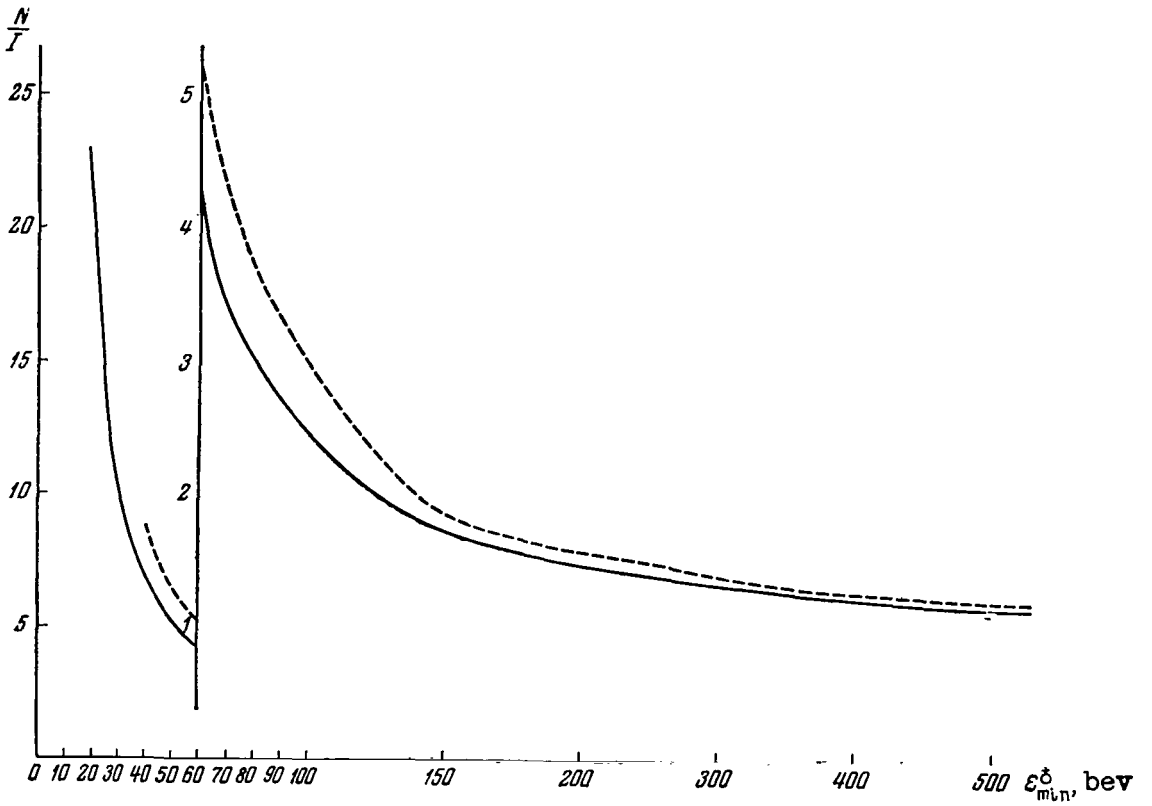

Fig. 3. Expected ratio of the amplitudes of the effects of cosmic rays in the middle latitudes as a function of the value of ε_{min} in formula (2)
Solid curve -- ratio of amplitudes of effects of the neutron component to the hard component at sea level; dotted curve -- neutron at mountain level to hard at sea level.

The scheme of a profile of type II is presented in the middle portion of Fig. 1. It can be seen from this scheme that first a rapid drop in the intensity occurs during the time t_{se} of the order of several hours, and then a smoother drop occurs down to the minimum of the intensity. Continuing the straight line of the smooth drop to intersection with the normal intensity level of cosmic rays (shown by a dotted line on the Figure), we find t_1. We believe that if a stream should capture the Earth with its side edge, the drop in the intensity would occur during the time t_1. Considering that the tangential velocity of the stream $u_t = 4 \cdot 10^7$ cm/sec, we obtain the fact that

$$l_1 = 4 \cdot 10^7 \cdot t_1 \text{ см}. \qquad (3)$$

We find analogously that

$$l_2 = 4 \cdot 10^7 \cdot t_2 \ см, \tag{4}$$

where t_2 is the time of restoration of the intensity from the minimum to the normal level. If the flux were homogeneous, we should expect that $l_1 = l_2$. Experimental data indicate that in practically all cases l_1 is less than l_2 (approximately one-half the value).

Since $H_1 l_1$ should be equal to $H_2 l_2$, where H_1 is the average value of the field in the forward portion of the stream, while H_2 is the average value in the rear portion, it follows from this that H_1 should be greater on the average than H_2, i.e. actually the field in the stream is inhomogeneous. After an examination of the experimental data, we turn to a consideration of the results that follow from this important fact. Here we note that although the theory of modulation of primary cosmic rays by regular magnetic fields, frozen in corpuscular streams, was developed for the case of a homogeneous magnetic field, it is also correct in a first approximation in our case of a regular, but not entirely homogeneous field.

In addition, as we have found ε_{min}, l_1, and l_2, it is easy to find the average field intensity in both parts of the stream

$$H_1 = \frac{\varepsilon_{min}/2}{300 \cdot l_1}; \quad H_2 = \frac{\varepsilon_{min}/2}{300 \cdot l_2}. \tag{5}$$

References [7, 2] have proposed the presence of a statistical relationship between the density of the energy of the magnetic field frozen in the stream and the density of irregular motions of the corpuscles within the stream. It was assumed that, on the average for many cases, the following relationship should be fulfilled

$$\frac{H^2}{8\pi} \approx \frac{\rho \bar{v}^2}{2}, \tag{6}$$

where ρ is the density of the stream, $\bar{v}$ is the thermal velocity of the corpuscles ($\bar{v} \sim 10^6$ cm/sec). This hypothesis was advanced in references [2, 7] in order to explain why streams causing large and very large magnetic storms, as a rule, cause an effect on cosmic rays and, consequently, carry considerable magnetic fields, while streams related to small or moderate magnetic storms cause an effect on cosmic rays only in rare cases. If we know H, ρ can be evaluated from the relationships cited:

$$\rho \approx \frac{H^2}{4\pi v^2}. \tag{7}$$

Although we shall sometimes use this relationship for evaluating ρ below, let us emphasize here once again that the results obtained are meaningful for the establishment of average principles, while in individual concrete cases they can greatly differ from the actual values of ρ. Such exceptions are observed, for example, in cases when very great magnetic storms produce no effect on the cosmic rays, while small ones cause an extremely great effect. This means that cases are possible when a stream with a large magnetic field possesses a low density, and when a stream with a negligible magnetic field possesses a high density.

Now we can find the path traversed by the Earth from the moment of its capture by the forward front until the moment when a break occurs in the drop in the cosmic ray intensity (see Fig. 1)

$$S = \frac{N_{6c}}{N} l_1. \tag{8}$$

This expression is correct in the case when the magnetic field H_1 in the forward portion of a stream with width l_1 is homogeneous. Although actually the field in the stream apparently changes continuously, we shall consider here, taking into account the approximate character of the calculation, that the field is homogeneous in both parts of the stream and changes abruptly at the line of separation. Knowing S and t_{se} of the rapid drop, it is easy to find the effective velocity of the forward front of the stream around the Earth [5]

$$u_r^* = \frac{S}{t_{6c}}. \tag{9}$$

Let us emphasize here that u_r^* will be equal to the actual velocity u_r of the forward front around the Earth only in the case when the magnetic field H_ϕ around the forward front is the same as the average field H_1 in the forward side portion of the stream. Let us assume first that this is so, i.e. that $H_1 = H_\phi$, and then that $u_r^* = u_r$.

According to the modern theories of geomagnetic storms, the corpuscular stream, striking the Earth's magnetic field with its forward front, compresses the Earth's field, causing an increase in the magnetic field intensity on the surface of the Earth (initial phase of the magnetic storm). According to D. T. Martyn [8], we can evaluate the amplitude of the increase in the intensity of the geomagnetic field ΔH_3 [2, p. 290] from the relationship

$$\frac{\rho_1 (u_r^*)^2}{2} = \frac{(\Delta H_3^*)^2}{\pi}, \tag{10}$$

from which

$$\Delta H_3^* \approx u_r^* \sqrt{\rho_1 \pi / 2}. \tag{11}$$

Here $\Delta H_3^* = \Delta H_3$ when $u_r^* = u_r$. In general $\Delta H_3 = \Delta H_3^* \cdot u_r / u_r^*$. Roughly determining the density of the stream according to the value of the frozen field according to function (7), we obtain:

$$\Delta H_3^* \approx \frac{u_r^* H_1}{3\bar{v}}. \tag{12}$$

In the consideration of concrete cases, an extremely large value of the effective velocity of the forward front u_r^* ($7 \cdot 10^8$-10^9 cm/sec) is sometimes obtained. At the same time, astrophysical data show that the actual velocity of the flux u_r can scarcely be greater than $3 \cdot 10^8$ cm/sec. This discrepancy is all the more striking in that our consideration gives a velocity of the stream directly around the Earth, while the astrophysical data pertain to the average velocity of the stream from the Sun to the Earth.

In view of this we propose below that the values of the velocity of the forward front that we have found may be high on account of the fact that the field, frozen close to the forward front, may be intensified on account of compression of the plasma when the stream is retarded by the interplanetary medium. If the field in such a "trap" is intensified, let us say, tripled in comparison with the average value of the field in the stream, the value of u_r^* found should be reduced to approximately one-third in order to find u_r. On the other hand, u_r can be found by any other method. Only the average value of the velocity of the stream during its motion from the Sun to the Earth, which should be greater than the true velocity of the stream u_r in direct proximity to the Earth, can be determined according to the lag in terrestrial phenomena with respect to solar phenomena. The velocity u_r can be determined, in principle, according to disturbed solar day variations of the cosmic rays, which are sensitive to the product $u_r H l_\delta$. Moreover, the quantities H and l_δ can in turn be determined according to the effect of cosmic rays during a magnetic storm.* Hence, let us assume that we have determined u_r by one method or another. Then we can find

---

* The determination of u_r by this method requires an additional thorough analysis, which we hope to perform in the near future.

the degree of compression of the plasma and the field along the forward front:

$$\frac{\rho_\Phi}{\rho_1} = \frac{H_\Phi}{H_1} = \frac{u_r^*}{u_r}, \tag{13}$$

from which

$$H_\Phi = \frac{u_r^*}{u_r} H_1; \quad \rho_\Phi = \frac{u_r^*}{u_r} \rho_1. \tag{14}$$

Since, according to [8],

$$\Delta H_3 = u_r \sqrt{\rho_\Phi \pi/2}, \tag{15}$$

then instead of (11), we should use the following expression in determining ΔH_3:

$$\Delta H_3 = \frac{H_1}{3v} \sqrt{u_r^* u_r}. \tag{16}$$

When we use (11), we obtain a value for ΔH_3 that is $\sqrt{u_r^*/u_r}$ times too high (which we have denoted by ΔH_3^*).

Profiles of types I and III. The calculations in these cases are conducted quite analogously. For profiles of type III we find the ratio N/I according to N and I, and then we find ε_{min} according to it, using the graph of Fig. 3, and the value of f according to the graphs of Fig. 2. We find $l_1 = u_t \cdot t_1$ according to the duration of the gradual drop t_1. We find l_2 analogously according to the duration t_2 of the restoration of intensity: $l_2 = u_t \cdot t_2$. Using the ε_{min} found, we find $H_1 = \varepsilon_{min}/300 \cdot 2 l_1$ and $H_2 = \varepsilon_{min}/300 \cdot 2 l_2$. From this we can evaluate ρ_1 and ρ_2 according to formula (7) if necessary.

Profiles of type I are calculated in the same way: we find the ratio of N and I, and then ε_{min} and f. We determine $l_2 = u_t \cdot t_2$ according to the duration of restoration t_2. From this we find $H_2 = \varepsilon_{min}/300 \cdot 2 l_2$. We can then evaluate ρ_2 according to formula (7). Since the minimum intensity of cosmic rays corresponds (assuming homogeneity of the field in the stream) to the position of the Earth when it is equidistant from the forward front of the stream and from its side edge (a distance equal to l_2), the effective velocity of the front u_r^* is determined during the time of the rapid drop t_{se}:

$$u_r^* = l_2 / t_{\text{бс}}. \tag{17}$$

If we can evaluate the actual velocity of the forward front u_r in some way, then we can find the degree of compression of the plasma and field

$$\frac{\rho_\Phi}{\rho_2} = \frac{H_\Phi}{H_2} = \frac{u_r^*}{u_r}, \tag{13'}$$

from which

$$\rho_\Phi = \frac{u_r^*}{u_r}\rho_2, \quad H_\Phi = \frac{u_r^*}{u_r}H_2. \tag{14'}$$

We can estimate the amplitude of a sudden beginning of a magnetic storm on the Earth according to formulas (11) and (16), where we should take H_2 instead of H_1.

Let us turn now to an investigation of individual cases. As has already been noted above, it is advisable to begin with profiles of type II. The general principles that would be revealed in their investigation facilitate an analysis of other profiles.

We shall see below that each individual case possesses its own specific features. Hence, in considering individual cases we shall pay attention not only to revealing general principles, but also to revealing the specific features. We shall attempt to relate these peculiarities to the specifics of the geomagnetic and solar phenomena in each case.

3. INDIVIDUAL PROFILES OF TYPE II AND PROPERTIES OF CORPUSCULAR STREAMS

3.1. Storms at the Beginning of September 1956

Fig. 4 presents data for the end of August - beginning of September for the stations of Mount Washington (N),* the schematic data of J. Lockwood [9], and the stations of Yakutsk and Moscow (I). For Yakutsk and Moscow, the temperature corrections, calculated according to the scheme of [2, 10] with the aid of radio sounding data, are also shown on the Figure with crosses.

Data on the K-index of the geomagnetic activity, the time of the beginning (↑), and the time of the end (↓) of the magnetic storm are also presented in the lower part of the Figure. The horizontal lines denote the active periods of the magnetic storm. Its characteristics are also indicated there. The first letter indicates the intensity of the storm: S -- small, M -- moderate, G -- great, VG -- very great;

---

* N -- neutron monitor, I -- ionization chamber, T -- cubic telescope.

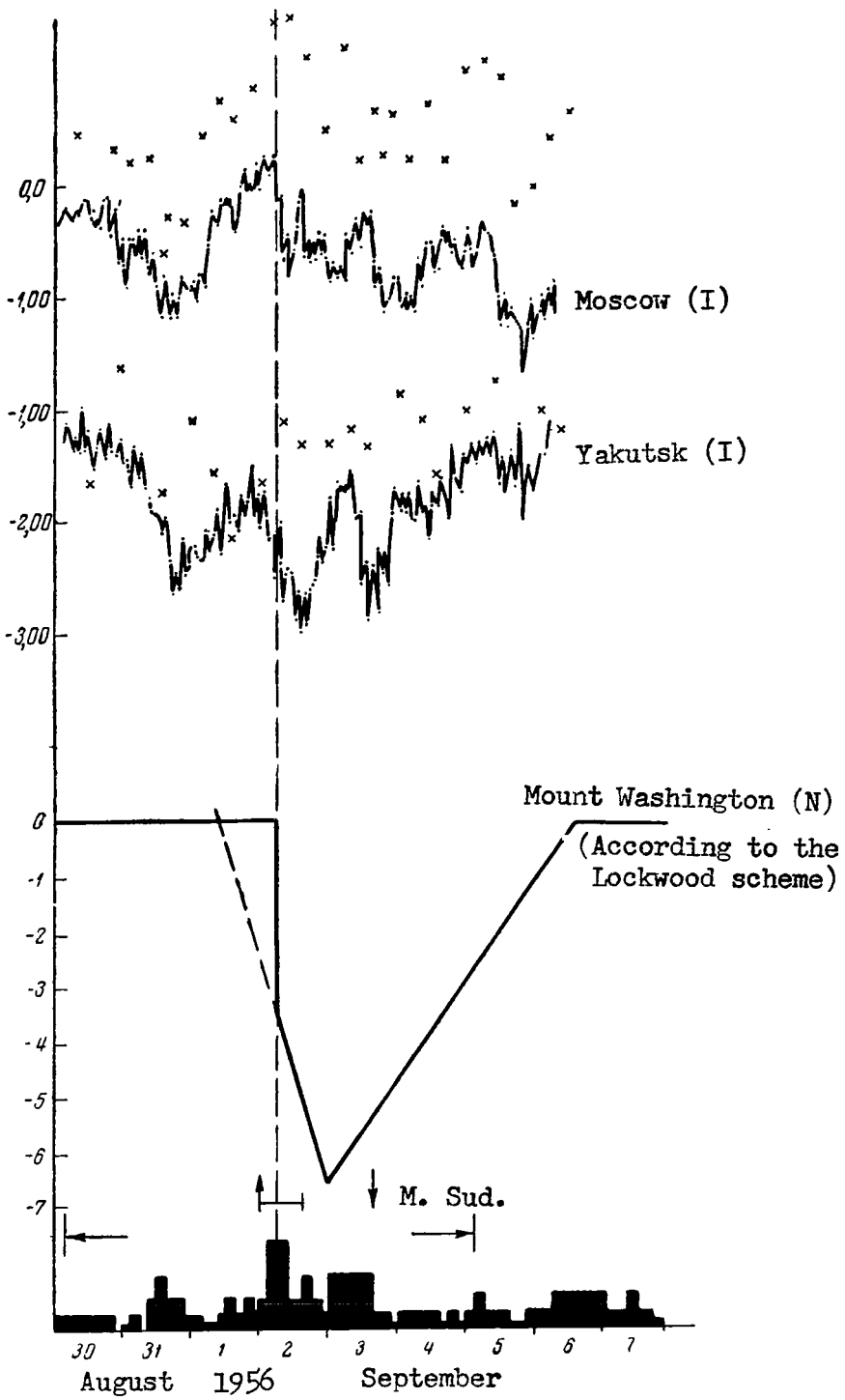

Fig. 4. Storms at the beginning of September 1956.

the second letter characterizes the beginning: Grad -- gradual, Sud -- sudden. The period when the active region that is believed to be responsible for the phenomenon on the Earth is passing through the central meridian of the Sun is shown by horizontal arrows. It can be seen from the Figure that a moderate storm with a sudden beginning at 01 hrs 18 min on 2 September caused a sharp drop* in the intensity of cosmic rays with a break in the line of the decrease, and then a gradual restoration, i.e. the formation of the profile characteristic of type II.

Since the amplitude of the decrease in the neutron component N = 6.5%, while that in the ionization chamber I = 1.7%, $N/I \approx 3.7$. From the graph of Fig. 5 we find $\varepsilon_{min} = 66$ bev. From this we find f = 0.115 according to Fig. 2 for this value of ε_{min} and N = 6.5%. Since $t_1 = 1.6$ days and $t_2 = 3.5$ days, $l_1 = 5.4 \cdot 10^{12}$ cm, while $l_2 = 1.2 \cdot 10^{13}$ cm. From this $H_1 = 2 \cdot 10^{-5}$ gauss, $H_2 = 0.9 \cdot 10^{-5}$ gauss. By means of (7) we find $\rho_1 = 60$ cm^{-3}, $\rho_2 = 11$ cm^{-3}. Since $S = l_1 \cdot 3.4/6.5 = 2.8 \cdot 10^{12}$ cm, and $t_{se} = 2$ hours, $u_r^* = 4 \cdot 10^8$ cm/sec. By means of (11) we find $\Delta H_3^* \approx 100\,\gamma$.

For a characterization of the structure of the stream, it is important to know the ratio l_1/l_2. In our case $l_1/l_2 = 0.46$. Since the active region passed through the central meridian from 30.2 August to 5.2 September [14] in the region of heliolatitudes 42-7° N, we assume that the width of the stream corresponded to the width of almost the entire active region with a radial emission of the stream (width of the region according to latitude -- 6 days, width of the stream according to the data of cosmic rays around the Earth -- 5 days). Such an agreement can scarcely be considered accidental. We have related the appearance of the stream to a class 3+ chromospheric flare, observed on 31 August at 13 hours (its coordinates were 16° N, 14° E). Hence, according to the lag in the moment of the beginning of the magnetic storm, the velocity of the stream $u_r = 1.3 \cdot 10^8$ cm/sec. Then the degree of compression of the forward front $u_r^*/u_r = 3$. From (13), (14), and (15) we find $\rho_\Phi = 180$ cm^{-3}, $H_\Phi = 6 \cdot 10^{-5}$ gauss, and $\Delta H_3 \approx 60\gamma$.

Let us turn our attention to still another interesting phenomenon. The magnetic storm ended at 15 hrs on 3 September, while the restoration of the intensity did not occur until midday of 6 September, i.e. the magnetic storm ended before the Earth passed out of the corpuscular stream. This fact can be understood in the following way. The stream can possess a substantial dispersion of velocities, where the rapid particles, being distorted to a lesser degree, move basically in the region of the forward portion of the stream, while the slow particles, whose trajectories are greatly distorted on account of the rotation of the Sun, are concentrated chiefly in the lagging side portion

---

* Let us note that the beginning of the sharp decrease coincides more with the beginning of the active period than with the beginning of the magnetic storm. Such a phenomenon, as we shall see from the following, occurs rather often.

of the stream. We found in addition that in the lagging side portion of the stream, the intensity of the frozen magnetic field is approximately one-half that in the forward portion. This corresponds to the lower plasma density in the lagging portion of the stream. Thus, we might expect that here the density of the kinetic energy $\rho u^2/2$ is substantially less than in the forward portion of the stream. Since the degree of geomagnetic disturbance is determined chiefly by the density of the kinetic energy of the stream, the disappearance (or substantial decrease) of the geomagnetic disturbance as the Earth moves into the lagging portion of the stream is quite natural.

3.2. Storm in January 1957

A very large magnetic storm with a sudden beginning at 12 hrs 55 min on 21 January (amplitude of the sudden beginning 35 γ, greatest amplitude of oscillations -- more than 400 γ) caused a change in the intensity of cosmic rays of type II, substantially distorted by another sort of mechanism -- the 11-year variation of cosmic rays (as has been noted by J. A. Lockwood [9]). Fig. 5 presents the data of ionization chambers in Moscow and Yakutsk, as well as the temperature corrections for these instruments. The data on the neutron component, obtained at Mount Washington Station, were taken from the article of J. A. Lockwood [9].

Since at the minimum intensity N = 17%, I = 4.8%, N/I = 3.54 and ε_{min} = 83 bev, hence f = 0.224. It follows from the scheme of the effect presented in Fig. 5 (lower graph) that t_1 = 2 days, t_2 = = 3 days, from which $l_1 = 0.68 \cdot 10^{13}$ cm, $l_2 = 1.02 \cdot 10^{13}$ cm. Hence $H_1 = 2 \cdot 10^{-5}$ gauss, $H_2 = 1.3 \cdot 10^{-5}$ gauss. Since $S = l_1 \cdot N_{se}/N = 0.68 \cdot 10^{13} \cdot 9.5/17 = 0.38 \cdot 10^{13}$ cm, the effective radial velocity of the forward front of the stream $u_r^* = 2\ S/t_{se} = 2.1 \cdot 10^8$ cm/sec. Let us further recall that ρ_1 = 55 cm^{-3}, ρ_2 = 23 cm^{-3}, and $\Delta H_3^* = 54\ \gamma$. The active region that caused this storm was located in the region of heliolatitudes of 2-45° S and the Kerrington latitudes from 336 to 93°. This region passed through the central meridian from 15.3 to 22.6 January, i.e. its angular width was about 5.3 days. This is close to the angular width of the stream, equal in our case to 5 days. According to the lag in the beginning of the storm with respect to the chromospheric flares with indices of 3 and 2+ (which occurred on 20 January at 11 hrs 20 min), we find: $u_r \lesssim 1.5 \cdot 10^8$ cm/sec. From this it follows that around the forward front of the stream approximately a 1.5-fold intensification of the field occurred. Thus, $H_\Phi \approx 3 \cdot 10^{-5}$ gauss, $\rho_\Phi \approx 80$ cm^{-3}, and a more accurate value of ΔH_3 according to (16) will be $\Delta H_3 \approx 45\gamma$, which is in good agreement with the experimentally observed amplitude of the sudden beginning of the disturbance in the horizontal component of the geomagnetic field (about 35 γ).

From Fig. 5 we extrapolated the restoration of intensity to the normal level before the storm, although actually, as can be seen from the experimental data and the work of J. A. Lockwood [9], the intensity

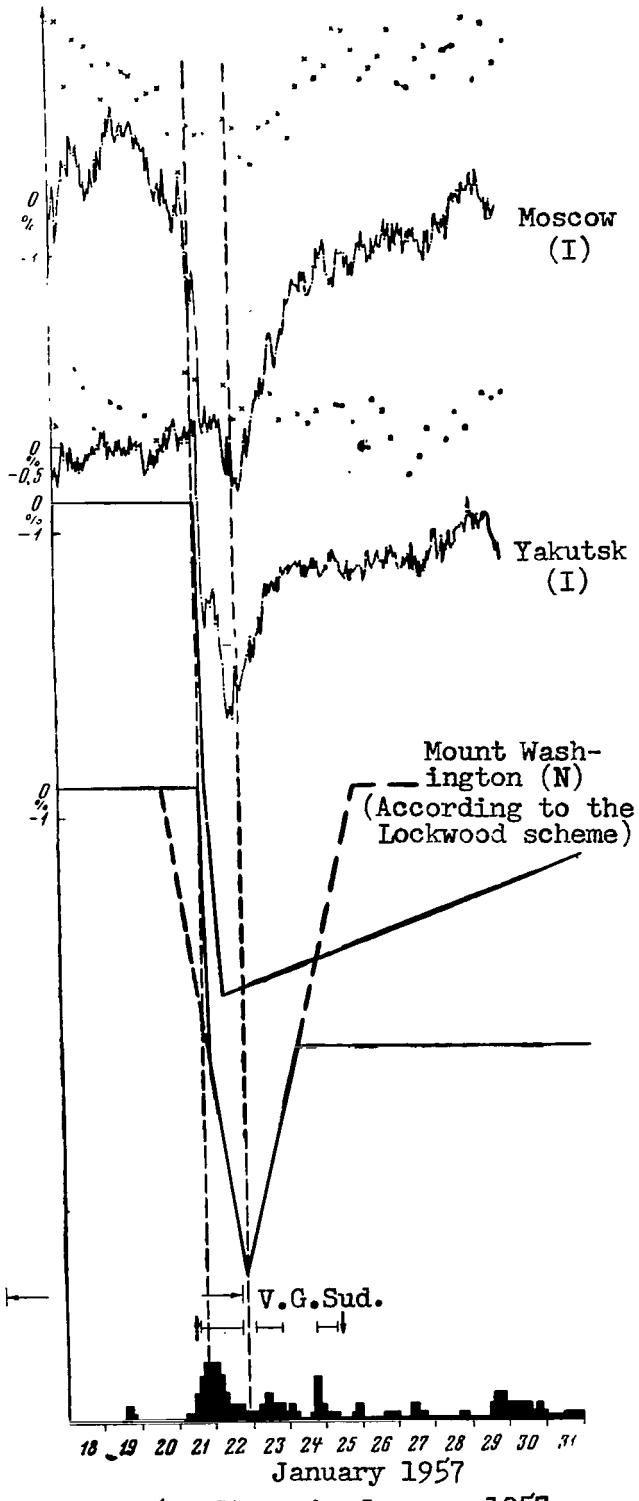

Fig. 5. Storm in January 1957

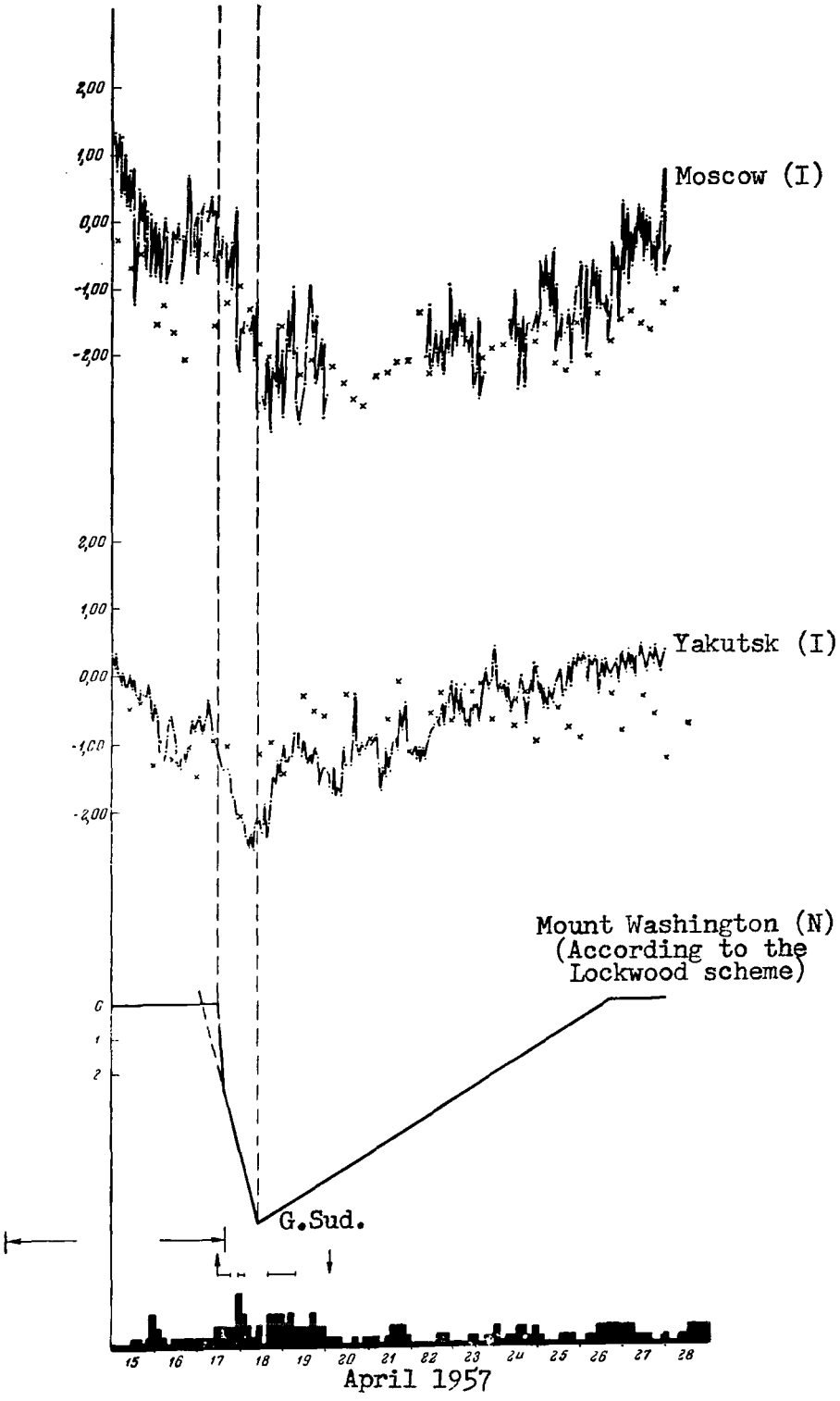

Fig. 6. Storm in April 1957

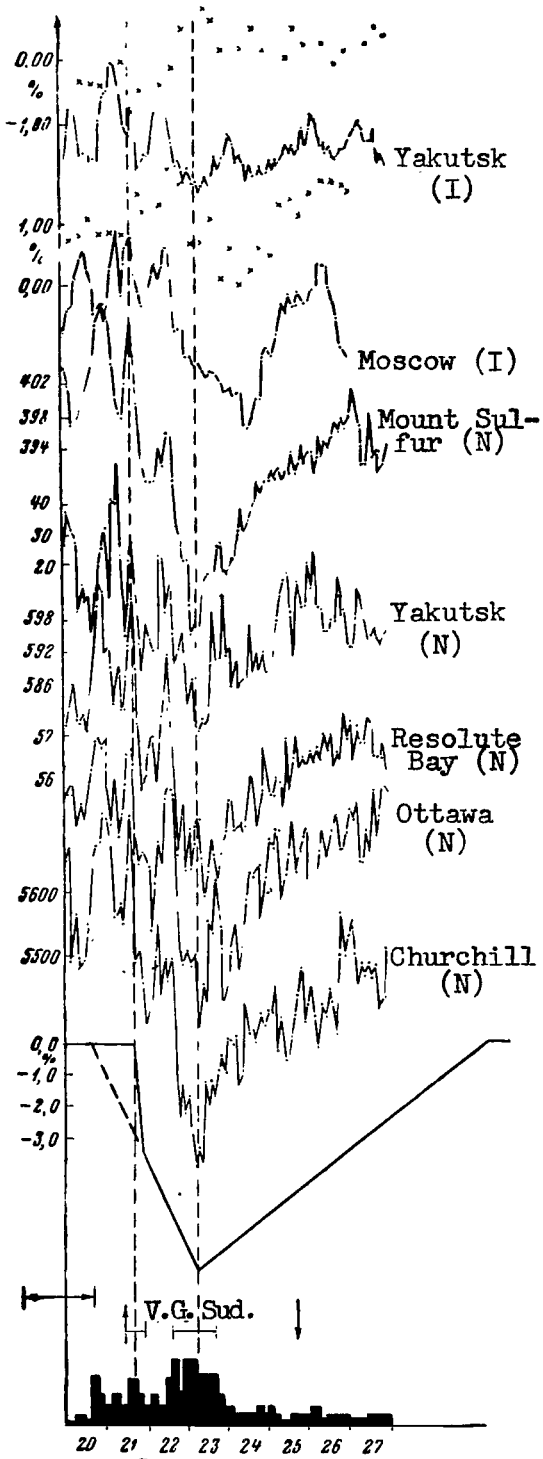

Fig. 7. Storm in the second half of September 1957.

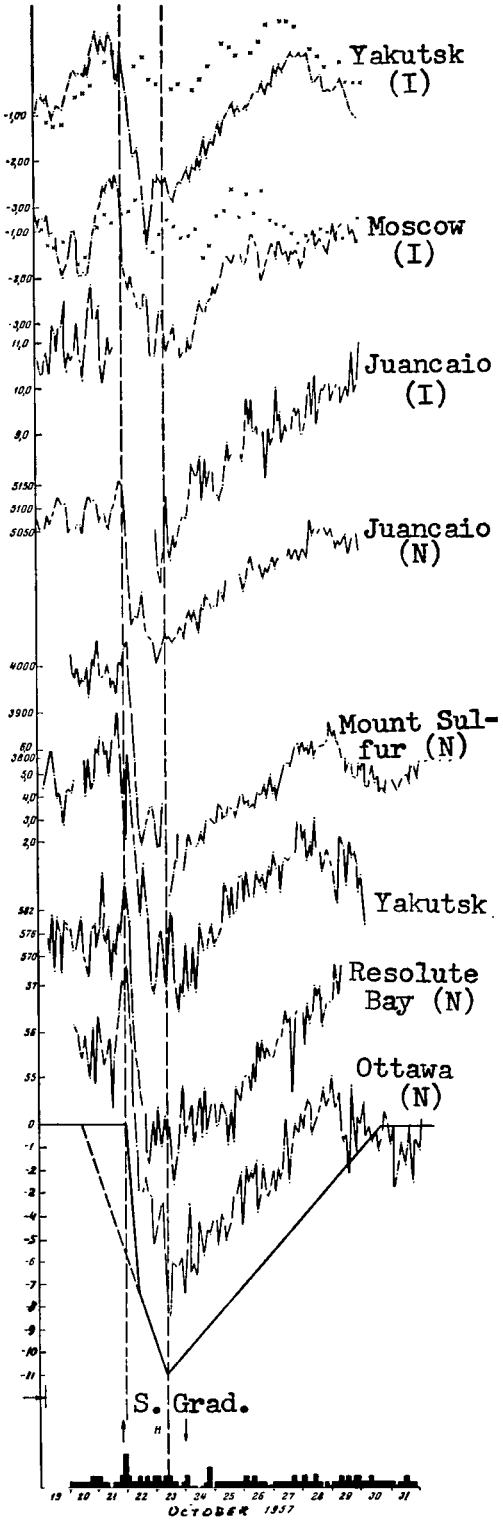

Fig. 8. Storm in October 1957.

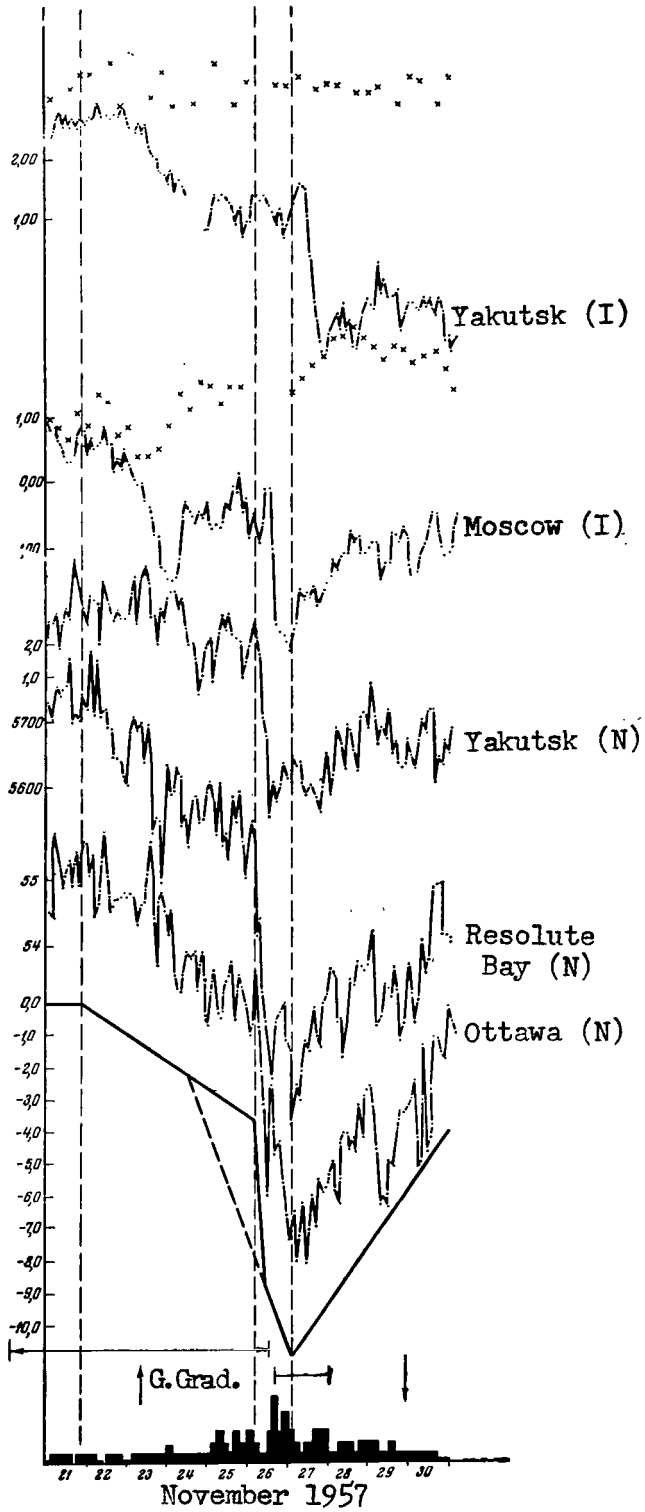

Fig. 9. Storm in November 1957.

of cosmic rays in the case under consideration was not fully restored. We believe that this was due to a general decrease in the cosmic ray intensity in the Earth-Sun neighborhood (i.e., outside the corpuscular stream), which occurred suddenly in a comparatively short time, while the Earth was within the stream. This general decrease was not related to the mechanism of modulation of cosmic rays when the Earth entered the corpuscular stream, and hence it will not be taken into consideration here. This decrease is related, in all probability, to the mechanism of the solar wind of Parker [11] and to Singer's antifermi mechanism of the retardation of particles in the interplanetary medium [12]. Apparently, simultaneously with the emission of a corpuscular stream in the direction of the Earth, characterizing an intensification of the solar activity, an intensification of corpuscular emission in other directions also occurs. The sudden intensification of corpuscular emission also leads to an abrupt decrease in the cosmic rays within the solar system in the period of time during which the Earth is found within the stream. A number of cases when the cosmic ray intensity was not restored to the normal level before the magnetic storm are encountered below.

3.3. Storm in April 1957

A large magnetic storm with a sudden beginning at 11 hrs 36 min on 17 April ended at 02 hrs on 20 April. This storm had three active periods with sudden beginnings (from 11 hrs 36 min to 17 hrs on 17 April, from 23 hrs 30 min 17 April to 02 hrs 18 April, and from 15 hrs 08 min on 18 April to 7 hrs on 19 April). The storm caused variations in the cosmic rays of type II. The data of the Moscow, Yakutsk, and Mount Washington stations are presented in Fig. 6. The profile of the effect is given according to J. A. Lockwood.

From Fig. 6 we find N = 6.5%, I = 1.75%, N/I = 3.7, from which ε_{min} = 78 bev and f = 0.09; according to t_1 = 1.16 days and t_2 = 8.6 days we find $l_1 = 0.4 \cdot 10^{13}$ cm and $l_2 = 2.9 \cdot 10^{13}$ cm. Hence $H_1 = 3.3 \cdot 10^{-5}$ gauss, $H_2 = 0.45 \cdot 10^{-5}$ gauss; $\rho_1 = 147$ cm^{-3}, $\rho_2 = 2.7$ cm^{-3}. According to N_{se} = 2.3%, we find $S = 0.14 \cdot 10^{13}$ cm, from which $u_r^* = 1.3 \cdot 10^8$ cm/sec and $\Delta H_3^* = 53\,\gamma$. The active region on the Sun, situated in the region of latitudes from 15 to 34° S and in the longitude region from 340 to 58°, passed through the central meridian from 11 to 17 April. The stream from this region could strike the Earth, since the heliolatitude of the Earth during this time was 6° S. This region with an angular width corresponding to passage through the central meridian in 6 days, could, it seems to us, cause a stream with an angular width of about 9.5 days. According to the lag in phenomena on the Earth with respect to the chromospheric flare of class 2, which occurred on 14 April at 14 hrs (25° S, 32° W), the average velocity of the forward front of the stream will be $u_r = 6 \cdot 10^7$ cm/sec, and the degree of compression of the forward front is about 4. Then ρ_Φ = 160 cm^{-3}, $H_\Phi = 6.8 \cdot 10^{-5}$ gauss, and $\Delta H_3 \approx 27\,\gamma$. Let us note that the

phenomena related to this storm are similar to the case in the beginning of September 1956, which we have already discussed in detail.

3.4. Storm in August-September 1957

The effects of cosmic rays during this storm are discussed in detail in reference [13]. Here let us note that during this period a complex superposition of the effects of several corpuscular streams, which requires a special consideration, occurred.

3.5. Storm in the Second Half of September 1957

A very large magnetic storm with a sudden beginning on 21 September at 10 hrs 06 min lasted until 15 hrs on 25 September. The storm had active periods from 10 to 20 hrs on 21 September and from 16 hrs 22 September to 18 hrs 23 September. The storm caused a change in the cosmic ray intensity, characteristic of type II. Data on the variations of cosmic rays at the Churchill (N), Ottawa (N), Resolute Bay (N), Yakutsk (N, I), Mount Sulfur (N), and Moscow (I) stations are presented in Fig. 7, and a profile of the effect is shown in the lower part of the Figure.

Let us present the results of calculations of the properties of the stream. Since $N \approx 7.5\%$, $I = 3\%$, $N/I \approx 2.5$, from which $\varepsilon_{min} \approx 100$ bev, $f \approx 0.10$. Since $t_1 = 3$ days, $t_2 = 7$ days, we find $l_1 = 10^{13}$ cm, $l_2 = 2.4 \cdot 10^{13}$ cm, from which $H_1 = 1.7 \cdot 10^{-5}$ gauss, $H_2 = 0.7 \cdot 10^{-5}$ gauss. Since $N_{se} = 4\%$, let us determine $S = 0.45 \cdot 10^{13}$ cm. When $t_{se} = 5$ hrs, this gives $u_r^* = 2.5 \cdot 10^8$ cm/sec, $\rho_1 = 40\ см^{-3}$, $\rho_2 = 7\ см^{-3}$, and $\Delta H_3^* = 55\gamma$. The active region on the Sun that caused this storm, situated in the region of latitudes 8-25° N and longitudes 90-65°, passed through the central meridian from 18.9 to 20.8 September. According to the 50-hour lag in phenomena on the Earth with respect to the class 3 chromospheric flare noted on 19 September at 8 hrs (22° N, 1° E), the average velocity of the forward front of the stream $u_r \approx 8 \cdot 10^7$ cm/sec, and the degree of compression of the forward front was equal to 3. Hence $H_\Phi = 5 \cdot 10^{-5}$ gauss, $\rho_\Phi = 120$ cm^{-3}, and $\Delta H_3 = 30\gamma$. Let us note that in this case the region with an angular width corresponding to passage through the central meridian for two days caused a stream with a considerably greater angular width, equal to approximately 10 days. This case is not distinguished by any peculiar features: the stream captured the Earth with its forward front and caused a very large magnetic storm with a sudden beginning, which ended somewhat before the intensity level of cosmic rays was restored, in agreement with the hypotheses developed in this article. Perhaps the only peculiar feature of the storm selected is its great increase in cosmic ray intensity on 22 September, which occurred on a background of a general decrease. Possibly this increase is related to intensification of the solar-diurnal variation or to an abrupt decrease in the geomagnetic activity during this period of time (which can be seen from the behavior

of the K-index in Fig. 7). It seems to us that this effect of the increase merits special analysis, since it may reflect some sort of specific interesting properties of the streams.

3.6. Storm in October 1957

The cosmic ray effect that began at the end of 21 October with an abrupt, then smoother decrease, and then a slow restoration to the normal level before the storm, coincides in time with the occurrence on the Earth of a small magnetic storm with a gradual beginning. Fig. 8 presents the experimental data from Ottawa (N), Resolute Bay (N), Yakutsk (N, I), Mount Sulfur (N), Juancaio (N, I), and Moscow (I) stations.

This case is characterized by the fact that a small magnetic storm with a gradual beginning caused a rather large effect on the cosmic rays, with an abrupt drop in the intensity, indicating that the Earth was captured not by the side edge of the stream, but by its forward front.

For the stations in the middle latitudes, we find N = 11%, I = = 4.2%, from which N/I = 2.62 and ε_{min} = 94 bev; f = 0.17. Since t_1 = 2.9 days, t_2 = 7.2 days, $l_1 = 10^{13}$ cm, $l_2 = 2.5 \cdot 10^{13}$ cm. Hence $H_1 = 1.56 \cdot 10^{-5}$ gauss, $H_2 = 0.64 \cdot 10^{-5}$ gauss, and ρ_1 = 31 cm^{-3}, ρ_2 = = 6 cm^{-3}. Since the neutron intensity during the rapid drop fell by N_{se} = 7.5%, $S = l_1 \cdot (7.5/11) = 0.68 \cdot 10^{13}$ cm. Since the rapid drop occurs after t_{se} = 10 hrs, we find $u_r^* = 2.8 \cdot 10^8$ cm/sec. From this $\Delta H_3^* = 54\gamma$ (the latter quantity scarcely has any physical meaning here, inasmuch as the storm had a gradual beginning). Since the stream under consideration caused a small magnetic storm, its actual density was very low, and the density of its kinetic energy was also extremely small. We think that the values we obtained for the density of the stream are quite high.

It is possible that the magnetic storm and the decrease in cosmic ray intensity are related to a stream that arose when a class 2+ flare arose on 16 October at 8 hrs (30° S, 20° E). Then $u_r = 2.9 \cdot 10^7$ cm/sec. From this the degree of compression of the forward front is about 10. We find that $H_\Phi = 1.6 \cdot 10^{-4}$ gauss, ρ_Φ = 310 cm^{-3}, and $\Delta H_3 = 17\gamma$. From the point of view of the hypotheses developed here, the investigated magnetic storm should have had a sudden beginning, and it is unclear to us how the fact that the magnetic storm had a gradual beginning can be explained. Here a further investigation, involving more complete data on the magnetic disturbances on the Earth and phenomena on the Sun during this period is required.

3.7. Storm in November 1957

Fig. 9 presents data on cosmic rays obtained at the stations at Yakutsk (N, I), Moscow (I), Resolute Bay (N), and Ottawa (N) in November. The cosmic ray effects in this period under consideration were

accompanied by a large magnetic storm with a gradual beginning at 08 hrs on 22 November and an end at 20 hrs on 29 November. This storm is characterized by an active period from 16 hrs 26 November to 23 hrs 27 November. The profile of the change in cosmic ray intensity is shown in the lower part of the Figure. We can see from the latter that a smooth decrease in the intensity began on 21 November and continued until 3 hrs, 26 November, when an abrupt decrease, lasting until 10 hrs on 26 November, occurred (during this time the intensity N dropped 5.2%). A smoother drop in the cosmic ray intensity began at this time, continuing until 2 hrs on 27 November (during this period the intensity N fell by another 2.3%), and then a slow restoration to the normal level before the beginning of the sharp drop at 3 hrs on 26 November began and continued up to the end of the day of 30 November. We believe that here there was a superposition of two effects: a broad corpuscular stream captured the Earth with its side edge and caused a decrease in intensity of type III, while a narrow stream traveling within it captured the Earth with its forward front and caused a decrease in intensity of type II.

Properties of the broad stream. Since N = 5% and I = 2.5%, N/I = 2.0 and ε_{min} = 115 bev; f = 0.07. Since t_1 = 6 days, l_1 = $= 2 \cdot 10^{13}$ cm, and $H_1 = 0.94 \cdot 10^{-5}$ gauss. We cannot determine the quantity l_2 here, but it apparently is no less than l_1 (since in all the cases considered in this work $l_1/l_2 < 1$); hence we might assume that the total width of the stream $l = l_1 + l_2$ is greater than $4 \cdot 10^{13}$ cm.

Properties of the narrow stream. Since N = 7.5%, I = 1.9%, then N/I = 3.95 and ε_{min} = 63 bev; f = 0.134. Inasmuch as t_1 = 2.6 days, t_2 = 4 days, $l_1 = 0.9 \cdot 10^{13}$ cm, $l_2 = 1.4 \cdot 10^{23}$ cm. Hence $H_1 = 1.2 \cdot 10^{-5}$ gauss, $H_2 = 0.8 \cdot 10^{-5}$ gauss, and ρ_1 = 19 cm^{-3}, ρ_2 = 8 cm^{-3}. Let us find $S = l_1 \cdot (5.2/7.5) = 0.6 \cdot 10^{13}$ cm. Considering the fact that the rapid drop occurred in t_{se} = 8 hrs, we find that $u_r^* = 2.2 \cdot 10^8$ cm/sec and $\Delta H_3^* = 43\gamma$.

During this period on the Sun, an active region in the northern hemisphere (its coordinates are 7-42° N, 349-265°) passed through the central meridian from 20.2 to 26.5 November; we believe it was related to the broad stream.

The narrow stream can apparently be related to a class 3+ flare, observed on 23 November at 8 hrs (25° N, 55° W). According to the lag in the abrupt decrease in cosmic ray intensity, we find $u_r = 10^8$ cm/sec and the degree of compression is about 2. From this H_Φ = $= 2.4 \cdot 10^{-5}$ gauss, ρ_Φ = 40 cm^{-3}, and $\Delta H_3 = 30\gamma$.

3.8. Storm in March of 1958

This storm is of special interest, since it apparently was caused by a corpuscular stream in which plasma without a field (or with a very weak field) moved ahead of the front with the frozen magnetic field. Experimental data on the changes in the cosmic ray intensity during this period at the Juancaio (N, I), Moscow (I), Yakutsk (I), and Heiss

Island (N) stations are presented in Fig. 10. During this period a moderate magnetic storm with a gradual beginning at 16 hrs on 24 March occurred, lasting until 06 hrs on 27 March. The active period of the storm lasted from 15 to 19 hrs on 25 March.

We can see from the data cited that the cosmic ray intensity was not restored to the normal level before the decrease. Here a phenomenon analogous to that which existed during the magnetic storm in January 1957, which we have taken up in detail above (3.2), apparently occurred. In the case under consideration we have a profile of a change of type II presented in the lower portion of Fig. 10 (we extrapolated the restoration of intensity to the normal level). Noteworthy is the fact that the magnetic storm began almost a day before the beginning of the sudden drop, which coincided with the active period of the storm. If we extrapolate the line of the smooth drop to the normal level of intensity, then we see from Fig. 10 that it intersects this level close to the point of the beginning of the magnetic storm. We interpret this case in the following way. The corpuscular stream ejected from the Sun at first did not carry a frozen magnetic field (or in any case, its intensity was very low, since it was not able to influence the cosmic ray intensity). The stream captured the Earth with its side front and caused a moderate magnetic storm with a gradual beginning. Since there was no magnetic field in this portion of the stream, the cosmic ray intensity did not change. When the magnetized portion of the stream came from the Sun and captured the Earth with its forward front, an abrupt drop occurred in the cosmic ray intensity. Around the magnetized front the plasma was compressed, the field was intensified (see below for calculations of this field H_ϕ); this caused the active period of the magnetic storm. Then, as the Earth gradually entered the magnetized stream, the cosmic ray intensity dropped comparatively sharply, after which, as the Earth left the stream, it was gradually restored. Now let us present calculations of the properties of the stream.

Since N = 7.5%, I = 3%, then N/I = 2.5 and ε_{min} = 100 bev; f = 0.108.

Considering that t_1 = 2 days, t_2 = 3 days, we find $l_1 = 0.7 \cdot 10^{13}$ cm, $l_2 = 10^{13}$ cm, from which $H_1 = 2.35 \cdot 10^{-5}$ gauss, $H_2 = 1.63 \cdot 10^{-5}$ gauss. Since the intensity N dropped sharply by N_{se} = 5% in t_{se} = 6 hours, S = $0.47 \cdot 10^{13}$ cm, and $u_r^* = 2.2 \cdot 10^8$ cm/sec, from which $\Delta H_3^* = 63\gamma$, $\rho_1 = 74\ см^{-3}$, $\rho_2 = 35\ см^{-3}$. Two active regions on the Sun passed through the central meridian during this period: one in the northern hemisphere, the other in the south. Inasmuch as the heliolatitude of the Earth was 7° S during this time, we should expect that the phenomenon under consideration was caused by the active region in the southern hemisphere, the coordinates of which were 0-35° S, 240-150°, and which passed through the central meridian from 17.7 to 24.6 March. The angular width of the region (corresponding to its passage through the central meridian in a period of seven days) agrees with the angular width of the stream of five days. According to the lag in the

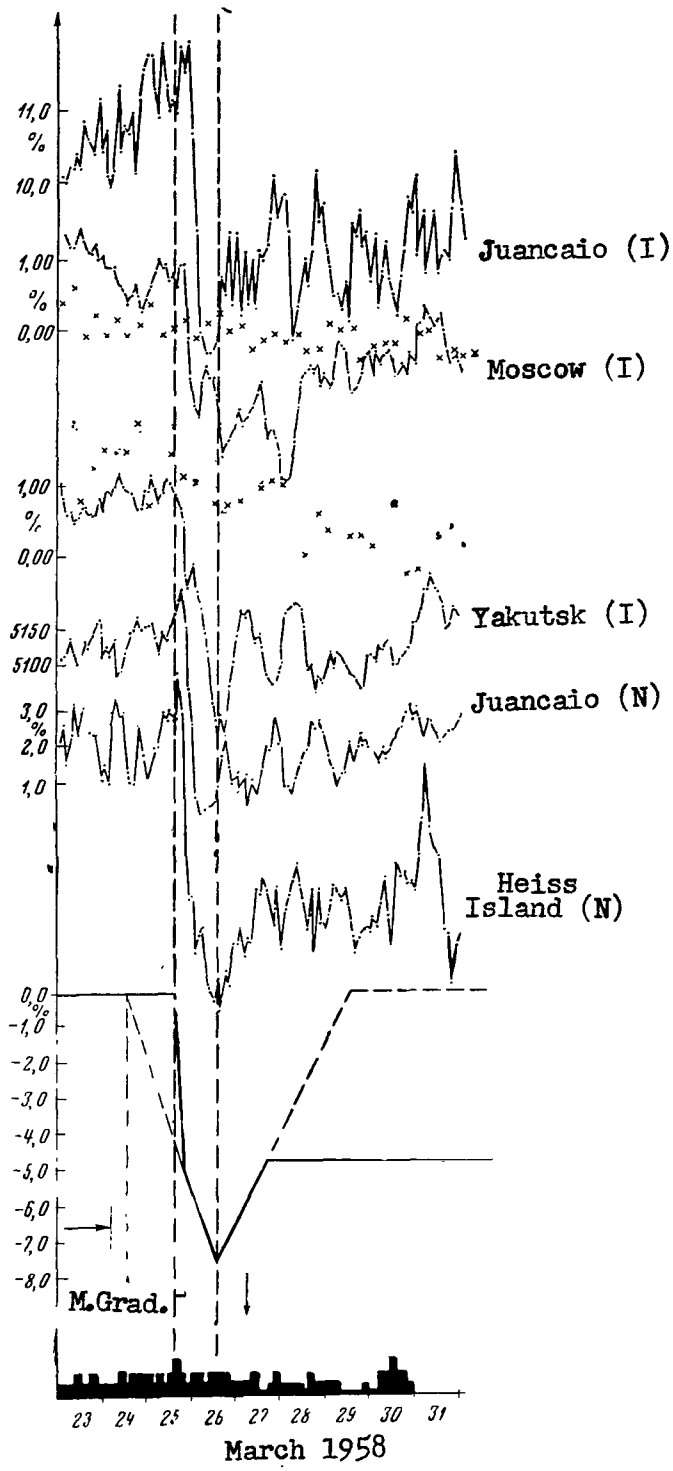

Fig. 10. Storm in March of 1958.

drop of the cosmic ray intensity with respect to the flare of ~53 hours, we find $u_r = 8 \cdot 10^7$ cm/sec, from which it follows that the field in the forward magnetized portion of the stream should be compressed approximately three-fold and should constitute $H_\Phi = 0.6 \cdot 10^{-4}$ gauss. Accordingly $\rho_\Phi \approx 190$ and $\Delta H_3 \approx 42\,\gamma$.

3.9. Storm in the First Half of July 1958

Fig. 11 presents experimental data for the period from 5 to 14 July at Heiss Island (N), Yakutsk (I), and Irkutsk (N) stations.

A very great magnetic storm (change in the H-component about 1500 γ) with a sudden beginning at 07 hrs 46 min on 8 July ended at 10 hrs on 10 July. This storm had an active period from 08 to 24 hrs, 8 July. We can see from Fig. 11 that the profile of the decrease in cosmic rays, caused by this storm, is characteristic of type II. Let us find the properties of the stream. According to the amplitude of the decrease in intensity of the neutron component N = 7% and the amplitude of decrease in intensity in the hard component I = 2%, we find N/I = 3.5, from which $\varepsilon_{min} = 68$ bev, f = 0.2. If the stream captured the Earth with its side edge, then, as we believe, the change in intensity would take place just as is shown by the dotted line in Fig. 11. Then the time of the hypothetical gradual drop in intensity $t_1 = 3.6$ days, the time of gradual restoration $t_2 = 4.2$ days, from which the extent of the stream from the forward side edge to the line of least intensity

$$l_1 = \frac{2\pi R_\odot \cdot 3{,}6}{27} = 1{,}22 \cdot 10^{13}\ см,$$

analogously $l_2 = 1.45 \cdot 10^{13}$ cm. From this we find the field intensity of the first half of the stream

$$H_1 = \frac{\varepsilon_{min}}{600\, l} = 0{,}94 \cdot 10^{-5}\ \text{gauss}$$

and in the second half -- $H_2 = 0.76 \cdot 10^{-5}$ gauss. During the sharp drop, the neutron intensity fell by 5.5%.

Let us find from this the distance from the place in the stream where the break in the intensity drop occurred, to the forward front of the stream (equal in the case of homogeneity of the field to the distance to the forward side edge of the stream) $S = l_1 \frac{5.5}{7} = 0.96 \cdot 10^{13}$ cm. Since a sharp drop occurred at 8 hrs, we find from this the velocity of the forward front of the stream (again assuming homogeneity of the field) $u_r^* = 3.4 \cdot 10^8$ cm/sec. The active region that caused the magnetic storm was situated on the Sun within the latitudes 10-50° N and

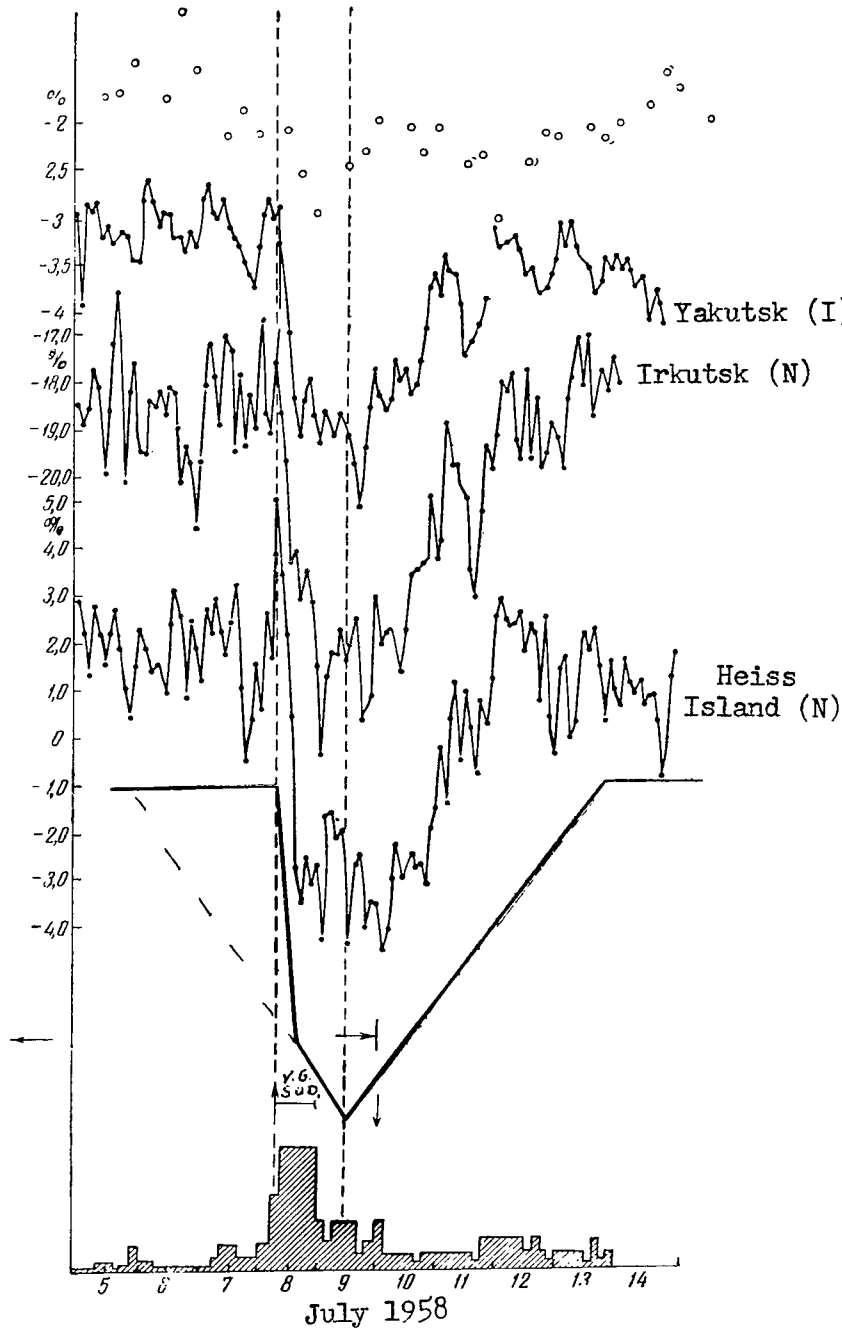

Fig. 11. Storm in the first half of July 1958.

longitudes 243-130° (the heliolatitude of the Earth during this period was 4° N). This region passed through the central meridian of the Sun from 4.4 to 10.0 July 1958, i.e. the angular width of the region was 8.6 days. We can see from Fig. 11 that if the Earth had been captured by the side edge, this would have occurred on 5.8 July, while the Earth would have left the stream on 13.8 July. Hence, the total width of the stream around the Earth corresponds to 8 days, which is in good agreement with the angular width of the active region, about 8.6 days. In this region an extremely powerful chromospheric flare with an area of 5304 millionths of the disc and a highest index of 3+ was observed close to the central meridian (26° N, 8° W) on 7 July during the period from 0 hrs 58 min to 4 hrs 14 min. According to the lag in the sudden beginning of the magnetic storm with respect to the flare, we find $u_r = 1.3 \cdot 10^8$ cm/sec. Hence, the degree of compression of the forward portion of the stream $u_r^*/u_r \approx 2.6$, and the field in it should be $H_\Phi \approx 2 \cdot 10\text{-}5$ gauss.

3.10. Storm in the Second Half of July 1958

Data on cosmic rays for the period from 18 to 26 July, obtained at the stations of Heiss Island (N), Irkutsk (I), and Moscow (I) are presented in Fig. 12. A moderate storm with a sudden beginning at 16 hrs 35 min on 21 July lasted until 15 hrs, 22 July. The active period occurred from 17 to 24 hrs on 21 July. The variation of intensity, as it seems to us, is characterized by type II. This can be seen from the data on the neutron component.

Since N = 4%, I = 1.5%, then N/I = 2.7% and ε_{min} = 93 bev; f = = 0.06. Since t_1 = 1.7 days, t_2 = 1.9 days, then $l_1 = 0.55 \cdot 10^{13}$ cm, $l_2 = 0.65 \cdot 10^{13}$ cm, from which $H_1 = 3 \cdot 10\text{-}5$ gauss, $H_2 = 2.5 \cdot 10\text{-}5$ gauss, and ρ_1 = 120 cm-3, ρ_2 = 83 cm-3. Since N_{se} = 3%, we find S = $0.4 \cdot 10^{13}$ cm, and since t_{se} = 8 hrs, we determine $u_r^* = 1.4 \cdot 10^8$ cm/sec, and $\Delta H_3^* = 55\,\gamma$. The active region that caused the investigated storm lay in the region of latitudes 2° N - 40° S and in the longitude region from 340-70°, and passed through the central meridian from 17.5 to 24.3 July 1958.

If we relate the formation of the stream to the class 2+ flare observed on 20 July at 12 hrs (22° S, 66° W), then $u_r = 1.4 \cdot 10^8$ cm/sec, and the degree of compression is about 1. The angular width of the region, in this case about 7 days, proves to be approximately twice as great as the angular width of the stream (about 3.5 days).

Storm in the Middle of August 1958

A magnetic storm with an unexpected beginning on 17 August at 06 hrs 22 min lasted until 14 hrs on 18 August. The active period of the storm occurred from 13 hrs on 17 August to 01 hrs on 18 August. Data from the Irkutsk (N, I) and Moscow (N) stations are presented in Fig. 13.

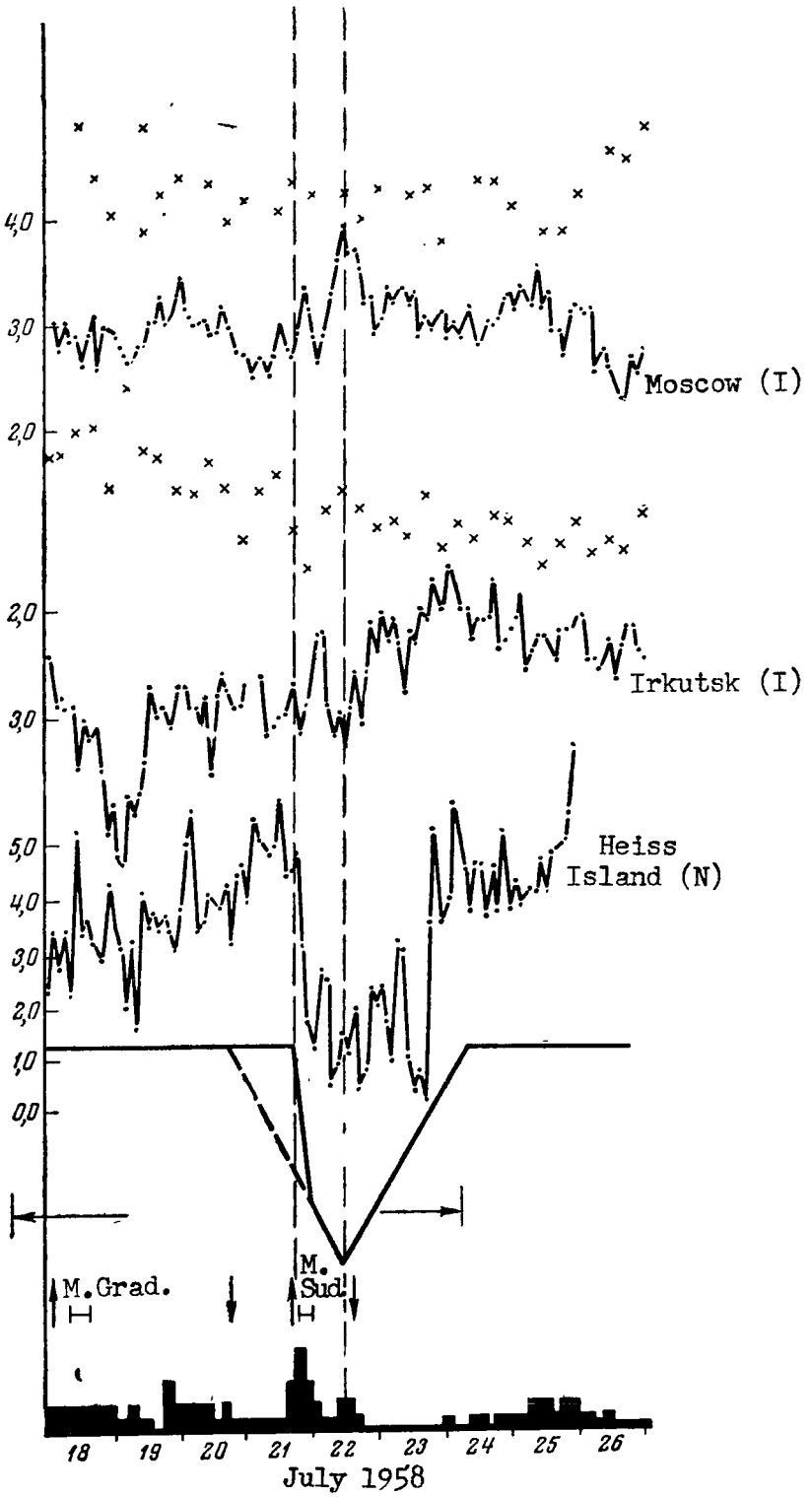

Fig. 12. Storm in the second half of July 1958.

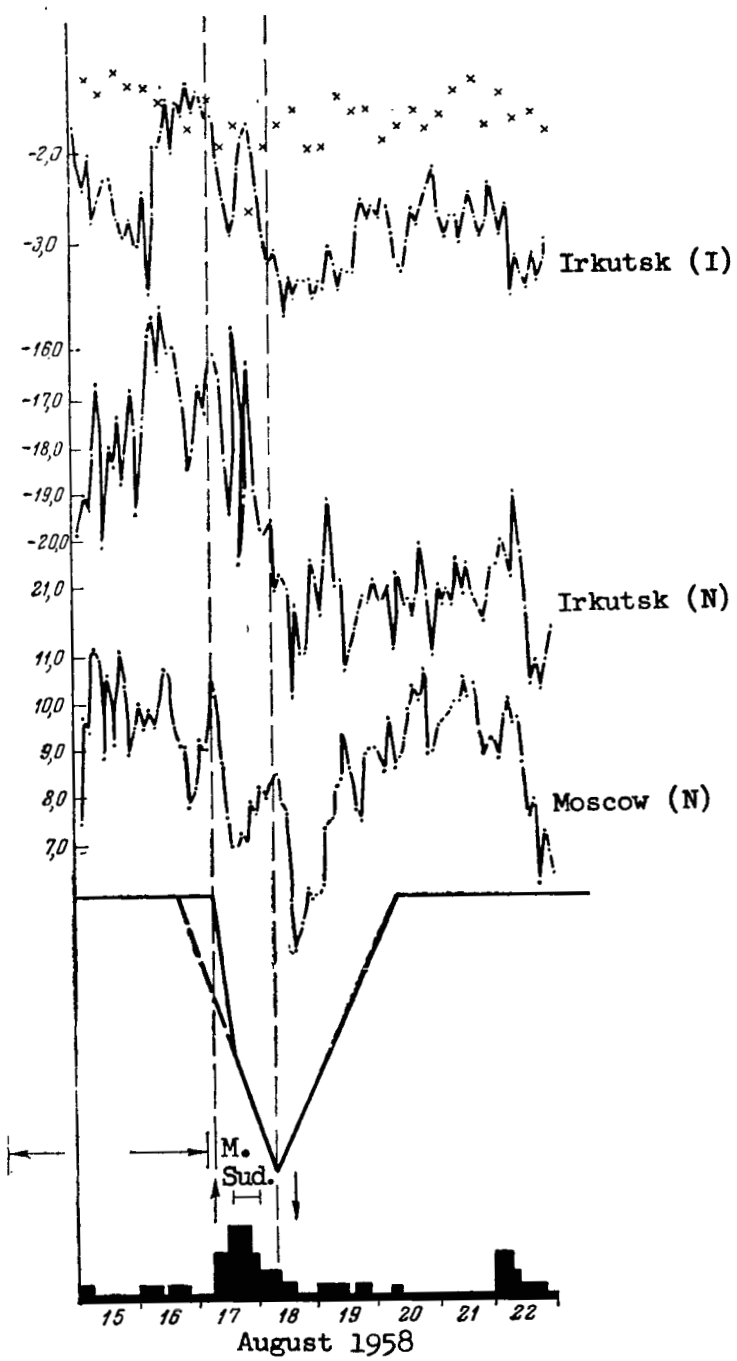

Fig. 13. Storm in the middle of August 1958.

Since $N \approx 6\%$, $I \approx 2.2\%$, we find $N/I \approx 2.7$ and $\varepsilon_{min} = 90$ bev; $f = 0.09$. Since $t_1 = 1.6$ days, $t_2 = 2$ days, then $l_1 = 0.55 \cdot 10^{13}$ cm; $l_2 = 0.68 \cdot 10^{13}$ cm, from which $H_1 = 2.7 \cdot 10^{-5}$ gauss, $H_2 = 2.2 \cdot 10^{-5}$ gauss. Since $N_{se} = 3.5\%$, we determine that $S = 0.3 \cdot 10^{13}$ cm, from which when $t_{se} = 7$ hrs, $u_r^* = 0.63 \cdot 10^8$ cm/sec. Further we find that $\rho_1 = 100$ cm^{-3}, $\rho_2 = 64$ cm^{-3}, $\Delta H_3^* = 22\gamma$. The active region that caused this stream was apparently situated in the northern hemisphere, since the heliographic latitude of the Earth during this period of time was about 6° N. This region, situated in the region of latitudes 1-30° N and in the longitude region 24-70°, passed through the central meridian from 13.7 to 17.2 August 1958. According to the lag in terrestrial phenomena with respect to a class 3 flare observed on 13 August at 13 hrs (13° S, 25° W) of approximately 3.5 days, we find $u_r \sim$ $\sim 5 \cdot 10^7$ cm/sec, which is close to u_r^*. Here the degree of compression was apparently close to 1.

3.12. Magnetic Storms at the End of August 1958

The last 10 days of August are characterized by an extremely interesting phenomenon -- a superposition of cosmic ray effects from several magnetic storms. During this period three magnetic storms occurred. The first was moderate with a sudden beginning at 02 hrs 28 min on 22 August. It continued until 15 hrs, 22 August. Then at 01 hrs 40 min on 24 August, a large storm with a sudden beginning occurred, lasting until 20 hrs on 25 August. And, finally, the third was moderate with a gradual beginning at 02 hrs, 27 August, and an end at 01 hrs, 28 August. During this storm there was an active period with a sudden beginning at 02 hrs 50 min on 27 August, which continued until 12 hrs, 27 August. Fig. 14 presents data on the stations at Irkutsk (N, I) and Moscow (N, I). The profile of the change in the cosmic ray intensity from 21 to 31 August 1958 is presented in the lower portion of Fig. 14 and can be broken up into three parts: 1) profile of type II, 2) profile of type I, 3) profile of type III.

We believe that all these profiles were caused by different streams. Let us turn to a calculation of the properties of the individual streams.

Calculation of the properties of the first stream. This stream caused a type II profile of the decrease. From $N = 4\%$, $I = 1.2\%$, we find $N/I = 3.4$ and $\varepsilon_{min} = 68$ bev; $f = 0.07$. Since $t_1 = 1.8$ days, we obtain $l_1 = 0.6 \cdot 10^{13}$ cm (t_2 and l_2 are unknown in this case, since the effect of another stream was superimposed during the restoration period). Hence $H_1 = 2.2 \cdot 10^{-5}$ gauss and $\rho_1 = 66$ cm^{-3}. Since $N_{se} = 3.2\%$, $t_{se} = 7$ hrs, $S = 0.5 \cdot 10^{13}$ cm, and $u_r^* = 2 \cdot 10^8$ cm/sec and $\Delta H_3^* = 56\gamma$. This stream was apparently caused by an active region situated on the Sun in the region of latitudes 30° N - 15° S and longitudes 227-333°, which passed through the central meridian from 21.1 to 30.1 August 1958.

If we relate the stream to several class 2 flares, observed on

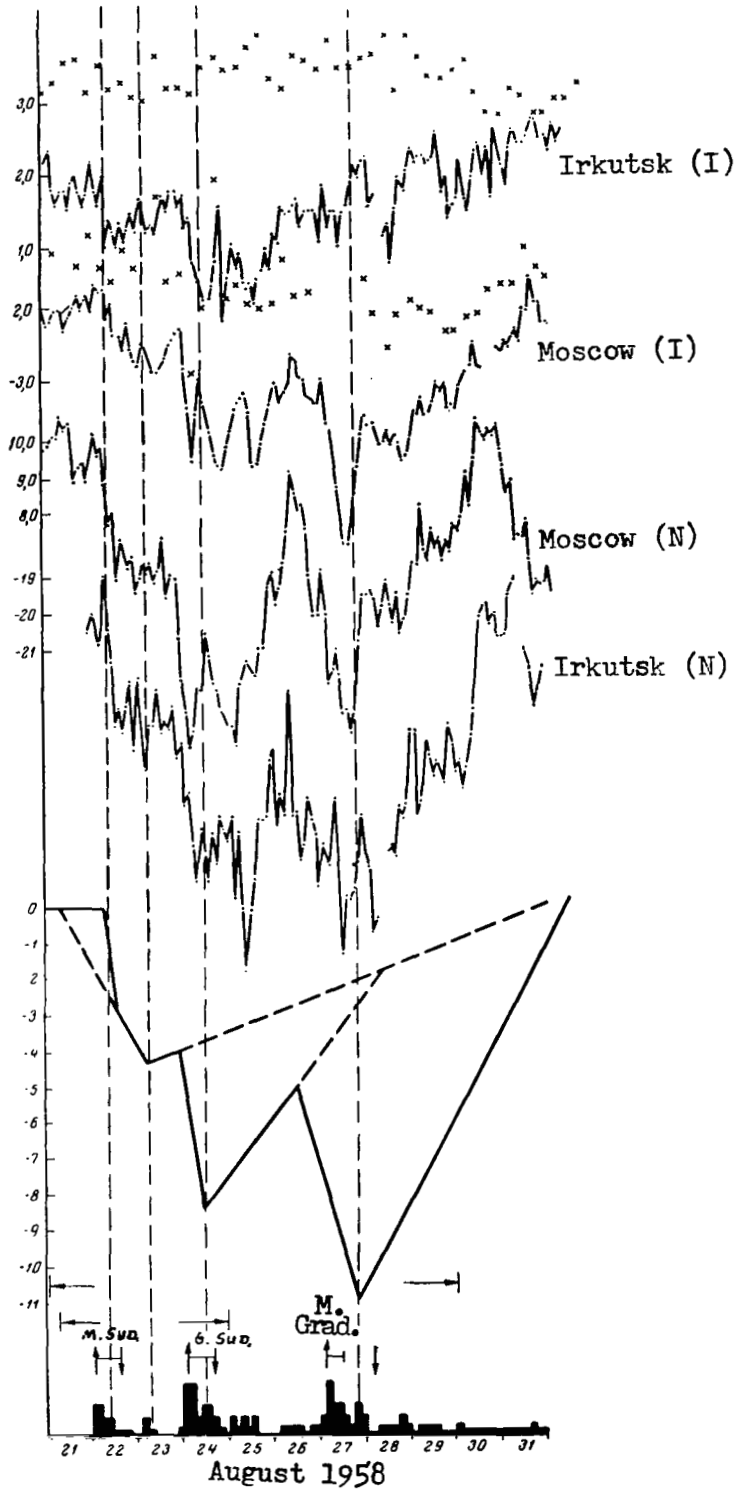

Fig. 14. Storm at the end of August 1958.

18 August at 9 hrs (20° N, 50° E), then from a lag of 90 hours we find $u_r = 0.5 \cdot 10^8$ cm/sec, and the degree of compression is close to 4. Hence $H_\phi = 9 \cdot 10\text{-}5$ gauss, $\rho_\phi = 260$ cm^{-3}, and $\Delta H_3 = 30\ \gamma$.

Calculation of the properties of the second stream. Here we have a profile of type I. This stream caused a large storm with a sudden beginning at 01 hrs 40 min on 24 August. From N = 4.5%, I = 1.3%, we find N/I = 3.46, $\mathcal{E}_{min} = 69$ bev, and f = 0.08. From $t_2 = 4.2$ days, we determine $l_2 = 1.9 \cdot 10^{13}$ cm and $H_2 = 0.6 \cdot 10\text{-}5$ gauss. Since $t_{se} = 10$ hrs, we obtain $u_r^* = 5.3 \cdot 10^8$ cm/sec, $\rho_1 = 5$ cm^{-3}, and $\Delta H_3^* = 40\ \gamma$. This storm was apparently caused by a class 3 flare, observed on 22 August at 16 hrs (19° N, 6° W). According to the 34-hour lag, we find $u_r \approx 1.2 \cdot 10^8$ cm/sec, and the degree of compression is about 4. Hence $H_\phi = 2.5 \cdot 10\text{-}5$ gauss, $\rho_\phi = 20$ cm^{-3}, and $\Delta H_3 = 20\ \gamma$.

Calculation of the properties of the third stream. Here there was a profile of type III, accompanied by a moderate storm with a gradual beginning. From N = 6% and I = 1.4%, we find N/I = 4.3 and $\mathcal{E}_{min} = 60$ bev; f = 0.11. Since $t_1 = 1.2$ days, $t_2 = 2.6$ days, we determine $l_1 = 0.42 \cdot 10^{13}$ cm, $l_2 = 0.88 \cdot 10^{13}$ cm. Hence $H_1 = 2.1 \cdot 10\text{-}5$ gauss, $H_2 = 1.2 \cdot 10\text{-}5$ gauss, and $\rho_1 = 60$ cm^{-3}, $\rho_2 = 18$ cm^{-3}.

3.13. Magnetic Storms in September-October 1958

Two magnetic storms with sudden beginnings, causing effects of a decrease in the cosmic ray intensity, occurred at the end of September: a large storm with a sudden beginning on 25 September at 04 hrs 08 min, ending on 26 September at 15 hrs, and a small storm with a sudden beginning on 30 September at 10 hrs 05 min, which ended on 1 October at 08 hrs. Fig. 15 presents data from Moscow (N, I) and Irkutsk (N) stations for this period of time.

Effect of the large storm with a sudden beginning on 25 September. As can be seen from Fig. 15, this storm caused an effect of a decrease in the cosmic ray intensity with a type II profile. From N = = 3.3%, I = 0.5%, we find N/I = 6.6 and $\mathcal{E}_{min} = 42$ bev; f = 0.075. From $t_1 = t_2 = 3$ days we determine $l_1 = l_2 = 1 \cdot 10^{13}$ cm, from which $H_1 = H_2 = 0.7 \cdot 10\text{-}5$ gauss; $\rho_1 = \rho_2 = 6$ cm^{-3}. From $N_{se} = 2.3\%$ and $t_{se} =$ = 6 hours, we obtain $S = 0.7 \cdot 10^{13}$ cm and $u_r^* = 3.3 \cdot 10^8$ cm/sec, $\Delta H_3^* =$ = $30\ \gamma$. This storm was caused by an active region on the Sun in the region of latitudes 7-41° S and longitudes 266-356°, which passed through the central meridian from 15.6 to 22.4 September. According to the lag with respect to the group of class 2 flares observed on 22 September at 8 hrs (20° S, 40° W) of 68 hours, we find $u_r \approx 6 \cdot 10^7$ cm/sec, and hence a degree of compression of approximately 5. Hence $H_\phi = 3.5 \cdot 10\text{-}5$ gauss, $\rho_\phi = 30$ cm^{-3}, $\Delta H_3 = 14\ \gamma$. The angular width of the region of 7 days corresponds to the angular width of the stream of 6 days.

Effect of the small storm with sudden beginning on 30 September. Here we have a type I profile. From N = 6%, I = 1.2%, we find N/I = 5 and $\mathcal{E}_{min} = 52$ bev, f = 0.12; since $t_2 = 3$ days, then $l_2 = 1 \cdot 10^{13}$ cm

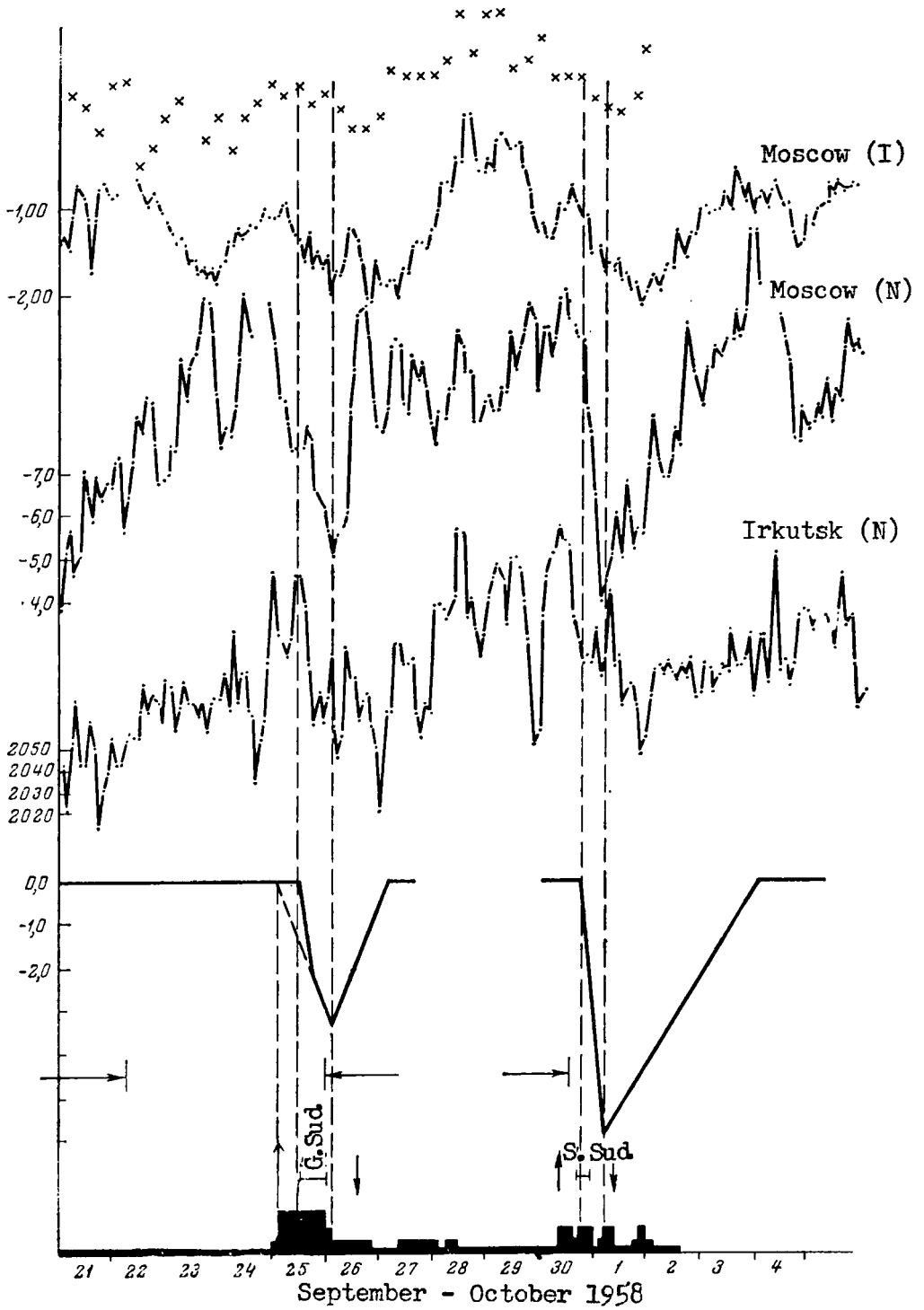

Fig. 15. Storm in September-October 1958.

and $H_2 = 0.8 \cdot 10^{-5}$ gauss, $\rho_2 = 10$ cm^{-3}. Since $t_{se} = 8$ hours, then $u_r^* = 3.5 \cdot 10^{-8}$ cm/sec, and $\Delta H_3^* = 38\,\gamma$. If this storm was caused by a class 2+ flare observed on 26 August at 1 hr (19° N, 85° W), then according to the lag of about 4 days we obtain $u_r = 4 \cdot 10^7$ cm/sec, and from this a degree of compression of about 8. Hence $H_\phi = 6 \cdot 10^{-5}$ gauss, $\rho_\phi = 50$ cm^{-3}, $\Delta H_3 = 10\,\gamma$. The angular width of the region, 5 days, corresponds to a half-width of the stream of about 3 days.

3.14. Storm in November 1954

We have few experimental data at our disposal on this storm, which occurred during the minimum of solar activity, but we have attempted to evaluate, albeit roughly, the parameters of the stream that caused it. Fig. 16 presents data on the variation of the cosmic ray intensity from 30 October to 11 November, obtained at the Mount Washington (N) (see the scheme of J. A. Lockwood [9]), Yakutsk (I), Moscow (I), and Cheltenham (I) stations. The change in cosmic ray intensity was accompanied by a moderate magnetic storm with a gradual beginning at 12 hrs on 31 October, lasting until 02 hrs on 3 November. Within this storm there was an active period from 14 hrs, 1 November, to 04 hrs, 2 November. The cosmic ray intensity began to drop approximately two days after the beginning of the magnetic storm. This case is analogous to that considered in connection with the storm in March of 1958 (see 3.8). Let us present the results of the calculations.

Since N = 6.2% and I = 1%, N/I = 6.2 and $\varepsilon_{min} = 54$ bev; f = = 0.1 (here the high altitude data on the neutron component were used). Since $t_1 = t_2 = 4.5$ days (we are extrapolating the restoration of intensity to intersection with the normal level before the storm and are not considering secondary modulation by the solar wind in interplanetary space), we find $l_1 = l_2 = 1.5 \cdot 10^{13}$ cm. Since $N_{se} = 2.8\%$ and $t_{se} = = 4$ hrs, we obtain $S = 0.7 \cdot 10^{13}$ cm and $u_r^* = 4.8 \cdot 10^8$ cm/sec. Further we find that $H_1 = H_2 = 0.6 \cdot 10^{-5}$ gauss, $\rho_1 = \rho_2 = 5$ cm^{-3}, and $\Delta H_3^* = 36\,\gamma$. The active region that apparently caused this storm intersected the central meridian from 23 to 28 October 1954. According to the lag, equal to approximately 5 days, we find $u_r \approx 2 \cdot 10^7$ cm/sec, from which the degree of compression of the plasma and field around the forward front of the stream is equal to approximately 15. Hence $H_\phi \approx 9 \cdot 10^{-5}$ gauss, $\rho_\phi = 75$ cm^{-3}, and $\Delta H_3 = 9\,\gamma$.

Here, just as in the case considered in Section 3.8, a corpuscular stream without magnetic field captured the Earth with its side edge and caused a magnetic storm with a gradual beginning. Approximately a day later the Earth was captured by the forward front of the magnetized portion of the stream, which led to a sharp drop in the cosmic ray intensity and to a further change in it, corresponding to a type II profile. In the case under consideration the width of the active region, of the order of five days, corresponds to a stream width of about 10 days.

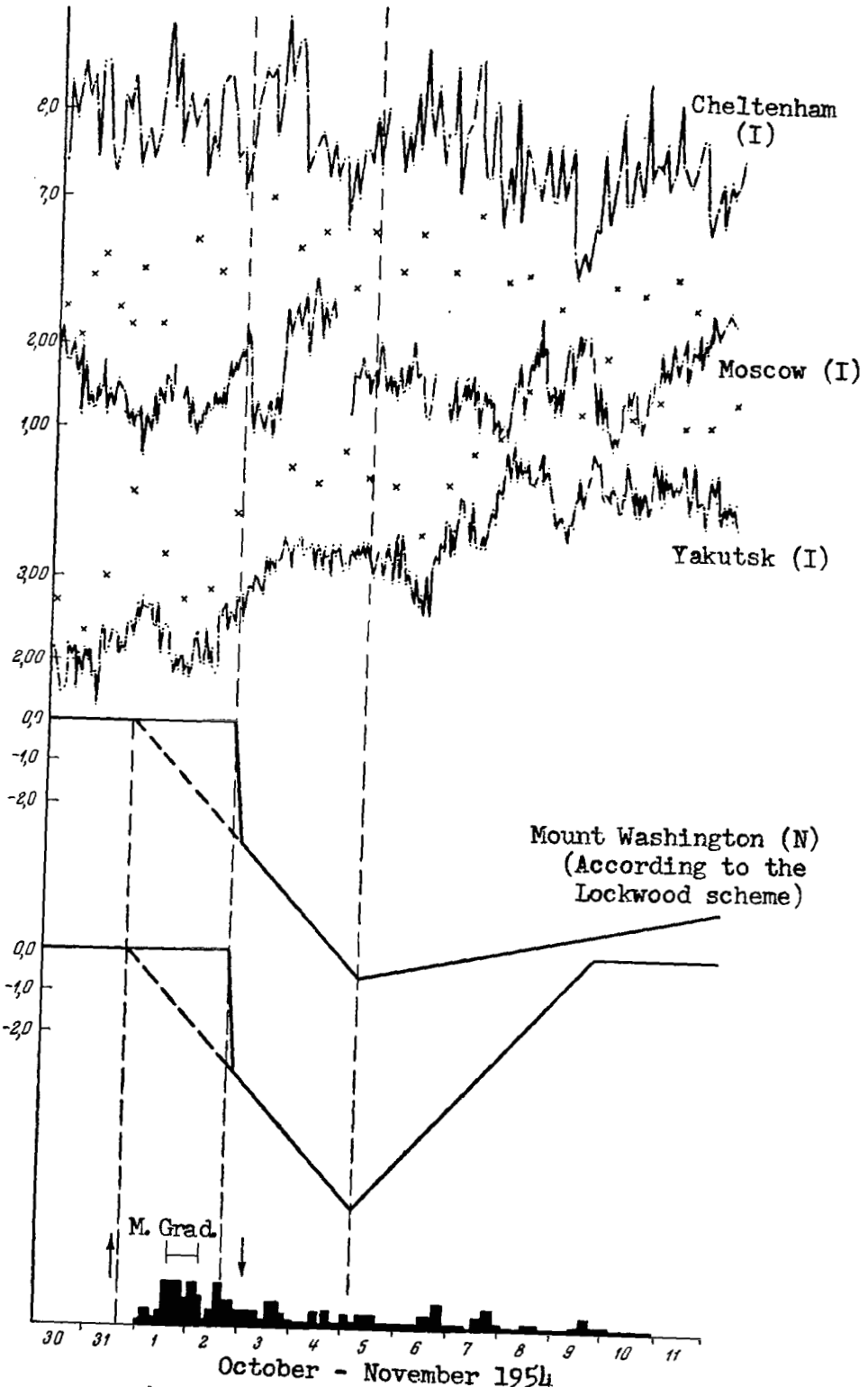
Cheltenham (I)
Moscow (I)
Yakutsk (I)
Mount Washington (N) (According to the Lockwood scheme)
M. Grad.
30 31 1 2 3 4 5 6 7 8 9 10 11
October - November 1954

Fig. 16. Storm in October-November 1954.

3.15. Storm in November 1956

Fig. 17 presents data on the variation of the cosmic ray intensity from 6 to 20 November at Mount Washington (N) [9], Yakutsk (I), and Moscow (I) stations. A moderate magnetic storm with a sudden beginning was noted on 9 November at 20 hrs 30 min. It continued until 04 hrs on 13 November. The decrease in the cosmic ray intensity began two to four hours after the beginning of the magnetic storm, although the active period occurred at 12 hrs on 10 November until 05 hrs on 11 November. The restoration of the intensity was interrupted on 15 November as a result of a new decrease, accompanying a large storm with a gradual beginning. Hence the time of restoration of intensity to the normal level was found by means of extrapolation.

The results of the calculations are the following. Since N = = 8.3%, I = 2.4%, then N/I = 3.5, ε_{min} = 85 bev, and f = 0.11. From the experimental data t_1 = 3.5 days, t_2 = 7 days, from which l_1 = = $1.2 \cdot 10^{13}$ cm, and $l_2 = 2.4 \cdot 10^{13}$ cm. Since N_{se} = 7.4% and t_{se} = 4 hrs, then S = $1.1 \cdot 10^{13}$ cm, and $u_r^* = 7.4 \cdot 10^8$ cm/sec. For the field intensity we find: $H_1 = 1.2 \cdot 10^{-5}$ gauss and $H_2 = 0.6 \cdot 10^{-5}$ gauss. And, finally, ρ_1 = 19 cm-3, ρ_2 = 5 cm-3, and ΔH_3^* = 110 γ. The active region apparently responsible for this storm intersected the central meridian from 6 to 13 November. If the storm was related to a class 3- flare, observed on 17 November at 12 hrs, then from the 56-hour lag we find $u_r = 0.75 \cdot 10^8$ cm/sec, and a degree of compression of about 10. Hence $H_\phi = 1.2 \cdot 10^{-4}$ gauss, ρ_ϕ = 190 cm-3, and ΔH_3 = 35 γ. In this case the width of the active region, equal to approximately 8 days, corresponds to a width of the stream equal to approximately 10-11 days.

4. INDIVIDUAL CASES OF MAGNETIC STORMS WITH TYPE I PROFILES OF THE DECREASE IN COSMIC RAY INTENSITY

4.1. Magnetic Storm in November 1955

Fig. 18 presents the data of a very great magnetic storm with a gradual beginning at 12 hrs on 18 November, and an end at 04 hrs, 21 November, according to the stations of Yakutsk (I), Mount Washington (N), Moscow (I), and Juancaio (I). The scheme of the profile was taken according to J. A. Lockwood [9]. The cosmic ray intensity began to drop abruptly approximately a day after the beginning of the magnetic storm at 16 hrs on 19 November. The sharp drop continued for t_{se} = 10 hrs. The restoration of the intensity continued for t_2 = 8 days.

From N = 5.5%, I = 2%, we find N/I = 2.75 and ε_{min} = 90 bev; f = 0.072. Since t_2 = 8 days, $l_2 = 2.7 \cdot 10^{13}$ cm, and $H_2 = 0.55 \cdot 10^{-5}$ gauss. Since t_{se} = 10 hrs, $u_r^* = 7.6 \cdot 10^8$ cm/sec, ρ_2 = 4 cm-3, ΔH_3^* = = 52 γ. The active region that caused this storm was situated on the Sun in the region of latitudes 10-30° N, longitudes 308-282°, and passed through the central meridian from 17.8-19.2 November. On account of the absence of complete data on the observations of solar

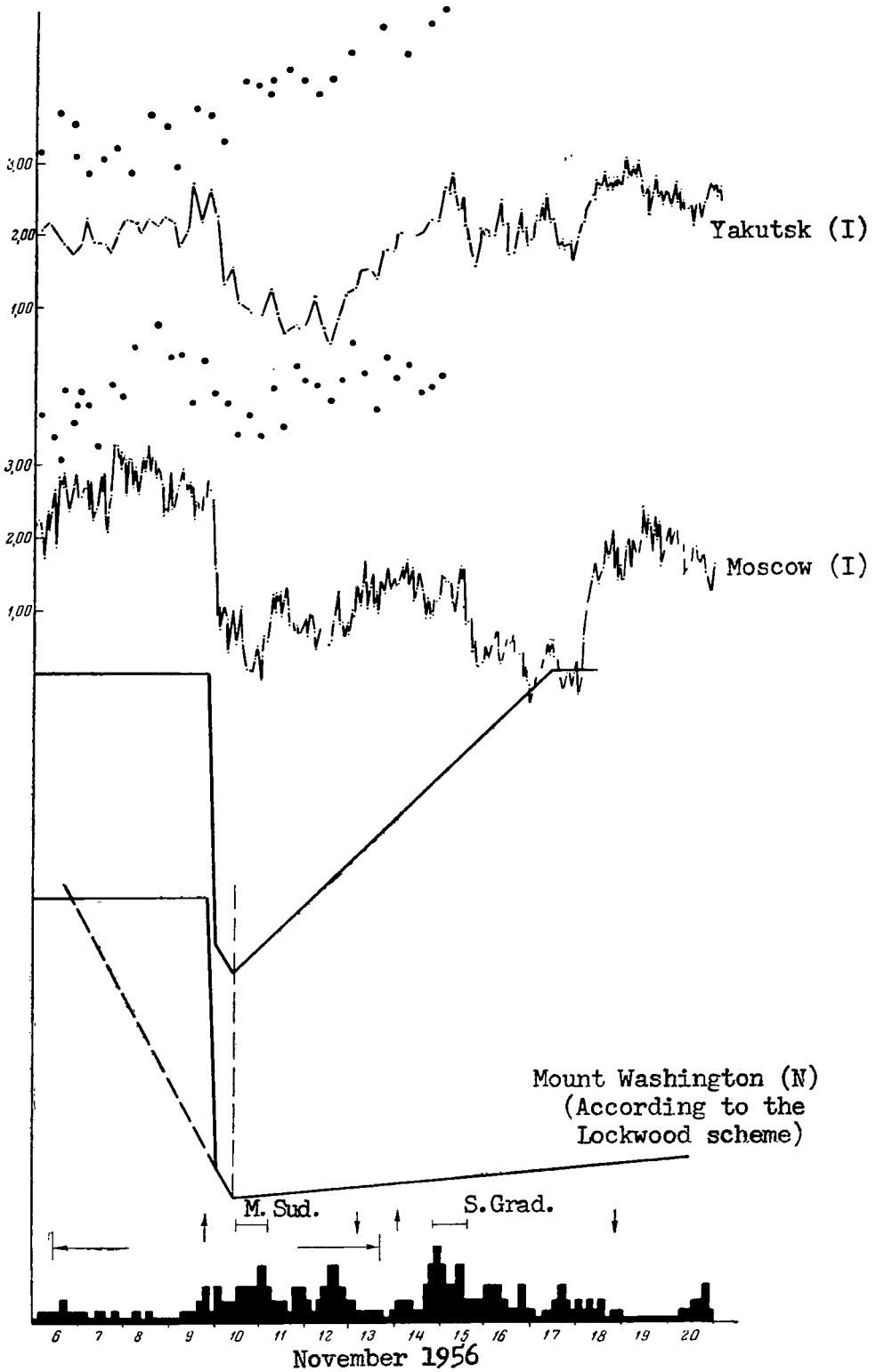

Fig. 17. Magnetic storm in November 1956.

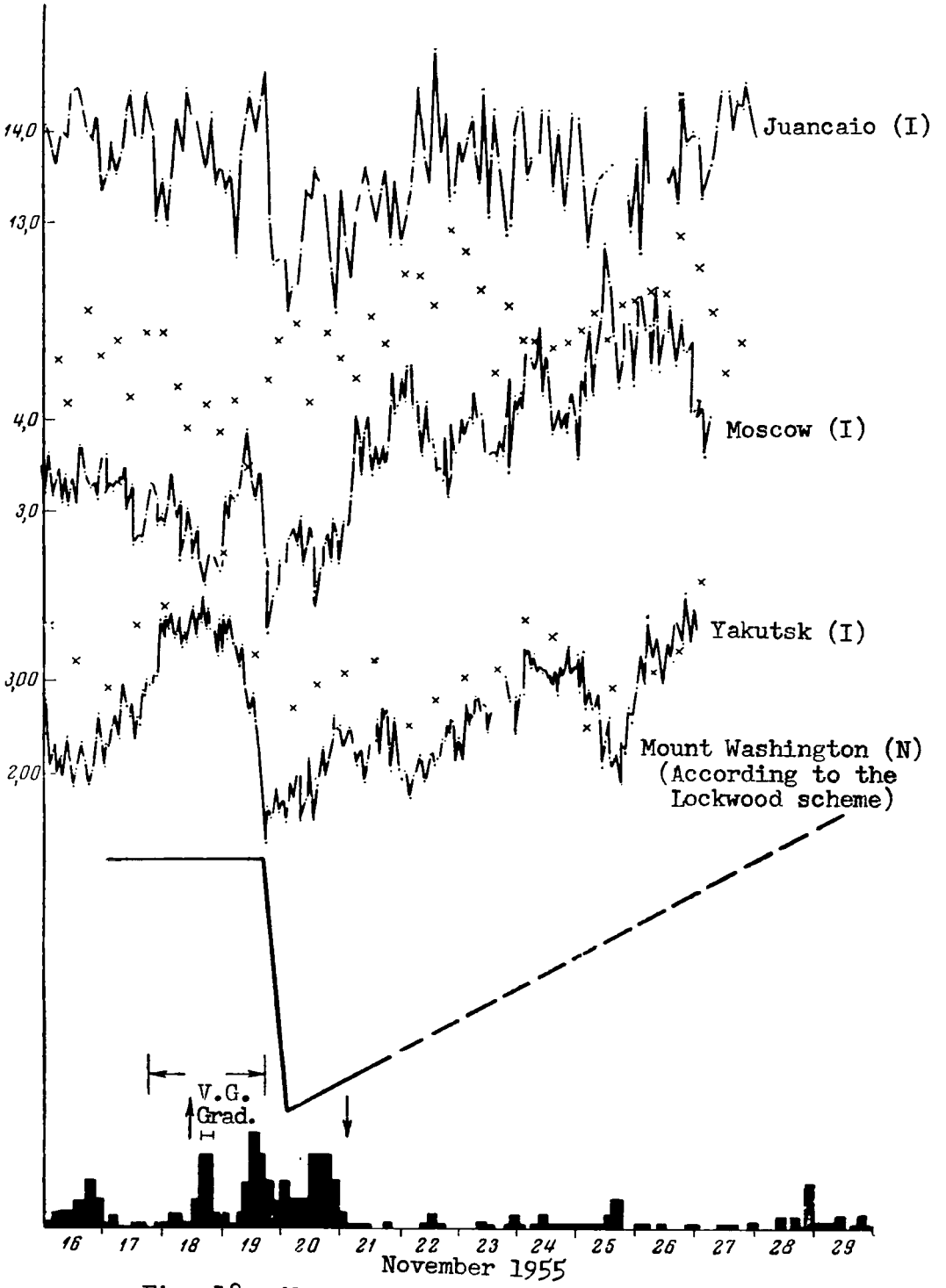

Fig. 18. Magnetic storm in November 1955.

flares, we can relate the observed phenomena only to a class 1 flare (23° N), noted on 16 November at 6 hrs. According to a lag of the order of two days, we find $u_r = 7 \cdot 10^7$ cm/sec, from which the degree of compression is approximately equal to 10 and $H_\phi = 5 \cdot 10^{-5}$ gauss, $\rho_\phi \approx 40$ cm^{-3}, and $\Delta H_3 = 17\,\gamma$. Here again there was a rather interesting case, when the unmagnetized portion of the corpuscular stream captured the Earth with its side edge and caused a storm with a gradual beginning. Not until approximately a day later did the magnetized portion of the stream approach the Earth, capturing it with its forward front, which caused an abrupt drop in the cosmic ray intensity. Nor is the possibility eliminated that the nonmagnetized portion of the stream had a diffuse forward front. In such cases capture of the Earth even by the forward front can cause a storm with a gradual beginning. Such a hypothesis seems more natural to us. In the opposite case, we should have expected that the stream would be sharply asymmetrical (that l_2 would be at least 10 times as great as l_1), while from a consideration of profiles of type II we have seen that l_2 is an average of twice as great as l_1. The active region with an angular width of approximately two days corresponds in our case to a stream with an angular half-width equal to approximately 10 days.

4.2. Storm in the Beginning of December 1955

Fig. 19 presents data for the first half of December at the stations of Mount Washington (N) [9] and Yakutsk (I). This case is extremely distinctive, since there was no magnetic storm during the decrease in cosmic ray intensity in the period from 6 to 15 December. A moderate magnetic storm with a gradual beginning occurred on 1 December from 13 to 23 hrs, i.e. took place approximately 5 days before the sharp drop in the cosmic rays. We believe that here the following phenomenon could have occurred. A broad corpuscular stream with an extremely low density captured the Earth with its side edge on 1 December and caused the storm with a gradual beginning noted above. As the Earth moved into the stream, the density of the kinetic energy of the plasma of the stream substantially decreased, and the intensity of the geomagnetic disturbances dropped (see the graph of K-indices in Fig. 9). Approximately five days later, a part of the stream with a frozen magnetic field arrived, causing the sharp decrease and gradual restoration characteristic of the type I profile.

From N = 5.4% and I = 2% we obtain N/I = 2.6, $\varepsilon_{min} = 117$ bev, f = 0.066. From $t_2 = 10$ days we find $l_2 = 3.4 \cdot 10^{13}$ cm and $H_2 = 0.6 \cdot 10^{-5}$ gauss, $\rho_3 = 4$ cm^{-3}, and from $t_{se} = 7$ hrs we find $u_r^* \approx 12 \cdot 10^8$ cm/sec, and $\Delta H_3^* \approx 90\,\gamma$. Since no active region was detected on the Sun, we are prevented from finding u_r, and therefore, the degree of compression around the forward magnetized portion of the stream as well.

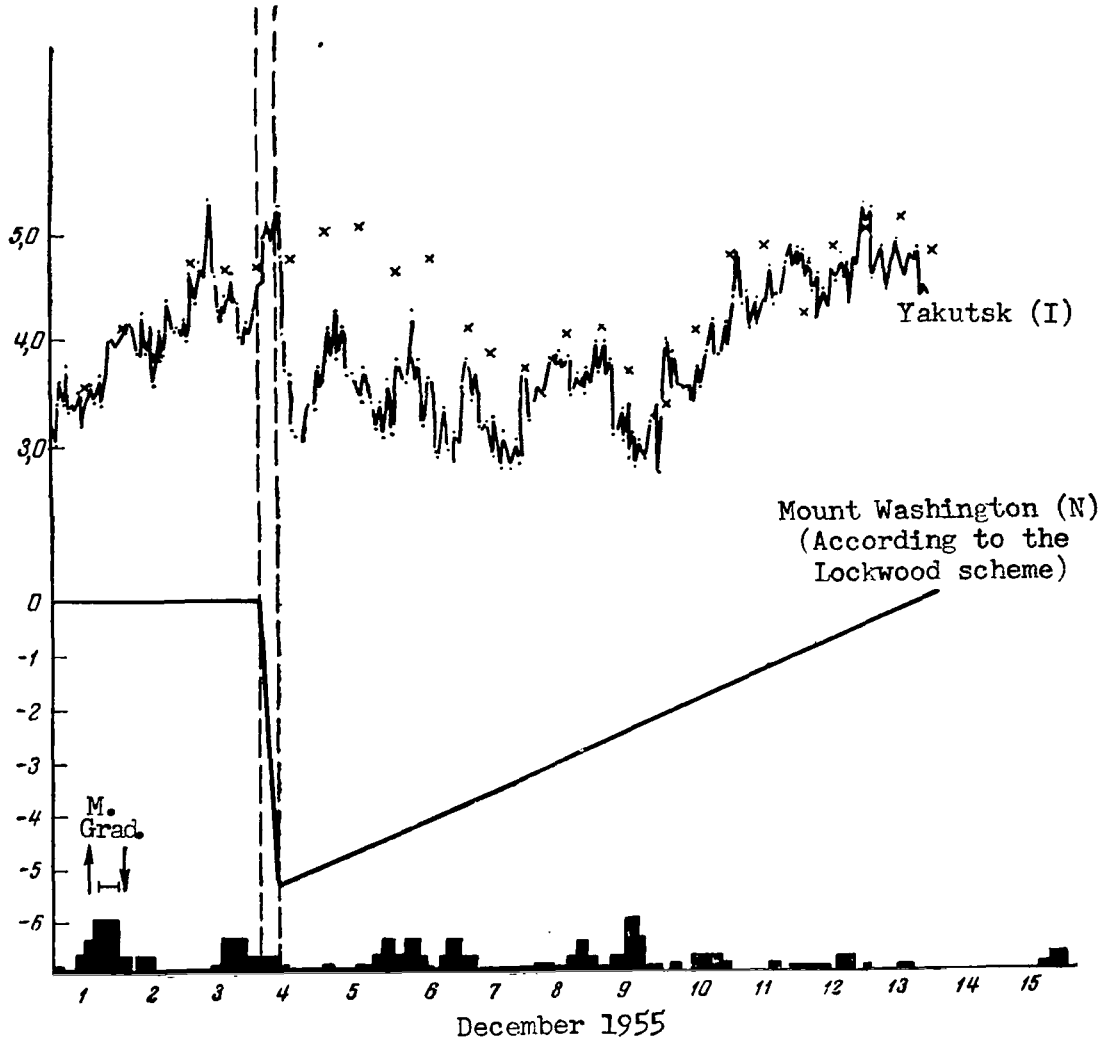

Fig. 19. Magnetic storm in December 1955.

4.3. Storm in the Beginning of March 1956

According to [14], a moderate magnetic storm with a sudden beginning at 23 hrs 41 min on 2 March lasted until 17 hrs on 4 March. The beginning of an abrupt decrease in the cosmic rays coincided with the beginning of the magnetic storm. Fig. 20 presents data from the Mount Washington (N) and Yakutsk (I) stations.

From N = 6.9%, I = 1.2%, we find N/I = 5.75, ε_{min} = 108 bev, f = 0.085; from t_2 = 5.5 days we obtain $l_2 = 1.9 \cdot 10^{13}$ cm, $H_2 = 10^{-5}$ gauss, and ρ_2 = 12 cm^{-3}; from t_{se} = 8 hours we determine $u_r^* = 6.5 \cdot 10^8$ cm/sec, from which $\Delta H_3^* = 78\gamma$. It seems to us that this storm could have been caused by an active region that passed through the central

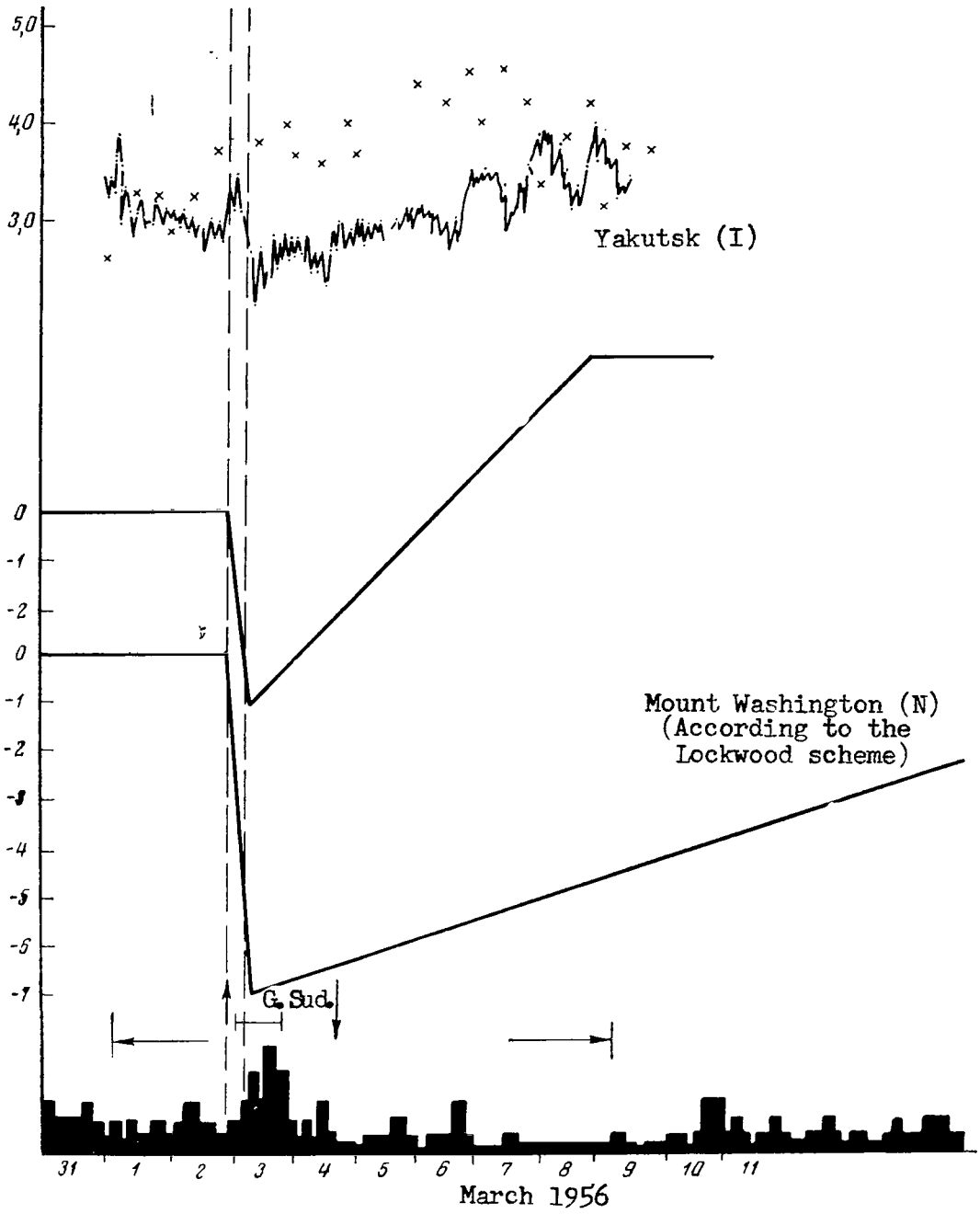

Fig. 20. Magnetic storm in the beginning of March 1956.

meridian from 1.1 to 9.2 March. According to the 1.8-day lag we find that $u_r \approx 8 \cdot 10^7$ cm/sec, and a degree of compression of the order of 8. Hence $H_\phi = 8 \cdot 10^{-5}$ gauss, $\rho_\phi \approx 100$ cm^{-3}, $\Delta H_3 \simeq 28\ \gamma$.

4.4. Magnetic Storm in March 1957

A large magnetic storm with a sudden beginning at 00 hrs 22 min on 10 March lasted until 01 hrs on 11 March and had an active period from 10 to 22 hrs, 10 March. Data on the cosmic ray intensity at the Moscow (I) and Mount Washington (N) [9] stations are presented in Fig. 21.

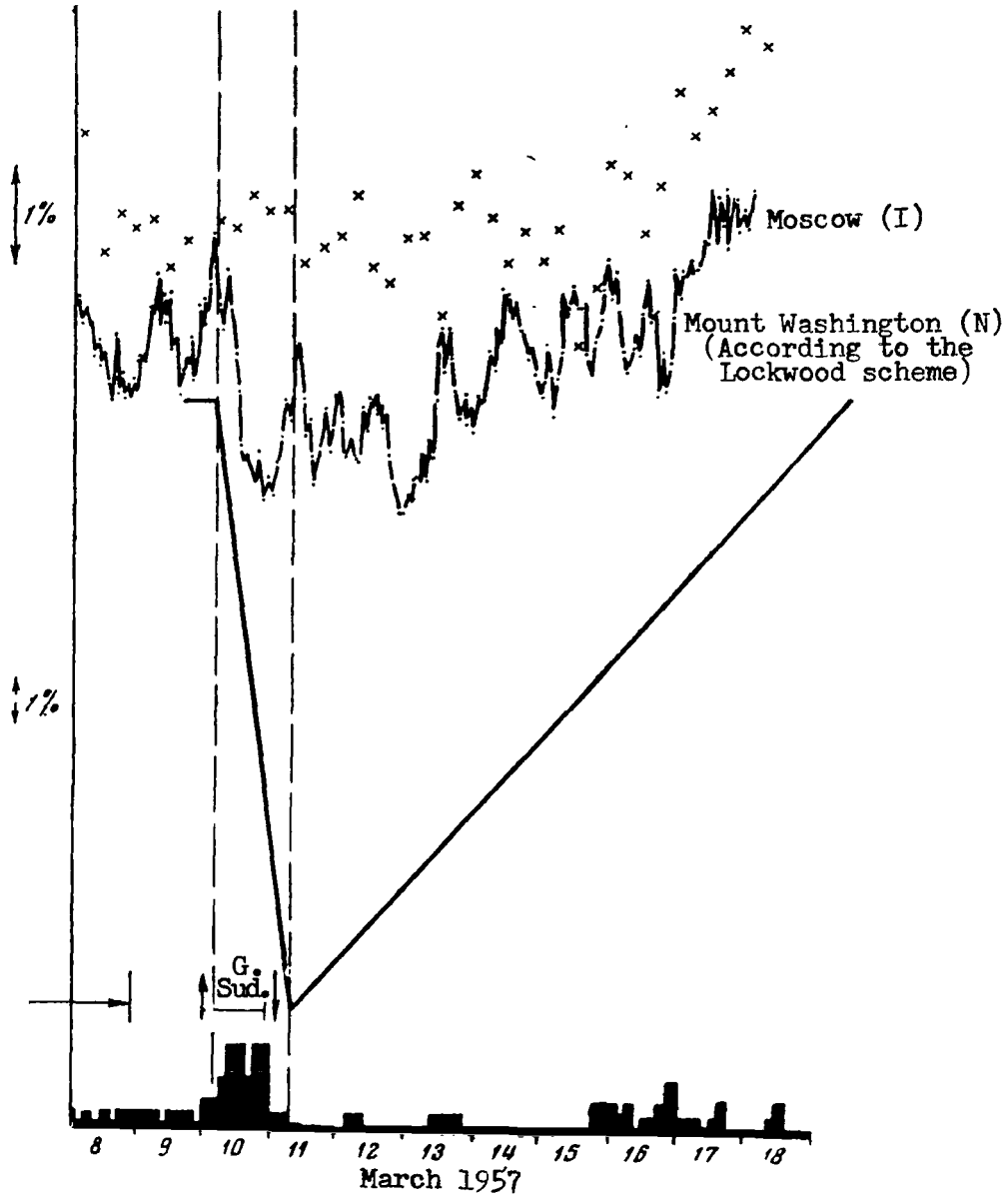

Fig. 21. Magnetic storm in March 1957.

From N = 11.5% and I = 2.2% we find N/I = 5.2 and ε_{min} = 60 bev; f = 0.175; from t_2 = 8.3 days we obtain $l_2 = 2.8 \cdot 10^{13}$ cm, from which $H_2 = 0.35 \cdot 10^{-5}$ gauss, ρ_2 = 1.7 cm^{-3}. Since t_{se} = 28 hrs, we determine $u_r^* = 2.8 \cdot 10^8$ cm/sec, from which $\Delta H_3^* = 12.4\gamma$. The active region that caused this storm could have been region No. 14 [14], which passed through the central meridian from 2.5 to 8.8 March, or No. 15, which passed through the central meridian from 10.6 to 15.8 March. If the stream was caused by the first region, then from the lag of about 5 days we find $u_r \approx 3 \cdot 10^7$ cm/sec and the degree of compression approximately 9. From this $H_\phi \approx 3 \cdot 10^{-5}$ gauss, ρ_ϕ = 15 cm^{-3} and $\Delta H_3 \approx 4\gamma$. If the storm was caused by the second region, then $u_r \approx u_r^* \approx 3 \cdot 10^8$ cm/sec, the degree of compression was approximately 1, and $H_\phi \approx$ $\approx 0.4 \cdot 10^{-5}$ gauss, $\rho_\phi \approx 2$ cm^{-3}, and $\Delta H_3 \approx 12\gamma$. Further investigation is needed for the identification of the region that caused the storm under consideration.

4.5. Magnetic Storm in August 1957

A moderate storm with a sudden beginning at 16 hrs on 3 August lasted until 04 hrs on 4 August. At 06 hrs on 5 August, a small storm with a sudden beginning was noted. According to the data on Fig. 22 (see inset opposite p. 40), we can see that the sharp drop in the intensity coincides with the beginning of the first magnetic storm.

From N = 9.3% and I = 2.6%, we find N/I = 3.6, ε_{min} = 82 bev, and f = 0.124. Since t_2 = 8 days, then $l_2 = 2.72 \cdot 10^{13}$ cm, H_2 = $= 0.5 \cdot 10^{-5}$ gauss, and ρ_2 = 3 cm^{-3}. From t_{se} = 35 hrs, we obtain u_r^* = $= 2.2 \cdot 10^8$ cm/sec and $\Delta H_3^* = 14\gamma$. If we relate this storm to the class 2+ flare (34° N, 7° W), then from the 58-hour lag we find u_r = $= 0.7 \cdot 10^8$ cm/sec, and the degree of compression about 3. From this $H_\phi = 1.5 \cdot 10^{-5}$ gauss, ρ_ϕ = 9 cm^{-3}, and $\Delta H_3 = 8\gamma$.

4.6. Magnetic Storm in the Middle of September 1957

A very great magnetic storm with a sudden beginning at 00 hrs 50 min on 13 September lasted until 15 hrs, 14 September, and had two active periods from 01 to 18 hrs on 13 September and from 09 to 15 hrs on 14 September. The data according to the stations at Juancaio (N), Resolute Bay (N), Mount Sulfur (N), Moscow (I), and Yakutsk (I) are presented in Fig. 23. The sharp drop began simultaneously with the sudden beginning of the magnetic storm, which corresponds to a capture of the Earth by the forward magnetized front of the stream.

From N = 3.9%, I = 1.3%, we find N/I = 3 and ε_{min} = 80 bev; f = 0.062; from t_2 = 4 days we obtain $l_2 = 1.36 \cdot 10^{13}$ cm, $H_2 = 10^{-5}$ gauss, ρ_2 = 13 cm^{-3}. From t_{se} = 6 hrs we determine $u_r^* = 6.3 \cdot 10^8$ cm/sec and $\Delta H_3^* = 77\gamma$. The active region that caused this storm passed through the central meridian from 9.5 to 12.4 September. According to the lag in the storm with respect to a solar class 3 flare (11 September from 3 to 5 hrs, coordinates 11° N, 3° W) of 45 hours,

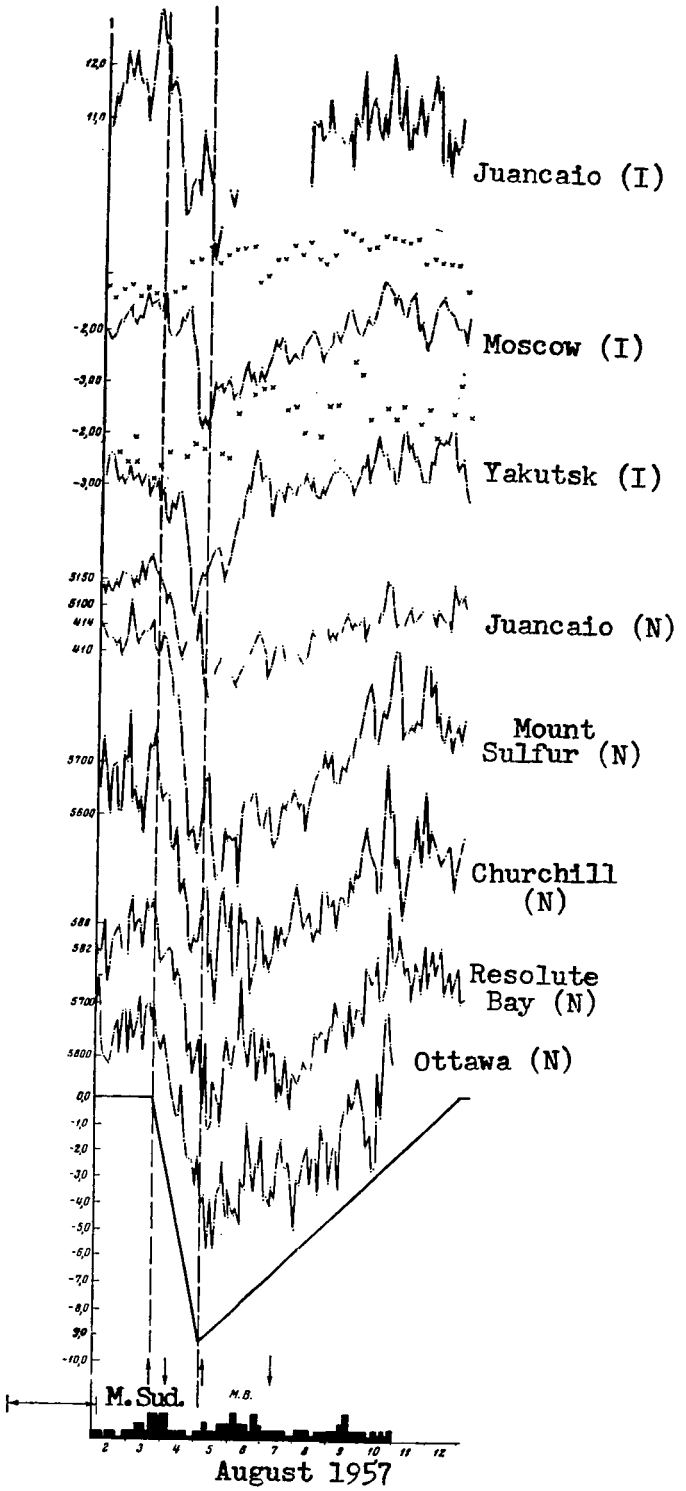

Fig. 22. Magnetic storm in August 1957.

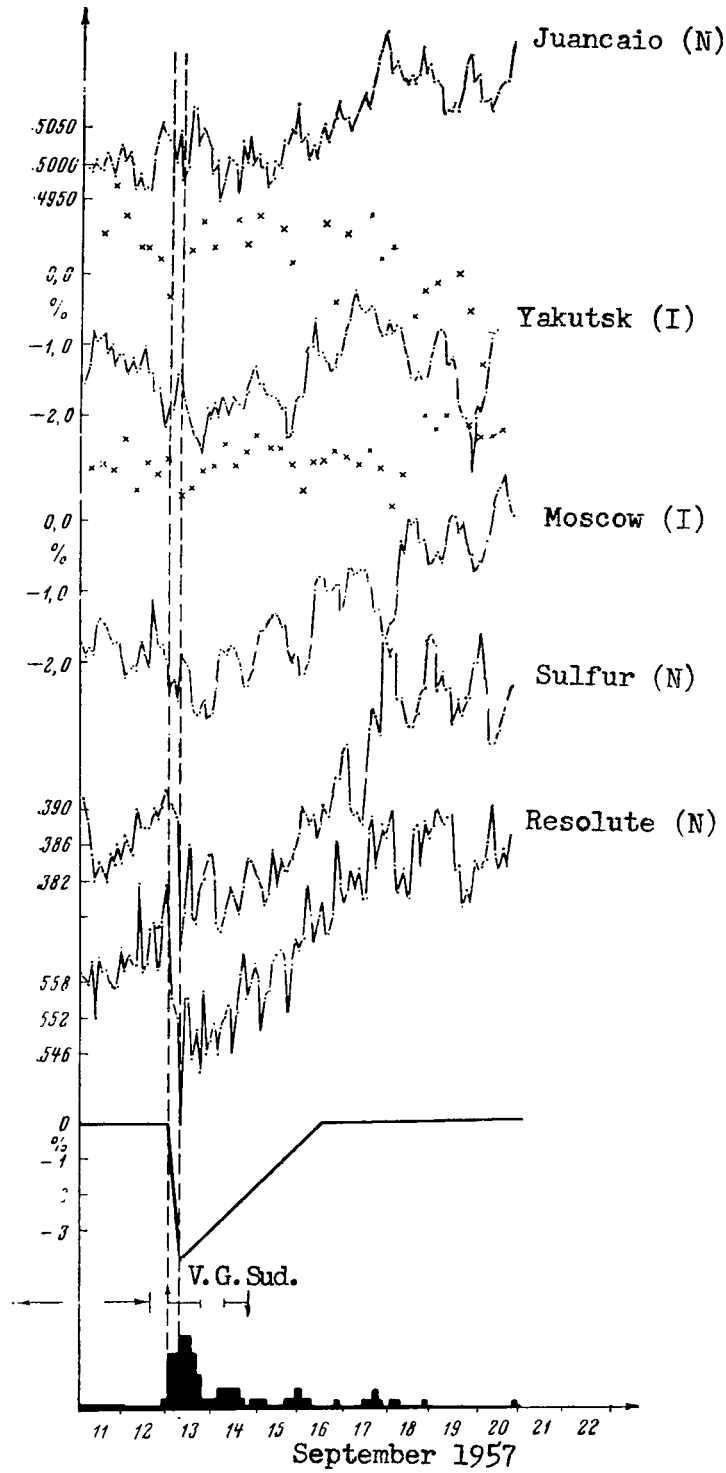

Fig. 23. Magnetic storm in the middle of September 1957.

we find $u_r \approx 9 \cdot 10^7$ cm/sec, from which the degree of compression is approximately 7, and $H_\phi \approx 0.7 \cdot 10^{-4}$ gauss, $\rho_\phi \approx 80$ cm^{-3}, and $\Delta H_3 \approx 30\gamma$. The width of the region of about 3 days corresponds to the half-width of the stream, of the same value.

4.7. Magnetic Storm at the End of September 1957

Experimental data for the period from 26 September to 5 October are presented in Fig. 24 for Ottawa (N), Churchill (N), Resolute Bay (N), Mount Sulfur (N), Yakutsk (I, N), Moscow (I), and Juancaio (N, I).

A very great magnetic storm with a sudden beginning at 00 hrs 15 min on 29 September lasted until 24 hrs, 30 September. The drop in the intensity began simultaneously with the sudden beginning of the magnetic storm, which indicates capture of the Earth by the forward magnetized front of the stream.

According to the data of Moscow and Yakutsk, N = 7.5%, I = 2.2%, and N/I = 3.4. Then $\mathcal{E}_{min} = 70$ bev and f = 0.127. Since $t_2 = 5$ days, $l_2 = 1.7 \cdot 10^{13}$ cm, $H_2 = 0.7 \cdot 10^{-5}$ gauss, and $\rho_2 = 7$ cm^{-3}. From $t_{se} = 20$ hrs we find $u_r^* = 2.4 \cdot 10^8$ cm/sec and $\Delta H_3^* = 21\gamma$. The active region that caused this storm passed through the central meridian from 26.4 to 29.5 September. The phenomena observed can apparently be related to a series of class 3 chromospheric flares, noted on 26 September at the end of the day. According to the lag of about 2 days, we find $u_r \approx 8 \cdot 10^7$ cm/sec, from which the degree of compression is approximately equal to 3, and $H_\phi \approx 2.1 \cdot 10^{-5}$ gauss, $\rho_\phi \approx 20$ cm^{-3}, and $\Delta H_3 \approx 12\ \gamma$. The width of the region, about 3 days, corresponds to a half-width of the stream of 5 days.

4.8. Magnetic Storm in February 1958

Fig. 25 presents experimental data for the period from 8 to 18 February at the stations of Mount Washington (N) [9], Ottawa (N), Resolute Bay (N), Moscow (I), Yakutsk (I), and Juancaio (N, I). A very great magnetic storm with a sudden beginning at 01 hrs 26 min on 11 February lasted until 24 hrs, 14 February, with an active period from 01 hrs 30 min to 14 hrs, on 14 February. The decrease in intensity coincided with the beginning of the magnetic storm; the restoration lasted for about 5 days.

From N = 6.5%, I = 1.8%, we obtain N/I = 3.6, $\mathcal{E}_{min} = 67$ bev, and f = 0.113. From $t_2 = 5$ days we find $l_2 = 1.7 \cdot 10^{13}$ cm, $H_2 = 0.66 \cdot 10^{-5}$ gauss, and $\rho_2 = 6$ cm^{-3}. Since $t_{se} = 4$ hrs, then $u_r^* = 1.2 \cdot 10^9$ cm/sec and $\Delta H_3^* = 98\gamma$.

The active region passed through the central meridian from 7.8 to 14.6 February. If the investigated magnetic field was related to the appearance of a class 2$^+$ chromospheric flare (11° S, 7° W) on 9 February at 22 hrs, then according to the lag of about 28 hrs we find that $u_r = 1.5 \cdot 10^8$ cm/sec, and the degree of compression is about 8.

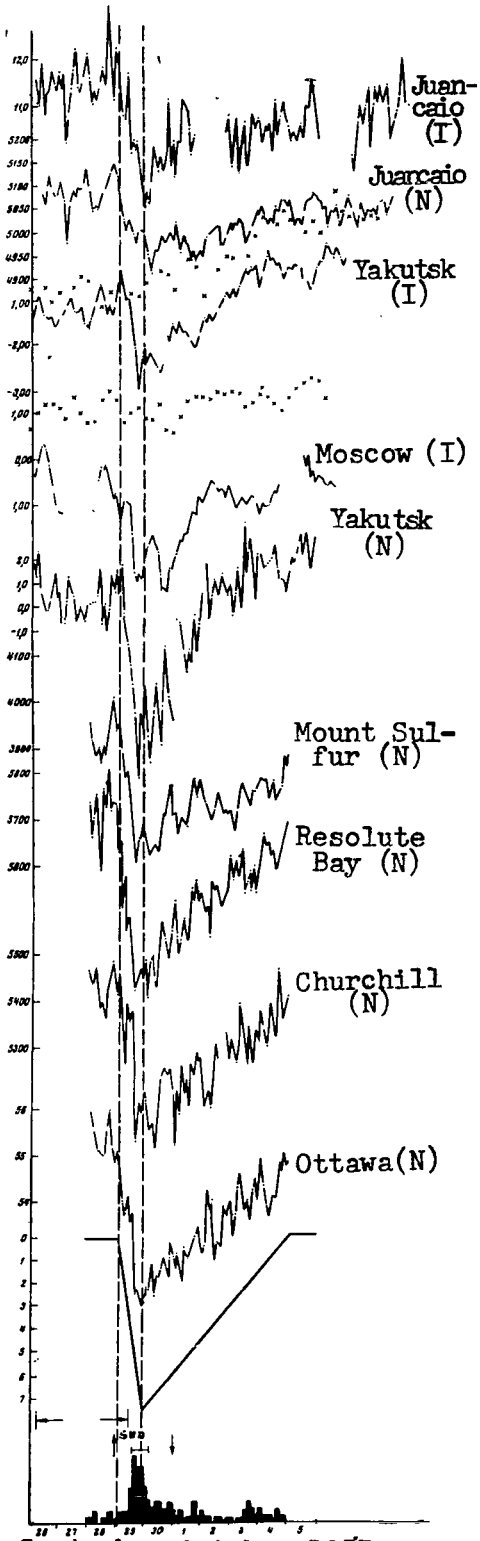

September-October 1957

Fig.24.Magnetic storm at the end of September 1957.

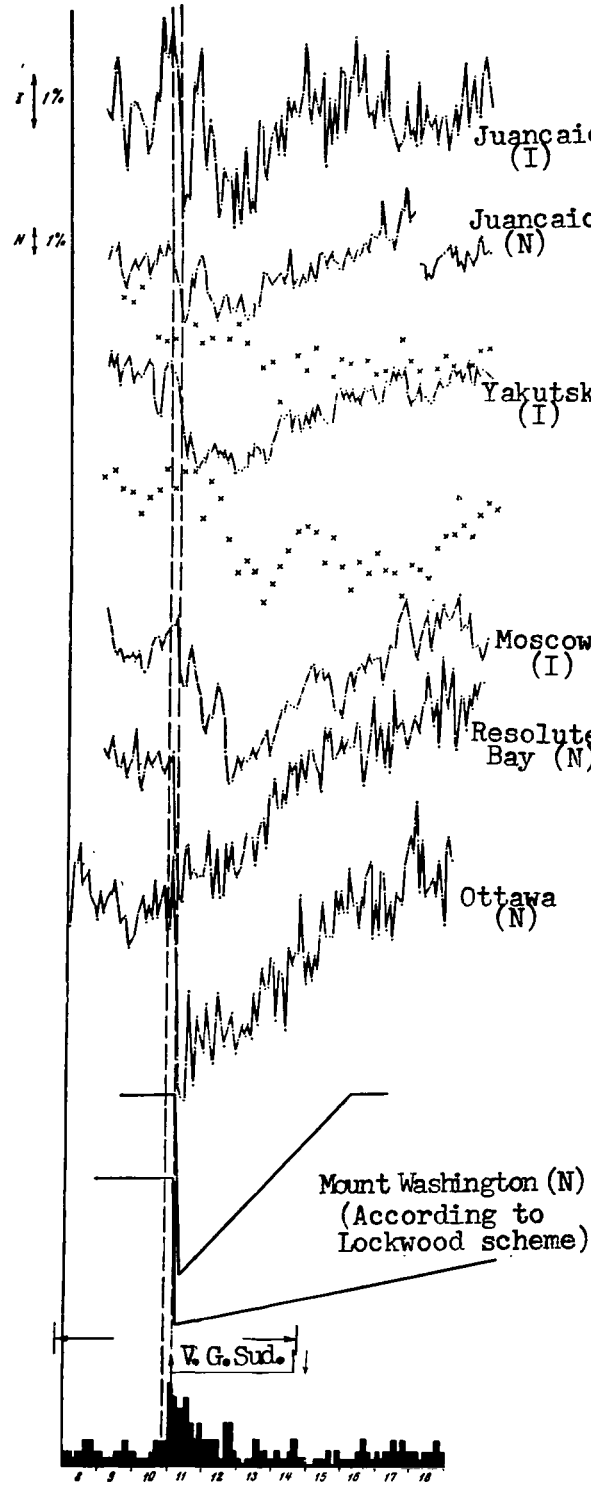

February 1958

Fig. 25. Magnetic storm in February 1958

From this $H_\phi = 5.3 \cdot 10^{-5}$ gauss, $\rho_\phi = 48$ cm^{-3}, and $\Delta H_3 = 35\gamma$. The width of the region, about 7 days, corresponds to a half-width of the stream of about 5 days.

4.9. Magnetic Storm at the End of October 1958

Experimental data for the period from 21 to 31 October at the stations of Moscow (N, I) and Irkutsk (N) are presented in Fig. 26. During this period two magnetic storms occurred. The first magnetic storm was a large one, with a sudden beginning at 03 hrs 15 min on 22 October, and ended at 09 hrs on 25 October. It had three active periods: 1) from 16 to 24 hrs, 22 October; 2) from 14 to 20 hrs, 23 October; 3) from 08 to 24 hrs, 24 October.

The second magnetic storm, moderate with a gradual beginning at 15 hrs on 27 October, ended at 17 hrs on 31 October. It had two active periods: 1) from 17 to 24 hrs, 27 October; 2) from 7 to 19 hrs, 28 October.

The sharp drop in the cosmic ray intensity coincided with the first active period of the large magnetic storm with sudden beginning at the end of the day of 22 October. We believe that the moderate storm with a gradual beginning was caused by the same stream (in our opinion, the latter storm is a continuation of the preceding one -- the large one with the sudden beginning; thus, they both represent essentially one storm).

According to N = 6% and I = 2%, we find N/I = 3 and $\varepsilon_{min} = 80$ bev, f = 0.09; from $t_2 = 5.5$ days we determine $l_2 = 1.9 \cdot 10^{13}$ cm, $H_2 = 0.7 \cdot 10^{-5}$ gauss, and $\rho_\infty = 7$ cm^{-3}. From $t_{se} = 10$ hrs we obtain $u_r^* = 5 \cdot 10^8$ cm/sec and $\Delta H_3^* = 47\gamma$. The active region that caused this storm passed through the central meridian from 19.0 to 26.7 October. According to the lag of about 3 days with respect to the three class 3 flares observed on 19 October at 7 hrs, we find $u_r \approx 5 \cdot 10^7$ cm/sec, from which the degree of compression is equal to approximately 10, and $H_\phi \approx 7 \cdot 10^{-5}$ gauss, $\rho_\phi \approx 70$ cm^{-3}, and $\Delta H_3 \approx 14\gamma$.

4.10. Magnetic Storm at the End of November 1958

Experimental data from 18 to 30 November at the stations of Moscow (I) and Yakutsk (N) are presented in Fig. 27.

A magnetic storm with a gradual beginning at 12 hrs on 25 November ended at 04 hrs on 26 November. At the moment when the magnetic storm ended, the cosmic ray intensity dropped sharply, and then began to be slowly restored up to 1 December 1958.

We interpret this phenomenon in the following way. The unmagnetized portion of the stream captured the Earth with its side edge and caused a small magnetic storm with a gradual beginning. This indicates that even at the forward edge of the stream, the density of the kinetic energy was low. Then the forward front of the magnetized portion of the stream captured the Earth and caused an abrupt decrease in

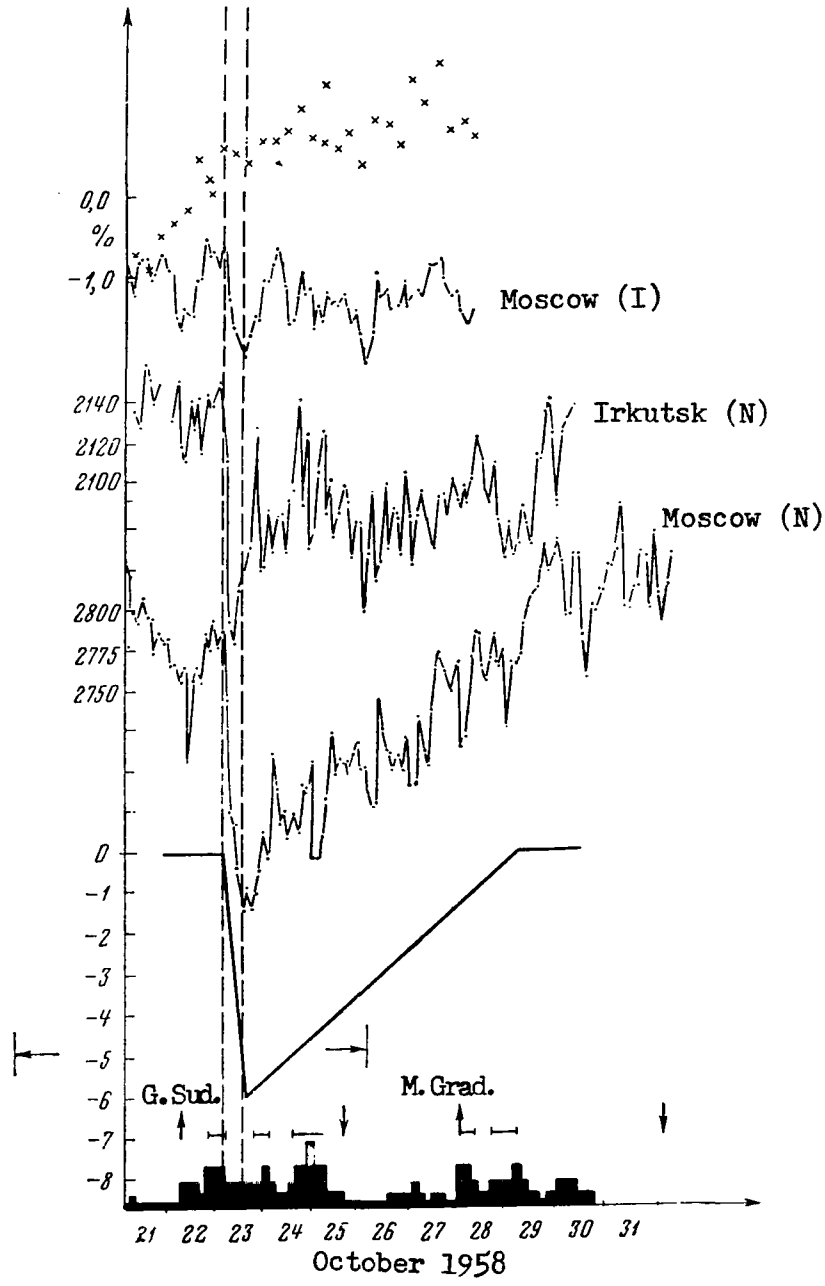

Fig. 26. Magnetic storm at the end of October 1958.

the cosmic ray intensity, followed by a gradual restoration. However, the plasma density of the magnetized portion of the stream was apparently still less than that in the unmagnetized portion. Thus, the weak magnetic disturbances observed (see the graph of the K-index in Fig. 27) could not be classified even as small magnetic storms.

From N = 5%, I = 0.5%, we find N/I = 10 and ε_{min} = 30 bev,

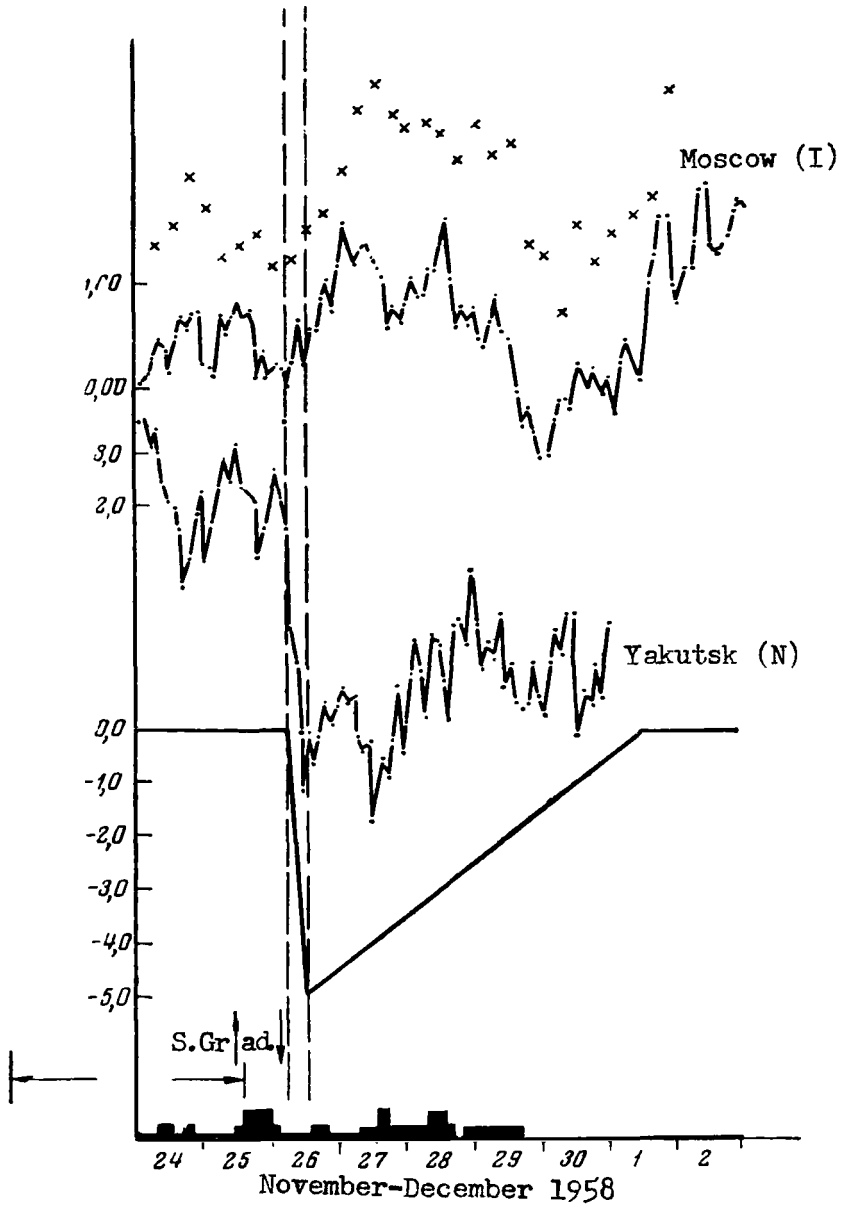

Fig. 27. Magnetic storm at the end of November 1958.

f = 0.16; from t_2 = 5 days we obtain $l_2 = 1.7 \cdot 10^{13}$ cm and H_2 = $= 0.3 \cdot 10^{-5}$ gauss, ρ_2 = 1 cm^{-3}. From t_{se} = 9 hrs we determine u_r^* = $= 5.2 \cdot 10^8$ cm/sec and $\Delta H_3^* \approx 19.3\,\gamma$. This storm can apparently be related to two class 3 flares observed on 17 November at 17 hrs (20° N, 10° E). According to the lag of about 35 hours, we find $u_r = 1.1 \cdot 10^8$ cm/sec and a degree of compression of about 5. From this H_Φ = $= 1.5 \cdot 10^{-5}$ gauss, ρ_Φ = 5 cm^{-3}, and $\Delta H_3 \approx 9\,\gamma$.

4.11. Magnetic Storm in March 1959

A very great magnetic storm (Fig. 28) with a sudden beginning at 06 hrs 42 min on 26 March was accompanied by a sharp decrease in the cosmic ray intensity. The first active period of the storm coincided with its beginning. The second that soon followed was accompanied by a new decrease in the intensity. Still another peculiarity of this example is the fact that a gradual decrease began more than a day before the magnetic storm. The restoration of the intensity lasted for approximately 5 days and ended when the storm ceased.

The insufficiency of experimental data did not allow us to perform a sufficiently detailed analysis of this case, but nevertheless, according to the material available to us, the following picture can be represented. On 25 March a stream carrying a magnetic field captured the Earth with its side edge, which caused a gradual decrease in the intensity with a type III profile. While found within the stream, on 26 March the Earth encountered the forward front of large-scale regions carrying stronger magnetic fields (active periods of the magnetic storm). After this followed a sharp decrease in the intensity with a type I profile. These large-scale formations could be related to the class 3 chromospheric flares observed on 24 March at 11 hrs (28° N, 75° W). According to the lag of about 45 hours, we find $u_r = 0.9 \cdot 10^8$ cm/sec. Let us turn to an evaluation of the parameters of the stream.

From N = 7% and I = 2.8% we find N/I = 2.5, $\mathcal{E}_{min}$ = 98 bev, and f = 0.102. Since t_2 = 5 days, then $l_2 = 1.7 \cdot 10^{13}$ cm, $H_2 = 10^{-5}$ gauss, and ρ_2 = 13 cm^{-3}. According to the total length of the sharp decrease in intensity $t_{se} \lesssim 12$ hrs, we find $u_r^* \gtrsim 4 \cdot 10^8$ cm/sec and $\Delta H_3^* \gtrsim 50\gamma$. According to the ratio of u_r^*/u_r we find the degree of compression to be about 5. From this $H_\Phi = 5 \cdot 10^{-5}$ gauss, ρ_Φ = 65 cm^{-3}, and $\Delta H_3 = 22\gamma$.

5. EFFECTS OF THE TYPE III DECREASE IN THE COSMIC RAY INTENSITY

5.1. Magnetic Storm in March 1955

Fig. 29 presents experimental data for the stations at Yakutsk (I), Moscow (I), Juancaio (I), and the scheme of J. A. Lockwood [9] for Mount Washington Station (N) for 12 days of March.

The change in the cosmic ray intensity was accompanied by a moderate magnetic storm with a gradual beginning at 09 hrs on 22 March, ending at 24 hrs on 23 March. Its active period was noted from 12 to 17 hrs on 22 March.

From N = 7%, I = 2% we find N/I = 3.5% and $\mathcal{E}_{min}$ = 84 bev, f = = 0.093; since t_1 = 1.2 days, t_2 = 6.6 days, we find $l_1 = 0.41 \cdot 10^{13}$ cm, $l_2 = 2.24 \cdot 10^{13}$ cm, from which $H_1 = 3.4 \cdot 10^{-5}$ gauss, $H_2 = 0.6 \cdot 10^{-5}$ gauss, ρ_1 = 153 cm^{-3}, ρ_2 = 5 cm^{-3}.

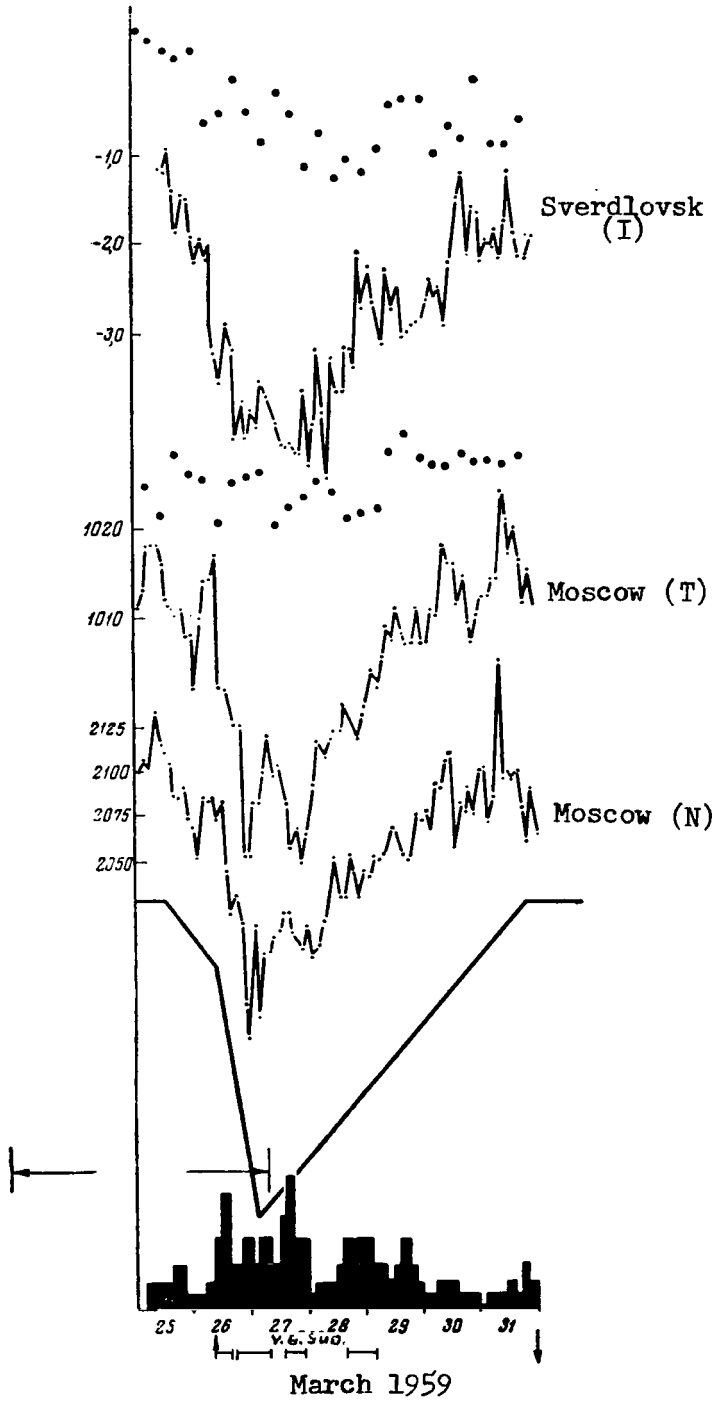

Fig. 28. Magnetic storm in March 1959.

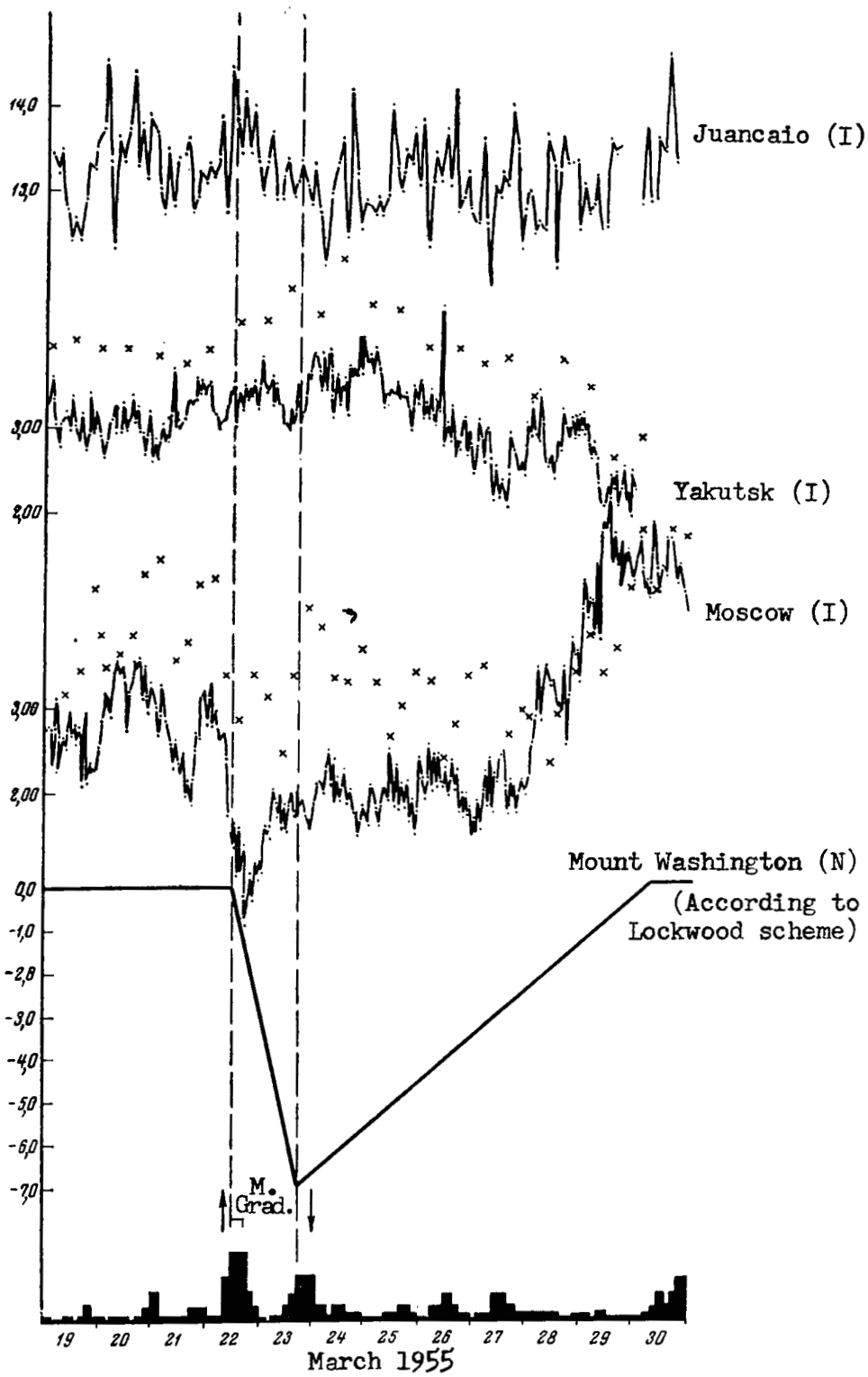

Fig. 29. Magnetic storm at the end of March 1955.

5.2. Magnetic Storm at the End of April 1956

Experimental data for the end of April 1956 at Yakutsk Station (I) and the scheme of J. A. Lockwood [9] for Mount Washington Station (N) are presented in Fig. 30. A large magnetic storm with a gradual beginning at 08 hrs 26 April, continuing until 11 hrs on 28 April, had an active period from 21 hrs 26 April to 05 hrs 28 April. This storm caused the characteristic change in the cosmic ray intensity with a type III profile.

The beginning of the decrease in intensity coincided with the beginning of the active period.

From N = 7.7%, I = 1.5% we find N/I = 5.1 and ε_{min} = 62 bev, f = 0.115. Since t_1 = 1.25 days and t_2 = 4.4 days, we determine l_1 = $= 0.42 \cdot 10^{13}$ cm, $l_2 = 1.5 \cdot 10^{13}$ cm, $H_1 = 2.4 \cdot 10^{-5}$ gauss, and H_2 = $= 0.7 \cdot 10^{-5}$ gauss, from which ρ_1 = 78 cm^{-3} and ρ_2 = 6.4 cm^{-3}. The active region on the Sun that caused the magnetic storm intersected the central meridian from 20.3 to 23.9 April. The width of the stream, 4.6 days, corresponds to a width of the active region of 3.6 days.

5.3. Magnetic Storm in the Middle of October 1957

A small magnetic storm with a gradual beginning at 20 hrs on 13 October ended at 01 hrs, 15 October. It caused the characteristic change in the cosmic ray intensity, with a type III profile.

Since the beginning of the decrease coincided with the beginning of the magnetic storm, we classify this case as capture of the Earth by the side edge of the magnetized corpuscular stream.

Experimental data from Yakutsk (N, I), Resolute Bay (N), and Mount Sulfur (N) stations are cited in Fig. 31.

From N = 2%, I = 0.8%, we find N/I = 2.5 and ε_{min} = 115 bev, f = 0.024. From t_1 = 1.16 days, t_2 = 1.60 days, we determine l_1 = $= 0.50 \cdot 10^{13}$ cm, $t_2 = 0.55 \cdot 10^{13}$ cm, and $H_1 = 3.9 \cdot 10^{-5}$ gauss, H_2 = $= 3.5 \cdot 10^{-5}$ gauss. From this ρ_1 = 204 cm^{-3}, ρ_2 = 163 cm^{-3}.

5.4. Magnetic Storm in December 1957

Fig. 32 presents experimental data characterizing the effect on cosmic rays during the magnetic storm of 19 December 1957. A small magnetic storm with a sudden beginning at 09 hrs 35 min on 19 December lasted until 09 hrs 21 December. Apparently there is an effect related to this storm on the cosmic rays. However, the gradual drop in intensity that began on 17 December is probably related to the small magnetic storm with a gradual beginning noted on 15 December. The cosmic ray intensity reached a minimum on 22 December and was restored on 29 December.

From N = 8% and I = 2.5% we find N/I = 3.2, ε_{min} = 74 bev, and f = 0.132. Since t_1 = 4.5 days and t_2 = 6.7 days, $l_1 = 1.53 \cdot 10^{13}$ cm, $l_2 = 2.28 \cdot 10^{13}$ cm, from which $H_1 = 0.8 \cdot 10^{-5}$ gauss and $H_2 = 0.5 \cdot 10^{-5}$

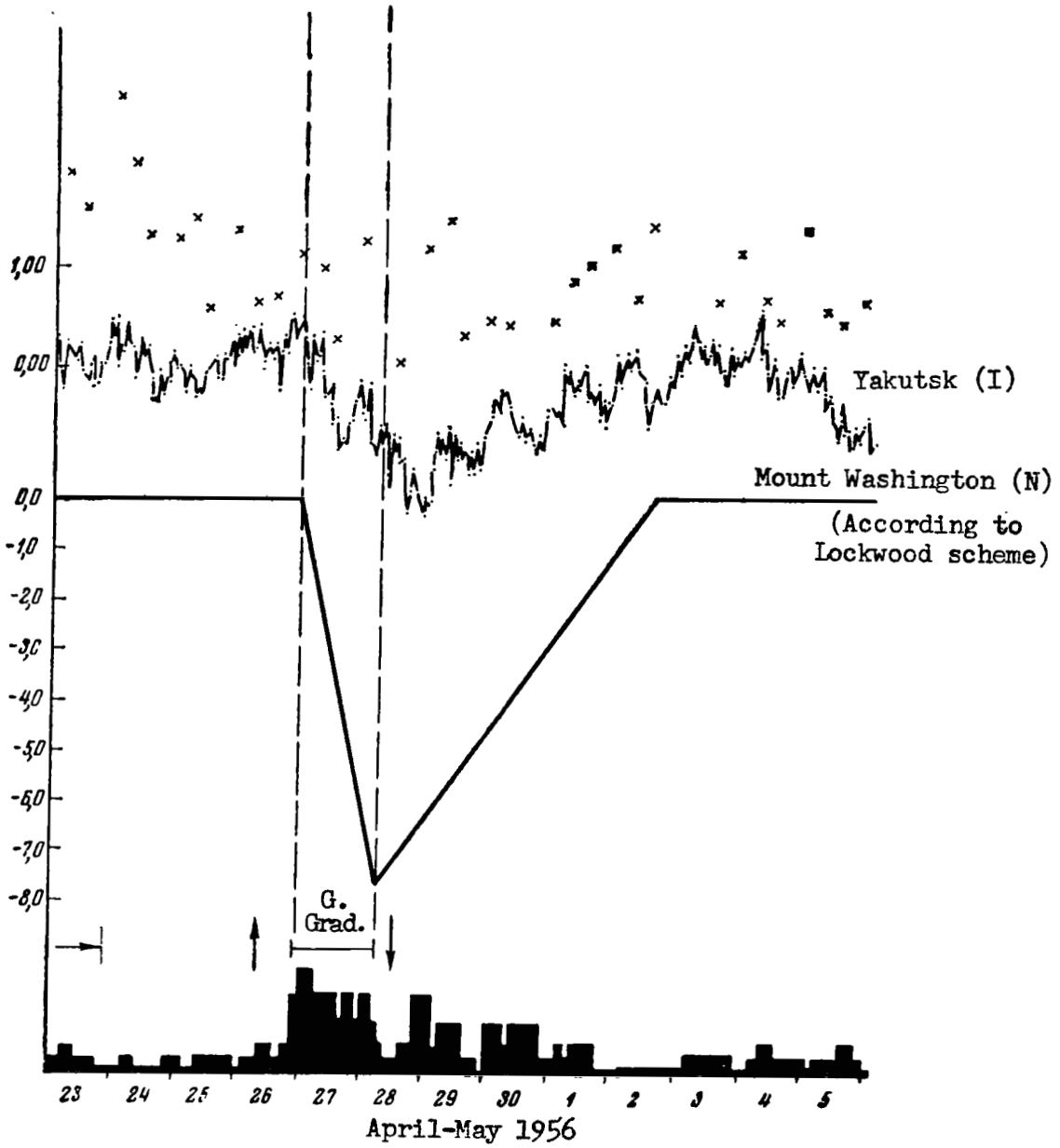

Fig. 30. Magnetic storm at the end of April 1956.

gauss, and $\rho_1 = 8$ cm^{-3}, $\rho_2 = 3$ cm^{-3}. The width of the stream $l = 3.8 \cdot 10^{13}$ cm and $l_1/l_2 = 0.67$.

5.5. Magnetic Storm in the End of May 1958

Fig. 33 presents experimental data for the period from 27 May

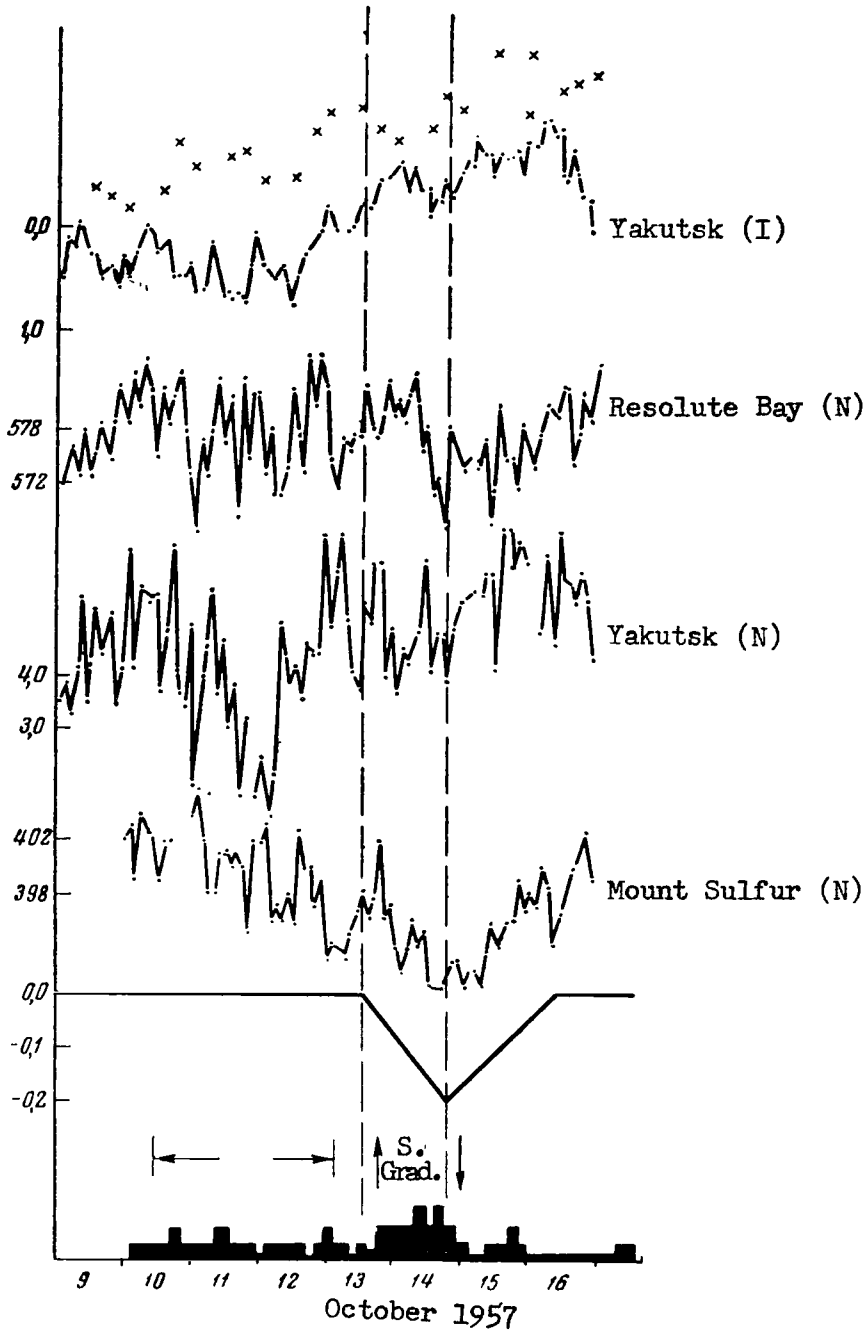

Fig. 31. Magnetic storm in the middle of October 1957.

to 4 June at the stations at Ottawa (N, T), Resolute Bay (N, T), Churchill (N, T), Irkutsk (N), Moscow (N, I), Yakutsk (I), and Tiksi Bay (I).

A moderate magnetic storm with a gradual beginning started at 01 hrs on 26 May, ending at 05 hrs, 30 May. The drop in intensity began on 29 May, and then a gradual restoration occurred until 4 June. From N = 6.5% and I = 2%, we find that N/I = 3.25, ε_{min} = 72 bev, and f = 0.109. Since t_1 = 2 days and t_2 = 3.3 days, $l_1 = 0.68 \cdot 10^{13}$ cm, $l_2 = 1.12 \cdot 10^{13}$ cm, $l = 1.8 \cdot 10^{13}$ cm, from which $H_1 = 1.75 \cdot 10^{-5}$ gauss, $H_2 = 1.06 \cdot 10^{-5}$ gauss, ρ_1 = 41 cm^{-3}, and ρ_2 = 15 cm^{-3}. The ratio l_1/l_2 = 0.6. The active region passed through the central meridian from 18.3 to 23.3 May. The width of the stream found, 5.3 days, corresponds to an angular width of the active region of 5.0 days.

5.6. Magnetic Storm in the Beginning of June 1958

Fig. 34 presents experimental data for the period from 5 to 17 June at the stations of Moscow (N, I), Yakutsk (I), and Resolute Bay (N, I). This period was accompanied by three magnetic storms.

A large magnetic storm with a gradual beginning started at 21 hrs, 6 June, ending at 20 hrs on 7 June. A moderate storm with a gradual beginning at 11 hrs on 9 June ended at 23 hrs on 11 June. And, finally, a moderate storm with a sudden beginning at 18 hrs 20 min on 14 June ended at 18 hrs on 15 June.

The cosmic ray intensity began to drop at the beginning of the day of 6 June, reached a minimum on 9 June, and then was slowly restored by 17 June.

From N = 6%, I = 0.8%, we find N/I = 7.5 and ε_{min} = 38 bev, f = 0.158; from t_1 = 3 days, t_2 = 9 days, we find $l_1 = 1 \cdot 10^{13}$ cm, $l_2 = 3 \cdot 10^{13}$ cm, from which $H_1 = 0.6 \cdot 10^{-5}$ gauss, $H_2 = 0.2 \cdot 10^{-5}$ gauss, and ρ_1 = 5.1 cm^{-3}, ρ_2 = 0.7 cm^{-3}. The ratio $l_1/l_2 = 1/3$. The active region on the Sun passed through the central meridian from 2.2 to 7.5 June. The width of the stream found, 12 days, corresponds to a width of the region of 5.3 days.

5.7. Magnetic Storm in the Middle of September 1958

A moderate magnetic storm with a gradual beginning at 05 hrs, 16 September, lasted until 07 hrs, 17 September. The active period lasted from 16 to 22 hrs, 16 September. We can see from the graphs of Fig. 35 that the decrease in the intensity began simultaneously or even somewhat before the start of disturbances in the magnetic field. The Figure presents the experimental data.

From N = 7% and I = 2.5%, we find N/I = 2.8, ε_{min} = 88 bev, and f = 0.107. Since t_1 = 2.5 days, t_2 = 8 days, then $l_1 = 0.85 \cdot 10^{13}$ cm, $l_2 = 2.72 \cdot 10^{13}$ cm, from which $H_1 = 1.7 \cdot 10^{-5}$ gauss, $H_2 = 0.5 \cdot 10^{-5}$ gauss, and ρ_1 = 39 cm^{-3}, ρ_2 = 4 cm^{-3}. The ratio l_1/l_2 = 0.31.

5.8. Magnetic Storm in the Beginning of December 1958

A moderate magnetic storm with a gradual beginning at 09 hrs on

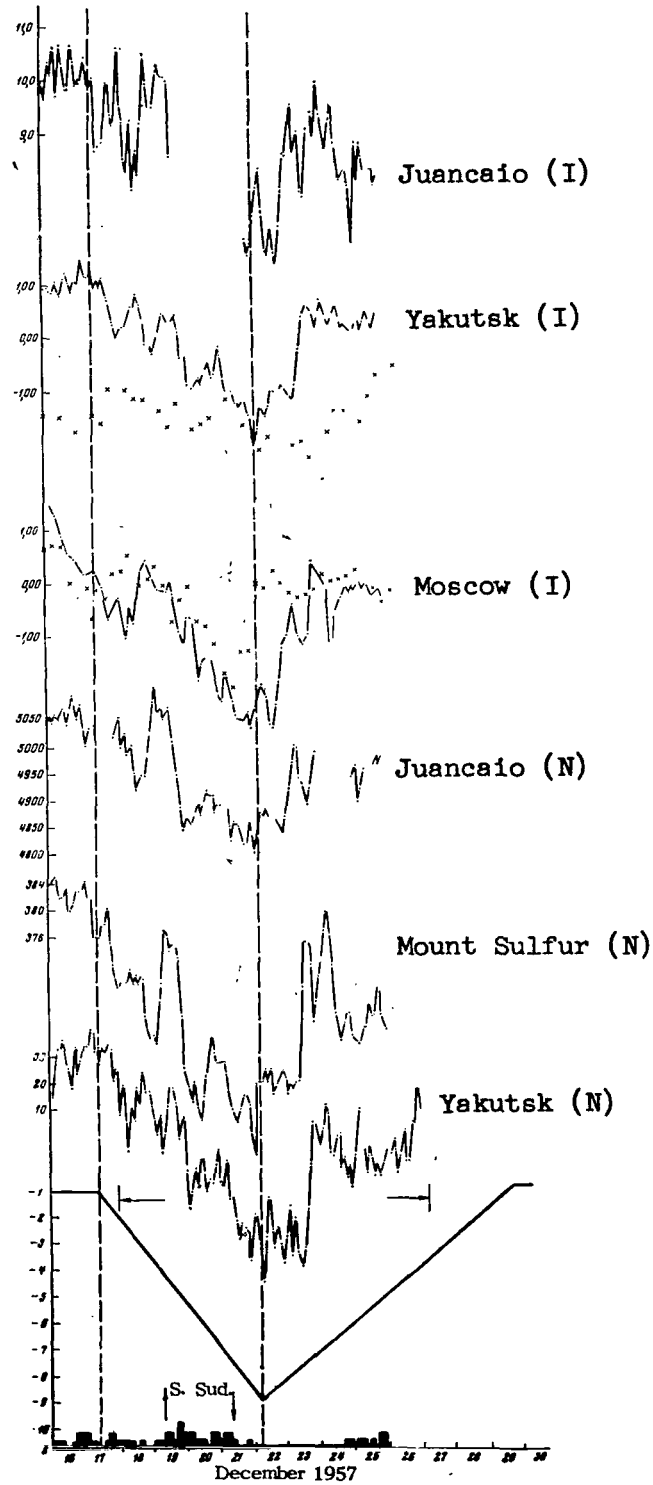

Fig. 32. Magnetic Storm in December 1957

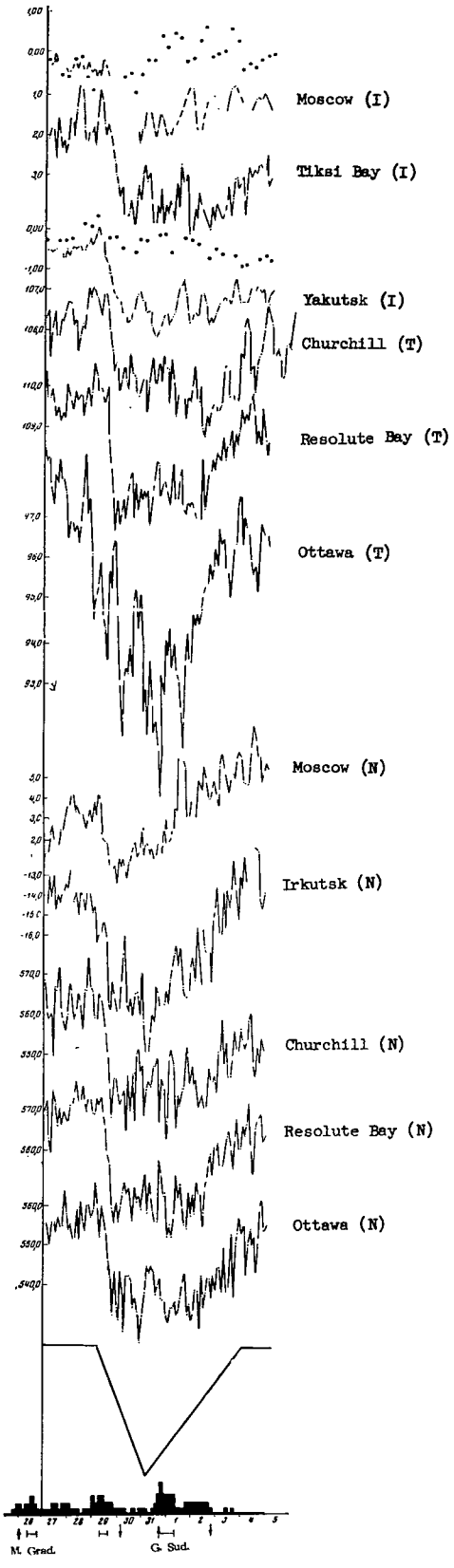

May - June 1958

Fig. 33. Magnetic Storm at the end of May 1958.

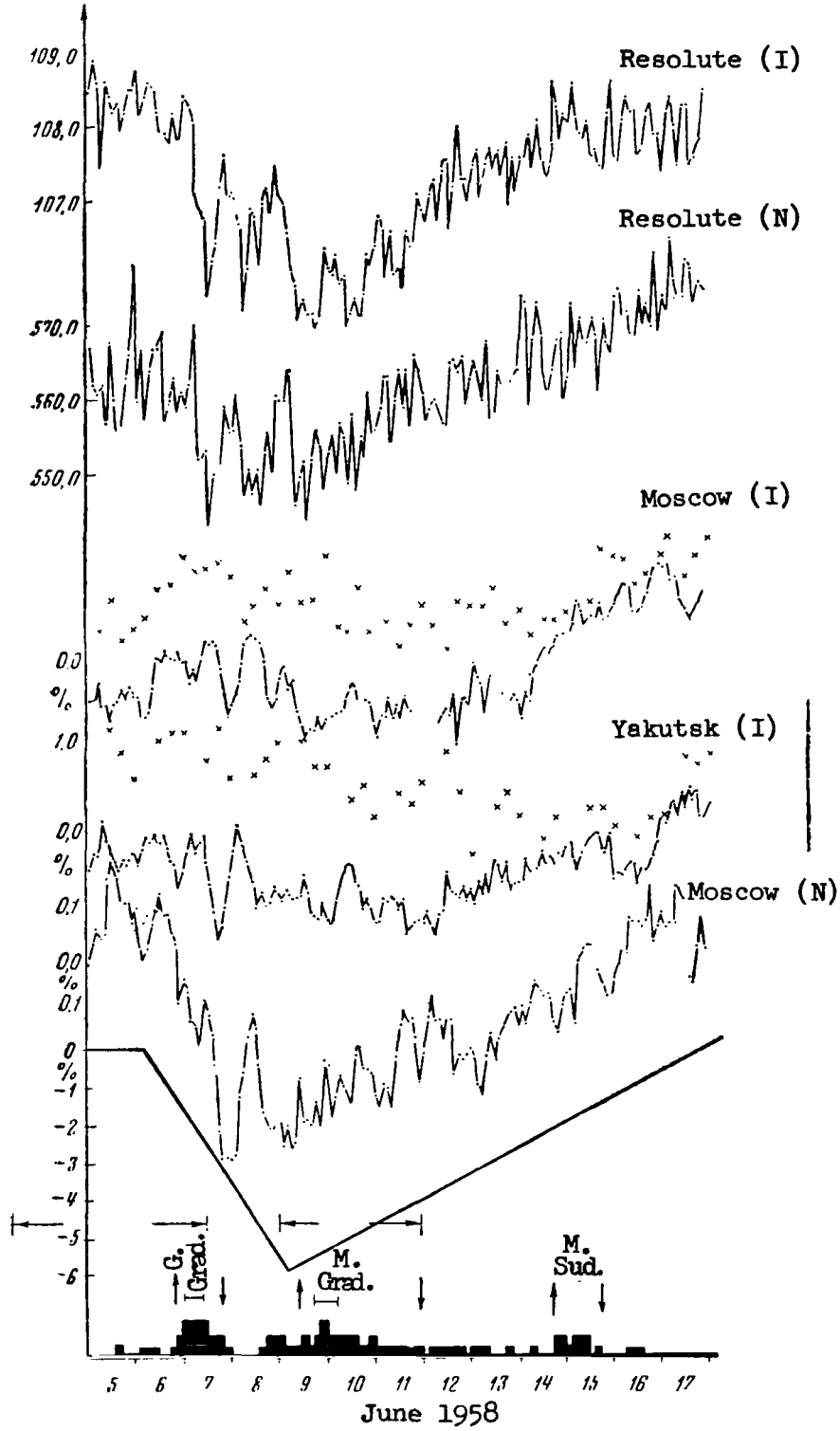

Fig. 34. Magnetic storm at the beginning of June 1958.

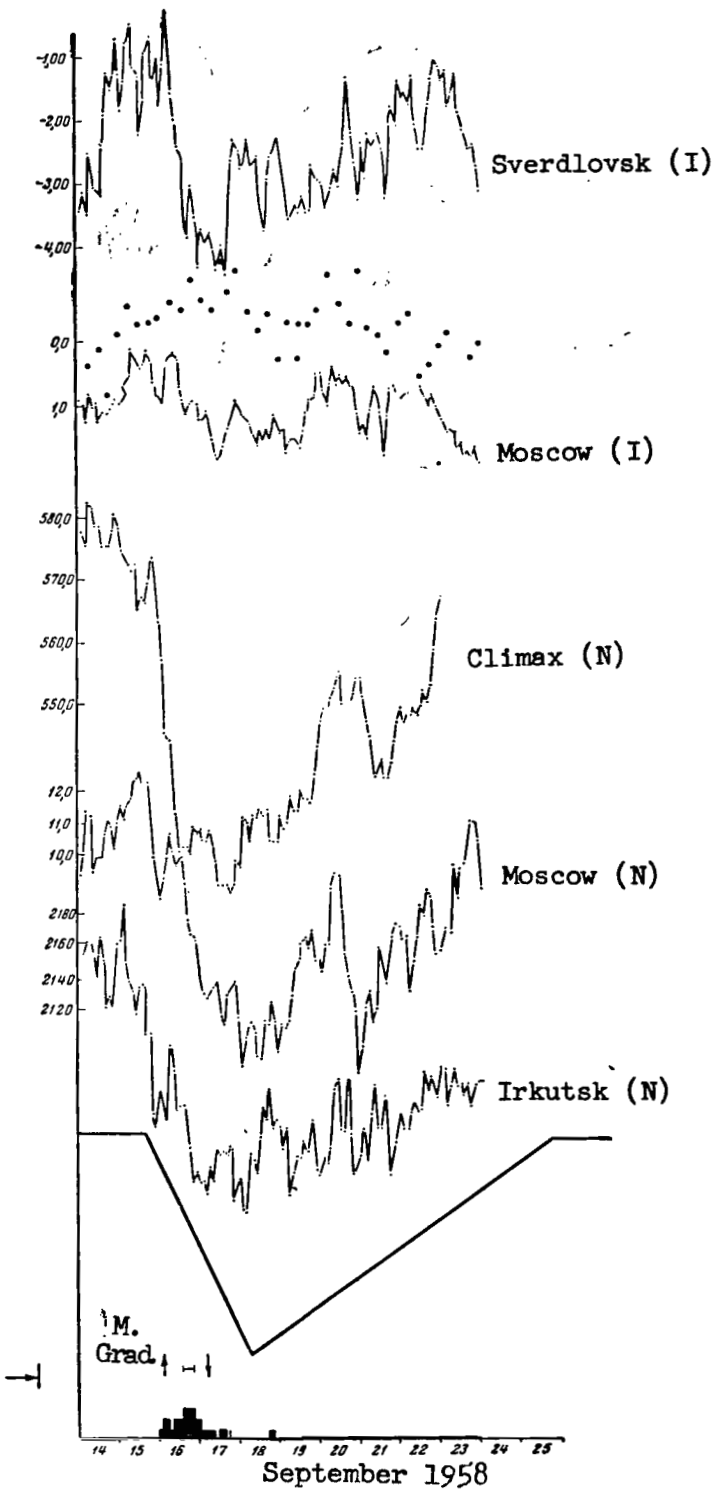

Fig. 35. Magnetic storm in the middle of September 1958.

2 December lasted until 04 hrs, 3 December. A day later, at 00 hrs on 4 December, a large storm with a sudden beginning, lasting until 15 hrs on 5 December, was noted.

Fig. 36 presents experimental data for the Murmansk (N), Moscow (I), and Irkutsk (I) stations.

From N = 5% and I = 2% we find N/I = 2.5, $\mathcal{E}_{min}$ = 100 bev, and f = 0.073. From t_1 = 2 days and t_2 = 2 days we find $l_1 = l_2 = 0.58 \cdot 10^{13}$ and $H_1 = H_2 = 2.9 \cdot 10^{-5}$ gauss, $\rho_1 = \rho_2$ = 110 cm^{-3}. Two active regions passed through the central meridian: 4-35° S from 27.1 November to 1.4 December and 2-43° N from 28.5 November to 3.5 December.

The width of the stream, 4 days, corresponds to widths of the region of 4.3 and 5 days for the southern and northern regions, respectively.

5.9. Magnetic Storm in the Middle of December 1958

A moderate magnetic storm with a gradual beginning at 15 hrs on 17 December lasted until 22 hrs, 20 December, and had an active period from 17 hrs, 17 December to 04 hrs, 18 December. This storm caused a characteristic change in the cosmic ray intensity with a type III profile. Inasmuch as the beginning of the decrease in cosmic ray intensity coincided with the beginning of the magnetic storm, we classify this case as capture of the Earth by the side edge of the magnetized corpuscular stream.

Experimental data for the Moscow (I), Cape Schmidt (I), and Murmansk (N) stations are presented in Fig. 37.

From N = 4%, I = 1.75%, we find N/I = 2.3 and $\mathcal{E}_{min}$ = 112 bev, f = 0.054. From t_1 = 0.75 days, t_2 = 3.5 days, we determine $l_1 = 0.25 \cdot 10^{13}$ cm, $l_2 = 1.2 \cdot 10^{13}$ cm, and $H_1 = 7.3 \cdot 10^{-5}$ gauss. $H_2 = 1.5 \cdot 10^{-5}$ gauss. From this ρ_1 = 720 cm^{-3}, ρ_2 = 31 cm^{-3}. The active region passed through the central meridian from 14.5 to 18.1 December. The width of the stream, 4.2 days, corresponds to an angular width of the active region of 3.7 days.

5.10. Magnetic Storm in January 1959

A moderate magnetic storm with a gradual beginning at 11 hrs on 9 January lasted until 11 January. Several active periods were noted during the storm. The change in intensity belongs to type III.

Experimental data for the stations at Moscow (N, T), Sverdlovsk (I), and Cape Schmidt (I) are presented in Fig. 38.

From N = 4%, I = 1.5% we find N/I = 2.67, $\mathcal{E}_{min}$ = 93 bev, and f = 0.06; from t_1 = 1.2 days and t_2 = 1.5 days we find $l_1 = 0.4 \cdot 10^{13}$ cm and $l_2 = 0.5 \cdot 10^{13}$ cm. Then $H_1 = 3.9 \cdot 10^{-5}$ gauss and $H_2 = 3.1 \cdot 10^{-5}$ gauss. From this ρ_1 = 204 cm^{-3} and ρ_2 = 129 cm^{-3}. The ratio $l_1/l_2 = 0.8$. The active region passed through the central meridian from 3.0 to 8.7 January. The width of the stream, 2.7 days, corresponds in

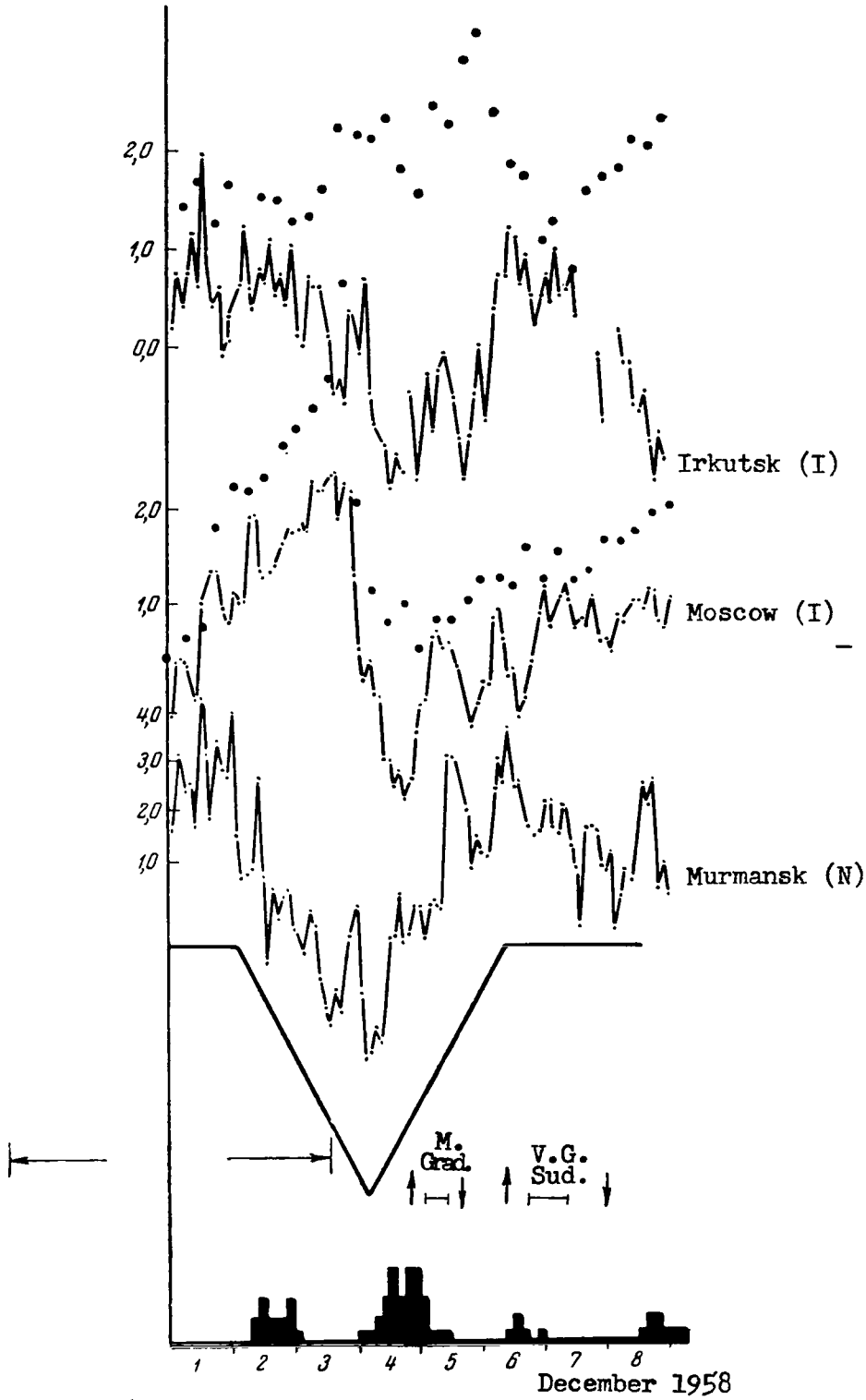

Fig. 36. Magnetic storm in the beginning of December 1958.

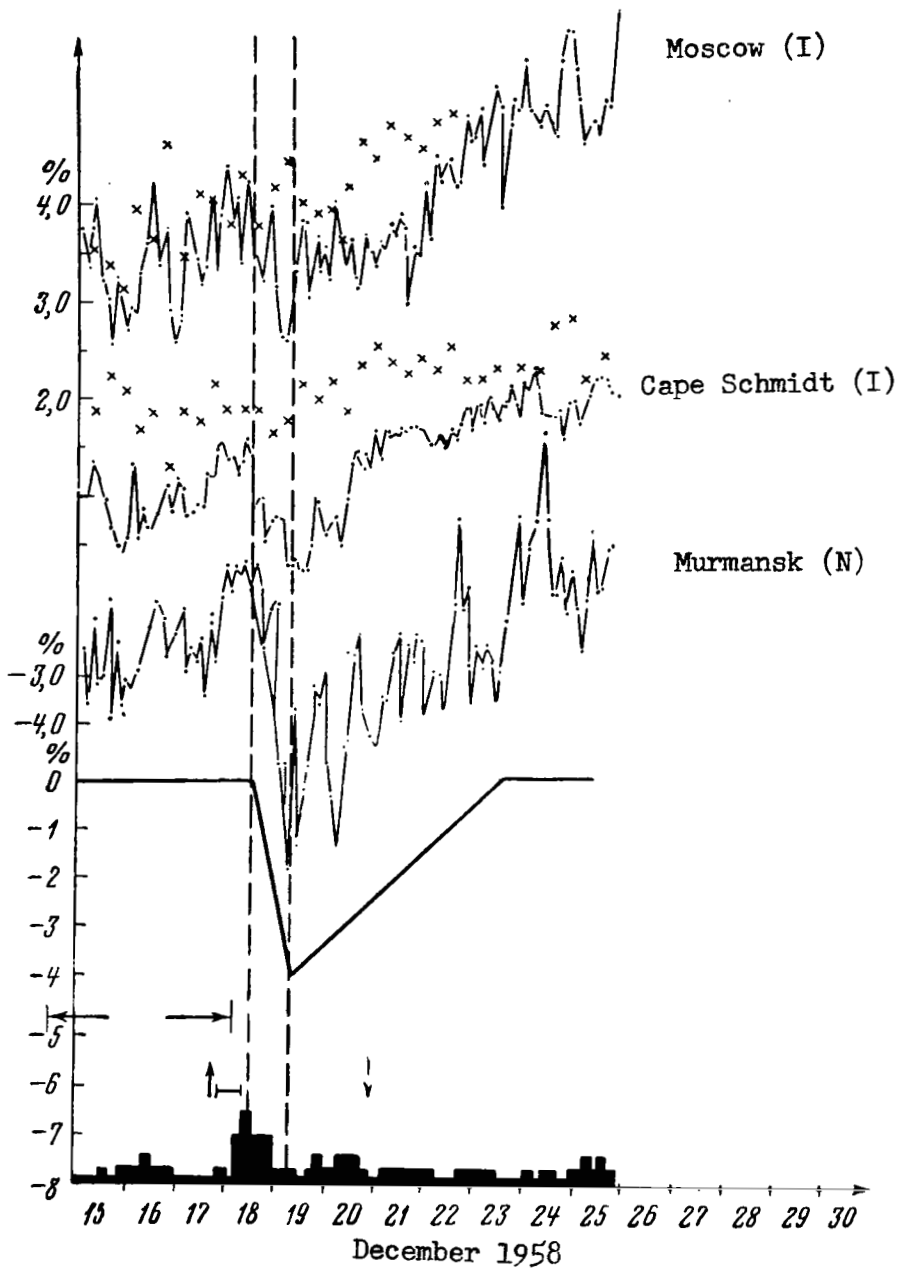

Fig. 37. Magnetic storm in the middle of December 1958.

this case to a width of the region of 5.7 days.

5.11. Magnetic Storm in February 1959

A moderate magnetic storm with a gradual beginning at 03 hrs,

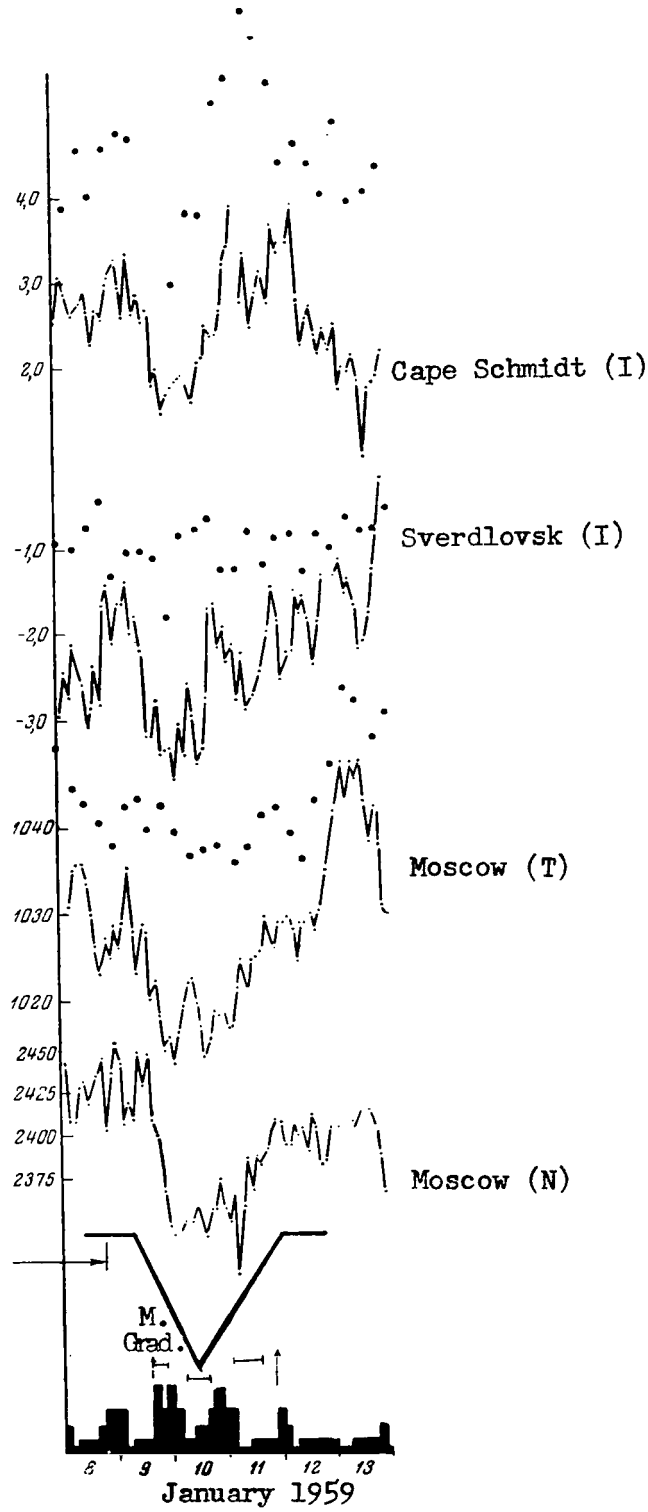

Fig. 38. Magnetic storm in January 1959.

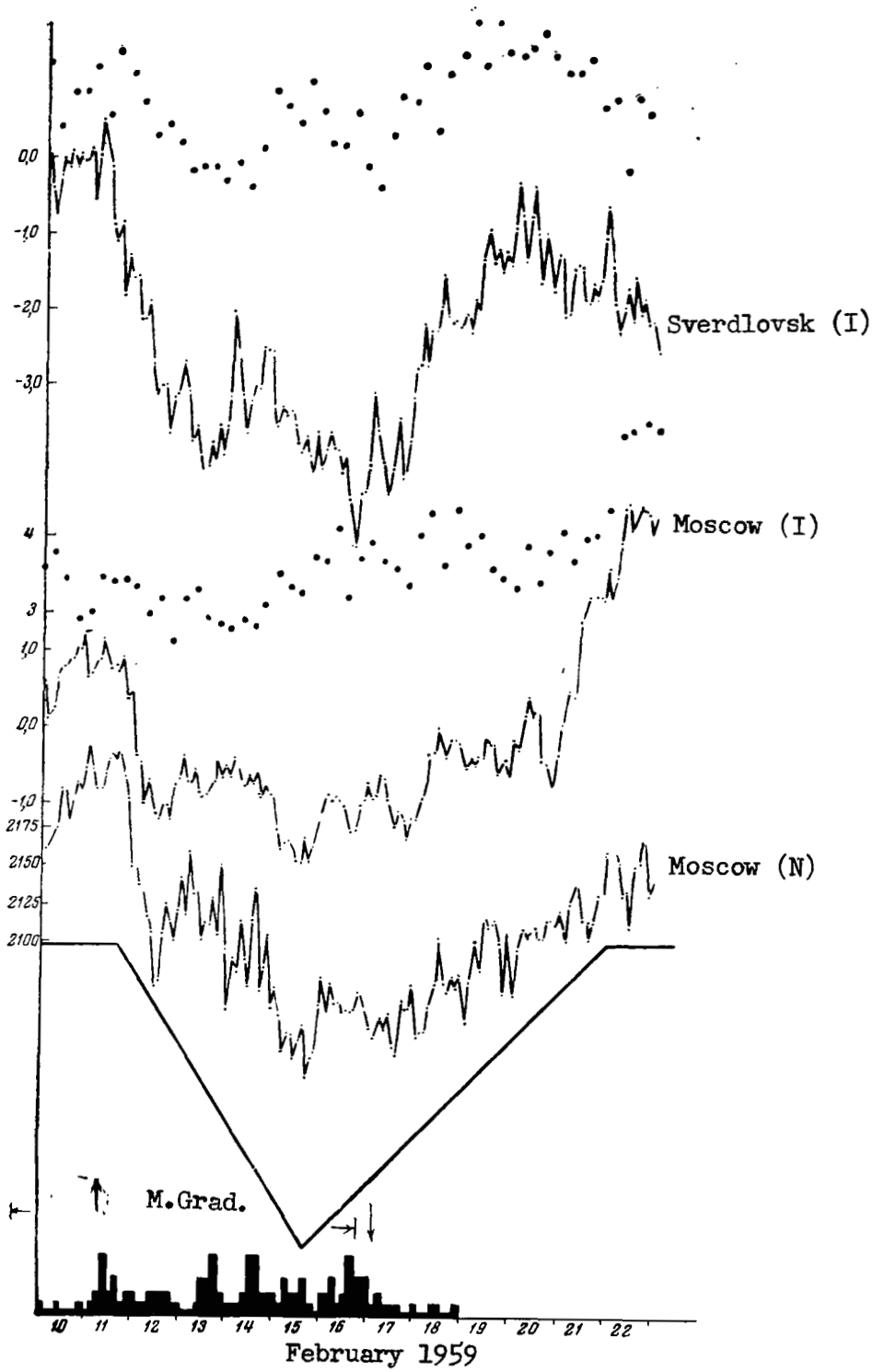

Fig. 39. Magnetic storm in February 1959.

11 February, lasted until 09 hrs on 17 February. The decrease in the cosmic ray intensity began on 11 and continued until 15 February, after which restoration began.

Experimental data for the stations at Moscow (N, I) and Sverdlovsk (I) are cited in Fig. 39.

From N = 8% and I = 3% we find N/I = 2.6, ε_{min} = 95 bev, and f = 0.117. Since the duration of the effect is approximately 10 days, $l = 3.4 \cdot 10^{13}$ cm. Then $H = 0.93 \cdot 10^{-5}$ gauss and $\rho = 12$ cm^{-3}. Two adjoining active regions in the northern hemisphere, which may be responsible for the phenomena under consideration, passed through the central meridian from 9.3 to 16.9 February. The width of the stream, about 10 days, corresponds in this case to a width of the regions of about 8 days.

6. INDIVIDUAL PROFILES AND THE EFFECT OF AN INCREASE BEFORE THE BEGINNING OF MAGNETIC STORMS

The effect of an increase in the cosmic ray intensity, due to acceleration of particles when they are reflected from the forward magnetized front of the stream, is considered in [4, 16, 17]. It follows from theoretical considerations that the effect of an increase in the cosmic ray intensity under consideration occurs only before magnetic storms causing profiles of decrease of types I and II, which characterize capture of the Earth by the forward magnetized front of the stream. Before magnetic storms with profiles of type III, which characterize capture of the Earth by the side edge of the stream, it should not be observed. Let us note that even if the storm has a gradual beginning, but its profile of decrease is of type I or II, in this case too the effect of an increase should occur, since such a case is interpreted as capture of the Earth by the side edge of the unmagnetized portion of the forward front, followed by its entry into the forward front of the magnetized portion of the stream. Table 1 presents data on the increase effect according to all the magnetic storms investigated in this work.

We can see from this Table that:

1) none of the 13 magnetic storms with profiles of type III caused the effect of increase in the cosmic ray intensity;

2) all the storms of types I and II caused a noticeable increase effect (with the exception of two or three storms where, if this effect does exist, it is difficult to distinguish it on a background of statistical errors and solar day variations).

CONCLUSIONS

From an investigation of the variations of cosmic rays and a comparison with geomagnetic data we have come to the following conclusions:

1. The field intensity in the preceding side portion of

Table 1

Types of Profiles and Effect of an Increase in the Cosmic Ray Intensity before Storms

Year, month	Time					Characteristics of storm	Type of profile	Effect of increase in cosmic rays
	Beginning of storm			End of storm				
	Date	Hr	Min	Date	Hr			
1954, November	31	12		3	02	M, Grad	II	present
1955, March	22	09		23	24	M, Grad	III	absent
1955, November	18	12		21	04	VG, Grad	I	present
1955, December	1	13		1	23	M, Grad	I	present
1956, February	11	10		12	13	M, Grad	III	absent
1956, March	2	23	41	4	17	M, Sud	I	present
1956, April	26	08		28	11	G, Grad	III	absent
1956, September	2	01	18	3	15	M, Sud	II	?
1957, January	21	12	55	23	20	VG, Sud	II	present
1957, March	10	00	22	11	01	G, Sud	I	?
1957, April	17	11	36	20	02	G, Sud	II	present
1957, August	3	16		4	04	M, Sud	I	present
1957, August	29	19	23	30	20	M, Sud	II	present
1957, September	13	00	50	14	15	VG, Sud	I	present
1957, September	21	10	06	25	15	VG, Sud	II	present
1957, September	29	00	15	30	24	VG, Sud	I	present
1957, October	21	20		23	23	S, Grad	II	present
1957, October	13	20		15	01	S, Grad	III	absent
1957, November	23	08		29	20	G, Grad	II	present
1957, December	15	05		15	20	S, Grad	III	absent
1958, February	11	01	26	14	24	VG, Sud	I	present
1958, March	24	16		27	06	M, Grad	II	present
1958, May	26	01		30	05	M, Grad	III	absent
1958, June	6	21		7	20	G, Grad	III	absent
1958, July	8	07	46	10	10	VG, Sud	II	present
1958, July	21	15	35	22	15	M, Sud	II	present
1958, August	17	06	22	18	14	M, Sud	II	present
1958, August	22	02	28	22	15	M, Sud	II	present
	24	01	40	25	20	G, Sud	I	present
	27	02		28	01	M, Grad	III	absent
1958, September	16	05		17	07	M, Grad	I	present
1958, September-	25	04	08	26	15	G, Sud	II	present
October	30	10	05	1	08	S, Sud	I	present
1958, October	22	03	15	25	09	G, Sud	I	present
1958, November	25	12		28	04	S, Grad	I	present

Characteristics of storm: S -- small, M -- moderate, G -- great, VG -- very great, Grad -- gradual beginning, Sud -- sudden beginning.

Continuation of Table 1

Year, month	Time: Beginning of storm: Date	Hr	Min	End of storm: Date	Hr	Characteristics of storm	Type of profile	Effect of increase in cosmic rays
1958, December	2	09		3	04	M, Grad	III	absent
1958, December	13	20		15	00	M, Grad	III	absent
1958, December	17	15		20	22	M, Grad	III	absent
1959, January	9	11		11	24	M, Grad	III	absent
1959, February	11	03		17	09	M, Grad	III	absent
1959, March	26	06	42	31	24	VG, Sud	I	present

streams is substantially greater than that in the lagging portion (this explains the sharper drop in comparison with the lag in the intensity of cosmic rays when the Earth is captured by the side front of the stream).

2. There is a substantial dispersion of the density of kinetic energy in the stream. It decreases significantly upon passage to the lagging side portion of the stream (this explains why magnetic disturbances end more rapidly than the increase in the cosmic ray intensity).

3. In the forward portion of the stream, a substantial thickening of its plasma and a corresponding intensification of the magnetic field frozen in it are formed (this explains the very sharp drop in the cosmic ray intensity during magnetic storms with sudden beginnings when the Earth is captured by the forward front of the stream).

4. Magnetic storms that give profiles of decrease of type III, characterizing capture of the Earth by the magnetized preceding portion of the stream, do not cause the effect of an increase in the cosmic ray intensity before magnetic storms.

5. Practically all magnetic storms giving profiles of types I or II, which characterize capture of the Earth by the forward magnetized front of the stream, cause a noticeable effect of increase in the cosmic ray intensity before the beginning of a magnetic storm.

These are average principles. Now, with the aid of an investigation of variations of cosmic rays, it is possible to study the properties of individual streams in rather great detail. On the basis of the analysis presented, we might assume that the profile of the change in cosmic ray intensity during magnetic storms is fully determined by the character of the Earth's entry into the stream, its velocity, and the distribution of the field in it. Consequently, a detailed investigation of this profile permits the obtaining of important information on the properties of streams.

In conclusion we shall take the opportunity to express our profound gratitude to Professor E. L. Feynberg and to L. I. Inozemtseva for their discussion of the results obtained. We shall also express our deep indebtedness to the researchers who supplied the experimental

data used in this work.

BIBLIOGRAPHY

1. Ya. L. Blokh, Ye. S. Glokova, L. I. Dorman. In the Collection "Variations of Cosmic Rays beneath the Earth, at Sea Level, and in the Stratosphere," Publishing House of the Academy of Sciences USSR, p. 7.
2. L. I. Dorman. Variations of Cosmic Rays. Moscow, State Technical Literature Publishing House, 1957.
3. S. Chapman, J. Bartels. Geomagnetism. Oxford, 1940.
4. L. I. Dorman. Works of the Yakut Branch of the Siberian Division, Academy of Sciences USSR, Physical Series, Publishing House of the Academy of Sciences USSR, 1960, No. 3.
5. L. I. Dorman. Works of the International Conference on Cosmic Rays, 1959, Publishing House of the Academy of Sciences USSR, 1960, Vol. 4, p. 113.
6. L. I. Dorman, Ye. L. Feynberg. In the Collection "Variations of Cosmic Rays beneath the Earth, at Sea Level, and in the Stratosphere," Publishing House of the Academy of Sciences USSR, 1959, p. 49.
7. L. I. Dorman. On the Nature of Variations of Cosmic Rays (Diss). Moscow, Scientific Research Institute of Terrestrial Magnetism -- Institute of Physics, Academy of Sciences, 1955.
8. D. T. Martyn. Nature, 1951, 167, p. 92.
9. J. A. Lockwood. Phys. Rev., 1958, 112, p. 1750.
10. L. I. Dorman, E. L. Feinberg. Memoria del V Congreso Int. de Radiacion Cosmica (Guanajuato, 1955), Mexico, 1958.
11. E. N. Parker. Phys. Rev., 1958, 110, p.6.
12. S. M. Singer. Nuovo Cimento, Supplemento, 1958, 7, p. 2.
13. Ya. L. Blokh, Ye. S. Glokova, L. I. Dorman, O. I. Inozemtseva. "Works of the International Conference on Cosmic Rays, 1959," Publishing House of the Academy of Sciences USSR, 1960, Vol. 4, p. 172.
14. Solar and Cosmic Data. Publishing House of the Academy of Sciences USSR and the NIZMIR.
15. L. I. Dorman. This Collection, p. 64.
16. L. I. Dorman. Works of the International Conference on Cosmic Rays, 1959, Publishing House of the Academy of Sciences USSR, 1960, Vol. 4, p. 132.
17. Ya. L. Blokh, L. I. Dorman, N. S. Kaminer. Works of the International Conference on Cosmic Rays, 1959, Publishing House of the Academy of Sciences USSR, 1960, Vol. 4, p. 178.

ABSTRACT

The paper gives an analysis of several cases of the decrease in the intensity of cosmic rays during the magnetic storms of different types (about 40 storms). For every case the profile is determined of the intensity variations (I, II and III types), the characteristics of which are connected with the properties of the magnetic storm (with sudden or gradual commencement), with the character of capture of the Earth in the corpuscular stream (by forward front or side edge), with the velocity of the stream and its geometric parameters and with the distribution and tension of the magnetic field frozen in the stream. On the basis of conceptions developed in [5] an interpretation is given of each case. The properties of streams appear to be largely different. However, general regularities are observed inherent to most of the streams: the angle width of the streams averagely amounts to the angle width of active region; the front edge of the stream is characterised by considerable increase of the magnetic field (and the corresponding compression of plasma); in the leading part of the streams the field is also somewhat increased compared with the field in the lagging edge; etc. Data are also given about the effect of the increase before the commencement of the magnetic storms under discussion.

VARIATIONS OF COSMIC RAY INTENSITY DURING THE PERIOD WHEN THE EARTH IS CAPTURED BY CORPUSCULAR STREAMS CARRYING HOMOGENEOUS AND INHOMOGENEOUS FROZEN MAGNETIC FIELDS

L. I. Dorman

1. INTRODUCTION

Reference [1] evaluated the change in cosmic ray intensity caused by scattering of particles by magnetic fields of streams in various cases of capture of the Earth. The scattering of particles by a homogeneous magnetic field in a plane perpendicular to the field was considered. The possible influence of inhomogeneity of the field was evaluated qualitatively. In this work we are expanding the calculations for the case of the homogeneous field and are presenting here the variation of the cosmic ray intensity in various cases of capture and at various values of $\varepsilon_{\delta} = 300\ H_{\delta} l_{\delta} =$ 40, 60, 80, 100, and 120 bev ([1] presented the results only for $\varepsilon_{\delta} =$ 100 bev). In addition, here we calculate the expected profile for various characters of inhomogeneity of the magnetic field. A comparison of these profiles with the experimental data permits us to evaluate the distribution of the field in the stream in each individual case.

2. CERTAIN SUPPLEMENTARY RESULTS OF THE CALCULATIONS FOR A HOMOGENEOUS FIELD

As a supplement to [1], Fig. 1 presents the results of calculations performed with the aid of the coupling constants according to the formula

$$\frac{\delta N_{\lambda}^{i}(h_0)}{N_{\lambda}^{i}(h_0)} = -\int_{\varepsilon_{\lambda}^{\min}}^{\infty} \frac{\delta D(\varepsilon)}{D(\varepsilon)} W_{\lambda}^{i}(\varepsilon, h_0)\, d\varepsilon, \tag{1}$$

where $\delta D(\varepsilon)/D(\varepsilon)$ is determined by the expression

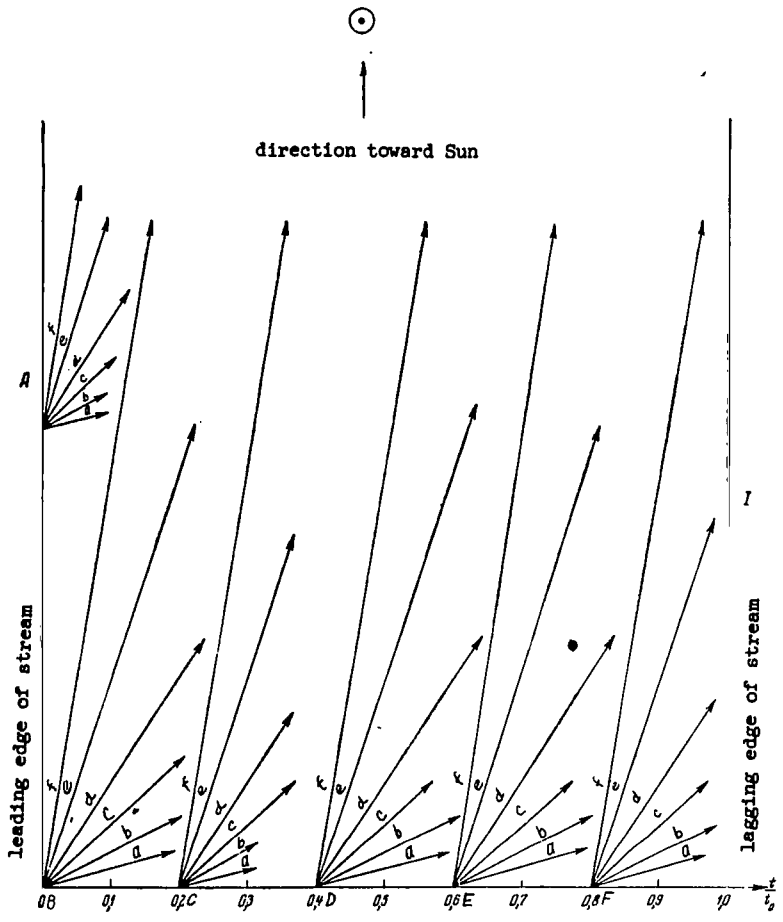
direction toward Sun
A
leading edge of stream
lagging edge of stream
I
front of stream

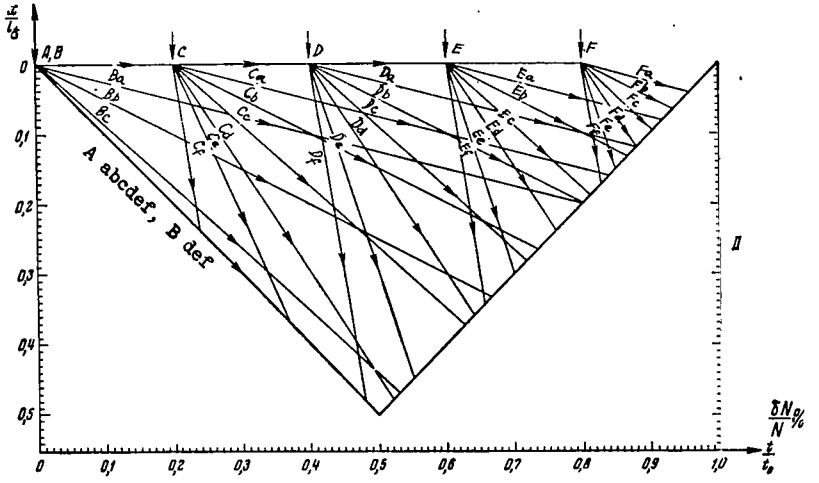
A,B
C
D
E
F
A abcdef, B def
II

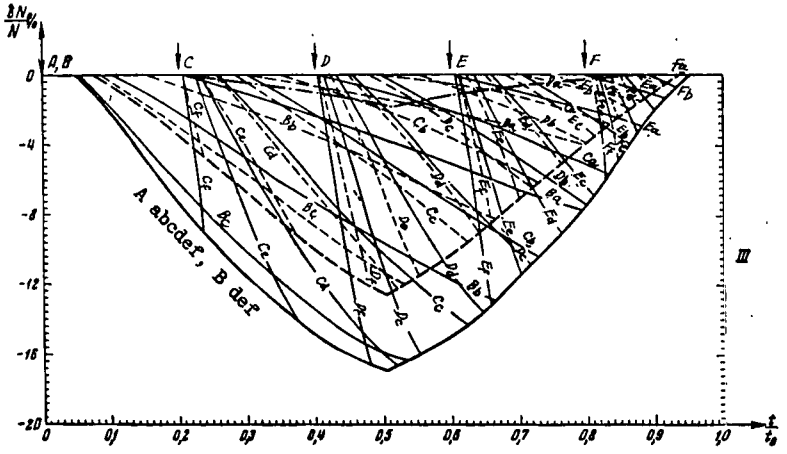
A,B
C
D
E
F
A abcdef, B def
III

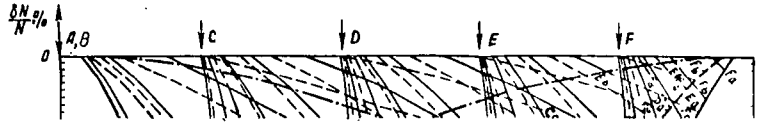
A,B
C
D
E
F

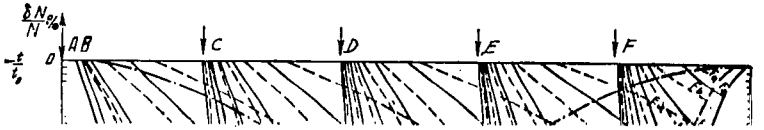
A,B
C
D
E
F

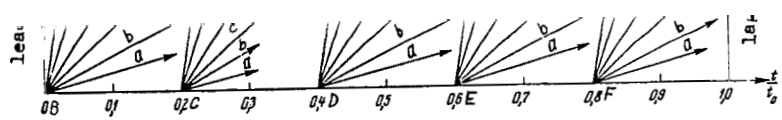

front of stream

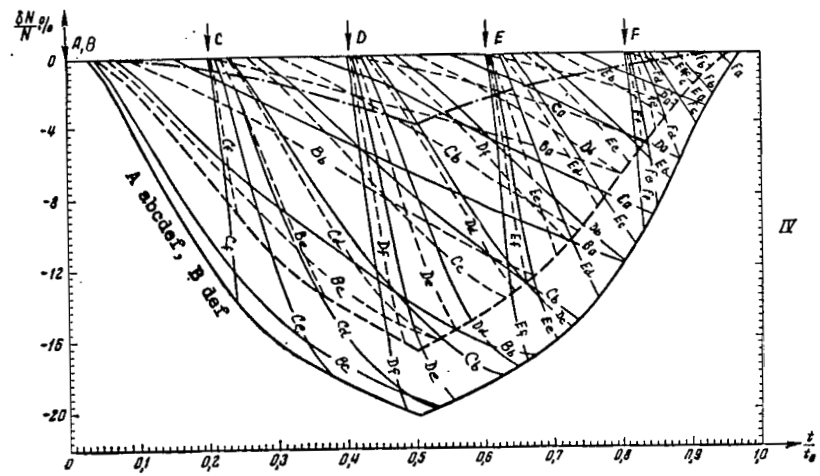

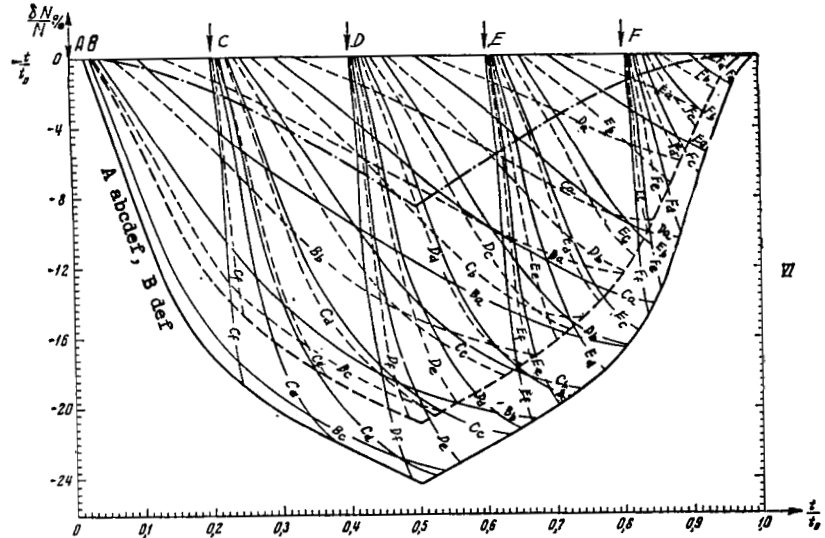

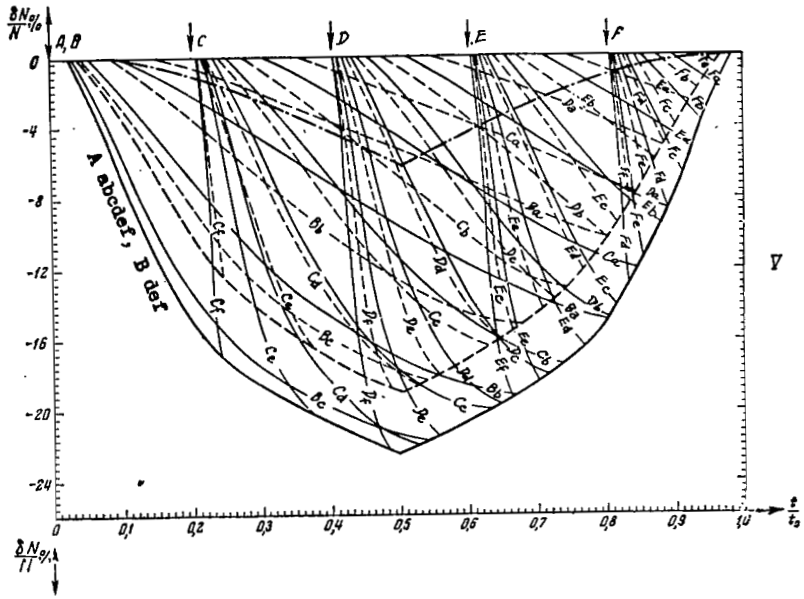

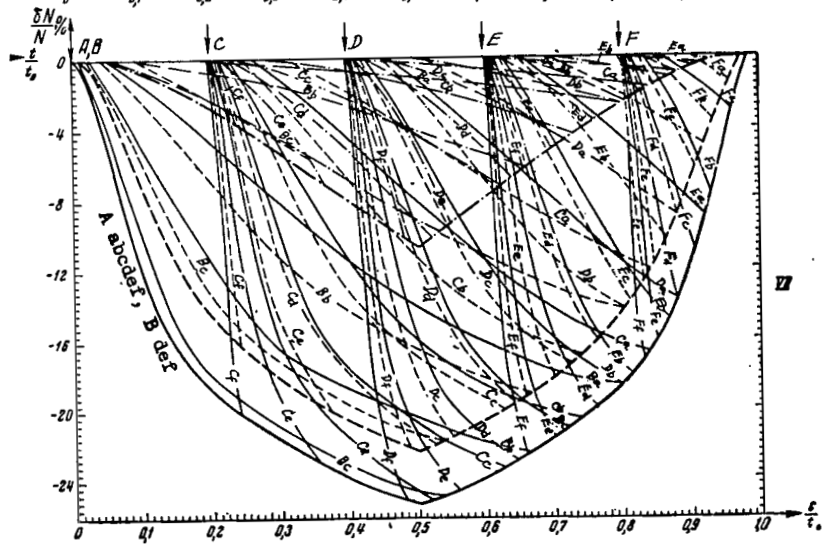

Beginning of magnetic storms

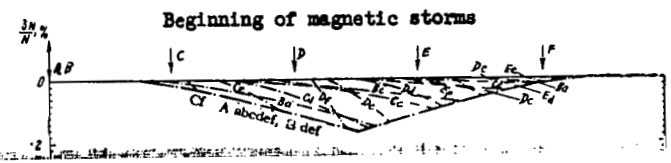

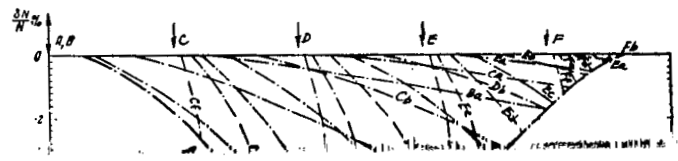

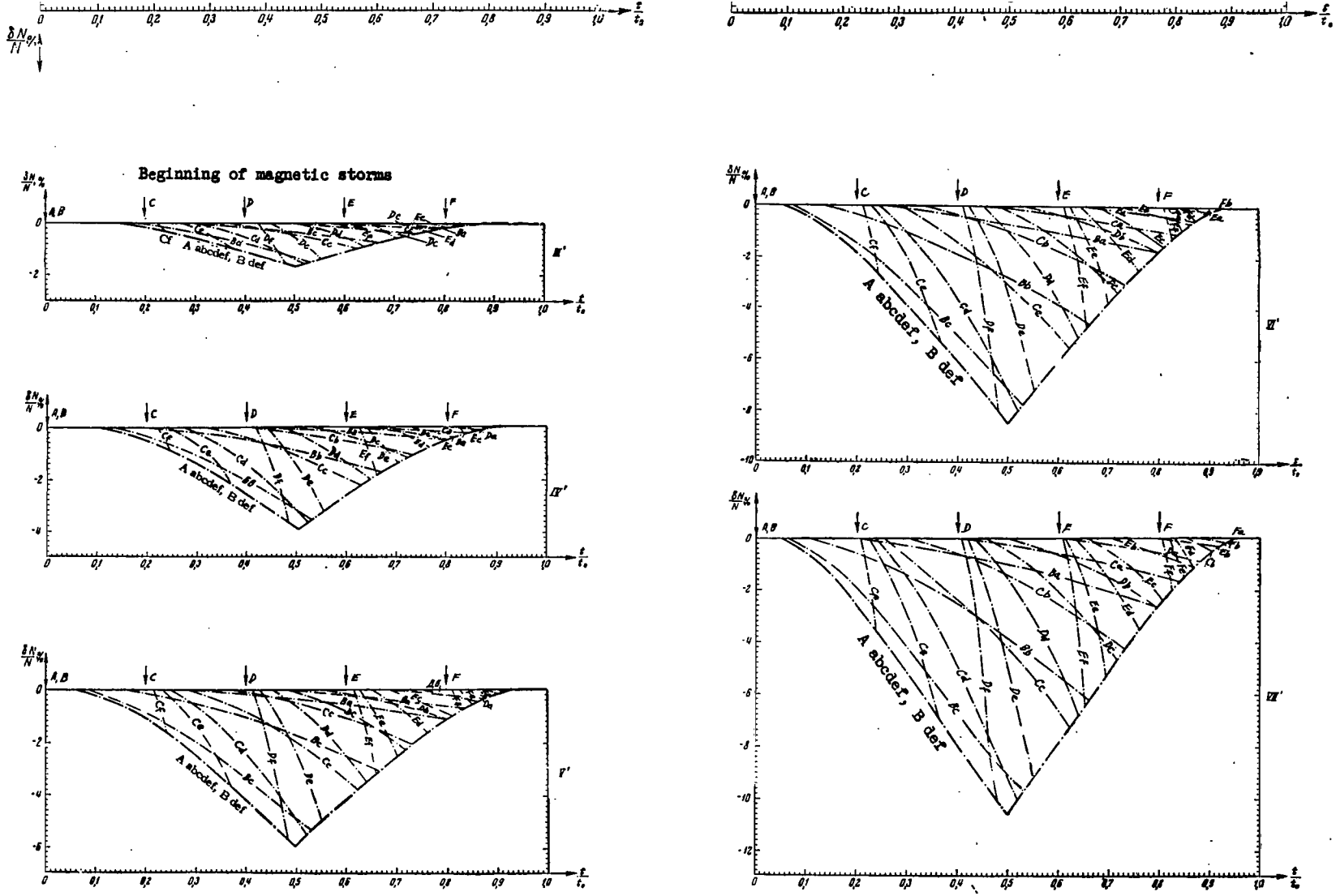

Fig. 1. Results of calculations for cases of a homogeneous magnetic field in the stream:

I -- path of the Earth in the stream; II -- profile of shortest distance; III -- variation of the cosmic ray intensity when $\varepsilon_\delta = 40$ bev; IV -- variation of cosmic ray intensity when $\varepsilon_\delta = 60$ bev; V -- variation of cosmic ray intensity when $\varepsilon_\delta = 80$ bev; VI -- variation of cosmic ray intensity when $\varepsilon_\delta = 100$ bev; VII -- variation of cosmic ray intensity when $\varepsilon_\delta = 120$ bev.
For the region of the middle latitudes $\lambda \sim 50°$: solid line -- neutron component at mountain level; dashed line -- neutron component at sea level; dashed-dotted line -- hard component at sea level. For greater clarity the results of the calculations for the hard component are also presented in a larger scale: (III', IV', V', VI', and VII' for various ε_δ, respectively). The velocities of the forward front of the stream are denoted by the following indices: a -- 10^7 cm/sec; b -- $2 \cdot 10^7$ cm/sec; c -- $3.5 \cdot 10^7$ cm/sec; d -- $6 \cdot 10^7$ cm/sec; e -- $2 \cdot 10^8$ cm/sec; f -- $3.4 \cdot 10^8$ cm/sec; A, B, C, D, E, F -- various cases of capture of the Earth by the stream and the corresponding beginnings of magnetic storms.

$$\frac{\delta D(\varepsilon)}{D(\varepsilon)} = f \begin{cases} -1, & \text{if} \quad \varepsilon \leqslant \frac{\varepsilon_{\min}}{4} \\ -\frac{2}{\pi} \arcsin\left(\frac{\varepsilon_{\min}}{2\varepsilon} - 1\right), & \text{if} \quad \frac{\varepsilon_{\min}}{4} \leqslant \varepsilon \leqslant \frac{\varepsilon_{\min}}{2}, \\ 0, & \text{if} \quad \varepsilon \geqslant \frac{\varepsilon_{\min}}{2}. \end{cases} \tag{2}$$

Here

$$\varepsilon_{\min} = 300 H_{\delta} \cdot 2x = \varepsilon_{\delta} \cdot \frac{2x}{l_{\delta}}. \tag{3}$$

where x is the shortest distance from the Earth to any edge of the stream. Graphs of the variation of x are presented for various cases of capture of the Earth by the stream in Fig. 1 (II). The same Figure (III-VII) presents the variations of the cosmic ray intensity of the neutron and hard components expected according to (1)(in the calculations it was assumed that f = 0.3). For greater clarity, the results of the calculations for the hard component are presented individually in Fig. 1 in a larger scale.

It follows from these graphs that:

1) The sharpness of the drop in intensity depends substantially on the radial velocity of the stream. The greater the velocity of the stream, the more rapid an intensity drop (with all other conditions equal) should be observed.

2) The relative rate of restoration should not depend on the radial velocity of the stream.

3) A certain lag in the beginning of the Forbush effect with respect to the beginning of the magnetic storm should be observed, where the magnitude of the lag should depend substantially on the radial velocity of the stream. As the velocity increases, the time lag should decrease. An especially large time lag should be observed for storms with gradual beginnings.

4) The profile of the Forbush effect and the time lag should depend somewhat on the type of the recorded component.

5) The more sensitive the given secondary component to the harder primary particles, the larger the time lag of the Forbush effect with respect to the beginning of the magnetic storm, the smaller the amplitude of the effect, and the more rapidly restoration of the cosmic ray intensity should occur.

A preliminary analysis [2] for many magnetic storms shows that these conclusions basically agree with the experimental data.

3. NATURE OF THE DISTRIBUTION OF THE FIELD IN THE STREAM

Reference [2] compared the observed profiles of the variation

of the cosmic ray intensity during various magnetic storms with the expected profiles, which were presented above. This comparison showed that in most streams the field is inhomogeneous: it is stronger in the leading portion of the stream and somewhat weaker in the lagging portion (with respect to the rotation of the Sun). Let us take a system of coordinates in such a way that the axis Oz is directed along the axis of the stream, Oy is perpendicular to the magnetic field. Here and in Sections 4-7 let us consider the case when the magnetic field intensity depends only on the coordinate y (we shall measure y in units of the stream width $l_{\odot}$ at a distance of the radius of the Earth's orbit $R_{\odot}$ from the Sun).*

Four types of field distribution are considered below, in Sections 4-7: 1) a linear drop from H_{max} in the leading edge of the stream to H_{min} in the lagging edge; 2) a parabolic drop from H_{max} to H_{min}; 3) a linear rise from zero at the leading edge to H_{max} at y_1 and then a linear drop to zero at the lagging edge; 4) a linear drop from H_{max} at the leading edge to zero at y = 0.5 and then a linear increase to H_{min} at the lagging edge.

In the case of an inhomogeneous field, the quantity $\int H dy$ will figure in the calculations instead of the shortest distance x, and formula (3) changes to

$$\varepsilon_{\min}(y) = ZeH_{\max} l_{\odot} 2 \cdot \varphi(y), \tag{4}$$

where

$$\varphi(y) = \frac{1}{H_{\max}} \cdot \min\left\{\int_0^y H\,dy;\ \int_y^1 H\,dy\right\}. \tag{5}$$

Here Ze is the charge of the primary particles.

In a first approximation the decrease in cosmic ray intensity will be proportional to the quantity $\varepsilon_{min}(y)$, and, consequently, to $\varphi(y)$ as well.

4. EXPECTED PROFILE OF THE INTENSITY IN THE CASE OF LINEAR VARIATION OF THE FIELD INTENSITY IN THE STREAM

If

$$\alpha \equiv \frac{H_{\min}}{H_{\max}}, \tag{6}$$

---

* This corresponds to the assumption that the Earth was captured by the side edge of a stream with an inhomogeneous magnetic field. The case of capture of the Earth by the forward front with an intensified magnetic field is considered below, in Section 8.

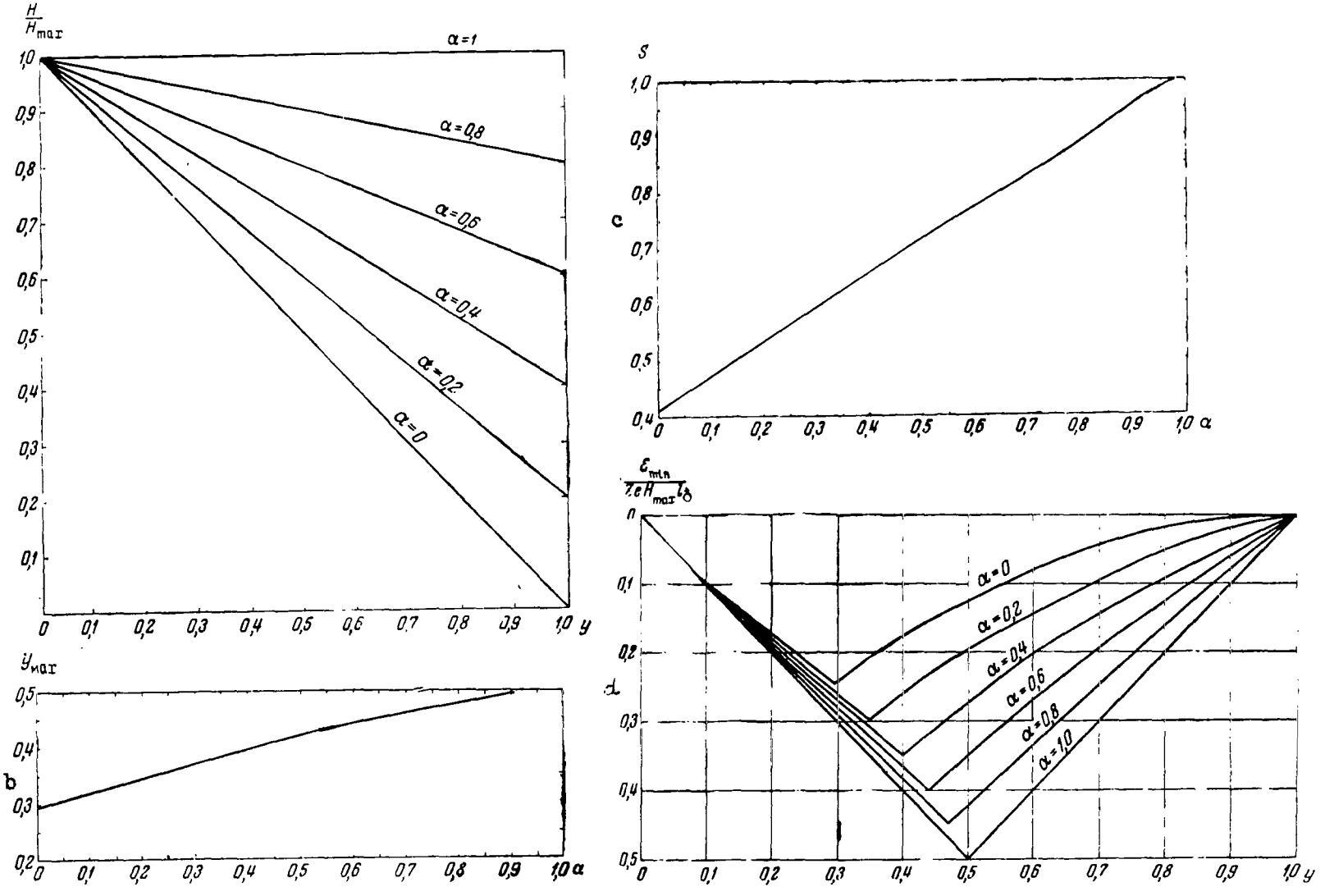

Fig. 2. Case of linear variation of the field intensity from H_{max} at the leading edge to H_{min} at the lagging edge of the stream.
a -- system of coordinates and profile of field; b -- dependence of y_{max} on α; c -- dependence of s on α; d -- profile of the variation of $\varepsilon_{min}/ZeH_{max}\, l_{\delta}$ for various α.

where H_{min} is the field intensity at the lagging edge of the stream, while H_{max} is the field intensity at the leading side edge of the stream, then in the case under consideration

$$H = H_{max}[1 - (1 - \alpha) y] \tag{7}$$

(the system of coordinates and profile of the field are shown in Fig. 2, a). Substituting (7) into (5), we find

$$\varphi(y) = \begin{cases} y - \frac{1}{2}(1 - \alpha) y^2, & \text{if } y \leqslant y_{max}, \\ 1 - y - \frac{1}{2}(1 - \alpha)(1 - y^2), & \text{if } y \geqslant y_{max}, \end{cases} \tag{8}$$

where the value of y_{max} at which $\varphi(y)$ reaches its maximum value (while the cosmic ray intensity, correspondingly, reaches its *minimum* value) is determined by the equation

$$y_{max} - \frac{1}{2}(1 - \alpha) y_{max}^2 = 1 - y_{max} - \frac{1}{2}(1 - \alpha)(1 - y_{max}^2). \tag{9}$$

From this

$$y_{max} = \frac{1 - \sqrt{\frac{1 + \alpha^2}{2}}}{1 - \alpha} \tag{10}$$

and

$$\varphi_{max} = \frac{1 + \alpha}{4}. \tag{11}$$

The dependence of y_{max} on α is shown in Fig. 2, b. Fig. 2, c also presents the ratio of the expected time of the drop in the cosmic ray intensity to the time of its restoration:

$$s = \frac{y_{max}}{1 - y_{max}}. \tag{12}$$

Fig. 2, d presents the profiles of $\varphi(y)$ for various α. From preliminary experimental data, cited in reference [2], it follows that in most cases the restoration period is approximately twice as great as the period of the intensity drop. Thus, if the assumption made on the distribution of the field is correct, then the case $\alpha = 0$ should occur most frequently, i.e. the field should most often fall linearly from H_{max} at the leading edge to zero at the lagging edge of the stream.

5. PARABOLIC VARIATION OF THE FIELD FROM H_{max} AT THE LEADING EDGE TO H_{min} AT THE LAGGING EDGE OF THE STREAM

Introducing the notation of (6) in this case too, we obtain

$$\frac{H}{H_{max}} = \alpha + (1-\alpha)(1-y)^2 \tag{13}$$

(see profile of field in Fig. 3, a). Substituting (13) into (15), we obtain

$$\varphi(y) = \begin{cases} y\left[1 - y(1-\alpha)\left(1 - \frac{y}{3}\right)\right], & \text{if } y \leqslant y_{max}, \\ (1-y)\left[1 - \frac{1}{3}(1-\alpha)(2+2y-y^2)\right], & \text{if } y \geqslant y_{max}, \end{cases} \tag{14}$$

where

$$y_{max} = 1 + \sqrt[3]{-\frac{1+2\alpha}{4(1-\alpha)} + \frac{1}{4(1-\alpha)}\sqrt{\frac{1+3\alpha+12\alpha^3}{1-\alpha}}} + \sqrt[3]{-\frac{1+2\alpha}{4(1-\alpha)} - \frac{1}{4(1-\alpha)}\sqrt{\frac{1+3\alpha+12\alpha^3}{1-\alpha}}}. \tag{15}$$

The graphs of $y_{max}(\alpha)$, $s(\alpha)$, and $\varphi(y)$ at various α are presented in Figs. 3,b, 3,c, and 3,d, respectively. We can see from these graphs that the variant with $\alpha \approx 0.2$-0.4 will apparently be realized most often.

6. PROFILE OF THE MAGNETIC FIELD INTENSITY IN THE FORM OF A TRIANGLE

In this case

$$H = \begin{cases} \frac{y}{y_1} H_{max}, & \text{if } y \leqslant y_1. \\ \frac{1-y}{1-y_1} H_{max}, & \text{if } y \geqslant y_1. \end{cases} \tag{16}$$

The profile of the field is shown in Fig. 4, a. Substituting

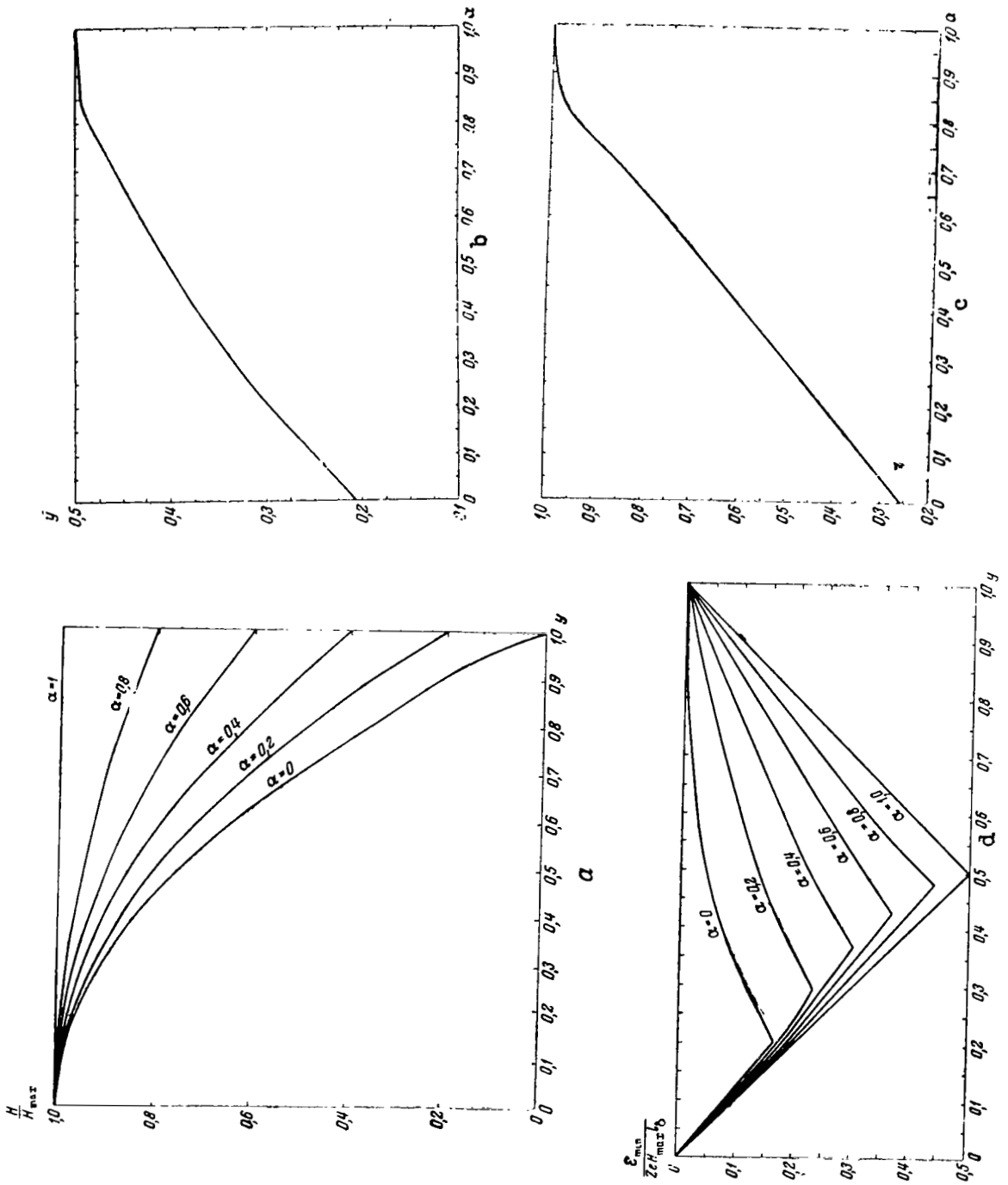

Fig. 3. Case of parabolic variation of the field from H_{max} at the leading edge to H_{min} at the lagging edge of the stream.
Notations the same as in Fig. 2.

(16) into (5), we obtain when $y_1 \leqslant 0.5$

$$\varphi(y) = \frac{\varepsilon_{\min}}{ZeH_{\max} l_{\delta}} = \begin{cases} \dfrac{y^2}{2y_1}, & \text{if } 0 \leqslant y \leqslant y_1, \\ \dfrac{2y - y_1 - y^2}{2(1-y_1)}, & \text{if } y_1 \leqslant y \leqslant y_{\max}, \\ \dfrac{(1-y)^2}{2(1-y_1)}, & \text{if } y_{\max} \leqslant y \leqslant 1, \end{cases} \tag{17}$$

where

$$y_{\max} = 1 - \sqrt{\frac{1-y_1}{2}}. \tag{18}$$

If $y_1 \geqslant 0.5$, then

$$\varphi(y) = \begin{cases} \dfrac{y^2}{2y_1}, & \text{if } 0 \leqslant y \leqslant y_{\max}, \\ \dfrac{1}{2} - \dfrac{y^2}{2y_1}, & \text{if } y_{\max} \leqslant y \leqslant y_1, \\ \dfrac{(1-y)^2}{2(1-y_1)}, & \text{if } y_1 \leqslant y \leqslant 1. \end{cases} \tag{19}$$

where

$$y_{\max} = \sqrt{\frac{y_1}{2}}. \tag{20}$$

The graphs of $y_{max}(y_1)$, $s(y_1)$, and $\varphi(y)$ are presented for various y_1 in Figs. 4,b, 4,c, and 4,d, respectively.

7. LINEAR DROP OF THE MAGNETIC FIELD INTENSITY FROM H_{max} AT THE LEADING EDGE TO ZERO AT Y = 0.5, FOLLOWED BY A LINEAR RISE TO H_{min} AT THE LAGGING EDGE

The profile of the field in this case is shown in Fig. 5, a. Adopting the notation of (6) for α, we obtain

$$H = H_{\max} \begin{cases} 1 - 2y, & \text{if } 0 \leqslant y \leqslant 0{,}5, \\ (2y-1)\alpha, & \text{if } 0{,}5 \leqslant y \leqslant 1. \end{cases} \tag{21}$$

Substituting (21) into (5), we obtain

$$\varphi(y) = \begin{cases} y - y^2, & \text{if } 0 \leqslant y \leqslant y_{\max}, \\ y^2 - y + \dfrac{1+\alpha}{4}, & \text{if } y_{\max} \leqslant y \leqslant 0{,}5, \\ \alpha(y - y^2), & \text{if } 0{,}5 \leqslant y \leqslant 1, \end{cases} \tag{22}$$

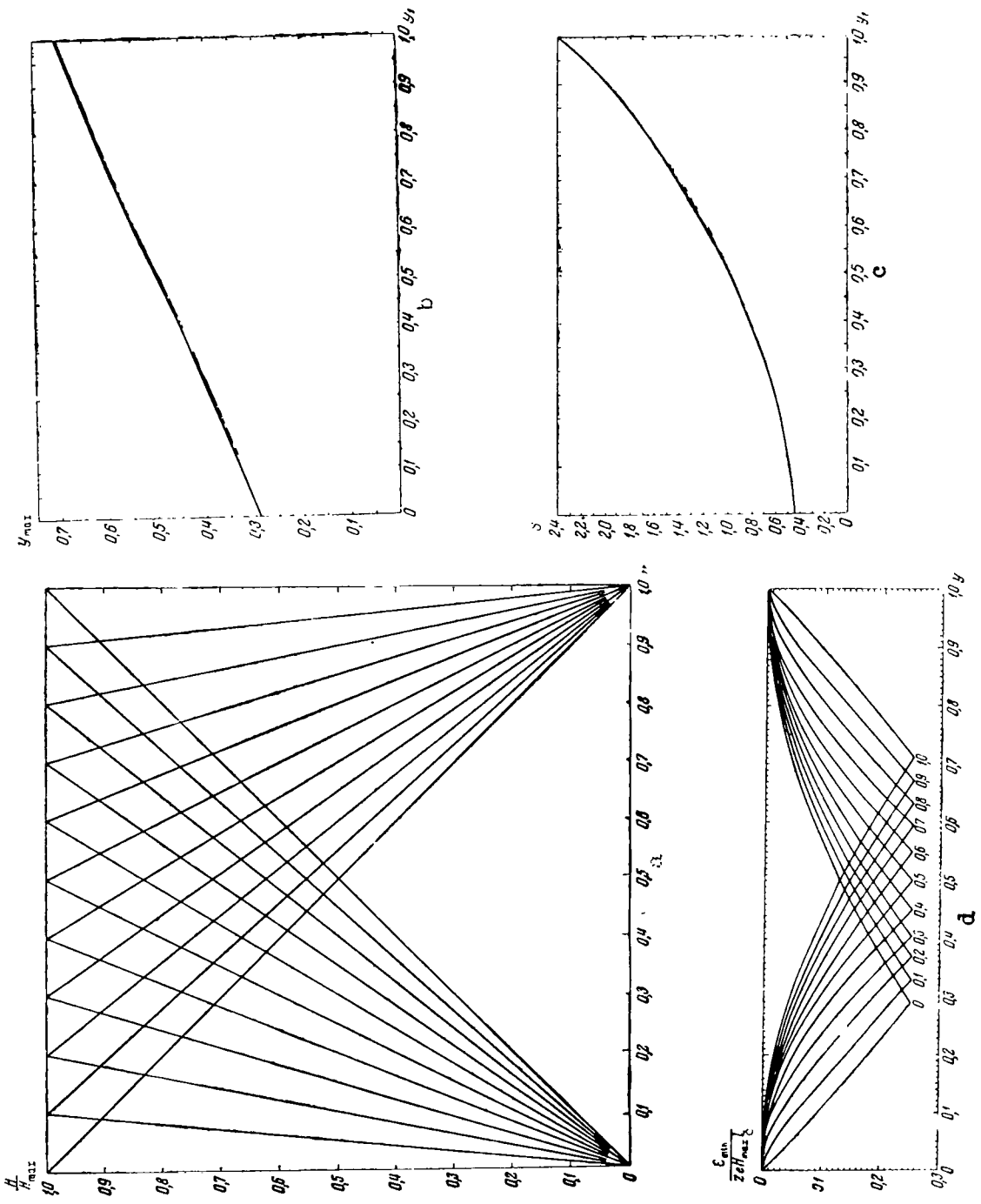

Fig. 4. Variant for the stream with a profile of the magnetic field having the form of a triangle with maximum at $y = y_1$.
Notations the same as in Fig. 2, but for various y_1 (0, 0.1, 0.2, 0.3, 0.4, 0.5, 0.6, 0.7, 0.8, 0.9, 1.0).

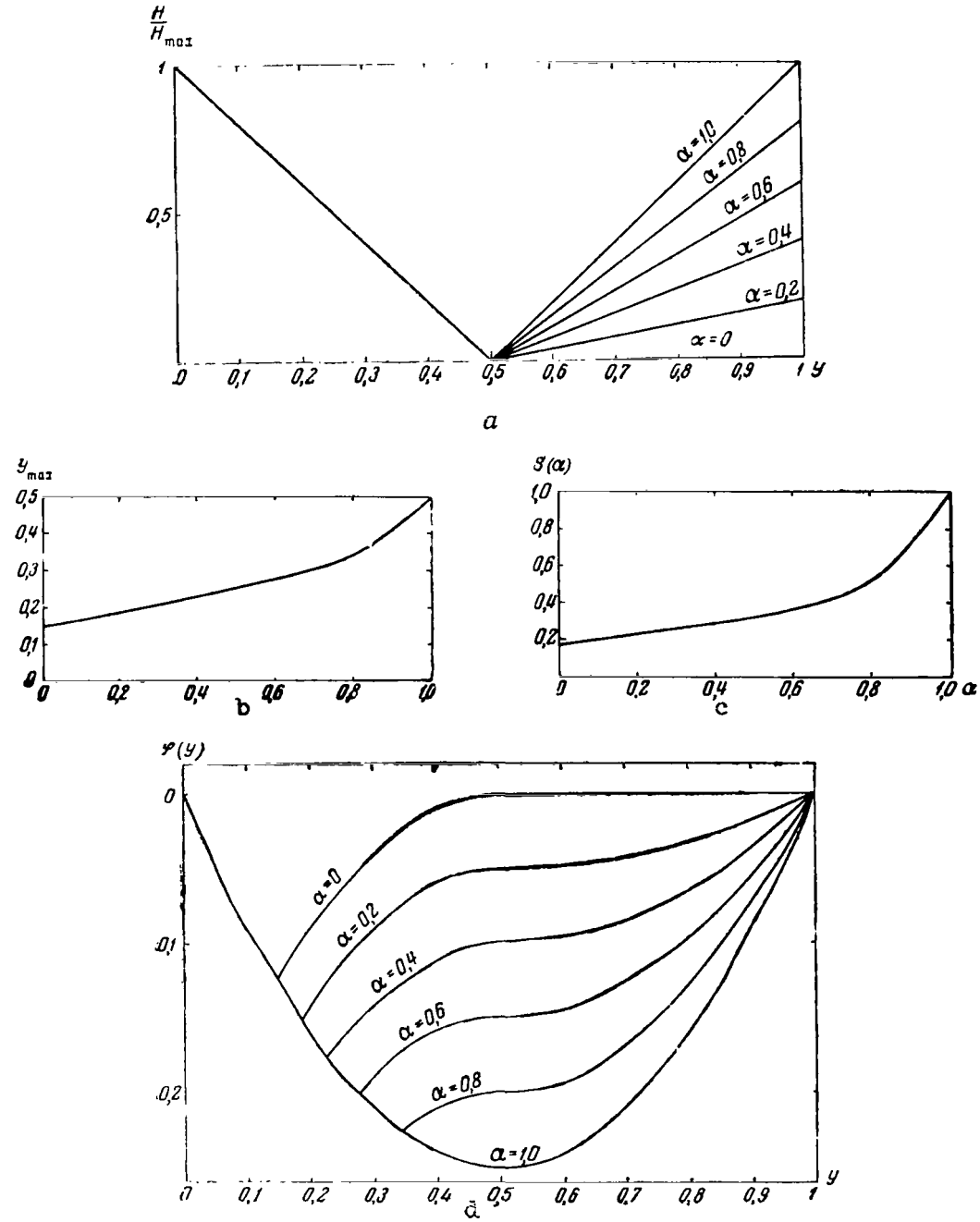

Fig. 5. Variant for a stream with a magnetic field intensity that drops linearly from H_{max} at the leading edge to zero at y = 0.5 and then rises linearly to H_{min} at the lagging edge of the stream.
Notations the same as in Fig. 2.

a

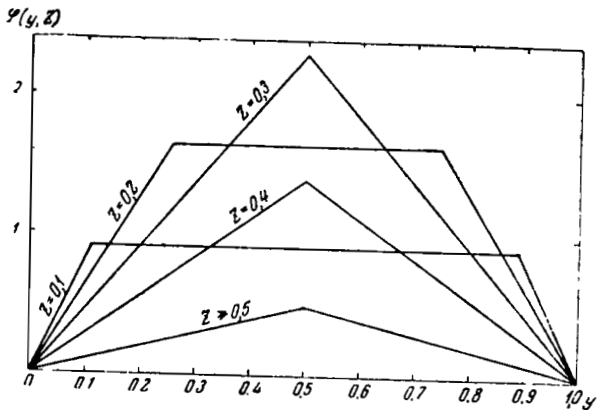
y(y, z)
z=0,3
z=0,2
z=0,4
z=0,1
z=0,5
0 0,1 0,2 0,3 0,4 0,5 0,6 0,7 0,8 0,9 1,0 y

b

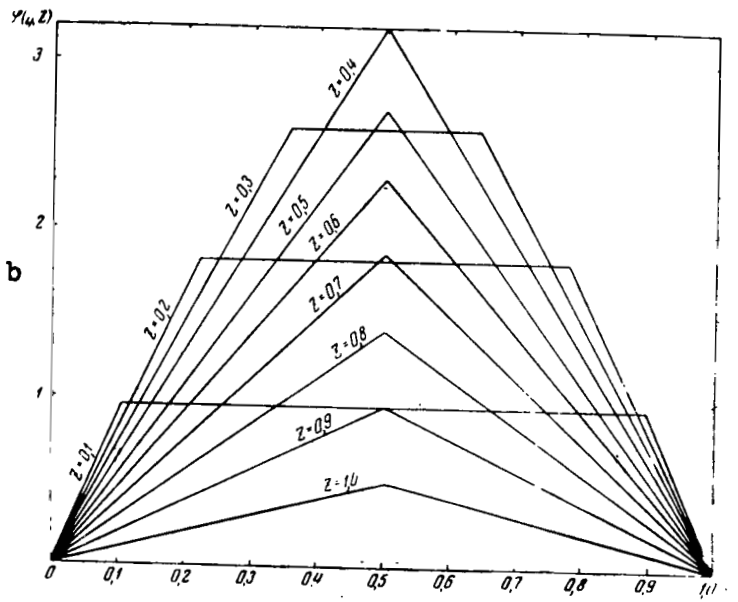
y(y, z)
z=0,4
z=0,3
z=0,5
z=0,6
z=0,2
z=0,7
z=0,8
z=0,9
z=0,1
z=1,0
0 0,1 0,2 0,3 0,4 0,5 0,6 0,7 0,8 0,9 1,0

c

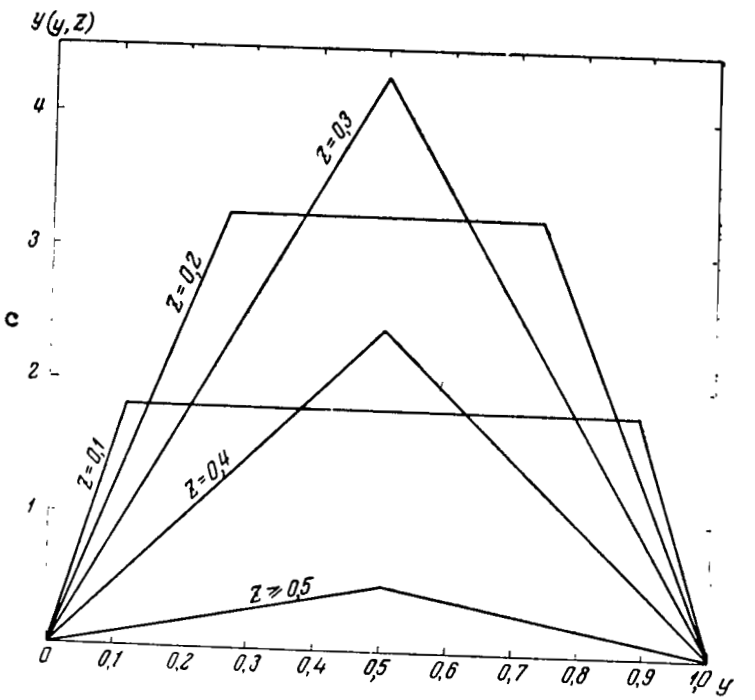
y(y, z)
z=0,3
z=0,2
z=0,1
z=0,4
z=0,5
0 0,1 0,2 0,3 0,4 0,5 0,6 0,7 0,8 0,9 1,0 y

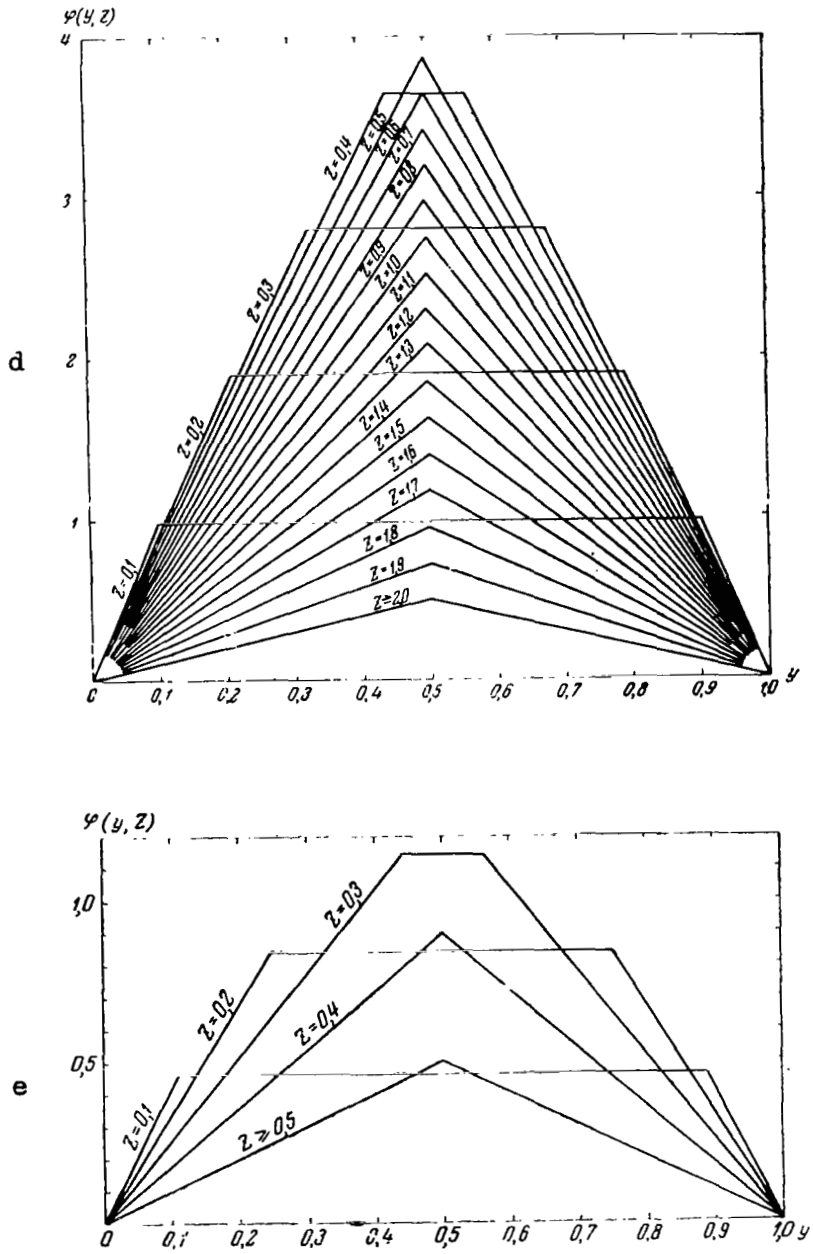

Fig. 6. Dependence of $\frac{\varepsilon_{\min}}{2ZeH_{\min}l_{\delta}} = \varphi(y, z)$ on y for various values of z when the Earth is captured by the forward front of a stream with an intensified field.

a — $\gamma = 10$, $\beta = 0{,}5$; b — $\gamma = 10$, $\beta = 1$; c — $\gamma = 10$, $\beta = 2$; d — $\gamma = 20$, $\beta = 0{,}5$; e — $\gamma = 5$, $\beta = 0{,}5$

where

$$y_{\max} = \frac{1 - \sqrt{\frac{1-\alpha}{2}}}{2}. \tag{23}$$

The graphs of y_{max} (α), s (α), and $\varphi(y)$ are presented in Figs. 5,b, c, and d, respectively, for various values of α.

8. CAPTURE OF THE EARTH BY THE FORWARD FRONT OF A STREAM WITH A FIELD INTENSIFIED IN THE FORWARD PORTION

It follows from reference [2] that in most corpuscular streams the plasma can be compressed in its forward portion on account of interaction of the stream with the interplanetary medium, and the magnetic field is correspondingly intensified. Hence it is of definite interest to find the expected change in the cosmic ray intensity under various assumptions on the nature of the field in the forward portion of the stream. Let us assume that the field falls linearly as the distance from the forward front of the stream increases, from H_{max} to H_{min} at a distance β from the front (in units of l_δ), and then, as the distance into the depth of the stream increases, the field intensity remains constant.

If z is the distance from the forward front of the stream, while y is the distance from the leading edge of the stream in units of l_δ, then

$$H(y, z) = H_{\min} \begin{cases} \gamma - \dfrac{\gamma - 1}{\beta} z, & \text{if } z \leqslant \beta, \\ 1, & \text{if } z \geqslant \beta, \end{cases} \tag{24}$$

where

$$\gamma \equiv \frac{H_{max}}{H_{\min}}. \tag{25}$$

The amplitude of the decrease in the cosmic ray intensity will be determined in a first approximation by the quantity entering into (2)

$$\varepsilon_{\min} = ZeH_{\min} l_\delta 2\varphi(y, z), \tag{26}$$

where

$$\varphi(y, z) = \frac{1}{H_{\min}} \min \left\{ \int_0^z H(y, z)\, dz;\ \int_0^y H(y, z)\, dy;\ \int_y^1 H(y, z)\, dy \right\}. \tag{27}$$

Table 1

Nature of the Variation of the Quantity $^{s}_{min}/ZeH_{min}\ ^{l}_{\delta}$ as y Varies for Various Velocities of the Stream (the Quantity $a = u_r/u_t$) and Various Cases of Capture of the Earth by the Stream (y_0) for $\gamma = 10$ and $\beta = 1$

a	y / y_0	0	0,1	0,2	0,3	0,4	0,5	0,6	0,7	0,8	0,9	1,0
	0	0	0,91	1,64	2,19	2,56	2,65	1,84	1,11	0,56	0,19	0
	0,1	0	0	0,955	1,82	2,60	3,20	2,10	1,38	0,74	0,28	0
	0,2	0	0	0	0,955	1,82	2,60	2,56	1,65	0,92	0,37	0
	0,3	0	0	0	0	0,955	1,82	2,60	1,92	1,10	0,46	0
1	0,4	0	0	0	0	0	0,955	1,82	2,19	1,28	0,55	0
	0,5	0	0	0	0	0	0	0,955	1,82	1,46	0,64	0
	0,6	0	0	0	0	0	0	0	0,955	1,64	0,73	0
	0,7	0	0	0	0	0	0	0	0	0,955	0,82	0
	0,8	0	0	0	0	0	0	0	0	0	0,91	0
	0	0	0,82	1,28	1,38	1,12	0,5	0,4	0,3	0,2	0,1	0
	0,1	0	0	1,64	1,92	1,84	1,40	0,4	0,3	0,2	0,1	0
	0,2	0	0	0	1,82	2,56	2,30	1,12	0,3	0,2	0,1	0
	0,3	0	0	0	0	1,82	3,20	1,84	0,84	0,2	0,1	0
2	0,4	0	0	0	0	0	1,82	2,56	1,38	0,56	0,28	0
	0,5	0	0	0	0	0	0	1,82	1,92	0,92	0,28	0
	0,6	0	0	0	0	0	0	0	1,82	1,28	0,46	0
	0,7	0	0	0	0	0	0	0	0	1,64	0,64	0
	0,8	0	0	0	0	0	0	0	0	0	0,82	0
	0	0	0,73	0,92	0,57	0,4	0,5	0,4	0,3	0,2	0,1	0
	0,1	0	0	1,46	1,38	0,76	0,5	0,4	0,3	0,2	0,1	0
	0,2	0	0	0	2,19	1,84	0,95	0,4	0,3	0,2	0,1	0
	0,3	0	0	0	0	2,60	2,30	0,76	0,3	0,2	0,1	0
	0,4	0	0	0	0	0	2,60	1,84	0,57	0,2	0,1	0
3	0,5	0	0	0	0	0	0	2,60	1,38	0,38	0,1	0
	0,6	0	0	0	0	0	0	0	2,19	0,92	0,19	0
	0,7	0	0	0	0	0	0	0	0	1,46	0,46	0
	0,8	0	0	0	0	0	0	0	0	0	0,73	0
	0	0	0,64	0,56	0,3	0,4	0,5	0,4	0,3	0,2	0,1	0
	0,1	0	0	1,28	0,84	0,4	0,5	0,4	0,3	0,2	0,1	0
	0,2	0	0	0	1,92	1,12	0,5	0,4	0,3	0,2	0,1	0
	0,3	0	0	0	0	2,56	1,40	0,4	0,3	0,2	0,1	0
	0,4	0	0	0	0	0	3,20	1,12	0,3	0,2	0,1	0
4	0,5	0	0	0	0	0	0	2,56	0,84	0,2	0,1	0
	0,6	0	0	0	0	0	0	0	1,92	0,56	0,1	0
	0,7	0	0	0	0	0	0	0	0	1,28	0,28	0
	0,8	0	0	0	0	0	0	0	0	0	0,64	0
	0	0	0,55	0,2	0,3	0,4	0,5	0,4	0,3	0,2	0,1	0
	0,1	0	0	1,10	0,3	0,4	0,5	0,4	0,3	0,2	0,1	0
	0,2	0	0	0	1,65	0,4	0,5	0,4	0,3	0,2	0,1	0
	0,3	0	0	0	0	2,10	0,5	0,4	0,3	0,2	0,1	0
	0,4	0	0	0	0	0	2,65	0,4	0,3	0,2	0,1	0
5	0,5	0	0	0	0	0	0	2,10	0,3	0,2	0,1	0
	0,6	0	0	0	0	0	0	0	1,65	0,2	0,1	0
	0,7	0	0	0	0	0	0	0	0	1,10	0,1	0
	0,8	0	0	0	0	0	0	0	0	0	0,55	0
	0	0	0,46	0,2	0,3	0,4	0,5	0,4	0,3	0,2	0,1	0
	0,1	0	0	0,93	0,3	0,4	0,5	0,4	0,3	0,2	0,1	0
	0,2	0	0	0	1,38	0,4	0,5	0,4	0,3	0,2	0,1	0
	0,3	0	0	0	0	1,84	0,5	0,4	0,3	0,2	0,1	0
	0,4	0	0	0	0	0	2,30	0,4	0,3	0,2	0,1	0
6	0,5	0	0	0	0	0	0	1,84	0,3	0,2	0,1	0
	0,6	0	0	0	0	0	0	0	1,38	0,2	0,1	0
	0,7	0	0	0	0	0	0	0	0	0,92	0,1	0
	0,8	0	0	0	0	0	0	0	0	0	0,46	0

Table 2

Nature of the Variation of the Quantity $\varepsilon_{min}/ZeH_{min}\, l_{\delta}$ as y Varies for Various Velocities of the Stream (the Quantity $a = u_r/u_t$) and Various Cases of Capture of the Earth by the Stream (y_0) for $\gamma = 10$ and $\beta = 2$

a	y_0 \ y	0	0,1	0,2	0,3	0,4	0,5	0,6	0,7	0,8	0,9	1,0
2	0	0	0,91	1,64	2,19	2,56	2,75	1,84	1,11	0,56	0,19	0
	0,1	0	0	1,82	2,46	2,92	3,20	2,20	1,38	0,74	0,28	0
	0,2	0	0	0	1,91	3,28	3,65	2,56	1,65	0,92	0,37	0
	0,3	0	0	0	0	1,91	3,64	2,92	1,92	1,10	0,46	0
	0,4	0	0	0	0	0	1,91	3,28	2,19	1,28	0,55	0
	0,5	0	0	0	0	0	0	1,91	2,46	1,46	0,64	0
	0,6	0	0	0	0	0	0	0	1,91	1,64	0,73	0
	0,7	0	0	0	0	0	0	0	0	1,82	0,82	0
	0,8	0	0	0	0	0	0	0	0	0	0,91	0
4	0	0	0,82	1,28	1,38	1,12	0,5	0,4	0,3	0,2	0,1	0
	0,1	0	0	1,64	1,92	1,84	1,40	0,4	0,3	0,2	0,1	0
	0,2	0	0	0	2,46	2,56	2,30	1,12	0,3	0,2	0,1	0
	0,3	0	0	0	0	3,28	3,20	1,84	0,84	0,2	0,1	0
	0,4	0	0	0	0	0	3,64	2,56	1,38	0,56	0,1	0
	0,5	0	0	0	0	0	0	3,28	1,92	0,92	0,28	0
	0,6	0	0	0	0	0	0	0	2,46	1,28	0,46	0
	0,7	0	0	0	0	0	0	0	0	1,64	0,64	0
	0,8	0	0	0	0	0	0	0	0	0	0,82	0
6	0	0	0,73	0,92	0,57	0,4	0,5	0,4	0,3	0,2	0,1	0
	0,1	0	0	1,46	1,38	0,76	0,5	0,4	0,3	0,2	0,1	0
	0,2	0	0	0	2,19	1,84	0,95	0,4	0,3	0,2	0,1	0
	0,3	0	0	0	0	2,92	2,30	0,76	0,3	0,2	0,1	0
	0,4	0	0	0	0	0	3,65	1,84	0,57	0,2	0,1	0
	0,5	0	0	0	0	0	0	2,92	1,38	0,38	0,1	0
	0,6	0	0	0	0	0	0	0	2,19	0,92	0,19	0
	0,7	0	0	0	0	0	0	0	0	1,46	0,46	0
	0,8	0	0	0	0	0	0	0	0	0	0,73	0

Table 3

Nature of the Variation of the Quantity $\varepsilon_{min}/ZeH_{min}\, l_{\delta}$ as y Varies for Various Velocities of the Stream (the Quantity $a = u_r/u_t$) and Various Cases of Capture of the Earth by the Stream (y_0) for $\gamma = 10$ and $\beta = 0,5$

a	y_0	0	0,1	0,2	0,3	0,4	0,5	0,6	0,7	0,8	0,9	1,0
2	0	0	0,64	0,56	0,3	0,4	0,5	0,4	0,3	0,2	0,1	0
	0,1	0	0	1,28	0,84	0,4	0,5	0,4	0,3	0,2	0,1	0
	0,2	0	0	0	1,64	1,12	0,5	0,4	0,3	0,2	0,1	0
	0,3	0	0	0	0	1,64	1,40	0,4	0,3	0,1	0,1	0
	0,4	0	0	0	0	0	1,64	1,12	0,3	0,2	0,1	0
	0,5	0	0	0	0	0	0	1,64	0,84	0,2	0,1	0
	0,6	0	0	0	0	0	0	0	1,64	0,56	0,1	0
	0,7	0	0	0	0	0	0	0	0	1,28	0,28	0
	0,8	0	0	0	0	0	0	0	0	0	0,64	0
4	0	0	0,28	0,2	0,3	0,4	0,5	0,4	0,3	0,2	0,1	0
	0,1	0	0	0,56	0,3	0,4	0,5	0,4	0,3	0,2	0,1	0
	0,2	0	0	0	0,84	0,4	0,5	0,4	0,3	0,2	0,1	0

Table 3 (Conclusion)

a	y_0 \ y	0	0,1	0,2	0,3	0,4	0,5	0,6	0,7	0,8	0,9	1,0
4	0,3	0	0	0	0	1, 12	0, 5	0, 4	0, 3	0, 2	0, 1	0
	0, 4	0	0	0	0	0	1, 40	0, 4	0, 3	0, 2	0, 1	0
	0, 5	0	0	0	0	0	0	1, 12	0, 3	0, 2	0, 1	0
	0, 6	0	0	0	0	0	0	0	0, 84	0, 2	0, 1	0
	0, 7	0	0	0	0	0	0	0	0	0, 56	0, 1	0
	0, 8	0	0	0	0	0	0	0	0	0	0, 28	0
6	0	0	0, 1	0, 2	0, 3	0, 4	0, 5	0, 4	0, 3	0, 2	0, 1	0
	0, 1	0	0	0, 2	0, 3	0, 4	0, 5	0, 4	0, 3	0, 2	0, 1	0
	0, 2	0	0	0	0, 3	0, 4	0, 5	0, 4	0, 3	0, 2	0, 1	0
	0, 3	0	0	0	0	0, 4	0, 5	0, 4	0, 3	0, 2	0, 1	0
	0, 4	0	0	0	0	0	0, 5	0, 4	0, 3	0, 2	0, 1	0
	0, 5	0	0	0	0	0	0	0, 4	0, 3	0, 2	0, 1	0
	0, 6	0	0	0	0	0	0	0	0, 3	0, 2	0, 1	0
	0, 7	0	0	0	0	0	0	0	0	0, 2	0, 1	0
	0, 8	0	0	0	0	0	0	0	0	0	0, 1	0

Table 4

Nature of the Variation of the Quantity $s_{min}/ZeH_{min}\, l_{\delta}$ as y Varies for Various Velocities of the Stream (the Quantity a $= u_r/u_t$) and Various Cases of Capture of the Earth by the Stream (y_0) for $\gamma = 20$ and $\beta = 0{,}5$

a	y_0 \ y	0	0,1	0,2	0,3	0,4	0,5	0,6	0,7	0,8	0,9	1,0
2	0	0	1, 24	0, 96	0, 3	0, 4	0, 5	0, 4	0, 3	0, 2	0, 1	0
	0, 1	0	0	2, 48	1, 44	0, 4	0, 5	0, 4	0, 3	0, 2	0, 1	0
	0, 2	0	0	0	3, 24	1, 92	0, 5	0, 4	0, 3	0, 2	0, 1	0
	0, 3	0	0	0	0	3, 24	2, 40	0, 4	0, 3	0, 2	0, 1	0
	0, 4	0	0	0	0	0	3, 24	1, 92	0, 3	0, 2	0, 1	0
	0, 5	0	0	0	0	0	0	3, 24	1, 44	0, 2	0, 1	0
	0, 6	0	0	0	0	0	0	0	3, 24	0, 96	0, 1	0
	0, 7	0	0	0	0	0	0	0	0	2, 48	0, 48	0
	0, 8	0	0	0	0	0	0	0	0	0	1, 24	0
4	0	0	0, 48	0, 2	0, 3	0, 4	0, 5	0, 4	0, 3	0, 2	0, 1	0
	0, 1	0	0	0, 96	0, 3	0, 4	0, 5	0, 4	0, 3	0, 2	0, 1	0
	0, 2	0	0	0	1, 44	0, 4	0, 5	0, 4	0, 3	0, 2	0, 1	0
	0, 3	0	0	0	0	1, 92	0, 5	0, 4	0, 3	0, 2	0, 1	0
	0, 4	0	0	0	0	0	2, 40	0, 4	0, 3	0, 2	0, 1	0
	0, 5	0	0	0	0	0	0	1, 92	0, 3	0, 2	0, 1	0
	0, 6	0	0	0	0	0	0	0	1, 44	0, 2	0, 1	0
	0, 7	0	0	0	0	0	0	0	0	0, 96	0, 1	0
	0, 8	0	0	0	0	0	0	0	0	0	0, 48	0
6	0	0	0, 1	0, 2	0, 3	0, 4	0, 5	0, 4	0, 3	0, 2	0, 1	0
	0, 1	0	0	0, 2	0, 3	0, 4	0, 5	0, 4	0, 3	0, 2	0, 1	0
	0, 2	0	0	0	0, 3	0, 4	0, 5	0, 4	0, 3	0, 2	0, 1	0
	0, 3	0	0	0	0	0, 4	0, 5	0, 4	0, 3	0, 2	0, 1	0
	0, 4	0	0	0	0	0	0, 5	0, 4	0, 3	0, 2	0, 1	0
	0, 5	0	0	0	0	0	0	0, 4	0, 3	0, 2	0, 1	0
	0, 6	0	0	0	0	0	0	0	0, 3	0, 2	0, 1	0
	0, 7	0	0	0	0	0	0	0	0	0, 2	0, 1	0
	0, 8	0	0	0	0	0	0	0	0	0	0, 1	0

Table 5

Nature of the Variation of the Quantity $\varepsilon_{min}/ZeH_{min}\, l_{\delta}$ as y Varies for Various Velocities of the Stream (the Quantity $a = u_r/u_t$) and Various Cases of Capture of the Earth by the Stream (y_0) for $\gamma = 5$ and $\beta = 0{,}5$

a	y_0 \ y	0	0,1	0,2	0,3	0,4	0,5	0,6	0,7	0,8	0,9	1,0
2	0	0	0,34	0,36	0,3	0,4	0,5	0,4	0,3	0,2	0,1	0
	0,1	0	0	0,68	0,54	0,4	0,5	0,4	0,3	0,2	0,1	0
	0,2	0	0	0	0,84	0,72	0,5	0,4	0,3	0,2	0,1	0
	0,3	0	0	0	0	0,84	0,90	0,4	0,3	0,2	0,1	0
	0,4	0	0	0	0	0	0,84	0,72	0,3	0,2	0,1	0
	0,5	0	0	0	0	0	0	0,84	0,54	0,2	0,1	0
	0,6	0	0	0	0	0	0	0	0,84	0,36	0,1	0
	0,7	0	0	0	0	0	0	0	0	0,68	0,18	0
	0,8	0	0	0	0	0	0	0	0	0	0,34	0
4	0	0	0,18	0,2	0,3	0,4	0,5	0,4	0,2	0,2	0,1	0
	0,1	0	0	0,36	0,3	0,4	0,5	0,4	0,3	0,2	0,1	0
	0,2	0	0	0	0,54	0,4	0,5	0,4	0,3	0,2	0,1	0
	0,3	0	0	0	0	0,72	0,5	0,4	0,3	0,2	0,1	0
	0,4	0	0	0	0	0	0,90	0,4	0,3	0,2	0,1	0
	0,5	0	0	0	0	0	0	0,72	0,3	0,2	0,1	0
	0,6	0	0	0	0	0	0	0	0,54	0,2	0,1	0
	0,7	0	0	0	0	0	0	0	0	0,36	0,1	0
	0,8	0	0	0	0	0	0	0	0	0	0,18	0
6	0	0	0,1	0,2	0,3	0,4	0,5	0,4	0,3	0,2	0,1	0
	0,1	0	0	0,2	0,3	0,4	0,5	0,4	0,3	0,2	0,1	0
	0,2	0	0	0	0,3	0,4	0,5	0,4	0,3	0,2	0,1	0
	0,3	0	0	0	0	0,4	0,5	0,4	0,3	0,2	0,1	0
	0,4	0	0	0	0	0	0,5	0,4	0,3	0,2	0,1	0
	0,5	0	0	0	0	0	0	0,4	0,3	0,2	0,1	0
	0,6	0	0	0	0	0	0	0	0,3	0,2	0,1	0
	0,7	0	0	0	0	0	0	0	0	0,2	0,1	0
	0,8	0	0	0	0	0	0	0	0	0	0,1	0

Substituting (24) into (27), we obtain

$$q(y, z) = \begin{cases} y\left(\gamma - \frac{\gamma-1}{\beta} z\right), & \text{if } y \leqslant z\,\frac{\gamma\beta - \frac{1}{2}(\gamma-1)z}{\gamma\beta - (\gamma-1)z} \\ (1-y)\left(\gamma - \frac{\gamma-1}{\beta} z\right), & \text{if } 1-y \leqslant z\,\frac{\gamma\beta - \frac{1}{2}(\gamma-1)z}{\gamma\beta - (\gamma-1)z} \\ \frac{z}{\beta}\left[\gamma\beta - \frac{1}{2}(\gamma-1)z\right], & \text{if } y;\ 1-y \geqslant z\,\frac{\gamma\beta - \frac{1}{2}(\gamma-1)z}{\gamma\beta - (\gamma-1)z} \end{cases} \text{when } z \leqslant \beta, \\ \begin{cases} y, & \text{if } y \leqslant 0{,}5 \\ 1-y, & \text{if } 1-y \leqslant 0{,}5 \end{cases} \text{when } z \geqslant \beta. \qquad (28)$$

Graphs of the function $\varphi(y, z)$, calculated according to (28) for various values of γ and β, are presented in Fig. 6 (a -- for $\gamma = 10$, $\beta = 0{,}5$; b -- for $\gamma = 10$. $\beta = 1$; c -- for $\gamma = 10$, $\beta = 2$; d -- for $\gamma = 20$; $\beta = 0{,}5$; e -- for $\gamma = 5$. $\beta = 0{,}5$).

It is easy to calculate the expected variation of the cosmic ray intensity by means of these graphs for various cases of capture of the Earth by the stream and various velocities of the latter. The trajectory of the Earth's motion in the stream

$$z = a(y - y_0), \tag{29}$$

where y_0 is the distance from the leading edge at which the Earth is captured by the forward front, while the coefficient

$$a = u_r / u_t, \tag{30}$$

i.e. represents the ratio of the radial component to the tangential component of the velocity of the stream with respect to the Earth. The results of the corresponding calculations of the quantity $\frac{\varepsilon_{min}}{2ZeH_{min}l_\delta}$ with the aid of the graphs of Fig. 6 are presented in Tables 1-5 for various a and y_0. We can see from the Table that intensification of the field in the forward portion of the stream should actually lead to a far sharper drop in the cosmic ray intensity than in the case of a homogeneous field.

BIBLIOGRAPHY

1. L. I. Dorman. Works of the International Conference on Cosmic Rays, 1959, Publishing House of the Academy of Sciences USSR, 1960, Vol. 4, p. 113.
2. Ya. L. Blokh, L. I. Dorman, N. S. Kaminer. This Collection, p 1.

ABSTRACT

The article presents results of calculations of the expected profile of the intensity variations of the neutron and the meson components of cosmic rays. The calculations are given for different cases of the Earth's capture in the stream with homogeneous frozen magnetic field with 300 $H_\delta l_\delta$ = 40, 60, 80, 100 and 120 Bev for the velocities of the front 10^7, $2 \cdot 1^7$, $3.5 \cdot 10^7$, $6 \cdot 10^7$, $1.2 \cdot 10^7$ and $2.4 \cdot 10^8$ cm/sec. The profile is determined of the variations of the boundary energy of the variations spectrum ε_{min} with the following distribution of the field in the stream: 1) lineary fall from H_{max} at the leading edge of the stream to H_{min} at the lagging edge (with the change of H_{min}/H_{max} from 0 to 1; 2) the fall along the parabola from H_{max} to H_{min}; 3) the profile of the field in a triangular form with the maximum at different distances from the leading edge of the stream; 4) the profile of the field with the minimum in the middle of the stream. The profile is also calculated of the ε_{min} changes with different suppositions about the character of field compression in the frontal part of the stream for different cases of the Earth's capture in a stream and for different values of the stream's velocity.

DIURNAL VARIATIONS OF THE HARD COMPONENT OF COSMIC RAYS NEAR THE MINIMUM OF SOLAR ACTIVITY

Ye. S. Glokova

1. INTRODUCTION

It has been established that the cosmic ray intensity observed at a given point varies with the rotation of the Earth around its axis. Until recently it was believed that there are considerable variations only with respect to solar time. They can be created partially by atmospheric effects, but certain facts leave no doubt that an anisotropy, closely related to the Sun and solar activity, exists in the intensity of primary cosmic rays. This anisotropy is apparently created in the solar system, possibly in the environs of the Earth. Variations with respect to solar time, if they do exist, are very small in comparison with the solar-diurnal variations. This is explained by the presence in the galaxy and in the solar system of magnetic fields, which confuse the trajectories of cosmic ray particles, as a result of which the sources of the latter in the galaxy cannot be detected.

In 1957, the work of A. M. Conforto and J. A. Simpson [1] was published, in which the authors express the opinion that in 1954, during a year of a deep minimum of the solar activity, a stellar-diurnal variation with a maximum at about 8-10 hrs, local stellar time, was observed in the intensity of the neutron and ionizing components of cosmic rays.

In this way the authors explained the anomalous variation of the phase of the solar-diurnal wave, which was observed in 1954 and was described by a number of authors [2, 3]. The problem of the cause of the unusual behavior of the diurnal variation in 1954 is closely related to an investigation of the properties of the space surrounding the Earth and merits a careful study.

By now the following experimental facts pertaining to this problem have been published.

1. In 1954 at the Juancaio station the average solar-diurnal vector for the year in the neutron component was close to zero. The monthly vectors showed a displacement of the phase 2π radians

counterclockwise for a period of 12 to 13 months.

2. A similar, although not exactly identical, phase displacement was observed in the neutron component at the Climax station and in the hard component at several stations.

3. When the vectors were arranged according to stellar time, a stellar-diurnal variation was obtained for all the stations with a maximum from 8 to 12 hrs, local stellar time.

4. There was a real solar-diurnal variation in the hard component of cosmic rays on the average for 1954.

5. The monthly and seasonal vectors showed an anomalous phase displacement toward the early morning hours. In the summer of 1954 the maximum of the intensity came at 2-3 hrs, local solar time.

6. In the minimum of solar activity in 1944, no such anomalous phase displacement was observed.

7. It was shown in reference [3] on the basis of the materials of three Soviet stations -- Moscow, Tbilisi, and Irkutsk -- that during the period 1953-1955, a phase displacement was observed not only for the seasonal or monthly vectors, but also for the average yearly vectors. When the seasonal vectors were averaged over the four seasons by the method of sliding means, the phase of the average yearly vectors was displaced to the earlier hours until the summer of 1954, after which it began to be displaced toward the later hours. Counterclockwise rotation of the seasonal vectors around the average yearly vectors was superimposed on this general phase displacement.

It was also shown that the rapid phase displacement of the average yearly vector close to the minimum of solar activity in 1954 may be the result of a temperature effect. After the introduction of temperature corrections, calculated according to aerological temperature data [3], the total phase displacement of the average yearly vector decreased to 50-60°, instead of the 130° found without considering temperature corrections.

The difference in amplitude and phase of the observed vector in the summer and winter seasons could also be explained by a seasonal difference in the value of the temperature correction. The problem of the possibility of explaining the seasonal counterclockwise rotation of the vector by a temperature effect remained open, since the temperature corrections for the spring and autumn were not determined.

This work has investigated the cause of the anomalous behavior of the diurnal variation in the minimum of the solar activity by comparing the diurnal variation in years of high and low solar activity on the basis of material of a number of stations. This work is a continuation of reference [3].

2. TREATMENT OF MATERIAL AND RESULTS OF THE TREATMENT

In preparing reference [3], the material was treated in the following way: the diurnal variations were calculated for each month,

excluding incomplete days in the process. An harmonic analysis was performed, and the harmonic coefficients of the first harmonic were averaged for the season. To obtain the average yearly vectors, the seasonal vectors were averaged over the four seasons by the method of sliding means. In this way consecutive average yearly vectors, lying one season apart, were obtained. Now we applied this method to the treatment of material from other stations. A list of stations whose data were used is presented in Table 1.

Table 1

Item No.	Stations	Geographical co-ordinates	Geomagnetic co-ordinates	Period of observations, years	Instrument
1	Tbilisi	41.7°N 44.8°E	36.3° 122.0°	1953-1955	I
2	Irkutsk	52.5 N 104.0 E	40.8 174.6	1953-1955	I
3	Moscow	55.0 N 37.3 E	50.8 120.5	1953-1956	I
				1957-1958	I
4	Yakutsk	61.0 N 129.7 E	51.0 193.8	1953-1956	I
				1957-1958	I
5	Freiburg [1]	47.9 N 7.8 E	49.3 89.3	1953-1955	I
6	Rome [1]	41.8 N 12.6 E	42.4 92.1	1954-1955	T
7	Christ Church [4]	43.5 N 172.6 W	-48.1 252.6	1943-1945	I
				1952-1955	I
				1957-1958	I
8	Cheltenham [7]	38.7 N 76.8 W	50.1 350.4	1943-1955	I
				1952-1955	I
				1957-1958	I
9	Juancaio [1, 4] (h=3350m)	12.0 S 75.3 W	-0.6 353.8	1943-1945	I
				1952-1955	I, N
				1957-1958	I
10	Climax [1] (h=3400m)	32.4 N 106.2 W	48.1 315.5	1953-1955	N

Note: I -- ionization chamber, T -- telescope, N -- neutron monitor.

In the treatment of material pertaining to the years of high solar activity 1957-1958, not only incomplete days, but also days in which a large effect of decrease in intensity, related to magnetic storms, was observed, were excluded. The same days were excluded for all the stations.

The variations of the average yearly and seasonal vectors are presented in Figs. 1 and 2. Each season includes three months: 1 -- December (of preceding year), January, February; 2 -- March, April, May; 3 -- June, July, August; 4 -- September, October, November. Each average yearly sliding vector (Fig. 1) is also denoted by numbers.

The number 1 denotes the vector averaged over seasons 2, 3, and 4 of 1951 and the first season of 1952, etc.

The numeration of the average yearly vectors (Fig. 1) is given in Table 2.

Data on the neutron component, obtained at the stations of Juancaio and Climax, as well as materials of observations using the cubic telescope at the Rome station during the period 1953-1955 were taken from reference [1]. The determination of the amplitude and phase of the diurnal variation of the neutron component in the work mentioned was performed by a method differing from that we used. In Figs. 1, 2, and 7, data on the neutron component are plotted in arbitrary units, while data on the hard component are plotted in percents of the average value. Hence the absolute values for the neutron and hard components are not comparable, but the general nature of the change in the vectors of the diurnal variation is rather comparable. The materials for 1957-1958 were obtained from the World Data Center B.

The seasonal variations and variations of the average yearly vectors (Figs. 1, 2) fully confirm the results obtained in reference [3]. As can be seen from Fig. 1, the effect of phase displacement of the average yearly vector of the hard component when the minimum of solar activity in 1954 is approached is observed at all stations situated in the Northern and Southern Hemispheres, and on the Equator. The 13th and 14th vectors, which are centered between the summer and autumn seasons of the Northern Hemisphere, have a minimum phase.

In Moscow there is a great increase in the amplitude after the minimum phase. The material for this station is not uniform. In July 1954, the instrument was transferred to another place with considerably less equivalent shielding on account of ceilings (instead of 120-130 g/cm^2, the shielding became equal to 35 g/cm^2).

Fig. 1 also shows the displacement of the average yearly vector in 1943-1945 for stations 7, 8, and 9 (Table 1). It is clearly evident from the figure that during the minimum of 1944, a decrease in the amplitude of the diurnal variation and a phase displacement toward the earlier hours was also observed, although the effect was not so sharply pronounced as in 1954.

Fig. 2 confirms the counterclockwise rotation of the seasonal vectors of the diurnal wave around the average yearly vector in 1954. This rotation is well expressed in the hard component at all the stations of the Northern Hemisphere, as well as in the neutron component at the equatorial station of Juancaio. The arrangement of the seasonal vectors is similar at all the stations of the Northern Hemisphere. At Christ Church station in the Southern Hemisphere, the seasonal variation is poorly expressed, and the arrangement of the seasonal vectors differs from their arrangement in the Northern Hemisphere, although the minimum phase, just as in the Northerm Hemisphere, comes at vectors 3-4. The phase displacement of the average

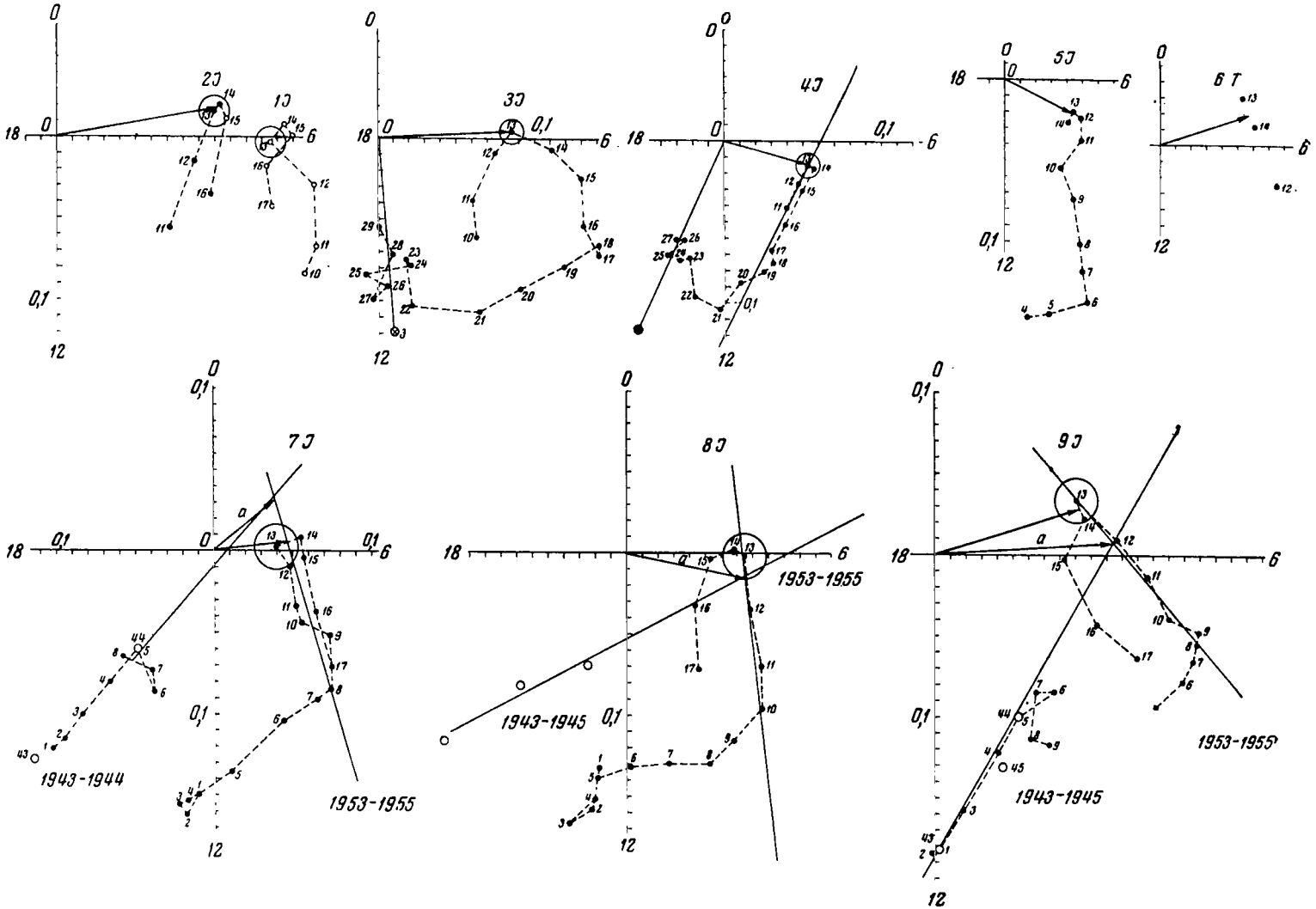

Fig. 1. Variation of the average yearly sliding vector on a harmonic dial

The ends of the vectors are connected with dotted lines. The numbers and letters around each figure show the number of the station in Table 1 and the instrument. The numeration of the vectors is given in Table 2. For stations 7, 8 and 9, the sliding vectors are also shown for the period from 1943 to 1945; the numeration begins with the average yearly vector for 1943. The circle around the end of vector 13 is traced by the radius of the probable error.

Table 2

Years	Seasons			
	1, 2, 3, 4	2, 3, 4, 1	3, 4, 1, 2	4, 1, 2, 3
1951—1952	1	2	3	4
1952—1953	5	6	7	8
1953—1954	9	10	11	12
1954—1955	13	14	15	16
1955—1956	17	18	19	20
1957—1958	21	22	23	24
1958—1959	25	26	27	28

yearly vector can also be seen clearly in Fig. 2. All the seasonal vectors are displaced in the direction of the earlier hours in 1954, and in the direction of later hours in 1955.

Identical ASK-1 instruments, which record variations with a very great accuracy, have been set up at the stations of Moscow and Yakutsk. Fig. 3 shows the arrangement of seasonal vectors at these two stations individually in 1954, 1955, and 1956; for the Moscow station -- also in 1951-1952.

In forming the seasonal vectors in this case, the average yearly sliding vector, centered around the given season, was subtracted.

A large seasonal variation of the diurnal vector is observed at both stations in 1954 and 1955. In 1956 it actually disappeared. In 1951-1952, a seasonal variation was observed in the arrangement of the vectors, similar to the variations of 1954-1955, but with a smaller amplitude.

Fig. 4 shows the seasonal path of the diurnal variation of the hard component, individually according to years, for stations 7, 8, and 9 from 1952 to 1955, after subtracting the sliding average yearly vector. Here no increase in the seasonal variation was noted in 1954. At the equatorial station (9) the seasonal variation was small, while at a station of the Northern Hemisphere (8) it was better expressed. The arrangement of the vectors was similar in 1952, 1953, and 1954; it changed in 1955. At the southern latitude station (7), there was no regular seasonal variation during these years, but in 1952 and 1953 a tendency toward the opposite arrangement of the seasonal variations in the Northern and Southern Hemispheres can be noted. This tendency disappeared in 1954 and reappeared in 1955.

Fig. 5, a presents the dependence of the amplitude of the vector of the average yearly diurnal wave, having a minimum phase (vectors 13, 14, Fig. 1), on the geographical latitude. We can see from Fig. 5 that the amplitude of the observable vector having a minimum phase varies in proportion to the geographical latitude of the station. Moreover, at the stations of the USSR the vectors of the minimum phase have greater values than at other stations situated

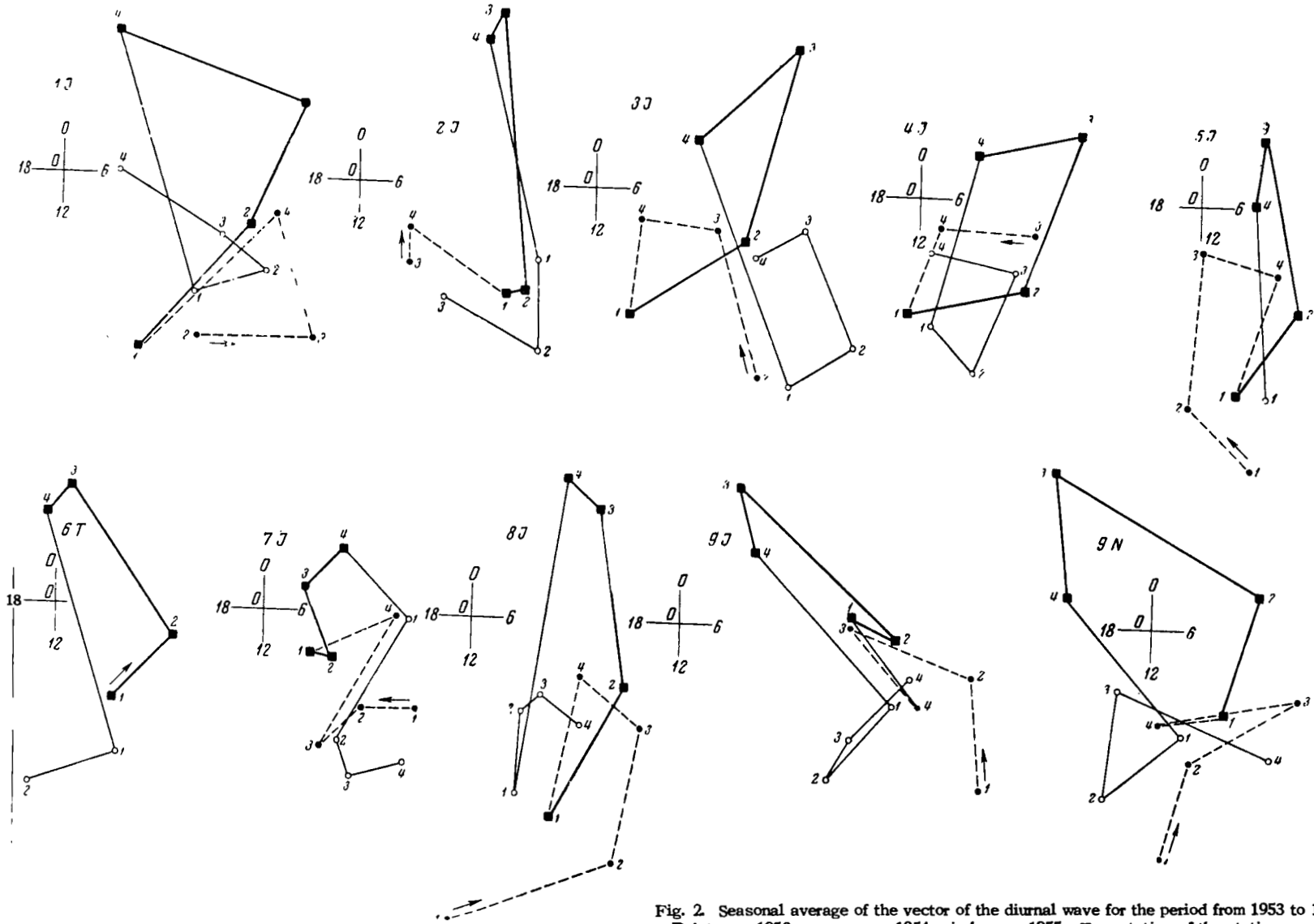

Fig. 2. Seasonal average of the vector of the diurnal wave for the period from 1953 to 1955. Points — 1953, squares — 1954, circles — 1955. For notation of the stations, see Table 1 on page 84, seasons — on page 84.

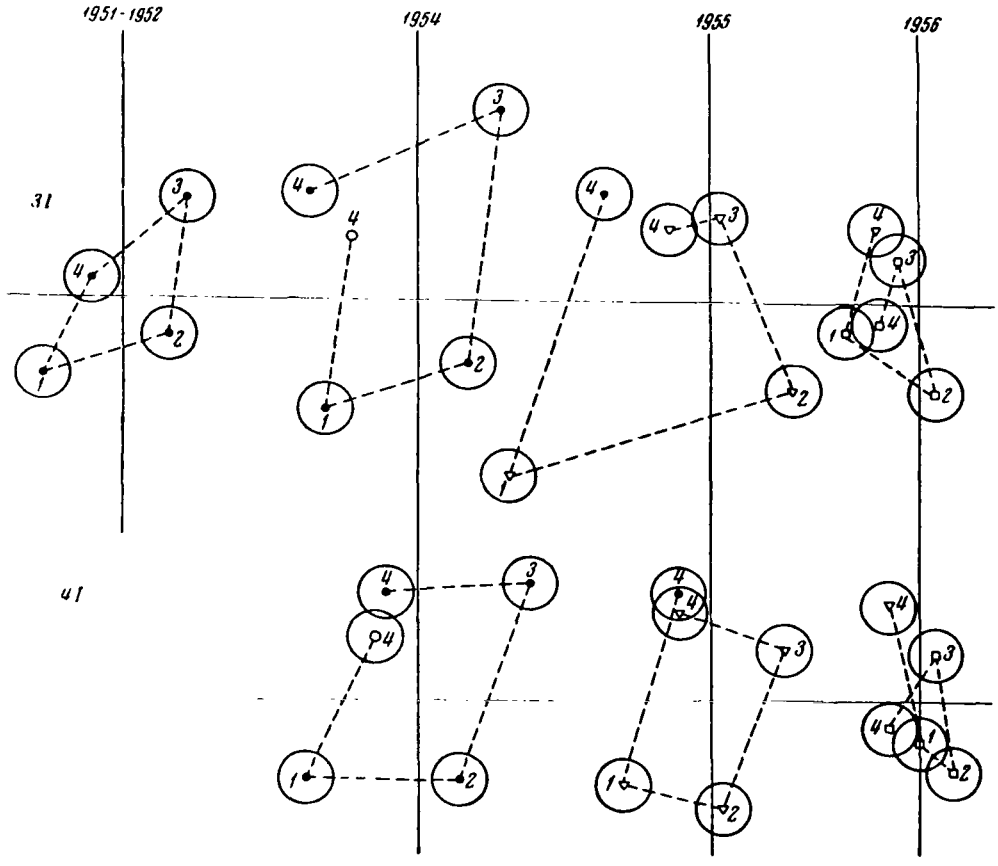

Fig. 3. Arrangement of the seasonal vectors individually according to years at stations 3 and 4 (see Table 1 on page 84). The average yearly sliding vector was calculated from the seasonal vectors.
For notation of seasons see page 84.

at the same geographical latitude. The straight line showing their latitude dependence is displaced to the right. When the stations are arranged according to geomagnetic latitude the dispersion of points obtained is considerably greater; the dependence of the amplitude of the vector of the minimum phase on the geomagnetic latitude is not as well expressed.

It is known that on the average for many years the vector of the diurnal variation of the hard component of cosmic rays does not show a clearly pronounced dependence on the latitude. Unfortunately, we had no data on the stations of Tbilisi and Irkutsk for the years of high solar activity and could not construct a dependence of the amplitude of the observed vector on the latitude for these stations.

Table 3 gives the ratios between the amplitudes of the average

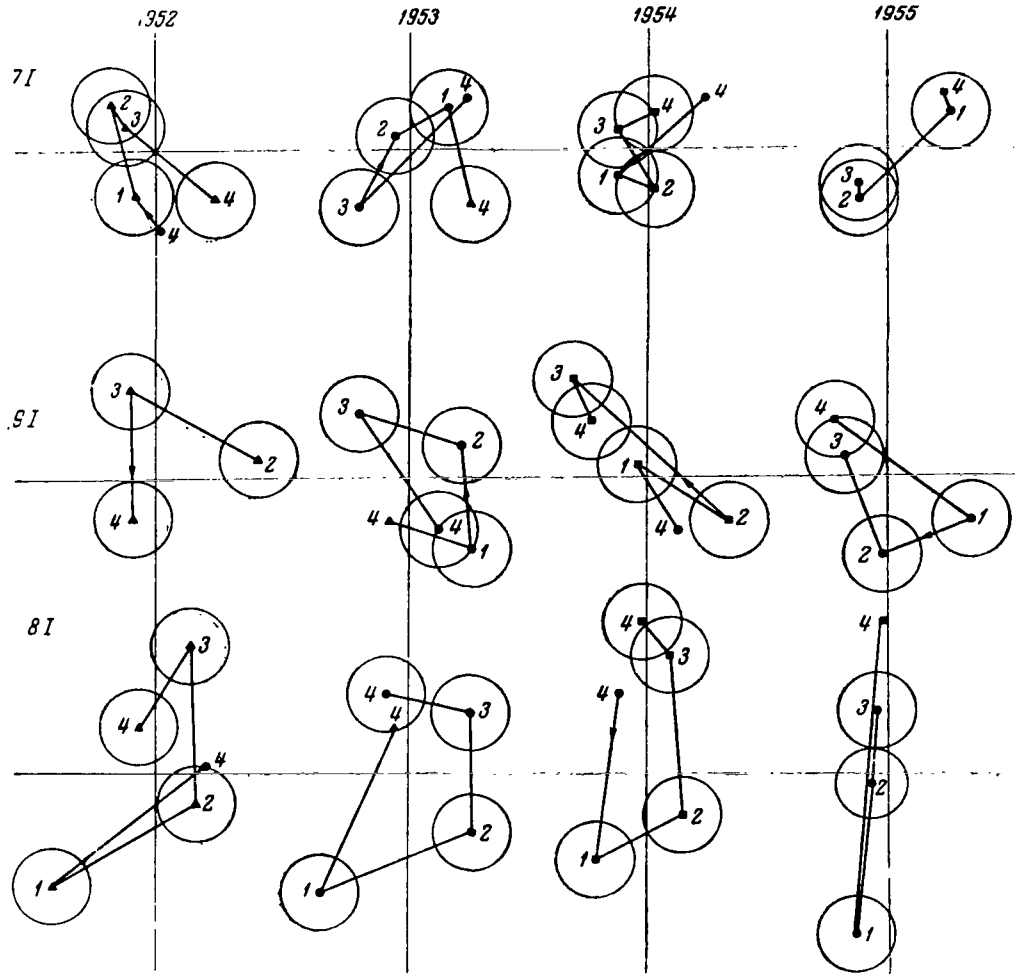

Fig. 4. Arrangement of seasonal vectors at stations 7, 9, 8 (p. 84). The average yearly sliding vector was subtracted from the seasonal vectors.
Numeration of the seasons is the same as on p. 84 .

yearly vectors for the stations Moscow - Yakutsk, Juancaio - Christ Church, Juancaio - Cheltenham in various years.

The indices 3, 4, 7, 8, 9 after the C denote the number of the station in Table 1.

We can see from Table 3 that during years of high solar activity this ratio is close to one, while during the years of the minimum it is considerably greater than one.

Thus, in addition to the results of reference [3], the following new data were obtained:

1) the picture of the phase displacement and decrease in amplitude of the average yearly vector of the diurnal wave of the hard

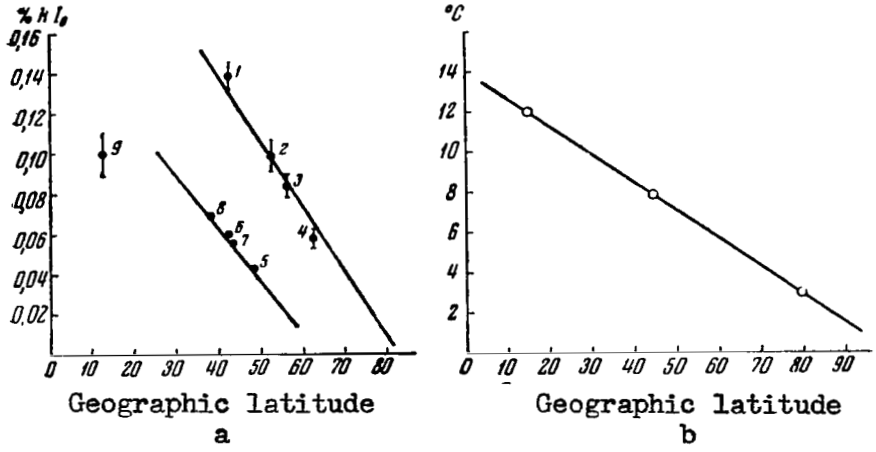

Fig. 5. Dependence on the geographic latitude according to stations (see p. 84):
a -- amplitudes of average yearly vector of diurnal variation of cosmic rays, having a minimum phase; b -- amplitudes of diurnal fluctuations of the terrestrial temperature.

Table 3

Ratios	Years						
	1944	1946	1948	1952	1954	1956,	VII 1957—VII 1958 гг.
$C_3 : C_4$	—	—	—	—	1,5	1,2	1,2
$C_9 : C_7$	1,5	1,0	0,8	1,1	2,0	—	—
$C_9 : C_8$	1,5	1,0	0,7	1,0	1,4	—	0,8

component of cosmic rays in 1953-1955 is repeated at stations situated in the Northern and Southern Hemispheres and on the Equator;

2) the counterclockwise seasonal rotation of the vector of the diurnal wave is well expressed in 1952-1954 at stations of the Northern Hemisphere; at the southern latitude station 7 the seasonal variation is poorly expressed;

3) the large seasonal variation of the diurnal vector of the hard component observed in Moscow and Yakutsk in 1954 and 1955 practically disappeared in 1956;

4) the observed average yearly vector of the diurnal variation in the minimum of solar activity has properties differing from the properties of the observed vector in the years of high solar activity

(a different ratio of the amplitudes of the variations for stations situated at different altitudes and latitudes).

3. ANALYSIS OF THE VARIATION OF THE AVERAGE YEARLY VECTOR

3.1. The Observed Vector as a Sum of Two Vectors

Data on the neutron component show that the amplitude of the average yearly diurnal variation of this component changed almost to zero in the minimum of solar activity (1954).

It seems probable that this decrease in the average yearly amplitude of the solar-diurnal wave in the neutron component is the result of the disappearance of anisotropy in the primary cosmic rays, related to solar activity.

During high solar activity, the observed amplitude of the diurnal wave in the neutron component is somewhat greater than the observed amplitude of the diurnal variation in the hard component. And yet, during the minimum of 1954 a solar-diurnal variation of considerable amplitude remained in the hard component, while the solar-diurnal variation in the neutron component disappeared. It is natural to suppose that the usually observed solar-diurnal variation in the hard component of cosmic rays can be represented as a sum of two vectors, one of which ($\underline{B}$) varies with the solar activity, while the second ($\underline{A}$) does not depend on the solar activity.

As the minimum of solar activity is approached, the amplitude of the variable vector decreases, while the observed vector should approach the constant vector* $\underline{A}$ in amplitude and phase.

Let the observed vector $\underline{C}$ represent a sum of two vectors $\underline{A}$ and $\underline{B}$, of which $\underline{A}$ = const, while $\underline{B}$ varies. Let us denote the amplitudes of these vectors by a, b, and c, respectively, and the phases by φ_a, φ_b, and φ_c. Let us consider the variation of c and φ_c under two assumptions:

1) only the amplitude of the vector $\underline{B}$ varies, φ_b = const;

2) only the phase of the vector $\underline{B}$ varies, b = const.

In the first case, as we can see from Fig. 6, the end of $\underline{C}$ will slide along a straight line parallel to the vector $\underline{B}$ and passing through the end of $\underline{A}$. The direction of this straight line apparently depends on the angle α between the components of the vectors** $\underline{A}$ and $\underline{B}$.

The second case is equivalent to a variation of the angle α with a constant amplitude b; in this case the observed vector $\underline{C}$ will

---

*The constancy of the vector $\underline{A}$ is of course conditional. It does not change with the solar activity, but can experience seasonal and other variations, independent of the solar activity.

**If the vector $\underline{A}$ = 0, then obviously the straight line will pass through the origin and its direction coincides with the direction of the vector $\underline{B}$.

slide around a circle whose center lies at the end of A and whose radius is equal to b. The amplitude c will increase as the angle α decreases and will decrease when it increases; when $\alpha = 0$, $c = b + a$, and when $\alpha = 180^\circ$, $c = b - a$. The difference between the amplitudes c and b for any angles α can be found from Fig. 6.

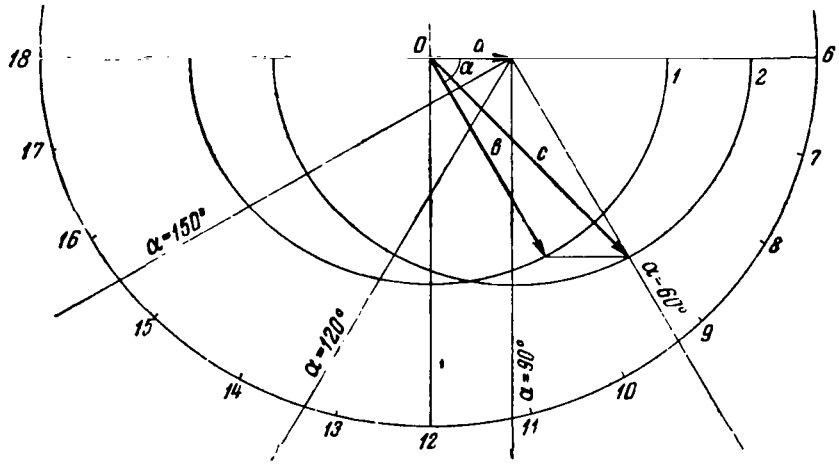

Fig. 6. Depiction of the vectors A, B, and C on an harmonic dial with a constant angle α and variation of the amplitude b. The end of C slides along the straight line $\alpha = 60^\circ$. When the angle α varies and the amplitude b is constant, the vector B describes a circle 1; then the end of the vector C describes a circle 2.

Considering the experimental curves of Fig. 1, we can see that close to the minimum of solar activity the end of the average yearly vector can actually be considered as sliding along a straight line. This can be noted especially well at stations 4 and 7, where during the rising and return motion of the observed vector, the points lie on one straight line. For the other stations, the traces of the direct and return motion of the vector diverge, but here too these traces are close to straight lines, the slope of which differs little in the rising and return motion of the vector.

The greatest discrepancy is observed in Moscow, but, as has been indicated, nonuniform material was used at this station.

The discrepancy in the rising and falling motions of the vector may be the result of a change in φ_b or of a change in the seasonal variation during 1954.

Averaging of data for four seasons can give sliding of the vector along one straight line only in the case of absence or constancy of the seasonal variations, as is the case at stations

7 and 4 (Figs. 3, 4). If the seasonal variation changes, for example, increases sharply, then it is not eliminated in the averaging, and the sliding average vector describes a curve. Such a picture occurs for the neutron component at station 9 (Fig. 7).

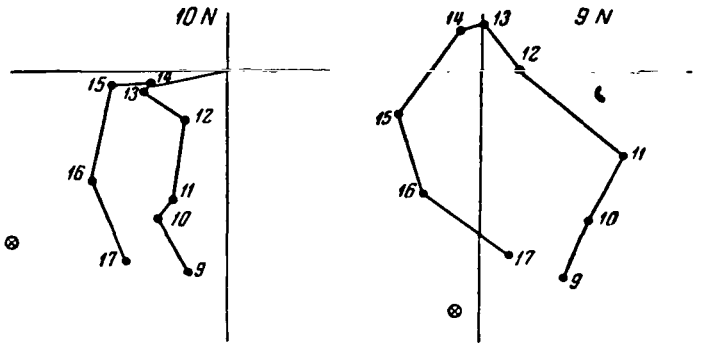

Fig. 7. Sliding average yearly vectors on harmonic dial for the diurnal variation of the neutron component at stations 9 and 10 (see p. 84).
Numeration of the vectors is indicated in Table 2 (p. 87).

For station 4, for which we have material for a long period after the minimum phase, we can see that the trace of the vector is rectilinear up to vectors 18-19. We can see from Table 3 that these vectors are centered around the beginning of 1956. After the 20th vector, the amplitude b stops increasing, and C begins to describe the curve corresponding to the second case.

For station 7 there is a great deal of material for the period preceding the minimum phase. Here sliding of the vector along the straight line begins with vectors 7-8, which are centered around the beginning of 1953. In the periods directly preceding vector 8 and following vector 18, we can consider that the change in the amplitude and phase of the observed vector may be the result of a simultaneous change of b and φ_b. A further change of φ_b exerts a dominant influence on the variation of the observed vector.

Sliding of the vector along a straight line was also observed close to the minimum of 1944, as can be seen from Fig. 1 for stations 7, 8, and 9.

We can show the cause of the change in amplitude and phase of the observed vector most convincingly according to the data of Climax station, Fig. 7. Here the constant vector of the neutron component proved to be directed oppositely to the constant vector in the hard component. As the minimum of solar activity is approached, the observed vector is displaced toward later hours, while in the case of

the opposite motion -- toward earlier hours. And yet, after the amplitude stopped changing, the direction of phase displacement became the same as in the hard component of the cosmic rays.

Thus, the experimental picture of the variation of the average yearly vector, depicted in Fig. 1, can be explained on the assumption that the observed vector is a sum of two, one of which remains constant. Close to the minimum of solar activity, the variation of the observed vector is determined basically by the variation of the amplitude of the variable vector, while during the year of high solar activity it is determined by the variation of its phase.

3.2. The Phase φ_b of the Extra-Atmospheric Vector for Various Stations

The relationship between the amplitude and phase of the observed vector when the amplitude of the vector B varies can be determined for various angles α from Fig. 6. From the triangle we have

$$\frac{a}{\sin A} = \frac{b}{\sin B} = \frac{c}{\sin C}. \tag{1}$$

Taking into consideration the fact that $\angle A = \alpha - \angle B$ and $\angle C = 180° - \alpha$, we obtain:

$$\frac{c}{a} = \frac{\sin \alpha}{\sin (\alpha - B)} = \frac{\sin (\varphi_b - \varphi_a)}{\sin (\varphi_b - \varphi_c)}, \tag{2}$$

where φ_a, φ_b, and φ_c are the phases of the vectors A, B, and C, counted in a clockwise direction from the Y-axis.

The phase φ_b is fully determined by the ratio between the amplitude and phase of the observed vector for various values of b and does not depend on the vector A. For two values of c we can write:

$$\frac{c_1}{c_2} = \frac{\sin (\varphi_b - \varphi_{c_2})}{\sin (\varphi_b - \varphi_{c_1})} = \frac{\sin \varphi_b \cos \varphi_{c_2} - \sin \varphi_{c_2} \cos \varphi_b}{\sin \varphi_b \cos \varphi_{c_1} - \sin \varphi_{c_1} \cos \varphi_b}$$

or

$$\sin \varphi_b (c_1 \cos \varphi_{c_1} - c_2 \cos \varphi_{c_2}) = \cos \varphi_b (c_1 \sin \varphi_{c_1} - c_2 \sin \varphi_{c_2}),$$

from which

$$\operatorname{tg}\varphi_b = \frac{c_1 \sin\varphi_{c_1} - c_2 \sin\varphi_{c_2}}{c_1 \cos\varphi_{c_1} - c_2 \cos\varphi_{c_2}}. \qquad (3)$$

Graphically the value of the angle φ_b is given by the slope of the straight line along which the observed vector slides (Fig. 6).

For a preliminary analysis according to experimental points of the rising motion of the vector, we constructed straight lines on Fig. 1 for the stations for which there was sufficient material.

From Fig. 1 we see that the slope of these straight lines, or φ_b, fluctuates around 180° and is different for the different stations. If we consider that the vector $\underline{B}$ is of extra-atmospheric origin, φ_b is the phase of the vector on the boundary of the atmosphere. If the extra-atmospheric vector is the result of anisotropy beyond the limits of the geomagnetic field, the difference of φ_b at various stations should be determined by the difference in the effective angle of deflection of particles in the geomagnetic field.

In a first approximation this actually is the case. The smallest phase φ_b determined according to the slope of the straight line is obtained at the equatorial high-altitude station of Juancaio. It is 30-40° less than for the middle-latitude stations. According to [5], for the ionizing component at the Equator in mountain altitudes the effective angle of deviation in a geomagnetic field for the spectrum of particles creating the extra-atmospheric diurnal variation is 30° greater than the effective angle for the hard component at the geomagnetic latitude 50°.

3.3. Determination of the Constant Vector $\underline{A}$

From the ratio of the observed values of φ_c, c, and the phase φ_b, we can say nothing of the magnitude and direction of the constant vector $\underline{A}$. At the same values of φ_b and c, we can have any values of φ_a and a; moreover, the value of b will vary. To determine $\underline{A}$ we must bring in supplementary data.

We can assume that in the minimum of solar activity in 1954, b = 0. In this case we can identify the constant vector $\underline{A}$ with the observed average yearly vector of the minimum phase.

If we have data for two minima of the solar activity at any station, we can determine the constant vector $\underline{A}$ by an independent method, without making any assumptions on the magnitude of the amplitude of the vector $\underline{B}$.

But in this case we must make an assumption that the value of the average yearly vector $\underline{A}$ remains constant during the entire time of the recording, i.e. in the two minima of the solar activity this value is the same.

Let us write formula (2) for two minima of the solar activity

at the same station:

$$c_1 \sin(\varphi_{b_1} - \varphi_{c_1}) = a \sin(\varphi_{b_1} - \varphi_a),$$
$$c_2 \sin(\varphi_{b_2} - \varphi_{c_2}) = a \sin(\varphi_{b_2} - \varphi_a).$$

From this we obtain

$$\frac{c_1 \sin(\varphi_{b_1} - \varphi_{c_1})}{c_2 \sin(\varphi_{b_2} - \varphi_{c_2})} = \frac{\sin(\varphi_{b_1} - \varphi_a)}{\sin(\varphi_{b_2} - \varphi_a)}.$$

In the left-hand portion all the values are known.

Let us denote

$$c_1 \sin(\varphi_{b_1} - \varphi_{c_1}) = k_1,$$
$$c_2 \sin(\varphi_{b_2} - \varphi_{c_2}) = k_2,$$

then we obtain

$$\cos\varphi_a \cdot (k_1 \sin\varphi_{b_2} - k_2 \sin\varphi_{b_1}) = \sin\varphi_a (k_1 \cos\varphi_{b_2} - k_2 \cos\varphi_{b_1}),$$

$$\operatorname{tg}\varphi_a = \frac{k_1 \sin\varphi_{b_2} - k_2 \sin\varphi_{b_1}}{k_1 \cos\varphi_{b_2} - k_2 \cos\varphi_{b_1}}, \qquad (4)$$

if the angle φ_a is known, then the value of a is determined according to formula (2). If we know $\underline{A}$ and $\underline{C}$ we can determine b. The vector $\underline{A}$ can also be determined graphically, by a simple construction, as is shown in Fig. 1 for stations 7, 8, and 9. The values of φ_a, a, and the values of b for various years, calculated according to the data of these stations, are presented in Table 4. We can see from it that φ_a and a found by the method described above differ little from φ_c and c of the vectors of the minimum phase observed.

3.4. Nature of the Constant Vector $\underline{A}$

As we can see from Table 4, the vector $\underline{B}$, which corresponds to the minimum phase of the vector $\underline{C}$, is small, and the amplitude c differs little from a. In a first approximation we can consider that the latitude dependence of the amplitude of the vector $\underline{C}$, depicted in Fig. 5,a corresponds to the latitude dependence of the amplitude of the vector $\underline{A}$.

The dependence shown in Fig. 5,a can serve as evidence in

Table 4

Station	Vector of minimum phase		Calculated values				
			A		B		
	c	φ_c	a	φ_a	1944 г.	1954 г.	1948 г.
7	0,046	80°	0,050	50°	0,124	0,030	0,164
8	0,072	90	0,076	100	0,110	0,015	0,164
9	0,096	72	0,112	86	0,116	0,030	0,136
Average . .					0,117	0,025	0,155

favor of the temperature origin of the vector A. Actually, if A is of temperature origin, then its value should be determined by the diurnal fluctuations of temperature and should depend on the geographic latitude. Fig. 5,b gives the usually used average latitude variation of the diurnal fluctuations of the Earth's temperature, which is in qualitative agreement with the latitude dependence of the vector A. It is natural to expect that the diurnal temperature fluctuations at stations with a sharp continental climate should be greater than at stations with a temperate or sea climate. This can explain the fact that the experimental points lie on two straight lines and that for the stations of the USSR the straight line is displaced to the right.

It seems very probable that the constant solar-diurnal vector A in the hard component is basically of temperature origin. However, the possibility is not excluded that this vector is complex and includes other atmospheric, and possibly also nonatmospheric effects, unrelated to the solar activity, in addition to the temperature effect. It may also include a diurnal variation of instrument origin.

We should note that it is difficult to explain the very great change in amplitude of the observed diurnal variation in Moscow after the instrument was moved to another place by a purely temperature increase in the vector A. When the shielding is decreased by 100 g/cm^2, the temperature effect can be increased by 10%, which cannot give an increase in the amplitude of the observed vector of almost double. The constant vector in the neutron component at Climax station also cannot be created by the temperature effect.

3.5. Amplitude of the Vector B in 1944 and 1954

We can see from Table 4 that in 1954 the vector B was actually close to zero, which confirms the conclusion of J. A. Simpson of the absence in 1954 of any disturbing factors of solar origin, creating

anisotropy of the cosmic rays.

In 1944 the vector B had an extremely considerable value, only approximately one and a half times less than in 1948.

Hence it is quite possible that the phenomena that could be observed in 1954, for example, variations with stellar time, could not be observed in 1944.

3.6. Displacement of the Phase of the Extra-Atmospheric Vector

Our results give 60° for the phase difference of the vector B between 1944 and 1954 for Christ Church station, and 70° for Cheltenham and Juancaio stations. As an average we obtained 66°, which is in good agreement with the results obtained in reference [3], introducing temperature corrections into the observed vectors.

After 1954 the phase displacement φ_c toward later hours was observed up to approximately the 24th to 25th vector, up to 1958, after which the phase of the vector stopped changing. This can be seen from the data of stations 3 and 4.

The vectors C before the minimum of solar activity in 1952 had the same phase at these stations.

In Fig. 7 we can see that the phase of C of the average diurnal variation of the neutron component for Climax and Juancaio stations was about 180° in 1954, while in 1957-1958 it was displaced to the left. Thus, it is possible that there is also a phase displacement in time for the neutron component of cosmic rays in the same direction as for the hard component of cosmic rays.

4. SEASONAL VARIATION OF THE DIURNAL WAVE

4.1. Geographical Distribution

For the hard component of cosmic rays, the experimental facts show a great seasonal variation of the diurnal wave at stations of the Northern Hemisphere during the period from 1952 to 1955. During the same time, no such variation was observed at station 7 in the Southern Hemisphere. On the Equator it was small, and the divergence of the seasonal vectors* differed from their divergence in the Northern Hemisphere.

Such a picture of the geographical distribution of the seasonal variation can be explained if we assume the simultaneous existence of seasonal variations of the temperature vector and the stellar-diurnal variation. Reference [3] showed that the difference in amplitude and phase of the observed diurnal vector in the winter and summer seasons in Moscow during the indicated period can be created

---

*In seasonal vector we are implying the deviation of the vector in the given season from the average yearly vector.

by differences in the values of the temperature corrections during these seasons. The role of the temperature effect in the seasonal variation of the diurnal vector is also indicated by the tendency toward the opposite arrangement of seasonal vectors at stations of the Northern and Southern Hemispheres (Fig. 4).

We might assume that at the equatorial station (9) the seasonal variation in the hard component has a different origin than in the northern latitudes. The divergence of the seasonal vectors here is close to that in the neutron component. Let us assume that at this station we are observing stellar-diurnal variation. If, in addition to the temperature variation, which has a maximum in the early morning hours, there is a stellar-diurnal variation with a maximum at 7-8 hrs, stellar time, the difference in the observed seasonal variation in the Northern and Southern Hemispheres is readily explained. Let us assume that the phase of the temperature vector remains constant, while the amplitude varies sinusoidally with the seasons. Under these conditions, the presence of stellar-diurnal variation leads to different results in the Northern and Southern Hemispheres with seasonal variations of the temperature vector the same in magnitude. As an illustration Fig. 8a, b, and c presents the divergence of the resultant seasonal vectors at the Equator, and in the Northern and Southern Hemispheres on a solar harmonic dial. In the construction we assumed: a maximum of the solar-diurnal variation at 8 hrs, stellar time (we considered that stellar and solar time coincide on 21 March); a maximum of the temperature variation at 3 hrs, local solar time [3]. The amplitude of the temperature wave during the winter season is equal to zero, while that during the summer is a maximum; in the spring and autumn it is equal to half the maximum value. The resultant vectors were constructed for three values of the amplitude of stellar-diurnal variation. On the Equator, where there are no seasonal fluctuations of the temperature vector, the stellar-diurnal vector describes a counterclockwise circle on the solar harmonic dial. In the Northern Hemisphere, as a result of the presence of seasonal variations in the temperature vector, the circle is stretched out into an ellipse, the distance between the winter and summer vectors is increased, and the observed seasonal variation is, as it were, intensified. In the Southern Hemisphere, superposition of the seasonal variation of the temperature vector decreases the distance between the winter and summer vectors. In determining the relationship between the amplitudes of the variation of the temperature and stellar-diurnal vectors, the ellipse is converted to a straight line, then the direction of rotation of the seasonal vector is changed to the reverse.

Thus, the seasonal variation of the diurnal vector in the hard component, created by stellar-diurnal variation, can be observed in an undistorted form only at the Equator. In the nothern latitudes it is, as it were, magnified, while the vectors are displaced, and in

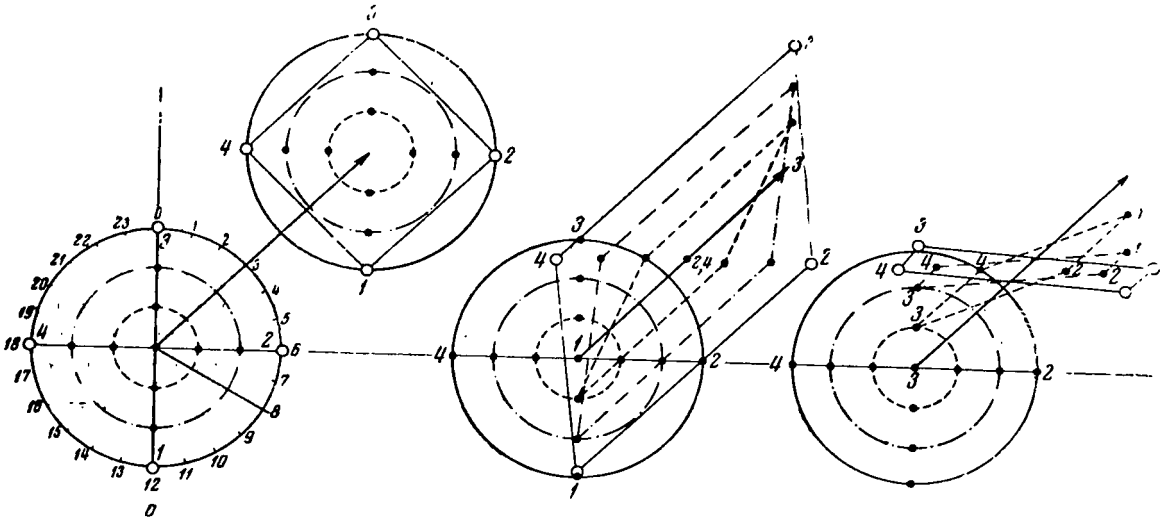

Fig. 8. Divergence of the seasonal vectors on harmonic dials in the presence of stellar-diurnal variation and seasonal variation of the amplitude of the temperature vector:
a -- at the Equator; b -- in the Northern Hemisphere; c -- in the Southern Hemisphere. Arrows indicate the temperature vector, circles -- the position of the resultant seasonal vectors. The numeration of the seasons is the same as on p. 84.

the southern latitudes it is minimized. It can be completely overcome by the seasonal variations of the temperature vector if they are large in comparison with the amplitude of the stellar vector.

The experimental picture depicted in Fig. 2 is in qualitative agreement with that presented in Fig. 8. In Fig. 2 we can note that in comparison with the arrangement of the seasonal vectors at the equatorial station (9I, 9N), the arrangement of the winter (1) and summer (3) vectors at most of the stations of the Northern Hemisphere in 1954 is displaced in a clockwise direction. This should also be observed if there are seasonal variations in the temperature vector.

4.2. Alternation of the Direction of Displacement of the Phase of the Observed Vector and Seasonal Variation

The experimental data presented in Fig. 2 show an increase in the seasonal variation in 1954 in comparison with 1953 at almost all the stations of the Northern Hemisphere. This apparent increase in the seasonal variation may be the result of a change in direction of the phase displacement of the observed vector in 1954.

As a result of the change in the amplitude of the vector B, the observed vector C slides upward along a straight line approximately until September 1954, when the phase has a minimum value. Then the direction of displacement of the vector changes to the opposite. During the year (from March 1954 to February 1955) the vector passes twice along the straight line in opposite directions. Thus, in 1954 an additional seasonal variation (D) arises. It has an arrangement of seasonal vectors close to the arrangement of the latter during other years in the Northern Hemisphere (vectors 3 and 4 upward). The superposition of the variation D leads to an apparent increase in the seasonal variation during 1954 at the stations of the Northern Hemisphere and to a displacement of the seasonal vectors at the Equator and in the Southern Hemisphere. As a result, at the southern-latitude station in 1954, the tendency toward an arrangement of the seasonal vectors opposite to that of the Northern Hemisphere disappears.

By subtracting from the seasonal vectors, the sliding average yearly vector for each season, centered around the same month as the given seasonal vector, we can eliminate the influence of the phase displacement in 1953 and in 1955, when the phase was displaced in the same direction. But such a procedure cannot completely eliminate the additional seasonal variation D in 1954, since the sliding average yearly vector does not give a correct amplitude of the variation when the direction of phase displacement changes.

4.3. Apparent Stellar-Diurnal Variation

As J. L. Thompson has shown [6], when stellar-diurnal variation is superimposed on solar-diurnal variation having a constant phase, the experimental points on the solar dial should be distributed in chronological order and describe a close curve during the year with a center at the end of the average yearly vector. With such a distribution of the experimental points, it can be described formally, without going into the nature of the effect, by means of the apparent stellar-diurnal variation and the seasonal variation of the amplitude of the solar-diurnal vector.

We have determined the apparent stellar-diurnal variation for the seasonal distribution of the vectors in 1954 according to the data presented in Fig. 2, and in 1952-1953 according to the materials of Fig. 4.

The stellar-diurnal vector was determined by a simple transfer of the seasonal vectors, counted from the end of the average yearly vector, to a stellar harmonic dial.*

---

*In reference [1], the presence of a constant average yearly vector in the hard component was not taken into consideration when the monthly vectors were transferred to a stellar harmonic dial.

The average stellar-diurnal vectors obtained from the eight seasons in 1952 and 1953 are presented in Fig. 9,a for stations 7, 8, and 9. The average stellar vectors for the four seasons of 1954 are presented in Fig. 9,b for various stations. The circles constructed around the average vectors in Fig. 9 show the dispersion of the seasonal vectors on the stellar harmonic dial. The radius of the circle $r = \sigma/\sqrt{n}$, where σ is the average quadratic deviation of the seasonal vectors from the mean stellar vector, n is the number of vectors from which the mean was determined (i.e. eight or four).

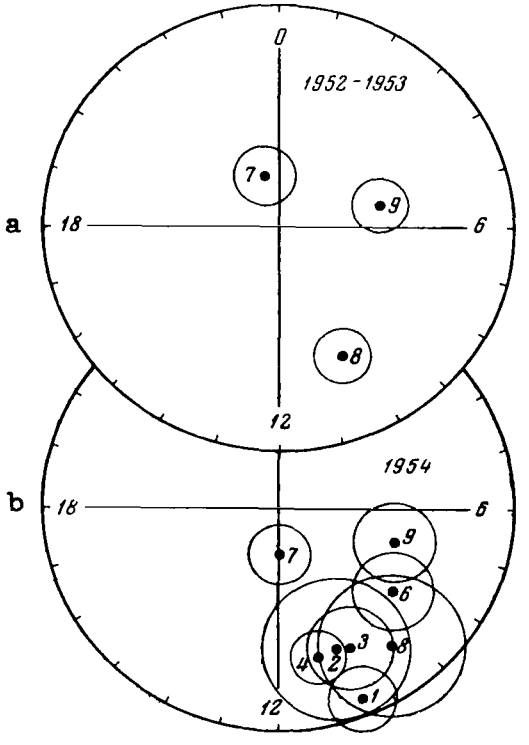

Fig. 9. Apparent stellar-diurnal variation on a stellar dial. The numbers show the number of the station in Table 1 (p. 84).
a -- for stations 7, 8, and 9 in 1952-1953; b -- for various stations in 1954.

We have also determined the apparent stellar-diurnal vector for the D-variation. In order to determine the phase of the stellar vector in the case when the experimental points lie on one straight line, it suffices to know the distribution of the dates and the slope of the straight line to the mean solar vector. We assumed that the sliding of the observed vector along the straight line occurs evenly. At the

extreme upper point it reaches 15 September.

As the average solar vector we took the average yearly sliding vector of the minimum phase. Under such assumptions it was found that the phase of the apparent stellar-diurnal wave of the D-variation according to the data for all stations (Fig. 1) fluctuates from 10 to 14 hrs, stellar time and is equal on the average to 12 hrs.

The amplitude of the stellar vector h is equal to half the length of the straight line describing the variation. This quantity can be evaluated by determining the length of the straight line on which the points from four seasons are situated, when the vector $\underline{C}$ slides in one direction. Such an evaluation gives an average of $h = 0.02\%$. Actually, h is apparently greater, since when the monthly vectors are averaged over the seasons, the length of the straight line decreases. It is obvious that the D-variation alone cannot create the observed seasonal variation in 1954, but it should increase the apparent stellar-diurnal variation at the stations of the Northern Hemisphere and displace the phase of the stellar variation at stations 7 and 9. From a comparison of the positions of the stellar vectors in Fig. 9,a and 9,b, we can observe this effect of a phase displacement in 1954 in comparison with 1952-1953.

From Fig. 9 we can see that during 1952-1953 at stations 7 and 8 the stellar vectors have opposite directions, which is naturally explained by the influence of the seasons and, consequently, of atmospheric effects.

We might note that the opposite nature of the phase of the stellar-diurnal wave for the Northern and Southern Hemispheres was first detected by A. R. Hogg [7]. The phases in 1952-1954 for the stations 7, 8 are in good agreement with the phases obtained by A. R. Hogg for the same stations on the average for a long period of time (from 1938 to 1945). Thus, these phases are rather stable. However, the phase for Juancaio station during 1952-1954 differs by 12-14 hrs from the phase found for this station by A. R. Hogg. It differs from the phase of the stellar-diurnal variation in the hard component found by H. Elliot and D. W. Dolbear by three independent methods [8] by approximately the same number of hours. These authors used materials from stations 7, 8, and 9 during approximately the same period as A. R. Hogg, as well as the data of telescopes in 1948, 1949.

As has already been indicated, the phase of the apparent stellar-diurnal variation in the hard component at station 9 in 1954 coincides with the phase of the stellar-diurnal variation in the neutron component. This variation practically disappears in 1955 in both components. However, in the hard component, a stellar-diurnal vector close in amplitude and phase to the 1954 vector was observed in 1952 and 1953. Thus, the indicated variation in the hard component appeared earlier and practically did not change its value in 1954. Hence we have no basis for believing that the seasonal variation observed in the hard component in 1954 has any other cause

than that in 1952 or 1953. The origin of the seasonal variation is apparently complex and requires further careful study not only during years of low, but also during years of high solar activity. The unexpected disappearance in 1956 of a clearly pronounced seasonal variation at stations 3 and 4 indicates that the vector B, which depends on the solar activity, should itself experience seasonal variations.

CONCLUSIONS

1. In a consideration of the changes in the diurnal variation of the cosmic ray intensity with the cycle of solar activity, the average yearly diurnal variation of the hard component can be represented in the form of a sum of two vectors. One of them varies with the solar activity and is related to the anisotropy of cosmic rays beyond the boundaries of the geomagnetic field, while the second -- atmospheric -- does not depend on the solar activity.

2. The change in amplitude and phase of the observed average yearly vector of the diurnal variation close to the minimum of solar activity (during approximately three years) is the result of a change in the amplitude of the extra-atmospheric vector.

3. During years of high solar activity the change in the observed vector is basically related to a change in the phase of the extra-atmospheric vector.

4. In the minimum of solar activity, 1954, the amplitude of the extra-atmospheric vector decreased almost to zero, and only the atmospheric vector remained. This explains the anomalous properties of the solar-diurnal variation in 1954.

5. The seasonal variation of the diurnal wave in the hard component of cosmic rays in the northern and southern latitudes is of atmospheric origin to a considerable degree. However, in addition to the atmospheric effects, there are other causes, creating a seasonal variation of the diurnal vector at the Equator and additional seasonal variations during years of high solar activity.

6. Experimental data on the hard component give no basis for assuming the appearance of any sort of special solar-diurnal variation in 1954, not observed in other years.

In conclusion I consider it my duty to express my gratitude to all the researchers whose materials were used in this work.

Let me also express my gratitude to senior technician M. K. Kulyukhina for performing the calculations and for aid in the formulation of the material.

BIBLIOGRAPHY

1. A. M. Conforto, J. A. Simpson. Nuovo Cimento, 1957, 5, p. 1052.
2. M. Possener, I. J. Van Heerden. Phil. Mag., 1956, 1, p. 253.
3. Ye. S. Glokova, N. S. Kaminer, N. A. Mishina. Tr. YaFAN SSSR, Seriya Fiz. (Works of the Yakut Branch of the Academy of

Sciences USSR, Physical Series), 1958, No. 2, p. 95.
4. I. Lange, S. E. Forbush. Cosmic Ray Results. Res. of the Department of Terr. Magn., 1948, 16; 1957, 20. Carnegie Institute of Washington Publ., 175.
5. L. I. Dorman. Variations of Cosmic Rays. Moscow, State Technical Literature Publishing House, 1957.
6. J. L. Thompson. Phys. Rev., 1939, 55, p. 11.
7. A. R. Hogg. J. Atm. Terr. Phys., 1950, 1, p. 114.
8. H. Elliot, D. W. Dolbear. J. Atm. Terr. Phys., 1951, 1, p. 205.

ABSTRACT

The paper shows that the mean yearly diurnal wave in the hard component of the cosmic rays could be expressed by the sum of two vectors. One of these vectors changes with the cycle of the solar activity, the other, being constant, does not depend on solar activity. When the minimum of solar activity approaches, the amplitude of the variable vector decreases, and this is the main cause of the changes of the observed diurnal wave near the minimum.

Data have been received proving the fact that the variable component is created by the anisotropy of cosmic rays outside the limits of the geomagnetic field, and the constant component is mainly of temperature origin.

The seasonal changes of the diurnal variation are discussed. The paper shows that the seasonal changes in the Northern and Southern latitudes is to a great extent connected with the temperature effect. However, there are other causes which produce the seasonal changes of the diurnal wave on the equator and the additional seasonal variation in the years of high solar activity. Experimental data on the hard component do not provide reasons to suppose that in 1954 a special stellar - diurnal variation appeared, which was absent from that component during other years.

DETERMINATION OF THE ENERGY SPECTRUM OF THE PRIMARY DIURNAL VARIATIONS OF THE COSMIC RAY INTENSITY*

T. M. Krupitskaya

1. INTRODUCTION

The experimental material of a number of stations of the World Network (Table 1), obtained during the IGY, was used to determine the energy spectrum of the diurnal variations.

The diurnal variation of the neutron and meson components was found at all stations by simple averaging of two-hour values individually for each section. All the results were reduced to constant barometric pressure and were treated by the methods of harmonic analysis. The amplitudes and phases of the first harmonic of the diurnal wave are presented in Table 1.

We can see from this Table that the amplitude of the diurnal variation for the neutron component is approximately twice as great as the amplitude of the diurnal variation of the meson component.

This fact is true both for individual stations (Heiss Island, Moscow, Berkeley, Resolute Bay) and on the average for all the stations. It is interesting to note for the high latitudes (Resolute Bay, Mirnyy, Heiss Island) the amplitude of the diurnal variations is less than for the middle latitudes, especially in the case of the meson component. The average moments of the maximum of the diurnal variation of the neutron and meson components are also in good agreement.

2. DETERMINATION OF THE PARAMETERS OF THE SPECTRUM OF DIURNAL VARIATIONS

We know from the theory of L. I. Dorman [1] that the energy

---

*The results of this article should be considered as doubly preliminary, since here no corrections are introduced for the temperature effect into the data of the meson component. The introduction of these corrections, as has been shown in certain investigations (for surveys see reference [1, Chapt. VII]), almost doubles the amplitude of the observed diurnal variation. -- (Note of Editor in Chief).

Table 1

Diurnal Variations of the Neutron and Meson Components

Item No.	Stations	A, %	Local time	Geomagnetic latitude	Period of observations
		Neutron Component			
1	Juancaio (3350 m)	0.24	11	-0°,6	June, July, Sept. 1957
2	Leeds	0.49	14	57.0	July-Dec. 1957
3	Berkeley	0.44	15	44.1	July-Dec. 1957
4	Zugspitze (2960 m)	0.42	14	48.2	July-Dec. 1957
5	Climax (3400 m)	0.33	15	48.1	June-Sept. 1957
6	Deep River	0.40	13	57.5	July-Nov. 1957
7	Resolute Bay	0.22	14	83.1	June-Sept. 1957
8	Moscow	0.29	15	50.8	Jan.-June 1958
9	Heiss Island	0.13	13	71.3	March-July 1958
	Average	0.33	14		
		Meson Component			
1	Berkeley	0.31	15	44°,1	July-Dec. 1957
2	Moscow	0.30	14	50.8	July-Dec. 1957
3	Moscow	0.16	12	50.8	July-Dec. 1957
4	Resolute Bay	0.12	12	83.1	June-Sept. 1957
5	Mirnyy	0.16	14	-77.0	June-Dec. 1957
6	Moscow	0.08	10	50.8	Jan.-June 1958
7	Moscow	0.16	15	50.8	Jan.-June 1958
8	Yakutsk	0.09	15	51.0	Jan.-June 1958
9	Heiss Island	0.09	11	71.3	March-July 1958
	Average	0.16	13		

spectrum of the primary variations of cosmic rays can be determined according to the observed secondary variations of various components at various latitudes and heights above sea level.

In this case the following basic formula is used:

$$\frac{\delta N^i_\lambda(h_0)}{N^i_\lambda(h_0)} = \int_{\varepsilon^{\min}_\lambda}^{\infty} W^i_\lambda(\varepsilon, h_0)\,\frac{\delta D(\varepsilon)}{D(\varepsilon)}\,d\varepsilon. \qquad (1)$$

Here

$$\frac{\delta N_\lambda^i(h_0)}{N_\lambda^i(h_0)},$$

-- the secondary variations I, obtained experimentally, $W_\lambda^i(\varepsilon, h_0)$ -- -- coefficient of the coupling between the primary and secondary variations I; $\frac{\delta D(\varepsilon)}{D(\varepsilon)}$ -- energy spectrum of the primary variations; h_0 -- level of observations, i -- index indicating the type of the component of the cosmic radiation (meson, neutron), λ -- geomagnetic latitude.

Obviously the energy spectrum of the primary variations can be determined more accurately the greater the number of components that can be drawn into finding the spectrum.

Usually it is assumed [1] that the energy spectrum of the primary variations represents a power function of the energy, beginning with some minimum energy ε_1, i.e. has the form:

$$\frac{\delta D(\varepsilon)}{D(\varepsilon)} = \begin{cases} a\varepsilon^{\alpha}, & \text{if } \varepsilon \geqslant \varepsilon_1, \\ 0, & \text{if } \varepsilon \leqslant \varepsilon_1, \end{cases} \tag{2}$$

where a and α are some constants.

Then formula (1) is rewritten in the form

$$\frac{\delta N_\lambda^i(h_0)}{N_\lambda^i(h_0)} = a\int_{\varepsilon_1}^{\infty} W_\lambda^i(\varepsilon, h_0)\,\varepsilon^{\alpha}\,d\varepsilon. \tag{3}$$

Three constants are unknown in this equation.

It is clear that to determine the energy spectrum of the primary variations, it is necessary to know at least three equations, i.e. experimental data for at least three independent components must be available. However, we had at our disposal data for only two of them. Hence we were able to proceed in the following way.

Let us write equation (3) for the neutron and meson components and divide the first by the second, where the coefficient a is reduced. We will have

$$\frac{\dfrac{\delta N_\lambda^{\text{H}}}{N_\lambda^{\text{H}}}}{\dfrac{\delta N_\lambda^{\text{M}}}{N_\lambda^{\text{M}}}} = \frac{\int_{\varepsilon_1}^{\infty} W_\lambda^{\text{H}}(\varepsilon, h_0)\,\varepsilon^{\alpha}\,d\varepsilon}{\int_{\varepsilon_1}^{\infty} W_\lambda^{\text{M}}(\varepsilon, h_0)\,\varepsilon^{\alpha}\,d\varepsilon}, \tag{4}$$

where $\frac{\delta N_\lambda^н}{N_\lambda^н} \Big/ \frac{\delta N_\lambda^м}{N_\lambda^м}$ is the ratio of the amplitudes of the neutron and meson components observed at the latitude λ.

We shall denote the integrals determined in the right-hand portion of (4) as $F_\lambda^н(\varepsilon_1, \alpha)$ and $F_\lambda^м(\varepsilon_1, \alpha)$. Let us denote the ratio of these integrals as $f(\varepsilon_1, \alpha)$, i.e.

$$\frac{F_\lambda^н(\varepsilon_1, \alpha)}{F_\lambda^м(\varepsilon_1, \alpha)} = f(\varepsilon_1, \alpha). \tag{5}$$

In equations (4) and (5), we have only two unknowns instead of three.

Let us find the function $f(\varepsilon_1, \alpha)$ for various values of α. We are assuming α to be equal to: 0, -0.5, -1.0, -2.0.

The values of the coupling coefficients $W_\lambda^i(\varepsilon_1)$ were determined for large energies by means of reference [1, Fig. 30]. In the region of low energies, more accurate curves for the coupling coefficients, cited in reference [2, Fig. 6] for the neutron, meson, and other components at the latitude 50° were used.

The integrals $F_\lambda^н(\varepsilon_1, \alpha)$ and $F_\lambda^м(\varepsilon_1, \alpha)$ were found by means of graphical integration.

Then the function $f(\varepsilon_1, \alpha)$ was determined for the neutron and meson components. These calculations are presented in the form of graphs (Fig. 1) of the dependence of the function f on ε_1 for various values of α. We should note that all the calculations of the integrals $F_\lambda^i(\varepsilon_1, \alpha)$ and the function f, performed for the neutron and meson components at sea level and latitude 50°, pertain also to the latitude 80°, since we can readily see from reference [1, Fig. 30] that the values of the coupling coefficients are the same for the same component for both latitudes 50° and 80°.

Furthermore, with the aid of the experimental data of Table 1, ratios of the amplitudes of the variation for the neutron and meson components were compiled both for the same and for different stations, i.e. the quantities

$$\frac{\delta N_\lambda^н}{N_\lambda^н} \Big/ \frac{\delta N_\lambda^м}{N_\lambda^м},$$

cited in Table 2 were determined. As can be seen from equation (4), the ratio of the observed values of the amplitudes should be equal to the value of $f(\varepsilon_1, \alpha)$. Hence, that value of ε_1 for which the observed ratio of the effects of the neutron and meson components is

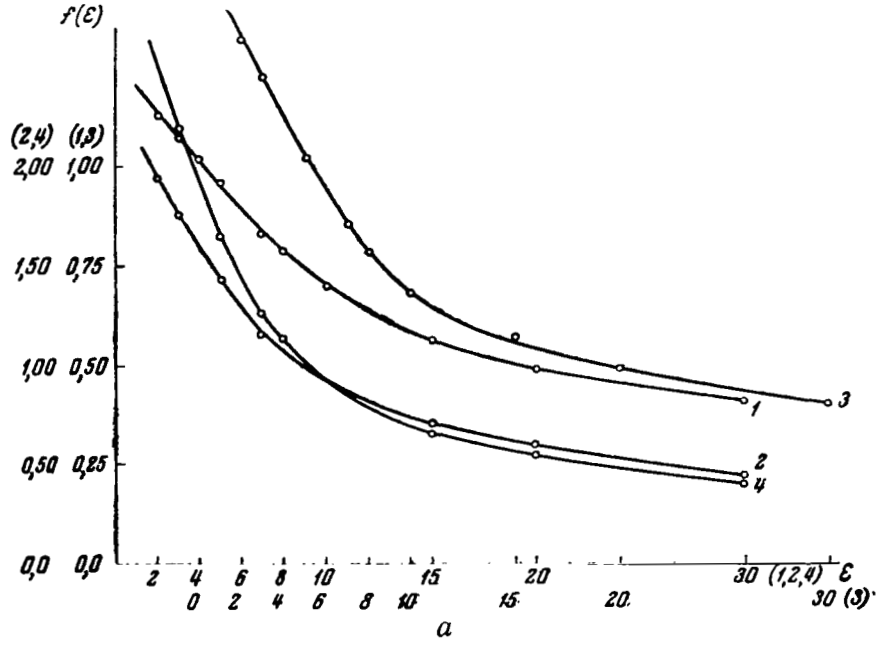

a

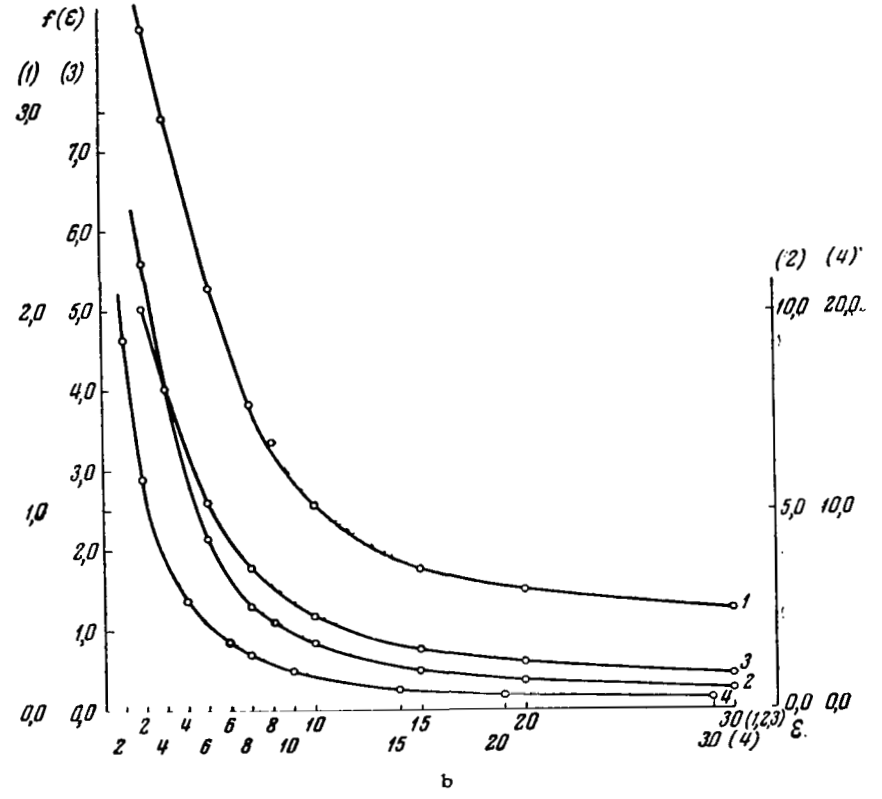

b

Fig. 1. Ratio of the integrals $F_{\lambda}^{i}(\varepsilon_1, h_0)$ for various (a and b) components to the integral $F_{\lambda}^{M}(\varepsilon_1, h_0)$ for the meson component at sea level as a function of ε_1 at various values of α and latitude 50°.
a–for the neutron component at sea level (1 – for $\alpha = 0$; 2 – for $\alpha = -0.5$); for the neutron component at mountain level (3 – for $\alpha = 0$; 4 – for $\alpha = -0.5$); b – for the neutron component at sea level (1 – for $\alpha = -1$; 2 – for $\alpha = -2$); for the neutron component at mountain level (3 – for $\alpha = -1$; 4 – for $\alpha = -2$).

equal to the theoretical function $f(\varepsilon_1, \alpha)$ will be the sought-after limiting value of the energy for the determined form of the spectrum and given α. Then it is easy to find the values of ε_1 from Fig. 1.

The results of the calculations of ε_1 are presented in Table 2. For each proposed form of the spectrum, i.e. for different values of α, we calculated the values of the coefficients a, which can be found by means of formula (3).

We can see from the table that when $\alpha = 0$ ε_1 and a generally are not determined by means of Fig. 1. Hence, this value of the parameter is generally unsuitable for characterizing the energy spectrum of the diurnal variations. When α = -0.5, -1.0, -2.0, the value of ε_1 varies within the interval from 2.6 to 6.3, from 5.9 to 8.7 and from 9.2 to 12.7, respectively, for different pairs of components. The average values of ε_1, a, and their dispersions show that it is difficult to select the value of α on the basis of the least value of the dispersion.

In order to select the value of α a comparison was made of the theoretically calculated amplitudes of the diurnal variations, proceeding from the assumed energy spectrum, with the experimental data for the neutron component at sea level, at mountain level, and for the meson component at sea level at the latitudes 50 and 80°. Let us assume that the sought-after spectrum of the diurnal variations represents a power function of one of three types:

$$\frac{\delta D(\varepsilon)}{D(\varepsilon)} = \begin{cases} a\varepsilon^{-0.5} & \text{— I,} \\ a\varepsilon^{-1} & \text{— II,} \\ a\varepsilon^{-2} & \text{— III.} \end{cases}$$

Let us calculate the amplitude of the diurnal variations for various cases by means of formula (1), using the corresponding coupling coefficients. In this case we shall limit the spectrum from below, taking as the lower limit of the spectrum the quantity obtained in Table 3 for the corresponding spectrum type. The value of a was selected in such a way that for the case when the meson component was recorded at sea level at a latitude of 50°, the theoretical value of the amplitude of the diurnal variation would coincide with the experimental.

The results of the calculations are presented in Table 3. From a comparison with the experimental data, it is not difficult to see that the best agreement of the theoretical and experimental values of the amplitude of the diurnal variations is observed for a type II spectrum at the latitude 50°. For the latitude 80° the agreement is somewhat less. This can possibly be explained, in the first place, by insufficient reliability of the experimental data at this latitude; in the second place, by the fact that the coupling coefficients at the latitudes 50 and 80° are assumed equal both for the neutron and for the meson component at sea level (Table 3).

Table 2

Energy Spectrum of the Diurnal Variations

Item No.	Stations	$\delta N_\lambda^H / N_\lambda^H$ / $\delta N_\lambda^M / N_\lambda^M$	$\alpha = 0$		$\alpha = -0,5$		$\alpha = -1,0$		$\alpha = -2,0$	
			ε_1	a	ε_1	a	ε_1	a	ε_1	a
	Neutron, meson									
1	Berkeley-Berkeley	1,42	—	—	5,2	0,024	7,4	0,13	11,0	3,4
2	Zugspitze-Moscow	1,82	—	—	4,3	0,018	6,9	0,10	10,5	2,6
3	Climax-Moscow	1,44	—	—	5,9	0,018	8,1	0,10	12,1	2,8
4	Deep River-Moscow	1.74	—	—	3,1	0,018	6,2	0,09	9,8	2,5
5	Zugspitze-Berkeley	1,35	—	—	6,3	0,025	8,7	0,13	12,7	4,2
6	Moscow-Moscow	1,80	—	—	2,8	0,013	6,0	0,07	9,4	1,6
7	Leeds-Berkeley	1,58	—	—	4,1	0,025	6,8	0,13	10,2	3,3
8	Resolute Bay-Resolute Bay .	1,83	—	—	2,6	0,009	5,9	0,05	9,2	1,2
9	Resolute Bay-Mirnyy	1,37	—	—	5,4	0,013	7,6	0,07	11,2	1,8
10	Heiss Island-Heiss Island .	1,45	—	—	4,9	0,007	7,6	0,04	10,8	1,0
	Average				4,5±1,2	0,017±0,006	7,1±0,9	0,09±0,03	10,7±1,1	2,4±1,0

Table 3

Assumed energy spectrum of the diurnal variation	Conditions of recording					
	Neutron component at sea level		Neutron component at mountain level		Meson component at sea level	
	50°	80°	50°	80°	50°	80°
$\frac{\delta D(\varepsilon)}{D(\varepsilon)} = \begin{cases} a\varepsilon^{-0,5}, & \text{if } \varepsilon_1 < \varepsilon \\ 0, & \text{if } \varepsilon_1 > \varepsilon \end{cases}$ $\varepsilon_1 = 4,5$ bev, $a = 0,01$	0,19	0,19	0,23	—	0,18	0,18
$\frac{\delta D(\varepsilon)}{D(\varepsilon)} = \begin{cases} a\varepsilon^{-1}, & \text{if } \varepsilon_1 < \varepsilon \\ 0, & \text{if } \varepsilon_1 > \varepsilon \end{cases}$ $\varepsilon_1 = 7,1$ bev, $a = 0,08$	0,30	0,30	0,36	—	0,18	0,18
$\frac{\delta D(\varepsilon)}{D(\varepsilon)} = \begin{cases} a\varepsilon^{-2}, & \text{if } \varepsilon_1 < \varepsilon \\ 0, & \text{if } \varepsilon_1 > \varepsilon \end{cases}$ $\varepsilon_1 = 10,7$ bev, $a = 2,2$	0,40	0,40	0,32	—	0,18	0,18
Experimental data	0,31	0,18	0,38	—	0,18	0,12

Thus, we arrive at the conclusion that the energy spectrum of the primary diurnal variations can be approximately represented in the form

$$\frac{\delta D(\varepsilon)}{D(\varepsilon)} = \begin{cases} a\varepsilon^{-1}, & \text{if} \quad \varepsilon > \varepsilon_1, \\ 0, & \text{if} \quad \varepsilon < \varepsilon_1, \end{cases}$$

$$\varepsilon_1 = (7{,}1 \pm 0{,}9) \text{ bev}, \quad a = 0{,}09 \pm 0{,}03.$$

This result differs negligibly from the results obtained by L. I. Dorman in reference [1] (ε_1 = 6.6 bev, a = 0.14).

BIBLIOGRAPHY

1. L. I. Dorman. Variations of Cosmic Rays. Moscow, State Technical Literature Publishing House, 1957.
2. L. I. Dorman, G. I. Freydman. Tr. Yakutskogo Fil. AN SSSR, Seriya Fiz. (Works of the Yakut Branch of the Academy of Sciences USSR, Physical Series), 1958, No. 2, p. 129.

ABSTRACT

The energy spectrum of the diurnal variations is determined according to the observations materials of the neutron and meson components obtained at a number of stations of the World network for the period of July 1957 - June 1958.

The relation of amplitudes of the neutron and meson components is applied in the determination of the parameters of the spectrum. It is found that the lower limit of the variations spectrum is (7.1 ± 0.9) Bev.

CHANGES IN THE AMPLITUDE OF THE DIURNAL VARIATION OF COSMIC RAY INTENSITY AS A FUNCTION OF THE MAGNETIC ACTIVITY

N. A. Zhukovskaya, A. I. Ol'

As is well known [1, 2, 3], as the magnetic activity increases, the amplitude of the diurnal variation of the cosmic ray intensity noticeably increases, while the moment of its maximum is displaced toward earlier hours.

However, in a study of the influence of magnetic activity on the value of the diurnal variation of the cosmic ray intensity (I), we obtained somewhat different results. We analyzed the intensity data obtained at a number of stations, cited in Table 1. All days entering into the observation period (chiefly the second half of 1957) were divided into groups characterized by different degrees of magnetic activity, i.e. different values of ΣKp. Group I included days when the values of Σ Kp varied from 0 to 12, group II -- days with Σ Kp equal to 13-18, III -- 19-23, IV -- 24-33, and V -- $\geqslant$ 34. The diurnal variation of I was found for each station individually according to groups, and its amplitude (Table 1) and phase were determined by the method of harmonic analysis.

We can see from Table 1 that as we pass from one group to another (with a greater Σ Kp) a continuous increase in the amplitude is not observed. The increase in the amplitude at most stations occurs in the first three groups; in the group with Σ Kp = 24-33, instead of the expected further increase, on the other hand, an abrupt decrease in the amplitude occurs, while when we pass to the next, fifth group with the greatest magnetic activity, a further increase [sic, decrease] in the amplitude is observed. To verify the assumption that the observed effect is not related to the period of greater solar activity, we analyzed data for Moscow, obtained by means of an ASK-1 ionization chamber in 1954 (year of the minimum solar activity). From Table 1 (station 2) we can see that in 1954 the detected effect also occurred.

In order to explain this effect, we constructed average curves of the average diurnal values of the cosmic ray intensity according to the method of superimposing periods in the interval -5 days to +5 days according to the data of the neutron monitor in Moscow,

Table 1

Item No.	Stations	Instrument	Amplitude, %				
			0 -12	13–18	19–23	24–33	≥34
1	Yakutsk	I	0,06	0,08	0,06	0,10	0,14
2	Moscow	I	0,06	0,18	0,12	0,10	0,32
3	Zugspitze	N	0,32	0,50	0,45	0,37	0,59
4	Amsterdam	I	0,04	0,05	0,06	0,02	0,06
5	Leeds	N	0,34	0,42	0,57	0,46	0,69
6	Deep River	N	0,32	0,44	0,52	0,24	0,25
7	Resolute Bay	N	0,17	0,35	0,14	0,13	0,22
8	Resolute Bay	T	0,11	0,12	0,06	0,06	0,20
9	Climax	N	0,25	0,40	0,44	0,36	0,32
10	Berkeley	N	0,24	0,49	0,42	0,47	0,51
11	Berkeley	T	0,33	0,39	0,28	0,20	0,40
12	Juancaio	N	0,35	0,39	0,22	0,12	0,13
13	Moscow	N	0,08	0,51	0,36	0,20	0,47
14	Moscow	T	0,23	0,22	0,17	0,09	0,27
15	Heiss Island	N	0,11	0,17	0,19	0,16	0,49

Note. I -- ionization chamber, N -- neutron monitor, T -- cubic telescope.

Berkeley, and Zugspitze (Fig. 1, a, b, c). Days entering into each group of magnetic activity, according to the division indicated above, were taken as zero days. The results obtained, presented in Fig. 1, gave no explanation for the effect of the decrease in the amplitude of the diurnal variation of I in the group with magnetic activity $\Sigma Kp = 24\text{-}33$, since the group with $\Sigma Kp = 24\text{-}33$ in this series of curves did not exhibit any anomalies. For Moscow the curve of the last group did not give a decrease in the intensity; its level again proved to be high. When computed according to the method of superimposing periods for group V ($\Sigma Kp \geq 34$), the lines when the average diurnal values in the interval -5 days to +5 days exhibited a distinct drop (nine days), then the lines with distinct rises (10 days) were averaged individually, and, finally, all the rest of the lines (eight days) were grouped. For each of these three groups, average diurnal variations were obtained. The application of methods of harmonic analysis gave the following results: for group I, after introducing corrections for noncyclic variation, the amplitude of the first harmonic (A) was obtained as equal to 0.31%, and for group II -- A = 0.78%.

Thus, proceeding from our results, obtained for Moscow for January-June 1958, a sharp decrease in the amplitude of the diurnal variation of the cosmic ray intensity in the group with $\Sigma Kp = 24\text{-}33$ might be explained by the presence in it of almost only drops in I with a small amplitude of the diurnal variation, while in the group with $\Sigma Kp \geq 34$, together with the drops, there are also rises. This

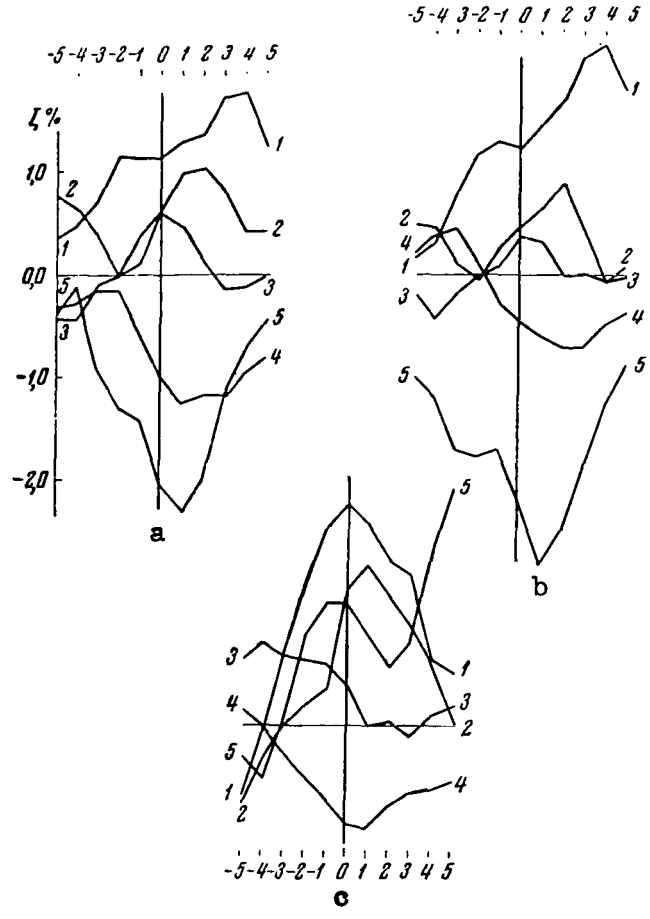

Fig. 1. Graphs of the average values of the cosmic radiation intensity:
a -- Berkeley (N); b -- Zugspitze (N); c -- Moscow (N).
The zero days for curves 1-5 pertain to the corresponding groups of magnetic disturbance.

was also responsible for the increase in the amplitude of the diurnal variation in this group. However, for the rest of the stations such an explanation is not suitable, since there the drop in I predominates in the group with $\Sigma Kp \geq 34$ (Fig. 1,a, b), while the effect of a decrease in the amplitude of the diurnal variation in the group with $\Sigma Kp = 24\text{-}33$ is rather sharply pronounced. Hence, the decrease in the diurnal variation observed in most cases in the group with $\Sigma Kp = 24\text{-}33$ cannot be explained in the manner indicated above.

Nor was the hypothesis that large drops or increases in the cosmic ray intensity during the day, which lead to a decrease in the diurnal variation, are concentrated in group IV of the magnetic activity, justified. It was found that large changes in I are

distributed over all groups of the magnetic activity.

Nor were positive results obtained in the explanation of the observed effect by excluding days (according to the data of the Zugspitze station) when the change in I was 2% and more over seven to eight successive hours from the analysis. Even after the exclusion of such days, the results presented in Table 2 were obtained.

Table 2

Σ Kp	0—12	13—18	19—23	24—33	⩾34
A, %	0,29	0,47	0,39	0,33	0,36

Thus, the effects of a decrease in the amplitude of the diurnal variation remain in group IV of the magnetic activity.

Still another attempt was made to explain the detected effect.

All the magnetic storms in the group with $\Sigma Kp = 24\text{-}33$ were divided into two groups: storms with sudden (Sc) and with gradual (G) beginnings. For each of these groups the diurnal variation was found, and after applying the methods of harmonic analysis, we obtained the results presented in Table 3.

Table 3

Stations	Instrument	A, % Storm (Sc)	A, % Storm (G)
Berkeley	T	0.18	0.26
Berkeley	N	0.46	0.53
Resolute Bay	T	0.05	0.11
Resolute Bay	N	0.06	0.28
Climax	N	0.33	0.52
Deep River	N	0.24	0.41
Zugspitze	N	0.38	0.38
Moscow	I	0.09	0.14

From Table 3 we can see that for all stations the amplitude of the diurnal variation of I during a storm Sc is considerably less than the amplitude during a storm G (only for Zugspitze were they obtained as equal).

We might advance the hypothesis that in the group with $\Sigma Kp = 24\text{-}33$ the decrease in the amplitude of the diurnal variation of I was due to storms Sc, characterized by a small amplitude. However, not only storms Sc give a decrease in the amplitude of

variation when one passes from the group with $\Sigma Kp = 19\text{-}23$ to the group with $\Sigma Kp = 24\text{-}33$. We determined the amplitude of the diurnal variation of I individually for storms Sc and G for these groups of magnetic activity according to the data of the neutron monitor of the Zugspitze station and the cubic telescope of Berkeley station. The results are presented in Table 4.

Table 4

Stations	Type of storm	A, %	
		$\Sigma Kp = 19\text{—}23$	$\Sigma Kp = 24\text{—}33$
Zugspitze	*Sc*	0,47	0,38
	G	0,44	0,38
Berkeley	*Sc*	0,33	0,18
	G	0,31	0,26

Thus, the problem of the nature of the effect of a decrease in the amplitude of the diurnal variation found in the group of days with $\Sigma Kp = 24\text{-}33$ remains open and is in need of further study, enlisting as great as possible a mass of observational material.

BIBLIOGRAPHY

1. J. C. Barton, J. H. Stockhausen. Phil. Mag., 1958, 3, p. 25.
2. A. E. Sandström. Tellus, 1955, 7, p. 2.
3. Y. Sekido, M. Kodama. Rep. Ionosph. Res. Jap., 1952, 6, p. 2.

ABSTRACT

The paper uses the data obtained at the 12 stations in the middle and high latitudes for 1957-1958 with corrections for barometric effect. The amplitude of the diurnal variation is determined by harmonic analysis (1 harmonic). The amplitudes thus received were averaged for several days with different rate of magnetic activity grouped together. The results obtained showed that on the background of continuous increase of the amplitude of diurnal variation with the increase of magnetic activity systematic decrease of amplitude is observed for the group of days with $\Sigma Kp = 24\text{-}33$.

The paper discusses the probable causes of the revealed effect.

ANISOTROPY OF COSMIC RAYS CAUSED BY THE ELECTRIC FIELD OF A CORPUSCULAR STREAM

L. I. Dorman

1. INTRODUCTION

Numerous observations of diurnal variations disturbed during magnetic storms show that the influence of an electric field on cosmic rays can be one of the basic causes resulting in anisotropy of the cosmic rays in the neighborhood of the Earth.

Inasmuch as the plasma of a corpuscular stream can be considered as superconducting, then only an electric field arising in the system of co-ordinates Sun-Earth as a result of motion of a corpuscular stream with a frozen magnetic field can exist in it. Since the velocity of the stream is much less than the velocity of light, the influence of this field on the trajectory of the particles can be neglected in comparison with the influence of the magnetic field. The stream of particles, arriving at the Earth, will change under the action of the electric field only on account of a change in the energy of the particles. Evaluations of the variations expected in this case have been made in many works [1-4]. In this article we are considering the distribution over the Earth of the spectrum of the expected variations caused by an electric field, under various assumptions on the structure of a regular inhomogeneous magnetic field. If in some energy interval $\varepsilon_1 < \varepsilon < \varepsilon_2$ the particles change their energy by $\Delta\varepsilon$, the spectrum of variations in this section will have the form

$$\frac{\delta D(\varepsilon)}{D(\varepsilon)} = a(1+\gamma)\frac{\Delta\varepsilon}{\varepsilon}, \quad \text{if} \quad \varepsilon_1 < \varepsilon < \varepsilon_2. \tag{1}$$

Here $1+\gamma$ is the exponent in the integral energy spectrum of primary undisturbed cosmic radiation and the coefficient $a \approx 1$ considers the variation of the solid angle of approach of the particles when the energy changes [1-4]. Thus, to determine the spectrum of anisotropy it suffices to find $\Delta\varepsilon$ and the intervals of the momenta in which one

energy change or another occurs.

2. VARIATION OF ENERGY OF THE PARTICLES ARRIVING AT THE EARTH

For definition, let the magnetic field H in the stream be directed perpendicular to the plane of the ecliptic and in the same direction as the Earth's field;* $H = \bar{H}f(y)$, where $\int_0^1 f(y)dy = 1$ and $l_\delta y$ is the distance from the leading edge of the stream, l_δ is the width of the stream near the Earth.

The maximum possible energy change of the particles under the action of the electric field that arises $E = \frac{u}{c} H$, where u is the velocity of the stream, will be

$$\Delta\varepsilon_m = Zel_\delta \int_0^1 E\,dy = \frac{Zeu}{c}\bar{H}l_\delta. \tag{2}$$

Here Ze is the charge of the particles.

When the Earth is found at a distance y from the advancing edge, the particles arriving at the Earth, intersecting the advancing edge (i.e. on Fig. 1 -- coming from the right), change their energy by

$$\Delta\varepsilon_- = -\Delta\varepsilon_m \int_0^y f(y)\,dy, \tag{3}$$

while those coming to the Earth through the lagging edge (i.e. on Fig. 1 -- coming from the left) change their energy by

$$\Delta\varepsilon_+ = \Delta\varepsilon_m \int_y^1 f(y)\,dy. \tag{4}$$

If the field is homogeneous, then $f(y) = 1$ and according to (3) and (4) we obtain

$$\Delta\varepsilon_- = -y\Delta\varepsilon_m; \quad \Delta\varepsilon_+ = (1-y)\Delta\varepsilon_m. \tag{5}$$

$\Delta\varepsilon_-$ and $\Delta\varepsilon_+$ can be obtained analogously for any distribution of the field.

---

*If the magnetic field in the stream has a different direction, the results obtained below can easily be changed analogously to the way it is done in reference [5].

3. INTERVALS OF MOMENTA IN WHICH A CHANGE OCCURS IN THE ENERGY OF PARTICLES WITH OPEN TRAJECTORIES

Since open trajectories are completely filled with particles, it suffices to determine in which direction the particles enter the stream in order to strike the Earth. First let us consider the case of a homogeneous field (Fig. 1). A consideration of the trajectories shows that the particles arriving at the Earth at an angle χ to the direction to the Sun will come from the left or the right (i.e. acquire or lose energy), depending on their momentum:

1) $0 \leqslant \chi \leqslant \pi$. In this case all the particles with a momentum

$$p_+ > p_1 = \frac{1-y}{2\cos^2\frac{\chi}{2}} \cdot \frac{Ze\bar{H}l_\delta}{c} \tag{6}$$

will come from the left (i.e. acquire energy), only if $y > \sin^2 \frac{\chi}{2}$.

If the latter condition is not fulfilled, then the particles whose momenta are included within the limits $p_1 \geqslant p_- \geqslant p_2$, where

$$p_2 = \frac{y}{2\sin^2\frac{\chi}{2}} \cdot \frac{Ze\bar{H}l_\delta}{c}, \tag{7}$$

will come from the right.

2) $\pi \leqslant \chi \leqslant 2\pi$. In this case all the particles with momenta

$$p_- > p_2 = \frac{y}{2\sin^2\frac{\chi}{2}} \cdot \frac{Ze\bar{H}l_\delta}{c} \tag{8}$$

come from the right, only if $y < \sin^2\frac{\chi}{2}$. In the opposite case, particles will also come from the left. Their momentum will be included within the limits $p_2 \geqslant p_+ \geqslant p_1$, where

$$p_1 = \frac{1-y}{2\cos^2\frac{\chi}{2}} \cdot \frac{Ze\bar{H}l_\delta}{c}. \tag{9}$$

A consideratinn of the trajectory of particles in an inhomogeneous field, the intensity of which depends only on y, shows that the results (6)-(9) remain unchanged, only in these expressions we should make the replacement

$$y \to \int_0^y f(y)\,dy; \quad 1-y \to \int_y^1 f(y)\,dy. \tag{10}$$

For example, in case (1) (for $0 \leqslant \chi \leqslant \gamma$) we obtain the result that all particles with momenta

$$p_+ > p_1 = \frac{\int_y^1 f(y)\,dy}{2\cos^2\frac{\chi}{2}} \cdot \frac{Ze\overline{Hl}_\delta}{c}, \tag{6'}$$

come from the left, only if $\int_0^y f(y)dy > \sin^2\frac{\chi}{2}$. If the latter condition is not fulfilled, particles with momenta $p_1 > p_- > p_2$, where

$$p_2 = \frac{\int_0^y f(y)\,dy}{2\sin^2\frac{\chi}{2}} \cdot \frac{Ze\overline{Hl}_\delta}{c}, \tag{7'}$$

will also come from the right. For other regions of the variation of χ we obtain analogous results.

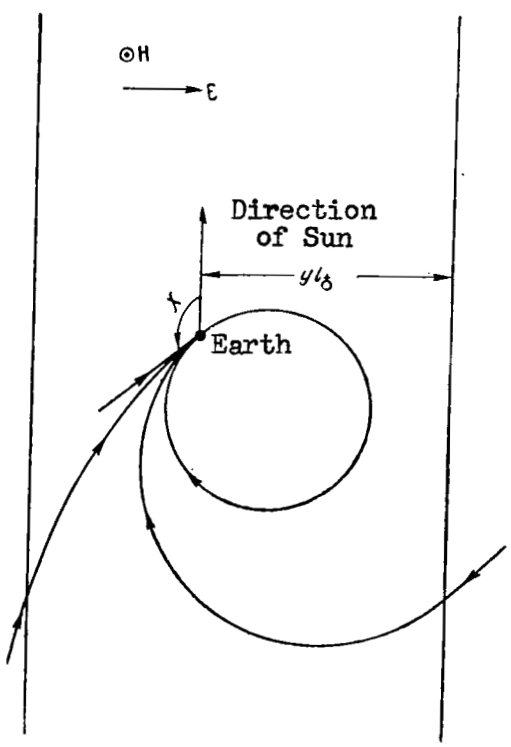

Fig. 1. Closed and open trajectories of particles in a stream with a homogeneous field (in an inhomogeneous field these trajectories will be somewhat more complex).

4. INTERVALS OF MOMENTA IN WHICH VARIATION OCCURS IN THE ENERGY OF PARTICLES WITH CLOSED TRAJECTORIES

If the trajectory is closed, then in spite of this it will not be completely empty, since nuclear absorption of particles by the plasma of the stream is negligibly small. Hence, if there are factors leading even to a small dispersion of particles from these trajectories (for example, particle drift, small inhomogeneities of the field, etc.), the closed trajectories are filled to a considerable degree. An investigation of the effects of a decrease in the cosmic ray intensity during magnetic storms [6] shows that the degree of filling of these orbitals 1 - f apparently reaches 0.8-0.9.

If a closed trajectory is symmetrical with respect to the axis of the stream, then in the case of a homogeneous field we should expect in it the same number of particles escaping from the left and from the right. For such trajectories variations of type (1) will be absent. If the trajectories are asymmetrical, the number of particles with p_- and p_+ will be different, and variations of type (1) will occur. In a first approximation we might assume that the number of particles with p_- will be greater the smaller the distance of the trajectory from the right, advancing edge. Analogously for p_+. Thus, if y_- and y_+ are the distances of the center of the trajectory from the advancing and lagging edges, respectively, the proportion of particles that decrease their energy will be $\varkappa_- = b/y_-$ and, analogously, $\varkappa_+ = b/y_+$. The coefficient b is found from the condition $1 - f = \varkappa_- + \varkappa_+$, from which

$$b = \frac{(1-f)\,y_-\,y_+}{y_- + y_+} = (1-f)\,y_-\,y_+. \tag{11}$$

Since

$$y_- = 1 - y - \frac{cp\cos\chi}{ZeHl_{\circlearrowleft}}\,;\quad y_+ = y + \frac{cp\cos\chi}{ZeHl_{\circlearrowright}}\,, \tag{12}$$

we obtain

$$\varkappa_- = (1-f)\left(y + \frac{cp\cos\chi}{ZeHl_{\circlearrowleft}}\right);\quad \varkappa_+ = (1-f)\left(1 - y - \frac{cp\cos\chi}{ZeHl_{\circlearrowleft}}\right). \tag{13}$$

Thus, considering (1), we obtain the spectrum of anisotropy for the particles from the closed trajectories

$$\frac{\delta D(\varepsilon)}{D(\varepsilon)} = \frac{a(1+\gamma)}{\varepsilon}\left(\Delta\varepsilon_-\,\varkappa_- + \Delta\varepsilon_+\,\varkappa_+\right), \tag{14}$$

where $\Delta\varepsilon_-$ and $\Delta\varepsilon_+$ are determined by expressions (3) and (4), while $\varkappa_-$ and $\varkappa_+$ are determined by expression (13).

In the case when the field is inhomogeneous, we obtain the same expression. But here we should make substitution (10). All particles with momenta

$$p < \min(p_1, p_2), \tag{15}$$

where p_1 and p_2 are determined by expressions (6)-(9), will be subject to variations of type (14).

We hope to consider the influence of the geomagnetic field in another work, and to determine the expected variations of various secondary components under various conditions of recording by means of the coupling coefficients, according to the spectrum of anisotropy found here.

BIBLIOGRAPHY

1. H. Alfven. Cosmic Electrodynamics. Translation from the English, Moscow, Publishing House of Foreign Literature, 1952.
2. J. A. Lunquist. Tellus, 1953, 5.
3. L. I. Dorman, E. L. Feinberg. Memoria del V Congreso Int. de Radiacion Cosmica (Guanajuato, 1955), Mexico, 1958.
4. L. I. Dorman, Variations of Cosmic Rays. Moscow, State Technical Literature Publishing House, 1957.
5. L. I. Dorman. This Collection, p.127.
6. Ya. L. Blokh, L. I. Dorman, N. S. Kaminer. This Collection, p. 1 .

ABSTRACT

The article gives results of the energy variations under the influence of the electric field and the impulse intervals where the particles acquire or lose energy (with consideration of the influence of the magnetic field in the streams on the trajectories of the particles). Calculations are made for different positions of the Earth in the stream and for different trajectories of the particles (closed and open).

The article presents the energy spectrum of the anisotropy which results from the influence of the electric field of corpuscular streams with regular homogeneous and inhomogeneous frozen magnetic field.

DIURNAL VARIATIONS OF COSMIC RAYS CAUSED BY ANISOTROPIC SCATTERING OF PARTICLES BY INHOMOGENEOUS MAGNETIC FIELDS OF CORPUSCULAR STREAMS

L. I. Dorman

1. INTRODUCTION

Reference [1] considered the anisotropy caused by the energy change of particles under the action of the electric field of a stream. Certain problems of the anisotropy of scattering of particles by a homogeneous magnetic field of a stream are considered in reference [2]. Here we are considering the anisotropy caused by an inhomogeneous magnetic field. The problem has been solved in the general case for a field perpendicular to the line of propagation of the stream, the intensity of which depends only on the distance to the advancing side edge.

The results of numerical calculations are cited for the case of a linear variation of the field from H_{max} at the advancing edge of the stream to H_{min} at the lagging side edge. The distortion of the trajectories of the particles by the geomagnetic field is considered approximately. A comparison with experimental data permits us to obtain information on the structure of the magnetic field in corpuscular streams.

2. TRAJECTORIES OF PARTICLES IN AN INHOMOGENEOUS FIELD, THE INTENSITY OF WHICH VARIES IN A DIRECTION PERPENDICULAR TO THE AXIS OF THE STREAM

Let the magnetic field in the stream H be directed perpendicular to the line of propagation, just as is shown in Fig. 1. All quantities with the dimensions of length will be measured in units of the stream width l_{δ} at a distance of the radius of the Earth's orbit R_{δ} from the Sun. Let us assume that H depends only on y

$$H(y) = \overline{H} f(y), \tag{1}$$

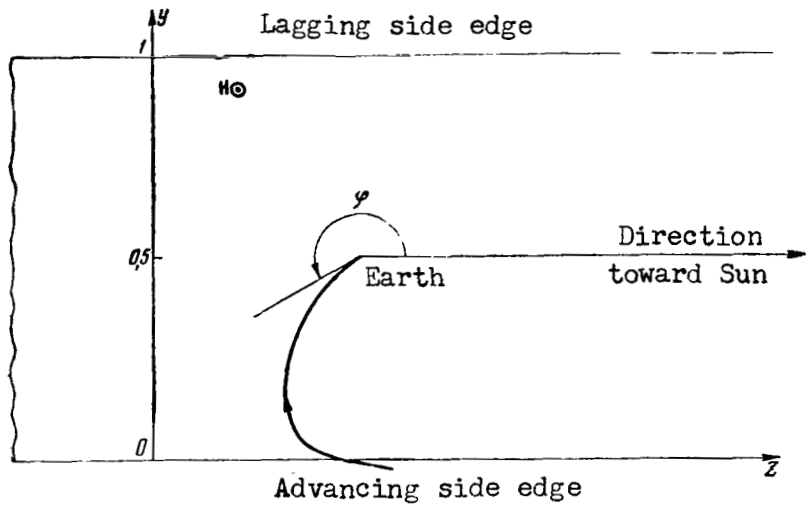

Fig. 1. Trajectory of particles in the plane perpendicular to the magnetic field of the stream. The case when the field is directed in the same way as the Earth's field is presented (the plane of the drawing coincides with the plane of the ecliptic).

where

$$\int_0^1 f(y)\,dy = 1. \tag{2}$$

The radius of curvature ρ of a particle with momentum p and charge Ze, moving in a plane perpendicular to the magnetic field (in the plane of the drawing of Fig. 1), will be

$$\rho(y)\,l_{\delta} = \frac{cp}{ZeHf(y)}. \tag{3}$$

Considering the fact that

$$\rho(y) = \frac{\left[1+\left(\frac{dy}{dz}\right)^2\right]^{3/2}}{\frac{d^2y}{dz^2}} \tag{4}$$

and substituting here $\rho(y)$ from (3), we obtain an equation for determining the trajectory of motion of a particle in the stream

$$y'' = \frac{f(y)}{k}[1 + y'^2]^{3/2}, \tag{5}$$

where

$$k = \frac{cp}{ZeHl_{\text{б}}}. \tag{6}$$

By means of the substitution

$$y' = \eta; \quad y'' = \eta \frac{d\eta}{dy} \tag{7}$$

we obtain

$$\frac{\eta d\eta}{(1 + \eta^2)^{3/2}} = \frac{f(y)\, dy}{k}, \tag{8}$$

from which

$$-\frac{1}{\sqrt{1 + \eta^2}}\Bigg|_{\eta(0)}^{\eta(y)} = \frac{1}{k}\int_0^y f(y)\, dy. \tag{9}$$

Since

$$\eta(y) = \operatorname{tg} \varphi(y), \tag{10}$$

where $\varphi(y)$ is the angle of inclination to the oz-axis of the tangent to the trajectory of motion of the particles, then substituting (10) into (9), we obtain

$$\cos \varphi(0) - \cos \varphi(y) = \frac{1}{k}\int_0^y f(y)\, dy. \tag{11}$$

Substituting here instead of k expression (6) and using the condition of entry of particles into the stream through the side edge, we find the value of the threshold momentum

$$cp_{\text{crit}} = \frac{ZeHl_{\text{б}}}{2}\beta(\varphi, y), \tag{12}$$

where $\beta(\varphi, y)$ for a field with a direction as in Fig. 1 (i.e. the same as in the geomagnetic field) has the form:

$$\beta(\varphi, y) = \begin{cases} \dfrac{\int_0^y f(y)\,dy}{\cos^2\frac{\varphi}{2}}, & \text{if} \quad \int_0^y f(y)\,dy \leqslant \cos^2\frac{\varphi}{2}, \\ \dfrac{\int_y^1 f(y)\,dy}{\sin^2\frac{\varphi}{2}}, & \text{if} \quad \int_0^y f(y)\,dy \geqslant \cos^2\frac{\varphi}{2}. \end{cases} \tag{13}$$

If the magnetic field in the stream is directed in the opposite direction, then

$$\beta(\varphi, y) = \begin{cases} \dfrac{\int_0^y f(y)\,dy}{\sin^2\frac{\varphi}{2}}, & \text{if} \quad \int_0^y f(y)\,dy \leqslant \sin^2\frac{\varphi}{2}, \\ \dfrac{\int_y^1 f(y)\,dy}{\cos^2\frac{\varphi}{2}}, & \text{if} \quad \int_0^y f(y)\,dy \geqslant \sin^2\frac{\varphi}{2}. \end{cases} \tag{14}$$

When the Earth is at a distance y from the advancing side edge of the stream, then only particles with momentum $p > p_{crit}$ (without considering the influence of the magnetic field) can approach at an angle φ to the Earth-Sun direction in a plane perpendicular to the force lines, i.e. if the distribution is originally isotropic, the spectrum of variations will have the form

$$\frac{\delta D(p, y, \varphi)}{D(p)} = f \begin{cases} -1, & \text{if} \quad p \leqslant p_{crit}, \\ 0, & \text{if} \quad p > p_{crit}, \end{cases} \tag{15}$$

where p_{crit} is determined by equation (12). Here the factor $f \approx 0.1$-0.3 determines the proportion of particles subject to the given variation [11].

3. DISTRIBUTION OF THE THRESHOLD MOMENTUM IN VARIOUS CASES OF THE INHOMOGENEOUS FIELD

The dependence of the threshold momentum cp_{crit} on φ and y for various distributions of the field in the stream f(y) can be found according to formulas (13) and (14). As an example, let us consider the case when the field decreases linearly from H_{max} at the advancing side edge to H_{min} at the lagging edge. In this case:

$$H = \bar{H} f(y), \tag{16}$$

where

$$\bar{H} = \frac{H_{max}(1+\alpha)}{2} = \frac{H_{max} + H_{min}}{2}, \tag{17}$$

$$f(y) = \frac{2}{1+\alpha}[1 - (1-\alpha)y]; \; 0 \leqslant y \leqslant 1, \tag{18}$$

$$\alpha \equiv \frac{H_{min}}{H_{max}}. \tag{19}$$

The results of calculations of $\beta(\varphi, y) = \frac{2cp_{crit}}{ZeHl_{\delta}}$ are presented in Table 1 for α = 0, 0.2, 0.4, 0.6, 0.8, and 1.0 (the last case corresponds to a homogeneous field).

Analogous calculations of $\beta(\varphi, y)$ have been performed for distributions of the magnetic field f(y), which were investigated in reference [3]. However, the results obtained are rather cumbersome, and we shall not cite them here. The basic peculiarities of the expected anisotropy can be seen from Table 1. The greatest anisotropy should be expected, under the assumptions made, when the Earth is close to any edge of the stream, since in this case the amplitude of variation of cp_{crit} is small. In the case of a homogeneous field (α = 1), the effect of anisotropy is the same in the advancing and in the lagging side edges. For an inhomogeneous field ($\alpha < 1$), the anisotropy is small at the lagging edge, where the magnetic field is weaker. The anisotropy should be the least in the middle of the stream. For example, in the case of a homogeneous field cp_{crit} should vary from $\frac{ZeH\bar{l}_{\delta}}{4}$ at $\varphi = 0^{\circ}$ and 180° to $\frac{ZeH\bar{l}_{\delta}}{2}$ at $\varphi = 90$ and 270°. This anisotropy should cause a semidiurnal variation. If the field is inhomogeneous, the amplitude of anisotropy in the middle of the field is increased, and the phase of the maximum cp_{crit} (i.e. the phase of the minimum cosmic ray intensity) is substantially displaced. Thus, when $\alpha = 0$, cp_{crit} should have a maximum when $\varphi = 60^{\circ}$ and 300°, in this case $cp_{crit} = \frac{ZeH\bar{l}_{\delta}}{2}$. The position of the minima of cp_{crit} remains as before, but the depth changes substantially: when $\varphi = 180^{\circ}$, $cp_{crit} = \frac{ZeH\bar{l}_{\delta}}{8}$, while when $\varphi = 0^{\circ}$, $cp_{crit} = \frac{3ZeH\bar{l}_{\delta}}{8}$. Thus, in this case the 24-hour wave will have considerable weight.

Table 1

Dependence of $\frac{2\,\varepsilon_{crit}}{ZeHl_{\delta}} = \beta(\varphi, y)$ on φ and y for Various Distributions of the Field in the Stream (Various Values of α).

Values of β Are Presented for $0° \leqslant \varphi \leqslant 180°$. If $\varphi > 180°$, β Will Be the Same as at $360° - \varphi$

α	y \ φ	0°	15°	30°	45°	60°	75°	90°	105°	120°	135°	150°	175°	180°
0	0,1	0,190	0,194	0,204	0,223	0,253	0,302	0,380	0,513	0,760	0,950	0,869	0,824	0,810
	0,2	0,360	0,366	0,386	0,422	0,480	0,572	0,720	0,972	0,800	0,750	0,686	0,651	0,640
	0,3	0,510	0,519	0,548	0,598	0,680	0,810	0,980	0,778	0,653	0,574	0,526	0,499	0,490
	0,4	0,640	0,651	0,686	0,751	0,853	0,971	0,720	0,572	0,480	0,422	0,386	0,366	0,360
	0,5	0,750	0,764	0,804	0,880	1,000	0,675	0,500	0,397	0,334	0,293	0,268	0,254	0,250
	0,6	0,840	0,855	0,900	0,984	0,640	0,432	0,320	0,254	0,213	0,188	0,173	0,166	0,160
	0,7	0,910	0,925	0,975	0,614	0,360	0,243	0,180	0,143	0,120	0,106	0,096	0,092	0,090
	0,8	0,960	0,977	0,598	0,273	0,160	0,108	0,08	0,064	0,053	0,047	0,043	0,041	0,040
	0,9	0,990	0,588	0,149	0,068	0,040	0,027	0,020	0,016	0,013	0,012	0,011	0,010	0,010
0,2	0,1	0,154	0,156	0,165	0,180	0,205	0,244	0,307	0,415	0,615	0,993	0,908	0,862	0,846
	0,2	0,303	0,308	0,325	0,355	0,404	0,481	0,606	0,820	0,930	0,818	0,748	0,710	0,697
	0,3	0,440	0,448	0,472	0,516	0,587	0,698	0,880	0,889	0,747	0,656	0,600	0,570	0,560
	0,4	0,554	0,564	0,594	0,650	0,738	0,880	0,892	0,708	0,595	0,523	0,478	0,453	0,446
	0,5	0,666	0,678	0,714	0,782	0,888	0,902	0,669	0,530	0,445	0,392	0,358	0,340	0,334
	0,6	0,760	0,774	0,804	0,877	0,960	0,648	0,480	0,381	0,320	0,281	0,257	0,244	0,240
	0,7	0,835	0,850	0,895	0,98	0,660	0,446	0,330	0,262	0,220	0,194	0,177	0,168	0,165
	0,8	0,904	0,920	0,969	0,656	0,384	0,259	0,194	0,152	0,128	0,112	0,103	0,098	0,096
	0,9	0,960	0,976	0,598	0,273	0,160	0,108	0,080	0,064	0,053	0,047	0,043	0,041	0,040
0,4	0,1	0,139	0,142	0,149	0,163	0,186	0,221	0,278	0,375	0,557	0,949	0,924	0,877	0,861
	0,2	0,268	0,273	0,288	0,314	0,357	0,426	0,536	0,723	0,978	0,860	0,785	0,746	0,732
	0,3	0,390	0,397	0,418	0,458	0,52	0,618	0,780	0,968	0,814	0,715	0,643	0,612	0,610
	0,4	0,502	0,510	0,538	0,587	0,668	0,796	0,996	0,790	0,664	0,584	0,534	0,507	0,498
	0,5	0,607	0,618	0,65	0,712	0,811	0,964	0,786	0,624	0,524	0,461	0,422	0,400	0,393
	0,6	0,703	0,716	0,753	0,825	0,937	0,802	0,594	0,472	0,396	0,348	0,318	0,302	0,297
	0,7	0,790	0,803	0,847	0,926	0,840	0,568	0,420	0,333	0,280	0,246	0,225	0,214	0,210
	0,8	0,867	0,883	0,93	0,908	0,530	0,360	0,266	0,212	0,178	0,156	0,142	0,135	0,133
	0,9	0,938	0,955	0,925	0,423	0.248	0,168	0,124	0.098	0,083	0,073	0,066	0,063	0,062

Table 1 (Conclusion)

a	y \ φ	0°	15°	30°	45°	60°	75°	90°	105°	120°	135°	150°	175°	180°
	0,1	0,122	0,125	0,132	0,144	0,164	0,194	0,245	0,331	0,491	0,836	0,942	0,894	0,878
	0,2	0,240	0,244	0,257	0,282	0,320	0,381	0,480	0,648	0,960	0,892	0,814	0,773	0,760
	0,3	0,352	0,358	0,377	0,412	0,470	0,559	0,705	0,952	0,864	0,759	0,694	0,659	0,648
	0,4	0,460	0,468	0,494	0,540	0,613	0,730	0,920	0,858	0,721	0,633	0,578	0,549	0,540
0,6	0,5	0,562	0,572	0,603	0,660	0,752	0,894	0,875	0,695	0,583	0,512	0,469	0,445	0,438
	0,6	0,660	0,672	0,708	0,775	0,880	0,920	0,680	0,540	0,454	0,399	0,364	0,346	0,340
	0,7	0,752	0,766	0,807	0,882	0,988	0,668	0,494	0,392	0,329	0,289	0,265	0,252	0,248
	0,8	0,840	0,855	0,902	0,985	0,640	0,432	0,320	0,254	0,214	0,188	0,172	0,162	0,160
	0,9	0,922	0,939	0,989	0,528	0,310	0,209	0,155	0,123	0,103	0,091	0,083	0,079	0,078
	0,1	0,110	0,112	0,118	0,129	0,147	0,175	0,220	0,297	0,441	0,752	0,954	0,905	0,890
	0,2	0,216	0,220	0,232	0,254	0,288	0,343	0,432	0,583	0,864	0,92	0,840	0,797	0,784
	0,3	0,291	0,296	0,312	0,341	0,388	0,462	0,582	0,786	0,945	0,831	0,760	0,722	0,709
	0,4	0,422	0,430	0,453	0,495	0,554	0,672	0,845	0,918	0,772	0,678	0,619	0,588	0,578
0,8	0,5	0,528	0,537	0,565	0,619	0,703	0,838	0,946	0,751	0,630	0,555	0,506	0,481	0,472
	0,6	0,625	0,637	0,672	0,734	0,835	0,934	0,748	0,594	0,499	0,438	0,402	0,381	0,374
	0,7	0,723	0,736	0,776	0,848	0,934	0,750	0,555	0,440	0,370	0,325	0,297	0,282	0,277
	0,8	0,818	0,833	0,877	0,958	0,723	0 492	0,354	0,289	0,243	0,214	0,195	0,185	0,182
	0,9	0,910	0,926	0,975	0,615	0,350	0,243	0,180	0,143	0,120	0,106	0,096	0,092	0,090
	0,1	0,100	0,102	0,107	0,118	0,134	0,159	0,200	0,270	0,400	0,684	0,965	0,916	0,900
	0,2	0,200	0,204	0,214	0,239	0,239	0,318	0,400	0,541	0,800	0,938	0,858	0,814	0,800
	0,3	0,300	0,305	0,322	0,352	0,400	0,477	0,600	0,810	0,935	0,820	0,750	0,712	0,700
	0,4	0,400	0,406	0,429	0,469	0,534	0,635	0,800	0,953	0,800	0,703	0,644	0,610	0,600
1,0	0,5	0,500	0,509	0,535	0,585	0,667	0,794	1,000	0,794	0,667	0,586	0,536	0,509	0,500
	0,6	0,600	0,610	0,644	0,703	0,800	0,953	0,800	0,635	0,534	0,469	0,429	0,406	0,400
	0,7	0,700	0,712	0,750	0,820	0,935	0,810	0,600	0,477	0,400	0,352	0,322	0,305	0,300
	0,8	0,800	0,814	0,858	0 938	0,800	0 541	0,400	0,318	0,269	0,239	0,214	0,204	0,200
	0,9	0,900	0,916	0,965	0,684	0,400	0,270	0,200	0,159	0,134	0,118	0,107	0,102	0,100

4. ANGULAR DISTRIBUTION OF THE INTENSITY OF VARIOUS COMPONENTS OF COSMIC RAYS (WITHOUT CONSIDERING THE INFLUENCE OF THE GEOMAGNETIC FIELD)

If $W_\lambda^i(\varepsilon, H_0)$ is the coupling coefficient between a type i component at the latitude λ, at an observation level with pressure h_0, and primary particles with total energy ε, the expected variation will be

$$\frac{\delta N_\lambda^i(h_0, y, \varphi)}{N_\lambda^i(h_0)} = \int_{\varepsilon_\lambda}^{\infty} \frac{\delta D(\varepsilon, y, \varphi)}{D(\varepsilon)} W_\lambda^i(\varepsilon, h_0)\, d\varepsilon. \tag{20}$$

Here ε_λ is the geomagnetic threshold for the given observation point, while $\frac{\delta D(\varepsilon, y, \varphi)}{D(\varepsilon)}$ is determined by expression (15), in which $\varepsilon_{crit} = \sqrt{c^2 p_{crit}^2 + m_0^2 c^4}$, will appear instead of p_{crit}, where m_0 is the rest mass of the primary particles, i.e.

$$\frac{\delta D(\varepsilon, y, \varphi)}{D(\varepsilon)} = \begin{cases} -f, & \text{if } \varepsilon \leqslant \varepsilon_{crit}, \\ 0, & \text{if } \varepsilon > \varepsilon_{crit}. \end{cases} \tag{21}$$

Here

$$\varepsilon_{crit} = \sqrt{\frac{Z^2 e^2 \overline{H}^2 l_\delta^2}{4} \beta^2(\varphi, y) + m_0^2 c^4} \approx \frac{Ze\overline{H} l_\delta}{2} \beta(\varphi, y). \tag{22}$$

The latter expression for ε_{crit} is correct with sufficient accuracy when $\frac{Ze\overline{H} l_\delta}{2} \beta(\varphi, y) > 2m_0 c^2$. Substituting (21) into (20), we obtain

$$\frac{\delta N_\lambda^i(h_0, y, \varphi)}{N_\lambda^i(h_0)} = \begin{cases} 0, & \text{if } \varepsilon_{crit} \leqslant \varepsilon_\lambda, \\ -f \int_{\varepsilon_\lambda}^{\varepsilon_{crit}(y, \varphi)} W_\lambda^i(\varepsilon, h_0)\, d\varepsilon, & \text{if } \varepsilon_{crit} > \varepsilon_\lambda. \end{cases} \tag{23}$$

By means of the graphs of Fig. 2, which give the dependence of

$$\int_{\varepsilon_\lambda}^{\varepsilon_{crit}} W_\lambda^i(\varepsilon, h_0)\, d\varepsilon$$

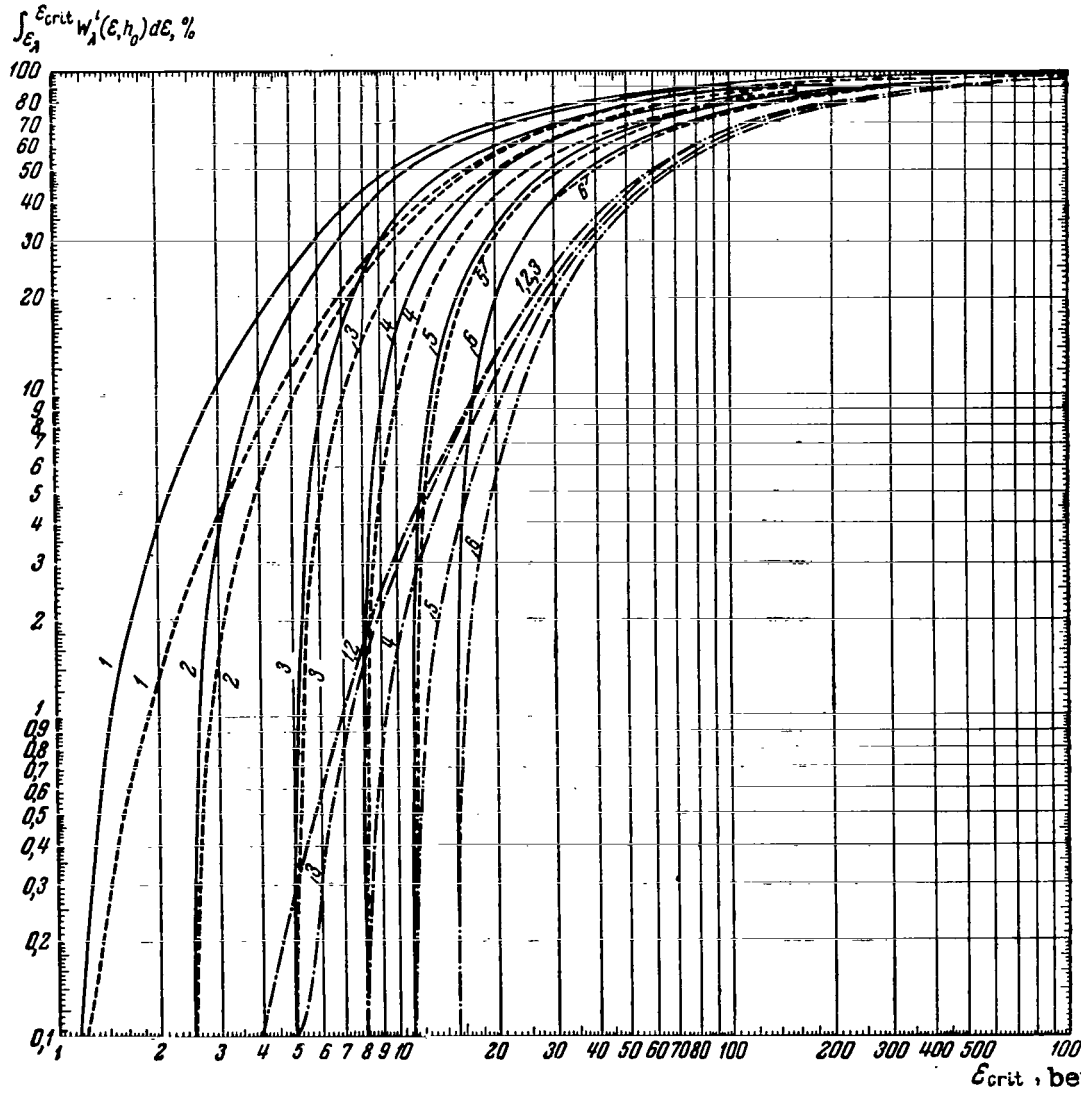

Fig. 2. Dependence of $\int_{\varepsilon_\lambda}^{\varepsilon_{crit}} W_\lambda^i(\varepsilon, h_0)\, d\varepsilon$ on ε_{crit} for various components of cosmic rays.
Solid curves -- neutron component at mountain level; dashed curves -- neutron component at sea level; dashed-dotted curves -- hard component at sea level. The numbers on the curves denote: 1 -- for ε_λ = 1 bev; 2 -- ε_λ = 2.5 bev; 3 -- ε_λ = 5 bev; 4 -- ε_λ = 8 bev; 5 -- ε_λ = 11 bev; 6 -- ε_λ = 15 bev.

on ε_{crit} for components of various types and various geomagnetic latitudes, it is easy to find the dependence of the intensities of various components at various latitudes on φ and y from Table 1 for any values of $Ze\bar{H}l_{\delta}$ and various distributions of the magnetic field in the stream. As an example, we shall present in Table 2 the results of calculations for $Ze\bar{H}l_{\delta}$ = 100 bev of the expected intensities of the neutron and hard components of cosmic rays for various positions of the Earth in the stream (various y). Here it is assumed that the coefficient f = 0.1. The calculations were performed for the cases of the homogeneous field (α = 1, see Table 1) and the field whose intensity drops linearly from H_{max} at the advancing side edge to zero at the lagging edge (α = 0, see Table 1). In these calculations we did not consider the influence of the Earth's magnetic field on the trajectories of the charged particles. This influence is a rather complex function of the latitude of the observation point, type of recording apparatus, and hardness of the particles, the intensity of which is modulated by the stream (i.e. depends also on the field intensity and its distribution in the stream). Hence below we shall attempt to evaluate only extremely roughly the role of the geomagnetic field. We should note that the expected distribution of intensity of cosmic rays cited in Table 2 pertains to measurements by instruments with an extremely narrow effective solid angle. The standard instruments (neutron monitors, ionization chambers, and cubic telescopes) are effective for particles arriving at angles within limits of approximately $\pm 30^{\circ}$ to the vertical [4]. This circumstance can be considered approximately by averaging the data of Table 2 by means of a sliding mean of five consecutive values

$$\left(\frac{\delta N}{N}\right)_{\varphi} = \frac{1}{5}\left[\left(\frac{\delta N}{N}\right)_{\varphi-30^{\circ}} + \left(\frac{\delta N}{N}\right)_{\varphi-15^{\circ}} + \left(\frac{\delta N}{N}\right)_{\varphi} + \left(\frac{\delta N}{N}\right)_{\varphi+15^{\circ}} + \left(\frac{\delta N}{N}\right)_{\varphi+30^{\circ}}\right].$$

Table 3, in which the results of such calculations are presented, shows that in this case the amplitude of the diurnal variation substantially decreases.

5. APPROXIMATE CONSIDERATION OF THE INFLUENCE OF THE GEOMAGNETIC FIELD ON THE TRAJECTORIES OF CHARGED PARTICLES, THE INTENSITY OF WHICH IS ANISOTROPICALLY MODULATED BY THE STREAM

The cosmic ray intensity recorded by neutron monitors and ionization chambers is determined basically by the primary particles that arrive at the Earth in a relatively small solid angle to the vertical. Hence the influence of the geomagnetic field on the trajectories of the particles can be approximately characterized by the effective angles for the particles falling along the vertical

$\psi_\lambda(\varepsilon)$ (the angle between the projection of the direction of motion of the particle far from the Earth on the plane of the geomagnetic equator and the projection on the same plane of the vertical to the observation point) and $\Phi_\lambda(\varepsilon)$ (the angle between the direction of motion of the particle far from the Earth and the plane of the geomagnetic equator) [1, 5, 6]. If at the moment when the Earth is at a distance y from the advancing edge of the stream, the local solar time of the observation point is t hrs, the angle χ between the projection of the direction of motion of the particles outside the action of the Earth's field on the plane of the geomagnetic equator and the Earth-Sun line will be

$$\chi = (t - 12) \cdot 15^\circ + \psi_\lambda(\varepsilon). \tag{24}$$

Let the magnetic field in the stream be perpendicular to the plane of the ecliptic. Then $\chi = \varphi$, and the angle $\Phi_\lambda(\varepsilon)$ characterizes the inclination of the trajectory of the particle in the stream to the plane perpendicular to the magnetic field of the stream. In this case a small inclination of the axis of rotation of the Earth toward the perpendicular to the plane of the ecliptic will cause a certain asymmetry between the variations in the Southern and Northern Hemispheres of the Earth, which we shall not consider as yet. The lack of coincidence of the rotational axis of the Earth with the axis of the geomagnetic dipole will cause a supplementary modulation, an evaluation of which has been given in [1, para. 27, section 4].

The power of the source of variations f may, generally speaking, depend on the inclination of the trajectory of the particles to the direction of the field in the stream, i.e. on the angle Φ [1].

Thus, the variations of the primary spectrum expected in this case can be represented in the form

$$\frac{\delta D(\varepsilon, t, y)}{D(\varepsilon)} = f(\Phi) \begin{cases} -1, & \text{if} \quad \varepsilon \leqslant \varepsilon_{\text{crit}}, \\ 0, & \text{if} \quad \varepsilon > \varepsilon_{\text{crit}}. \end{cases} \tag{25}$$

Here

$$\varepsilon_{\text{crit}} = \frac{Ze\bar{H}l_\delta}{2} \beta[(t - 12) \cdot 15^\circ + \psi_\lambda(\varepsilon), y], \tag{26}$$

where $\beta(\varphi, y)$ is determined by expression (13) or by expression (14) depending on the direction of the field in the stream.

If the field in the stream is parallel to the plane of the ecliptic, then φ and Φ will be determined by more complex expressions.

Table 2

Expected Decrease (in Percent) in the Intensity of Various Components of Cosmic Rays in the Middle Latitudes (ε_λ = 2.5 bev) and at the Equator (ε_λ = 15 bev) as a Function of y and φ for Various Distributions of the Magnetic Field in the Stream (α = 0 and 1). It is Assumed that f = 0.1; 300 $\overline{H}l_\delta$ = 100 bev. All the Values in the Table are Negative. Values are Presented for $0^\circ \leqslant \varphi \leqslant 180^\circ$. If $\varphi > 180^\circ$, the Amplitude of the Decrease will be the Same as at $360^\circ - \varphi$

Secondary component	ε_λ, bev	$\alpha = 1$													
		y \ φ	0°	15°	30°	45°	60°	75°	90°	105°	120°	135°	150°	175°	180°
		1	2	3	4	5	6	7	8	9	10	11	12	13	14
Neutron at mountain level	2,5	0,1	1,8	1,9	2,0	2,4	2,8	3,5	4,5	5,6	6,6	7,7	8,3	8,2	8,0
		0,2	4,5	4,6	4,8	5,2	5,6	6,0	6,6	7,2	7,9	8,2	8,1	8,0	7,9
		0,3	5,9	5,9	6,0	6,3	6,7	7,0	7,4	8,0	8,2	8,0	7,9	7,9	7,8
		0,4	6,6	6,6	6,9	7,0	7,2	7,7	8,0	8,2	7,9	7,8	7,6	7,4	7,4
		0,5	7,0	7,0	7,2	7,4	7,6	7,9	8,2	7,9	7,6	7,4	7,2	7,0	7,0
		0,6	7,4	7,4	7,6	7,8	7,9	8,2	8,0	7,7	7,2	7,0	6,9	6,6	6,6
		0,7	7,8	7,9	7,9	8,0	8,2	8,0	7,4	7,0	6,7	6,3	6,0	5,9	5,9
		0,8	7,9	8,0	8,1	8,2	7,9	7,2	6,6	6,0	5,6	5,2	4,8	4,6	4,5
		0,9	8,0	8,2	8,3	7,7	6,6	5,6	4,5	3,5	2,8	2,4	2,0	1,9	1,8
	15	0,1	0	0	0	0	0	0	0	0	2,0	4,6	5,8	5,6	5,6
		0,2	0	0	0	0	0	0	2,0	3,5	5,2	5,9	5,4	5,2	5,2
		0,3	0	0	0,5	1,0	2,0	3,0	4,0	5,2	5,8	5,2	4,9	4,7	4,8
		0,4	2,0	2,0	2,3	2,7	3,5	4,2	5,2	5,8	5,2	4,7	4,2	4,0	4,0
		0,5	3,2	3,2	3,5	3,8	4,3	5,2	6,0	5,2	4,3	3,8	3,5	3,2	3,2
		0,6	4,0	4,0	4,2	4,7	5,2	5,8	5,2	4,2	3,5	2,7	2,3	2,0	2,0
		0,7	4,8	4,7	4,9	5,2	5,8	5,2	4,0	3,0	2,0	1,0	0,50	0	0
		0,8	5,2	5,2	5,4	5,9	5,2	3,5	2,0	0	0	0	0	0	0
		0,9	5,6	5,6	5,8	4,6	2,0	0	0	0	0	0	0	0	0

Neutron at sea level		0,1	0,94	1,0	1,2	1,3	1,6	2,1	3,05	4,1	5,5	6,8	8,2	7,6	7,5
		0,2	3,1	3,1	3,3	3,7	4,0	4,7	5,7	6,7	7,4	7,6	7,4	7,2	7,2
		0,3	4,5	4,5	4,7	5,1	5,5	6,0	6,6	7,2	7,6	7,4	7,2	7,0	7,0
		0,4	5,6	5,6	5,8	6,0	6,4	6,7	7,3	7,6	7,2	7,0	6,8	6,6	6,6
	2,5	0,5	6,2	6,2	6,4	6,6	6,8	7,2	7,8	7,2	6,8	6,6	6,4	6,2	6,2
		0,6	6,6	6,6	6,8	7,0	7,2	7,6	7,2	6,7	6,4	6,0	5,8	5,6	5,6
		0,7	7,0	7,0	7,2	7,4	7,6	7,2	6,6	6,0	5,5	5,1	4,7	4,5	4,5
		0,8	7,2	7,2	7,4	7,6	7,4	6,7	5,5	4,7	4,0	3,7	3,3	3,1	3,1
		0,9	7,5	7,6	8,2	6,8	5,5	4,1	3,05	2,1	1,6	1,3	1,2	1,0	0,94
Hard at sea level		0,1	0,027	0,03	0,034	0,05	0,09	0,16	0,31	0,6	1,3	2,9	4,2	4,0	4,0
		0,2	0,31	0,31	0,36	0,48	0,6	0,82	1,3	2,1	3,4	4,1	3,7	3,4	3,4
		0,3	0,78	0,78	0,86	0,96	1,3	1,75	2,4	3,5	4,1	3,6	3,2	3,0	3,0
		0,4	1,3	1,3	1,4	1,7	2,0	2,60	3,4	4,2	3,4	3,0	2,7	2,4	2,4
	2,5	0,5	1,9	1,9	2,1	2,4	2,7	3,4	4,3	3,4	2,7	2,4	2,1	1,9	1,9
		0,6	2,4	2,4	2,7	3,0	3,4	4,2	3,4	2,6	2,0	1,70	1,4	1,3	1,3
		0,7	3,0	3,0	3,2	3,6	4,1	3,5	2,4	1,75	1,3	0,96	0,86	0,78	0,78
		0,8	3,4	3,4	3,7	4,1	3,4	2,1	1,3	0,82	0,6	0,48	0,36	0,31	0,31
		0,9	4,0	4,0	4,2	2,9	1,3	0,60	0,31	0,16	0,09	0,05	0,034	0,03	0,027
		0,1	0	0	0	0	0	0	0	0	0,60	2,3	3,6	3,5	3,5
		0,2	0	0	0	0	0	0,02	0,6	1,4	2,9	3,6	3,2	3,0	3,0
		0,3	0	0	0,16	0,3	0,6	1,00	1,8	3,0	3,6	3,0	2,6	2,5	2,5
		0,4	0,6	0,6	0,7	0,96	1,4	2,0	3,0	3,6	3,0	2,4	2,1	1,8	1,8
	15	0,5	1,2	1,2	1,4	1,70	2,2	2,9	3,8	2,9	2,2	1,7	1,4	1,2	1,2
		0,6	1,8	1,8	2,1	2,4	3,0	3,6	2,9	2,0	1,4	0,96	0,70	0,6	0,6
		0,7	2,5	2,5	2,6	3,0	3,6	3,0	1,8	1,00	0,6	0,30	0,16	0	0
		0,8	3,0	3,0	3,2	3,6	2,9	1,4	0,6	0,02	0	0	0	0	0
		0,9	3,5	3,5	3,6	2,3	0,6	0	0	0	0	0	0	0	0

Table 2 (Conclusion)

Secondary component	ε_λ, bev	$\alpha = 0$													
		y \ φ	0°	15°	30°	45°	60°	75°	90°	105°	120°	135°	150°	175°	180°
		1	15	16	17	18	19	20	21	22	23	24	25	26	27
Neutron at mountain level		0,1	4,2	4,2	4,6	5,0	5,4	6,0	6,6	7,2	7,8	8,2	8,0	8,0	7,9
		0,2	6,4	6,4	6,5	6,8	7,0	7,4	7,8	8,2	7,9	7,8	7,7	7,6	7,6
		0,3	7,2	7,2	7,3	7,4	7,6	8,0	8,2	7,9	7,6	7,4	7,2	7,0	7,0
		0,4	7,6	7,6	7,7	7,8	8,0	8,2	7,8	7,3	7,0	6,7	6,5	6,4	6,4
	2,5	0,5	7,8	7,8	7,9	8,0	8,3	7,6	7,0	6,4	6,2	5,8	5,4	5,3	5,3
		0,6	8,0	8,0	8,2	8,3	7,6	6,8	6,0	5,2	4,5	4,2	3,8	3,7	3,6
		0,7	8,2	8,2	8,2	7,5	6,4	5,1	4,1	3,0	2,4	1,8	1,7	1,6	1,5
		0,8	8,2	8,2	7,4	5,8	3,6	2,1	1,1	0,48	0,1	0	0	0	0
		0,9	8,2	7,4	3,3	0,64	0	0	0	0	0	0	0	0	0
		0,1	0	0	0	0	0	0	1,7	3,4	5,0	5,8	5,4	5,2	5,2
		0,2	1,4	1,4	1,7	2,3	3,0	3,8	4,8	5,8	5,2	4,9	4,5	4,3	4,3
		0,3	3,2	3,2	3,5	4,0	4,5	5,2	5,8	5,1	4,3	3,8	3,4	3,2	3,2
		0,4	4,3	4,3	4,5	5,0	5,4	5,8	4,8	3,8	3,0	2,3	1,8	1,4	1,4
		0,5	4,9	5,0	5,2	5,6	6,0	4,3	3,2	2,0	0,6	0	0	0	0
		0,6	5,4	5,4	5,6	5,8	4,3	2,4	0,58	0	0	0	0	0	0
		0,7	5,6	5,7	5,8	4,0	1,4	0	0	0	0	0	0	0	0
		0,8	5,8	5,8	4,0	0	0	0	0	0	0	0	0	0	0
		0,9	6,0	3,9	0	0	0	0	0	0	0	0	0	0	0

Neutron at sea level		0,1	2,9	2,9	3,1	3,4	3,8	4,5	5,4	6,3	7,2	7,6	7,4	7,3	7,3
		0,2	5,2	5,2	5,4	5,7	6,0	6,4	7,0	7,6	7,3	7,1	6,9	6,8	6,8
		0,3	6,2	6,2	6,4	6,6	6,8	7,3	7,7	7,2	6,7	6,6	6,3	6,1	6,1
		0,4	6,8	6,8	6,9	7,2	7,4	7,6	7,0	6,4	6,0	5,7	5,4	5,2	5,2
	2,5	0.5	7,8	7,2	7,3	7,5	7,8	6,8	6,2	5,4	5,2	4,4	4,0	3,9	3,9
		0,6	7,4	7,4	7,6	7,7	6,8	5,7	4,8	3,8	3,2	2,8	2,5	2,4	2,3
		0,7	7,5	7,5	7,7	6,6	5,2	3,7	2,7	1,85	1,4	1,05	0,88	0,74	0,72
		0,8	7,6	7,6	6,6	4,1	2,3	1,15	0,52	0,22	0,02	0	0	0	0
		0,9	7,7	6,6	2,0	0,29	0	0	0	0	0	0	0	0	0
Hard at sea level		0,1	0,28	0,28	0,31	0,4	0,52	0,86	1,05	2,0	3,6	4,1	3,7	3,6	3,5
		0,2	1,05	1,05	1,2	1,4	1,75	2,3	3,1	4,4	4,3	3,2	2,9	2,7	2,7
		0,3	1,9	1,9	2,2	2,4	2,9	3,4	4,4	3,4	2,7	2,3	2,1	2,0	2,0
		0,4	2,7	2,7	2,9	3,2	3,7	4,4	3,1	2,3	1,8	1,4	1,2	1,05	1,05
	2,5	0,5	3,2	3,3	3,4	3,8	4,3	2,8	1,95	1,3	1,05	0,69	0,58	0,5	0,5
		0,6	3,7	3,7	4,0	4,3	2,7	1,25	0,94	0,52	0,31	0,26	0,2	0,18	0,18
		0,7	4,0	4,0	4,2	2,5	1,05	0,48	0,24	0,11	0,06	0,03	0,024	0,017	0,017
		0,8	4,2	4,2	2,4	0,58	0,17	0,03	0,01	0	0	0	0	0	0
		0,9	4,3	2,4	0,1	0	0	0	0	0	0	0	0	0	0
		0,1	0	0	0	0	0	0	0,58	1,4	2,7	3,6	3,2	3,1	2,9
		0,2	0,35	0,35	0,48	0,72	1,1	1,45	2,5	3,6	2,9	2,6	2,3	2,0	2,0
		0,3	1,25	1,25	1,5	1,8	2,3	2,9	3,7	2,8	2,2	1,6	1,4	1,2	1,2
		0,4	2,1	2,1	2,3	2,7	3,2	3,6	2,5	1,6	1,1	0,72	0,52	0,35	0,35
	15	0,5	2,6	2,7	2,9	3,3	3,8	2,3	1,2	0,6	0,14	0	0	0	0
		0,6	3,1	3,1	3,4	3,7	2,1	0,8	0,12	0	0	0	0	0	0
		0,7	3,5	3,5	3,7	1,9	0,32	0	0	0	0	0	0	0	0
		0,8	3,6	3,6	1,8	0	0	0	0	0	0	0	0	0	0
		0,9	3,7	1,75	0	0	0	0	0	0	0	0	0	0	0

Table 3

The Same as in Table 2, but for Sliding Means from $\varphi - 30^\circ$ to $\varphi + 30^\circ$. Values are Presented for $0^\circ \leqslant \varphi \leqslant 180^\circ$. If $\varphi > 180^\circ$, the Amplitude of the Decrease will be the Same as at $360^\circ - \varphi$

Secondary component	ε_λ, bev	$\alpha = 1$												
		y \ φ	0°	15°	30°	45°	60°	75°	90°	105°	120°	135°	150°	175°	180°
Neutron at mountain level	2,5	0,1	1,92	2,00	2,18	2,52	3,04	3,76	4,60	5,58	6,54	7,28	7,76	8,08	8,20
		0,2	4,66	4,74	4,94	5,24	5,64	6,12	6,66	7,18	7,60	7,88	8,02	8,04	8,02
		0,3	5,94	6,00	6,16	6,38	6,68	7,08	7,46	7,72	7,90	8,00	7,96	7,90	7,88
		0,4	6,72	6,74	6,86	7,08	7,36	7,62	7,80	7,92	7,90	7,78	7,62	7,52	7,48
		0,5	7,08	7,12	7,24	7,42	7,66	7,80	7,84	7,80	7,66	7,42	7,24	7,12	7,08
		0,6	7,48	7,52	7,62	7,78	7,90	7,92	7,80	7,62	7,36	7,08	6,86	6,74	6,72
		0,7	7,88	7,90	7,96	8,00	7,90	7,72	7,46	7,08	6,68	6,38	6,16	6,00	5,94
		0,8	8,02	8,04	8,02	7,88	7,60	7,18	6,66	6,12	5,64	5,24	4,94	4,74	4,66
		0,9	8,20	8,08	7,76	7,28	6,54	5,58	4,60	3,76	3,04	2,52	2,18	2,00	1,92
	15	0,1	0	0	0	0	0	0	0,40	1,32	2,48	3,60	4,72	5,44	5,68
		0,2	0	0	0	0	0,4	1,10	2,14	3,32	4,40	5,04	5,38	5,38	5,28
		0,3	0,20	0,30	0,70	1,30	2,10	3,04	4,0	4,64	5,02	5,16	5,08	4,86	4,80
		0,4	2,12	2,20	2,50	2,94	3,58	4,28	4,78	5,02	5,02	4,78	4,42	4,20	4,08
		0,5	3,32	3,38	3,60	4,00	4,56	4,90	5,00	4,90	4,56	4,00	3,60	3,38	3,32
		0,6	4,08	4,20	4,42	4,78	5,02	5,02	4,78	4,28	3,58	2,94	2,50	2,20	2,12
		0,7	4,80	4,86	5,08	5,16	5,02	4,64	4,00	3,04	2,10	1,30	0,70	0,30	0,20
		0,8	5,28	5,38	5,38	5,04	4,40	3,32	2,14	1,10	0,40	0	0	0	0
		0,9	5,68	5,44	4,72	3,60	2,48	1,32	0,4	0	0	0	0	0	0
Neutron at sea level		0,1	1,06	1,08	1,20	1,44	1,84	2,42	3,18	4,30	5,44	6,36	7,04	7,46	7,74
		0,2	3,18	3,26	3,46	3,76	4,24	4,92	5,70	6,42	6,92	7,26	7,36	7,32	7,28
		0,3	4,58	4,66	4,86	5,08	5,60	6,08	6,50	6,96	7,20	7,28	7,24	7,12	7,08
		0,4	5,68	5,72	5,88	6,10	6,44	6,78	7,06	7,16	7,18	7,04	6,84	6,72	6,68

Neutron at sea level	2,5	0,5	6,28	6,32	6,44	6,64	6,96	7,12	7,18	7,12	6,96	6,64	6,44	6,32	6,28
		0,6	6,68	6,72	6,84	7,04	7,18	7,16	7,04	6,78	6,44	6,10	5,88	5,72	5,68
		0,7	7,08	7,12	7,24	7,28	7,20	6,96	6,60	6,08	5,60	5,08	4,86	4,66	4,58
		0,8	7,28	7,32	7,36	7,26	6,92	6,42	5,66	4,92	4,24	3,76	3,46	3,26	3,18
		0,9	7,74	7,46	7,04	6,36	5,44	4,30	3,32	2,42	1,84	1,44	1,20	1,08	1,06
Hard at sea level		0,1	0,03	0,034	0,046	0,08	0,13	0,24	0,488	1,05	1,86	2,60	3,28	3,82	4,08
		0,2	0,33	0,50	0,41	0,60	0,70	1,06	1,128	2,34	2,92	3,34	3,60	3,60	3,52
		0,3	0,82	0,83	0,94	1,12	1,45	1,98	2,59	3,06	3,36	3,48	3,38	3,16	3,08
		0,4	1,34	1,40	1,54	1,80	2,22	2,76	3,10	3,32	3,32	3,14	2,78	2,58	2,52
	2,5	0,5	1,98	2,02	2,18	2,50	2,98	3,24	3,30	3,24	2,98	2,50	2,18	2,02	1,98
		0,6	2,52	2,58	2,78	3,14	3,32	3,32	3,14	2,76	2,22	1,80	1,54	1,40	1,34
		0,7	3,08	3,16	3,38	3,48	3,36	3,06	2,60	1,98	1,45	1,12	0,94	0,83	0,82
		0,8	3,52	3,60	3,60	3,34	2,92	2,34	1,64	1,06	0,70	0,60	0,41	0,50	0,33
		0,9	4,08	3,82	3,28	2,60	1,86	1,05	0,05	0,24	0,13	0,08	0,046	0,034	0,03
		0,1	0	0	0	0	0	0	0,12	0,58	1,30	2,00	2,70	3,28	3,54
		0,2	0	0	0	0,04	0,12	0,40	0,96	1,70	2,80	2,82	3,14	3,16	3,08
		0,3	0,06	0,08	0,22	0,42	0,78	1,34	2,0	2,50	2,80	2,94	2,84	2,60	2,52
		0,4	0,64	0,70	0,86	1,14	1,62	2,20	2,60	2,78	2,80	2,58	2,22	1,98	1,92
		0,5	1,28	1,34	1,54	1,88	2,40	2,70	2,80	2,70	2,40	1,88	1,54	1,34	1,28
	15	0,6	1,92	1,98	2,22	2,58	2,80	2,78	2,58	2,20	1,62	1,14	0,86	0,70	0,64
		0,7	2,52	2,60	2,84	2,94	2,80	2,50	2,02	1,34	0,78	0,42	0,22	0,08	0,06
		0,8	3,08	3,16	3,14	2,82	2,80	1,70	1,00	0,40	0,12	0,04	0	0	0
		0,9	3,54	3,28	2,70	2,00	1,30	0,58	0,12	0	0	0	0	0	0

Table 3 (Conclusion)

Secondary component	ε_λ, bev	$\alpha = 0$; φ / γ	0°	15°	30°	45°	60°	75°	90°	105°	120°	135°	150°	175°	180°
Neutron at mountain level	2,5	0,1	4,36	4,44	4,68	5,04	5,52	6,04	6,60	7,16	7,56	7,84	7,98	8,02	7,98
		0,2	6,44	6,50	6,62	6,82	7,10	7,44	7,66	7,82	7,88	7,84	7,72	7,66	7,64
		0,3	7,20	7,22	7,30	7,50	7,70	7,82	7,86	7,82	7,66	7,42	7,24	7,12	7,08
		0,4	7,64	7,66	7,74	7,86	7,90	7,82	7,66	7,40	7,06	6,78	6,60	6,48	6,44
		0,5	7,84	7,86	7,96	7,92	7,76	7,46	7,10	6,60	6,16	5,82	5,60	5,42	5,34
		0,6	8,08	8,10	8,02	7,78	7,38	6,78	6,02	5,34	4,74	4,28	3,96	3,80	3,72
		0,7	8,20	8,06	8,04	7,08	6,26	5,22	4,20	3,28	2,60	2,10	1,80	1,64	1,62
		0,8	7,88	7,56	6,64	5,42	4,00	2,62	1,48	0,76	0,24	0,12	0,02	0	0
		0,9	5,92	5,38	3,9	2,26	0,78	0,12	0	0	0	0	0	0	0
	15	0,1	0	0	0	0	0,34	1,02	2,02	3,18	4,26	4,96	5,32	5,36	5,28
		0,2	1,52	1,64	1,96	2,44	3,12	3,94	4,52	4,90	5,04	4,96	4,64	4,46	4,38
		0,3	3,32	3,42	3,68	4,08	4,60	4,92	4,98	4,84	4,48	3,96	3,58	3,36	3,28
		0.4	4,38	4,48	4,70	5,0	5,10	4,96	4,56	3,94	3,14	2,46	1,96	1,66	1,56
		0,5	5,06	5,14	5,34	5,22	4,86	4,22	3,22	2,02	1,16	0,52	0,12	0	0
		0,6	5,48	5,52	5,30	4,70	3,74	2,62	1,46	0,60	0,12	0	0	0	0
		0,7	5,72	5,36	4,50	3,38	2,24	1,08	1,28	0	0	0	0	0	0
		0,8	5,08	4,28	3,12	1,96	0,80	0	0	0	0	0	0	0	0
		0,9	2,76	2,76	1,96	0,78	0	0	0	0	0	0	0	0	0
Neutron at sea level	2,5	0,1	2,98	3,04	3,22	3,54	4,04	4,68	5,44	6,20	6,78	7,16	7,36	7,38	7,34
		0,2	5,28	5,34	5,50	5,74	6,10	6,54	6,86	7,08	7,18	7,14	6,98	6,88	6,84
		0,3	6,28	6,32	6,44	6,66	6,96	7,12	7,14	7,10	6,90	6,58	6,36	6,24	6,18
		0,4	6,84	6,90	7,02	7,18	7,22	7,12	6,88	6,54	6,10	5,74	5,50	5,34	5,28

Neutron at sea level	2,5	0,5	7,20	7,24	7,36	7,32	7,12	6,74	6,28	5,60	5,04	4,58	4,28	4,02	3,94
		0,6	7,48	7,50	7,38	7,04	6,52	5,76	4,86	4,06	3,42	2,94	2,64	2,48	2,42
		0,7	7,58	7,36	6,90	6,14	5,18	4,01	2,98	2,15	1,60	1,20	0,96	0,82	0,8
		0,8	7,20	6,70	5,64	4,35	2,93	1,65	0,84	0,38	0,15	0,04	0	0	0
		0,9	4,98	4,64	3,32	1,78	0,46	0,06	0	0	0	0	0	0	0
Hard at sea level		0,1	0,29	0,31	0,36	0,47	0,628	0,97	1,66	2,32	2,88	3,40	3,70	3,70	3,62
		0,2	1,11	1,14	1,28	1,54	1,96	2,60	3,00	3,30	3,42	3,34	3,00	2,86	2,80
		0,3	2,02	2,06	2,26	2,56	3,06	3,30	3,36	3,24	2,98	2,52	2,22	2,08	2,04
		0,4	2,78	2,84	3,04	3,34	3,42	3,34	3,06	2,60	1,96	1,54	1,28	1,12	1,08
	2,5	0,5	3,32	3,40	3,60	3,52	3,26	2,84	2,28	1,56	1,12	0,82	0,66	0,56	0,54
		0,6	3,82	3,84	3,68	3,20	2,62	1,92	1,12	0,64	0,46	0,30	0,26	0,22	0,20
		0,7	4,08	3,74	3,14	2,44	1,68	0,86	0,38	0,2	0,09	0,05	0,03	0,02	0,02
		0,8	3,48	3,12	2,32	1,47	0,63	0,16	0,042	0,008	0,002	0	0	0	0
		0,9	1,86	1,84	1,36	0,50	0,02	0	0	0	0	0	0	0	0
		0,1	0	0	0	0	0,12	0,40	0,94	1,66	2,30	2,80	3,10	3,18	3,10
		0,2	0,44	0,48	0,62	0,82	1,24	1,86	2,30	2,60	2,78	2,68	2,36	2,18	2,12
		0,3	1,32	1,38	1,60	1,94	2,44	2,70	2,78	2,64	2,34	1,84	1,52	1,32	1,28
		0,4	2,18	2,26	2,48	2,78	2,86	2,72	2,40	1,90	1,28	0,86	0,60	0,46	0,42
	15	0,5	2,76	2,84	3,06	3,00	2,70	2,24	1,60	0,84	0,38	0,14	0,02	0	0
		0,6	3,22	3,28	3,08	2,62	2,02	1,34	0,60	0,18	0,02	0	0	0	0
		0,7	3,58	3,22	2,58	1,88	1,18	0,44	0,06	0	0	0	0	0	0
		0,8	2,88	2,52	1,80	1,08	0,36	0	0	0	0	0	0	0	0
		0,9	1,42	1,42	1,08	0,34	0	0	0	0	0	0	0	0	0

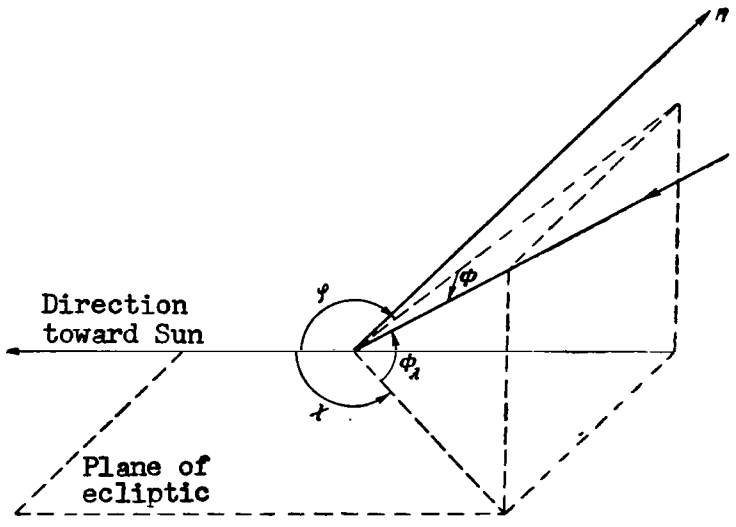

Fig. 3. Determination of the angles φ and Φ in the case when the magnetic field of the stream lies in the plane of the ecliptic.

For definition, let the field in the stream be directed along the revolution of the Earth around the Sun. Then, as can be seen from Fig. 3, the angle Φ will be determined by the expression

$$\sin \Phi = -\sin \chi \cos \Phi_\lambda, \tag{27}$$

while the angle φ will be defined by the expression

$$\sin \Phi = \sin \Phi_\lambda \cos \Phi, \tag{28}$$

[sic] where χ is determined by expression (24). Substituting Φ and φ found from (27) and (28) into (13), we find the dependence of β, and, consequently, ε_{crit} as well, on t and ψ_λ. Then the sought after variation of the intensity $\delta N/N$ of various secondary components can be found by means of formula (23) as functions of t and y for various λ.

For approximate estimations of the expected diurnal variations caused by anisotropic scattering of the particles by inhomogeneous magnetic fields of the streams, it is possible to use the results cited in Table 1 and in Fig. 2. The influence of the magnetic field of course, can be considered extremely approximately by means of certain effective values of the angles $\overline{\psi}_\lambda^i$ and Φ_λ^i for secondary components of the i type and observation points with the geomagnetic

threshold ε_λ [1 (15.7), (15.8)].

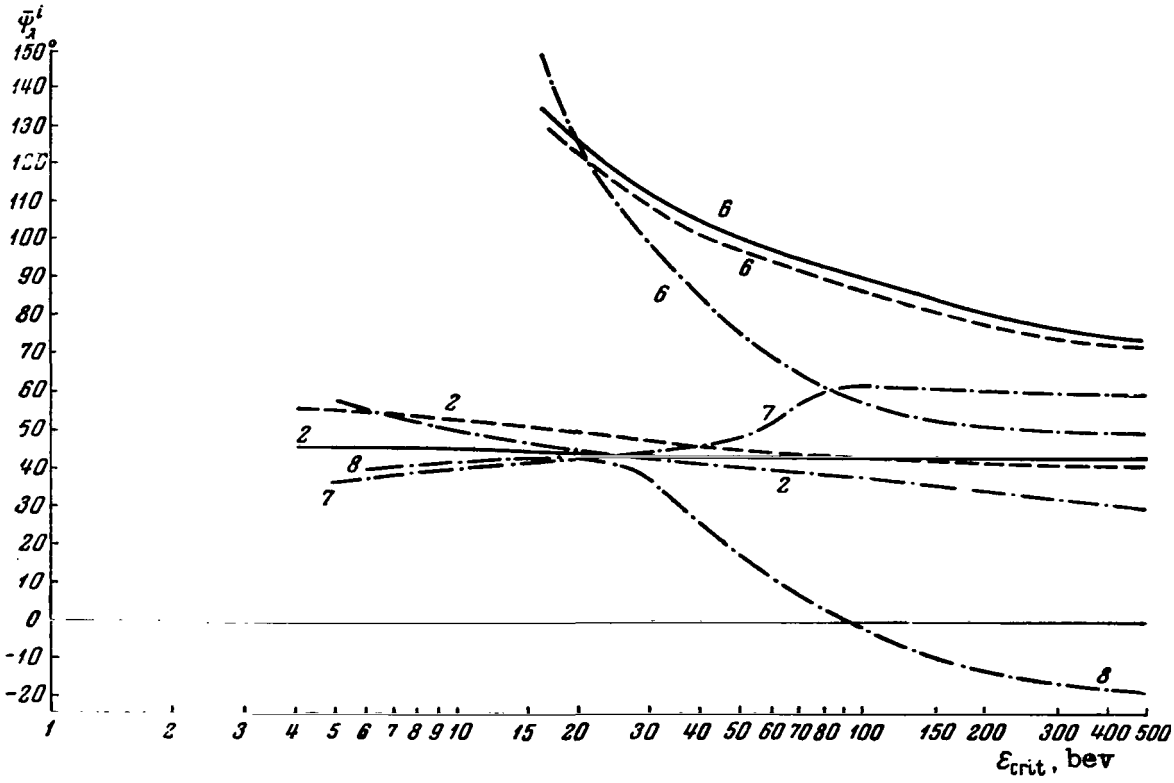

Fig. 4. Dependence of $\bar{\psi}^i_\lambda$ on ε_{crit} for various components of cosmic rays and various latitudes. Notations of curves the same as in Fig. 2. Only curves for $\lambda = 0^\circ$ and $\lambda = 50^\circ$ are presented; curves 7 and 8 -- for particles approaching at an angle of 48° from the east and from the west, respectively.

In this case we must consider that $\bar{\psi}^i_\lambda$ will depend essentially on the type of the component, ε_λ and ε_{crit}. According to (21) and [1, (15.8)], we obtain:

$$\bar{\psi}^i_\lambda = \frac{\int_{\varepsilon_\lambda}^{\varepsilon_{crit}} W^i_\lambda(\varepsilon, h_0)\,\psi_\lambda(\varepsilon)\,d\varepsilon}{\int_{\varepsilon_\lambda}^{\varepsilon_{crit}} W^i_\lambda(\varepsilon, h_0)\,d\varepsilon}. \qquad (29)$$

The dependence of $\bar{\psi}^i_\lambda$ on ε_{crit} for various secondary components

and various λ is presented in Fig. 4. Since ε_{crit} depends in turn on φ and y (see Table 1), $\bar{\psi}^i_\lambda$ also will depend correspondingly on φ and y. The angle $\bar{\Phi}^i_\lambda$ can be found analogously according to (21) and [1, (15.7)]. Its dependence on ε_{crit} is shown in Fig. 5.

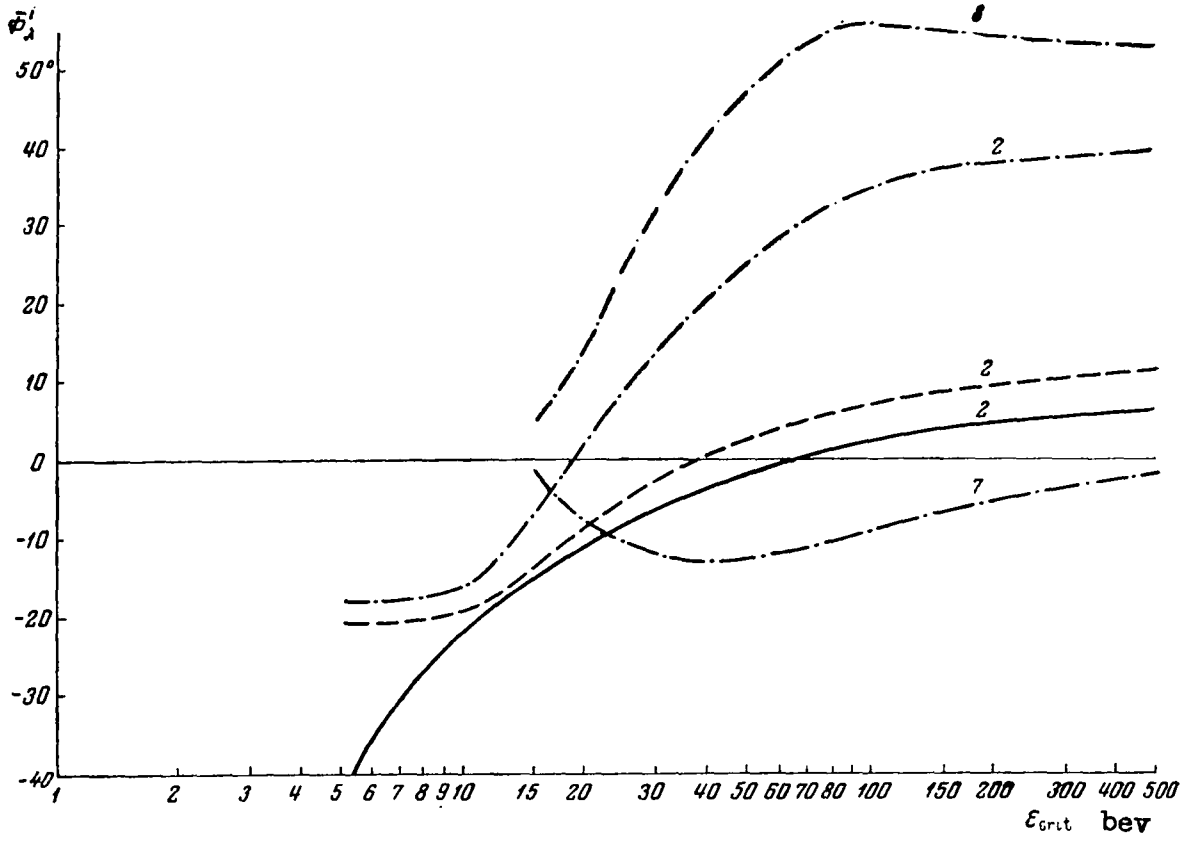

Fig. 5. Dependence of $\bar{\Phi}^i_\lambda$ on ε_{crit} for various components of cosmic rays.
Notations of curves the same as in Fig. 2. Curves are presented only for $\lambda = 50^\circ$; curves 7 and 8 -- for particles arriving at an angle of 48° from the east and from the west, respectively.

Let the magnetic field in the stream be perpendicular to the plane of the ecliptic and directed in the same way as the Earth's field. Then we should compare the local time (in hours) to each value of φ in Tables 1 and 2

$$t = \frac{\varphi - \bar{\psi}^i_\lambda}{15^\circ} + 12. \qquad (24')$$

If the value of $ZeHl_{\delta}$ characterizing the given stream has been determined (for example, from data on the maximum decrease in the intensity of the neutron and hard components of cosmic rays during a magnetic storm [7]), then for given quantities φ and y it is possible to find the value of δ_{crit} by means of Table 1, and the expected decrease in the intensity for various cases of recording and values of $\bar{\psi}_{\lambda}^{i}$ by means of the graphs of Figs. 2 and 4. Finally, with the aid of (24) we find the local time when this decrease is expected. Since the moment when the Earth was captured by the stream is known according to the beginning of the magnetic storm, then for each t in each concrete case the value of y will be known, and thus for each individual magnetic storm we will obtain the expected dependence of the cosmic ray intensity on the time, including the effect of anisotropy (y will vary according to the world time, while χ will vary according to the local time).

The variation of the cosmic ray intensity can be found analogously in the case when the field in the stream is parallel to the plane of the ecliptic: first for given φ and y (the latter is determined by the interval of time from the beginning of the magnetic storm) we find the corresponding δ_{crit} with the aid of Table 1; we find the expected decrease in intensity according to the graphs of Fig. 2, and the values of $\bar{\psi}_{\lambda}^{i}$ and $\bar{\Phi}_{\lambda}^{i}$ according to the graphs of Figs. 4 and 5.

We find χ and Φ by means of functions (27) and (28). From this we find the local time

$$t = \frac{\chi - \bar{\psi}_{\lambda}^{i}}{15^{\circ}} + 12, \qquad (24'')$$

to which the decrease in cosmic ray intensity pertains [the angle Φ may influence the amplitude of the decrease if the coefficient f in (25) depends on Φ]. Thus, in this case too, we can find the change in cosmic ray intensity and solar-diurnal variations expected for each concrete magnetic storm under various assumptions, by means of the graphs and tables presented here.

In conclusion let us note once again that in investigating the anisotropy of cosmic rays during the capture of the Earth by a stream, not only the effect considered here, but also the anisotropy caused by the energy change of the particles under the influence of the electric field of the stream must be taken into consideration. This anisotropy will possess a completely different spectrum from that found here.

The problem of the anisotropy of cosmic rays caused by the energy change of particles on account of the influence of an electric field arising when a corpuscular stream with an inhomogeneous magnetic field passes is considered in reference [3].

Let us take the opportunity to express our profound gratitude to laboratory worker R. T. Gushchina for her aid in performing the numerical calculations.

BIBLIOGRAPHY

1. L. I. Dorman. Variations of Cosmic Rays. Moscow, State Technical Literature Publishing House, 1957.
2. L. I. Dorman. Works of the International Conference on Cosmic Rays, 1959, Publishing House of the Academy of Sciences USSR, 1960, Vol. 4, p. 113.
3. L. I. Dorman. This Collection, p. 121.
4. E. A. Brunberg. Arkiv Fysik, 1958, 14-16, p. 195.
5. E. A. Brunberg, Tellus, 1953, 5, p. 135.
6. E. A. Brunberg, A. Dattner, Tellus, 1953, 5, p. 269.
7. Ya. L. Blokh, L. I. Dorman, N. S. Kaminer. This Collection, p. 1 .

ABSTRACT

The paper discusses diurnal variations of cosmic rays which result from the anisotropic scattering of particles by the frozen regular homogeneous and inhomogeneous magnetic fields. The problem is solved in the general aspect for the field lying perpendicular to the line of the distribution of the stream. The energy spectrum of the variations is found as the function of the local time for different distributions of the magnetic field in the stream without consideration and with approximate consideration of further influence of the magnetic field on the trajectories of the particles. With the applicance of the caupling coefficients the expected variations of the intensity of the neutron and meson components of cosmic rays are determined on the sea level and on the mountain level at stations with different geomagnetic threshold for different distributions of the frozen field and for different positions of the Earth in the stream. The article gives approximated values of the changes of results in calculation of the diagram of the instruments' direction.

VARIATION OF COSMIC RAY INTENSITY DURING MAGNETIC STORMS WITH SUDDEN AND GRADUAL BEGINNINGS

A. I. Ol'

Magnetic storms with sudden and gradual beginnings (in the future we shall call them Sc and G storms) are so different in their characteristic features that they should be considered as due to solar corpuscular streams of two different classes [1, 2]. E. R. Mustel' [3] has come to the conclusion that corpuscular streams causing Sc and G storms should be distinguished according to the following physical parameters: a) velocity of the stream, b) concentrations of the ions in the stream, and c) intensity of the magnetic field related to the stream. E. R. Mustel' believes also that the appearance of Sc storms is caused by streams carrying with them greater frozen magnetic fields than in the case of the streams responsible for G storms. It is known that during magnetic storms noticeable changes are frequently observed in the cosmic ray intensity (I). As a rule, drops in I prove to be related to magnetic storms. According to references [4, 5], considerable drops in I are observed during magnetic storms with sudden beginnings, while G storms, as a rule, do not prove effective in this respect. This is in full agreement with the conclusion of E. R. Mustel' indicated above.

We have undertaken a study of the variations of I during magnetic storms of both types (Sc and G) on the material of observations of the meson component of cosmic radiation at the network of stations of Carnegie Institute (US): Godhavn, Cheltenham, Juancaio, and Christchurch for 1937-1946 [6]. We had no aerological information; hence it was impossible to introduce temperature corrections. We were able to use only a very rough method of eliminating temperature effects, consisting of averaging the values of I for several stations situated at great distances from one another. We might consider that the temperature change from day to day takes place independently at distant stations, i.e. averaging of the values of I leads to an elimination of the temperature effect (although in a first approximation). To eliminate the influence of smooth variations of the temperature during the year and gradual changes in I

of instrumental origin, means were taken not of the values of I themselves, but of their deviations from a smoothed curve constructed according to values of I averaged for the month. By this method we obtained average deviations of I, where the values of the deviations of I (ΔI) for Juancaio were given double the weight. This was due to the fact that the temperature changes of the upper atmosphere from day to day at this equatorial station are small in comparison with the changes at the middle-latitude stations, and, especially, at the high-latitude stations. Average values of ΔI were found from April 1937 to December 1946 (there were no data for October 1943 and May 1946).

A list of all the drops in I no less than 1% was compiled on the basis of these data. The following were taken as characteristics of the drops: the duration of the drop (Δt) in days (i.e. the number of days when consecutive values of ΔI were $\geqslant 1\%$), the greatest negative value of ΔI during the drop, the sum of the negative ΔI during the drop ($\Sigma \Delta I$), and the sum of the values of the 10-point index of the magnetic activity C during the drop (ΣC). From April 1937 to December 1946 a total of 42 drops in the intensity with $\Delta I \geqslant 1\%$ were observed. Of them 32 proved to be related to Sc storms, eight to G storms, and two were not related to magnetic disturbances. It was found that a certain positive correlation exists between the greatest negative value of ΔI during the drop and the duration of the drop: for Δt = 1-2 days, the average $\Delta I = 1.3\%$; for Δt = 3-4 days, $\Delta I = 2.2\%$; and for Δt = 5-6 days, $\Delta I = 3.0\%$. A rather close curvilinear correlation, also positive, exists between ΣC and $\Sigma \Delta I$. However, the three strongest and positive drops (1 March 1942, 5 February and 27 July 1946) differ sharply from this dependence.

To explain the general character of the relationship between magnetic disturbance and the drops in I, we constructed a graph of the average magnetic activity (C) according to the method of superposition of periods (Fig. 1), where dates of the beginnings of the drops with $\Delta I \geqslant 1\%$ were considered as the zero days (there were 31 such days). This figure shows the distribution of the dates of sudden beginnings of magnetic disturbances with respect to the zero days. The data on sudden beginnings were taken from the catalog of world magnetic storms we compiled. It follows from Fig. 1 that the magnetic activity experiences a considerable rise on the average during the day of the beginning of the drop in I. The number of sudden beginnings increases sharply during the day before the beginning of the drop in I. The difference in the moments of the maxima of the two curves in Fig. 1 is explained by the fact that, as a rule, the magnetic activity reaches the greatest value not on the day of the sudden beginning, but on the following day.

For a sharper exposure of the role of sudden beginning in the appearance of drops in I, we constructed a graph (also according to the method of superposition of periods) of average values of ΔI, where the zero days were days with significant $C \geqslant 7$, entering into

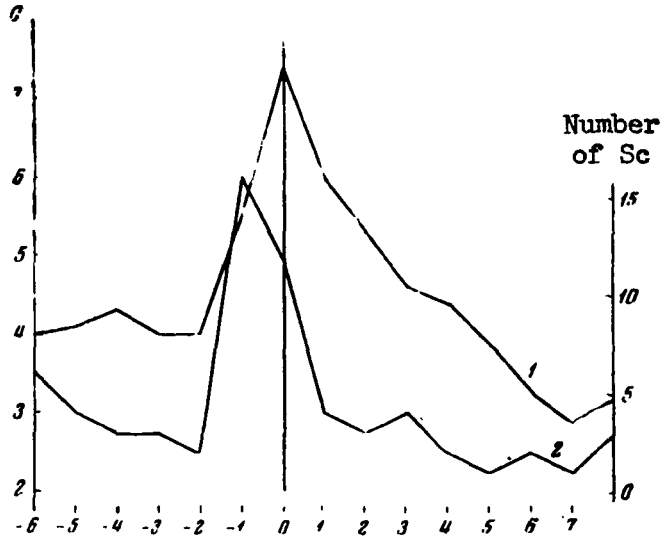

Fig. 1. Graph of the average magnetic activity C (curve 1) and number of magnetic storms with sudden beginnings (curve 2). Zero days -- dates of drops $\Delta I \geqslant 1\%$ in 1937-1946.

the composition of Sc and G storms (Fig. 2,a). The drop in I during a G storm is so small that it cannot be considered as real, since its value is less than triple the root-mean-square error of the values of I, which is of the order of 0.2% [7]. A drop in I during an Sc storm should be considered real. Fig. 2,b shows analogous graphs of the average values of ΔI for days with C = 7, 8, and 9, included among Sc storms. We can see that the average drop in ΔI increases as the disturbance increases. The same graphs were constructed for individual years in 1937-1946. The appearance of drops in I during Sc storms and the absence of drops during G storms holds true in all years, but the drops in I are most weakly pronounced during the period of the minimum of solar activity (1944-1945). This is quite natural, since the Sc storms arising during this period are on the average less intense than those during the period of the maximum.

Then we constructed a graph (Fig. 3) of the variation from year to year of the Wolff number (W), the numbers of Sc and G storms during the year, and the number of negative values of ΔI exceeding 0.6%. From a consideration of Fig. 3 we can conclude that a variation of the number of drops in I occurs generally parallel to the variation of the number of Sc storms and has little in common, especially at the end of the cycle, with the variation of the number of G storms (the corresponding coefficients of the correlation are

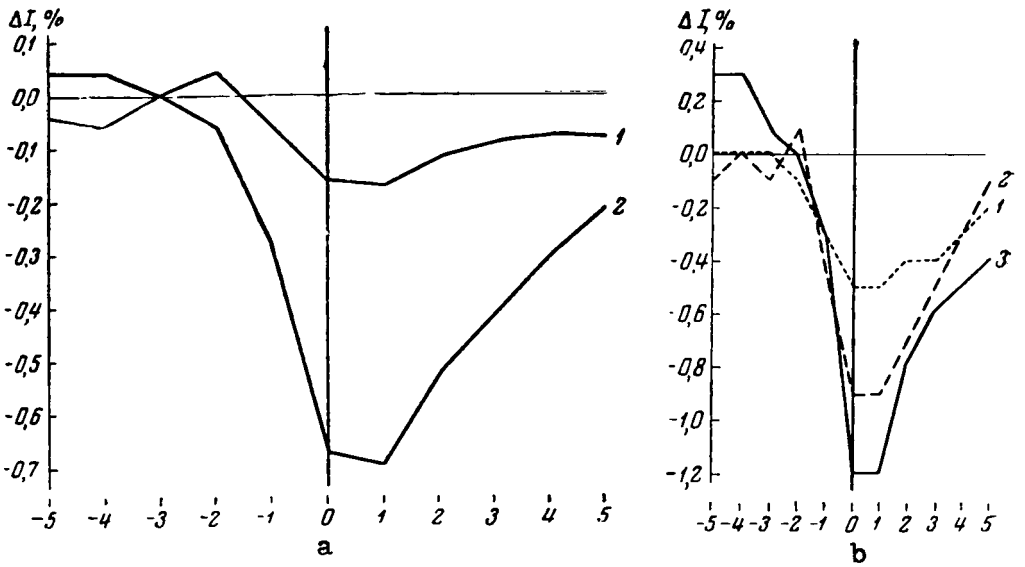

Fig. 2. Graph of the average cosmic ray intensity (ΔI) a -- zero days -- dates of magnetic storms with gradual (curve 1) and sudden beginnings (curve 2); b -- zero days -- storms with sudden beginnings, C = 7 (curve 1), C = 8 (curve 2), C = 9 (curve 3).

equal to $+0.94 \pm 0.04$ and -0.47 ± 0.24).

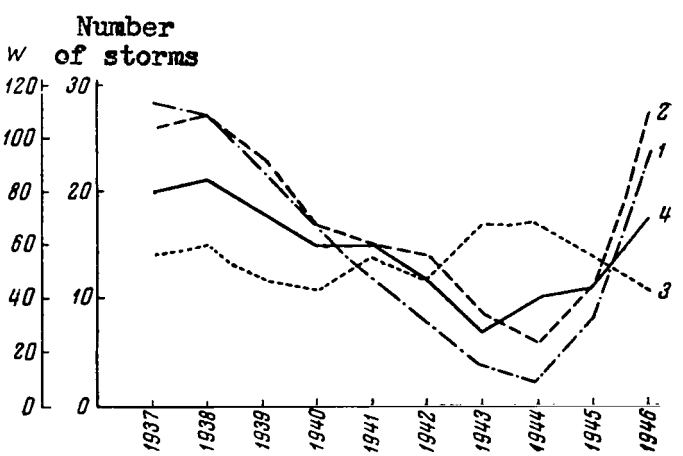

Fig. 3. Changes from year to year of the Wolff number (curve 1), number of storms with sudden beginnings (curve 2), number of storms with gradual beginnings (curve 3), and number of drops $\Delta I \geqslant 0.6\%$ (curve 4).

Thus we can assert that large drops in I are caused chiefly (although not exclusively) by the solar corpuscular streams responsible for magnetic storms with sudden beginnings, while the streams causing storms with gradual beginnings are accompanied by drops in I only in very rare cases, as it also follows from theoretical considerations.

In addition, together with drops in I, sometimes cases are observed of an anomalous increase in I, having the character of strong transitory flareups of the intensity, and lasting for a number of days. Such increases in I are especially noticeable in the neutron component of cosmic radiation. Two interpretations of these phenomena are possible. Increased values in I can be considered the normal level of I, corresponding to quiet conditions on the Sun, i.e. the absence of corpuscular streams that cause drops in I, or as some anomalous phenomenon, possibly related to some sort of special conditions on the Sun.

Several years ago J. A. Simpson [8] discovered that passage through the central meridian of the Sun (in April-September 1953) of the so-called unipolar magnetic regions, discovered by H. W. Babcock and H. D. Babcock, were accompanied by considerable increases in the intensity of the neutron component of cosmic radiation and magnetic disturbances, i.e. ejections of corpuscular radiation from the Sun.

Thus, at least in individual cases, increases in I were not simply "the absence of drops", but special anomalous phenomena.

In the treatment of the data of recording of the neutron component of cosmic rays at the high-latitude observatory of Heiss Island, which began work on the IGY program in January 1958, noticeable increases in I were also detected. When a graph (Fig. 4,a) of the average intensity of the neutron component (during March-July 1959) was constructed according to the method of superposition of periods (in this case the dates of the beginnings of Sc magnetic storms and days with $\Sigma Kp \geqslant 34$, included in G storms, were considered as the zero days), it was found that Sc storms are related to noticeable drops in I (on the average, by ~2%), while G storms were accompanied by increases in the neutron intensity (on the average, by ~1.5%).

We have constructed analogous graphs according to the data of the middle-latitude stations both for the neutron and for the meson component of cosmic radiation. For this we used the results of observations (in 1957-1958) at the stations at Moscow, Zugspitze (German Federated Republic) and Berkeley (US).

Figs. 4,b-e present the results obtained. It follows from these graphs that increases in I during G storms were observed in 1957-1958, both in the high, and in the middle latitudes, and not only in the neutron, but also in the meson components of cosmic radiation. We might therefore advance the hypothesis that the increases in I observed in 1957-1958 were related to the anomalously

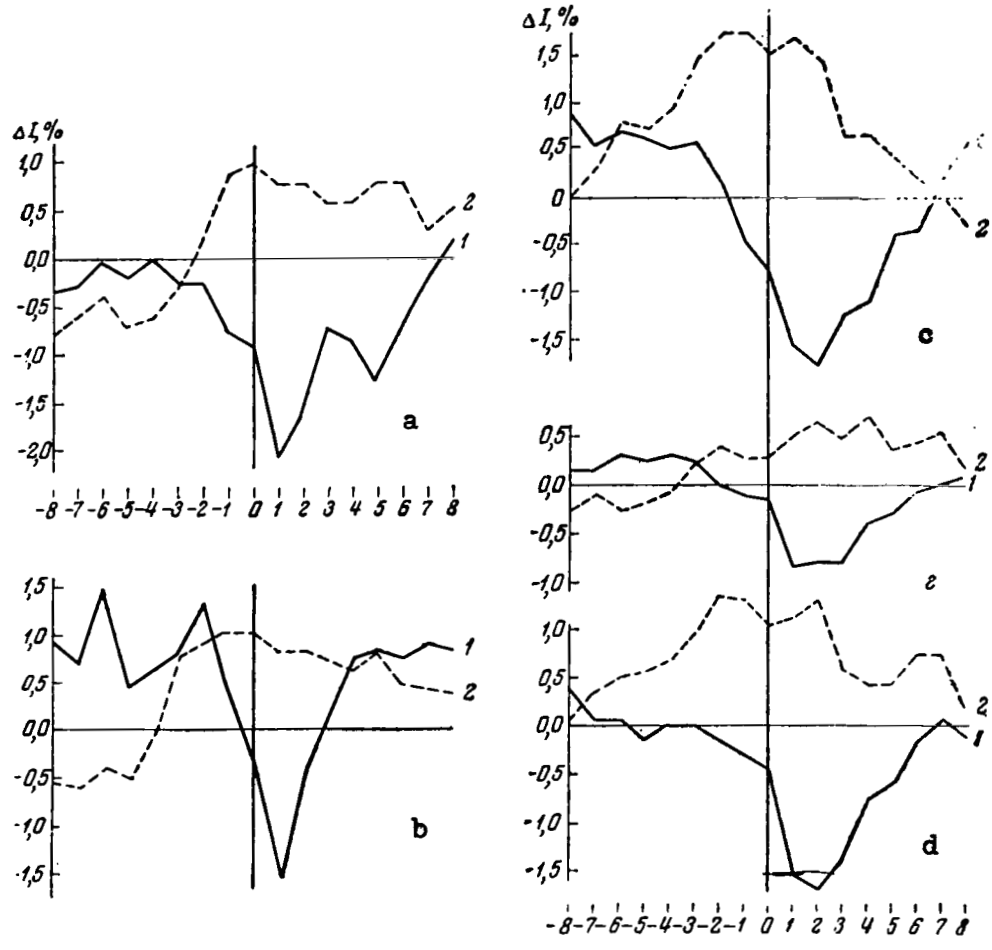

Fig. 4. Graphs of the average cosmic ray intensity (ΔI).
a -- neutron monitor (Heiss Island); b -- neutron monitor (Moscow); c -- neutron monitor (Zugspitze); d -- cubic telescope (Berkeley); e -- neutron monitor (Berkeley). Zero days -- dates of storms with sudden (curve 1) and gradual (curve 2) beginnings.

high solar activity during this period, since in 1937-1946, no increases in I during G storms were observed. It has been shown that a consideration of the 27-day variations does not eliminate the indicated effect.

The physical nature of the increases we have found is not clear. In their report to the International Conference on Cosmic Rays in Moscow (July 1959), I. Kondo, K. Nagashima, and S. Ioshida

indicated that they observed analogous increases in I during very strong magnetic storms on 11-15 September 1957 and 9-13 February 1958. They explained the increases in I by a decrease in the cutoff energy, as a result of a general decrease in the intensity of the geomagnetic field during the smooth phase of magnetic storms. We might also propose another explanation: the emission by the Sun of high-energy corpuscles from small flares or calcium floccules, causing magnetic storms with gradual beginnings [9]. Such emission should occur only during periods of anomalously high solar activity.

BIBLIOGRAPHY

1. A. I. Ol'. Priroda (Nature), 1948, p. 7.
2. A. I. Ol'. In the Collection "The Physics of Corpuscular Streams and their Influence on the Upper Atmosphere of the Earth", Publishing House of the Academy of Sciences USSR, 1957, 34, p. 1.
3. E. R. Mustel'. Astr. Zh. (Astronomical Journal), 1957, 34, 1.
4. M. Kitamura. Jap. J. Meteorol. Geophys., 1954, 5.
5. I. Sekido et al. Rep. Ionosph. Res. Jap., 1955, 9, p. 3.
6. I. Lange, S. E. Forbush. Pub. Carnegie Inst., N175; Res. Dept. Terr. Mag., Washington, 1948, 14.
7. S. E. Forbush. J. Geophys. Res., 1954, 59, p. 4.
8. J. A. Simpson, H. W. Babcock, and H. D. Babcock. Phys. Rev., 1955, 98, p. 5.
9. E. R. Mustel', O. N. Mitropol'skaya. Izv. Krymskoy Astrofiz. Observ. (News of the Crimean Astrophysical Observatory), 1958, 18.

ABSTRACT

According to the observation materials of the meson and neutron components of cosmic radiation obtained at the Heiss I. high latitude observatory and at some middle latitude stations it has been found that in 1957-1958 the magnetic storms with gradual commencement were followed by the increase in the intensity of cosmic rays, while the storms with sudden commencement -- by the decrease. In 1937-1946 the storms with gradual commencement were not connected with any significant variations in the intensity of cosmic rays, and large storms with sudden commencement were followed by the decrease.

A supposition is offered that the increase in the intensity observed during the magnetic storms with gradual commencement could be characteristic only of this cycle of solar activity due to its extraordinary high level.

RELATIONSHIP OF THE COSMIC RAY INTENSITY TO SOLAR ACTIVITY

K. K. Fedchenko

As a result of numerous investigations conducted earlier [1] and recently [2, 3], the inverse relationship between the variations of the cosmic ray intensity and solar activity has been shown. Now we can consider it established that as the solar activity increases, the cosmic ray intensity, as a rule, decreases. Moreover, the magnitude of the decrease is proportional to the degree of solar activity: the Wolff numbers, area of spots, floccules, etc. Among the manifestations of this dependence are, for example, such well known facts as the 11-year variation of the cosmic ray intensity, in phase opposition to the cyclic variation of solar activity and the well pronounced 27-day variation of the intensity during the year of the maximum solar activity, while these variations are absent during the year of the minimum.

According to E. R. Mustel' [4], the geoactive influence of such different sources of solar corpuscular streams as the spots and calcium floccules is apparently not the same. It is of interest to explain what influence these two types of sources of corpuscular streams exert on the cosmic ray intensity in various periods of the solar cycle.

Average diurnal values of the intensity of the hard and neutron components* for the period of the maximum (1958) and minimum (1954-1955) solar activity, obtained at the high latitude stations of Tikhaya Bay (hard component, 1954-1955), Heiss Island (hard and neutron, 1958), as well as at the Moscow Station (hard and neutron, 1954-1955, 1958) served as material for the investigation. Data on the solar activity -- the area of spots and calcium floccules in the central zone of the Sun (45° from the center of the visible disc) -- were selected from the bulletin "Solar Data" [5, 6], as well as from the "Catalog of Solar Activity" [7].

The results of the investigation are represented graphically (Fig. 1) in the form of curves obtained according to the method of superposition of periods. The upper portion of Fig. 1 pertains to the

---

* In this article data freed from the temperature and barometric effects were used.

period of the minimum solar activity, while the lower portion pertains to the period of the maximum. In the left-hand portion of the Figure the zero days denote the dates of passage of spots maximum in area through the central zone of the Sun, while in the right-hand portion they represent dates with floccules maximum in area. We can conclude from this Figure that the cosmic ray effect related to solar activity during the period of the maximum is determined by the spots to a far greater degree than by the floccules.

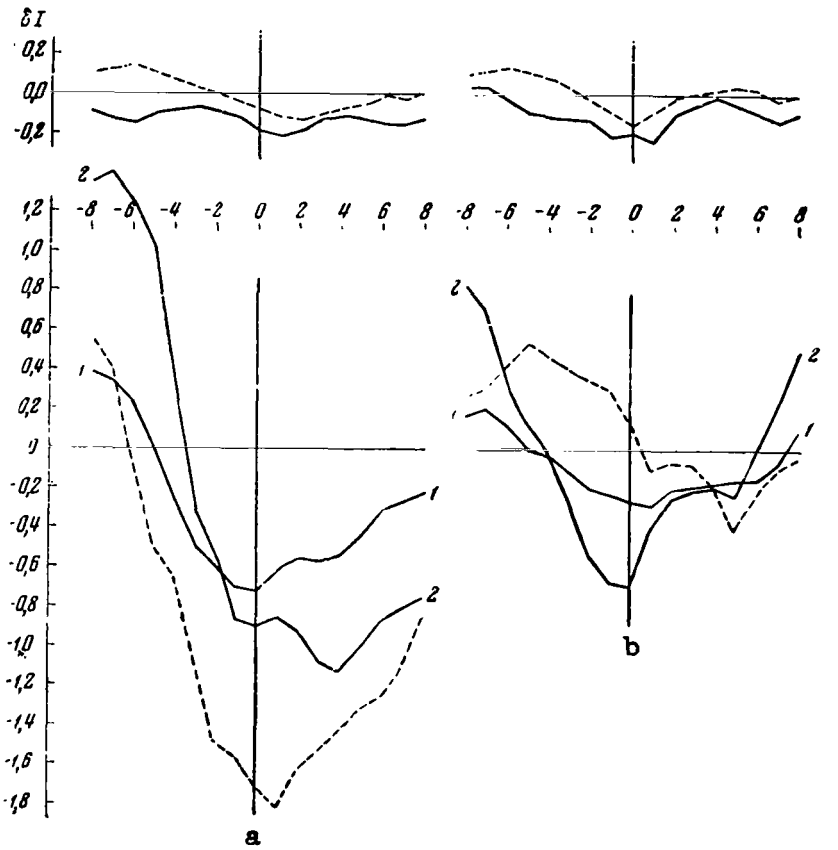

Fig. 1. Variation of the cosmic ray intensity in various phases of the solar cycle as a function of spots (a) and calcium floccules (b).
Above -- for period of minimum, below -- for period of maximum. Dashed curves -- according to data of Moscow Station; solid curves: above -- according to data of Tikhaya Bay Station, below -- according to data of Heiss Island Station (1 -- cubic telescope, 2 -- neutron monitor).

The result cited agrees with the proposal of E. R. Mustel' [4], that the calcium floccules, responsible chiefly for magnetic storms of

gradual beginnings, serve as a source of streams in which the intensity of the magnetic field carried away from the Sun is far less (more than an order of magnitude) than the intensity of the frozen magnetic field in streams originating in spots and responsible chiefly for storms with sudden beginnings. This can also serve as an indication of the different chemical nature of the two types of streams responsible for magnetic storms with different characters of the commencement; this has also been indicated by E. R. Mustel' [4].

We know that during the period of the maximum in 1957-1958 the solar activity reached an extremely high value. For example, the areas of certain large spots reached values above 3000 in September 1957, while one spot (19 September 1957) reached a value of 10,000 millionths of a hemisphere. In view of this it is of interest to reveal what changes in the cosmic ray intensity are caused by large spots that pass through the central zone of the Sun.

Average diurnal values of the meson and neutron cosmic ray intensities, obtained during the IGY period at the stations of Moscow, Zugspitze and Berkeley, served as material for the investigation. Bulletins [5, 6] were used to select the solar data.

The method of superposition of periods was also used for an analysis of the data. But, in contrast to the preceding case, days in which the largest spots with areas exceeding 2000 millionths of a hemisphere passed through the central zone of the Sun were taken as the zero days here. During the period of observations from July to December 1957, there were 26 such days. Most of these spots [5, 6], which passed through the central zone of the Sun, caused a drop in the intensity. The group largest in area, which passed through the central zone of the Sun during a period of four days (18-21 September 1957), was accompanied by a noticeable increase in the cosmic ray intensity both in the neutron (up to 4%) and in the hard (up to 1.5%) components at all three stations -- Moscow, Zugspitze, and Berkeley.

Fig. 2 presents the results of the investigation. In the upper portion curves for the stations mentioned above are depicted. In this case the dates of passage of the largest group of spots accompanied by an increase in the intensity through the central zone of the Sun were taken as the zero days. Below curves are depicted for the same stations, but in this case the dates when large groups of spots accompanied by a drop in the intensity passed through the central zone of the Sun served as the zero days. From a consideration of the Figure we should conclude that not all large spots cause a decrease in the cosmic ray intensity. A noticeable increase in the intensity is apparently caused by the largest groups of spots, encountered only in years of high solar activity.

Noteworthy in a discussion of Fig. 2 is the fact that all the curves, both upper (in the case of an increased intensity), and the lower (in the case of a drop) reach their extreme values on the zero day. This means that both increases and drops in the cosmic ray intensity, occurring when very large spots pass through the central zone,

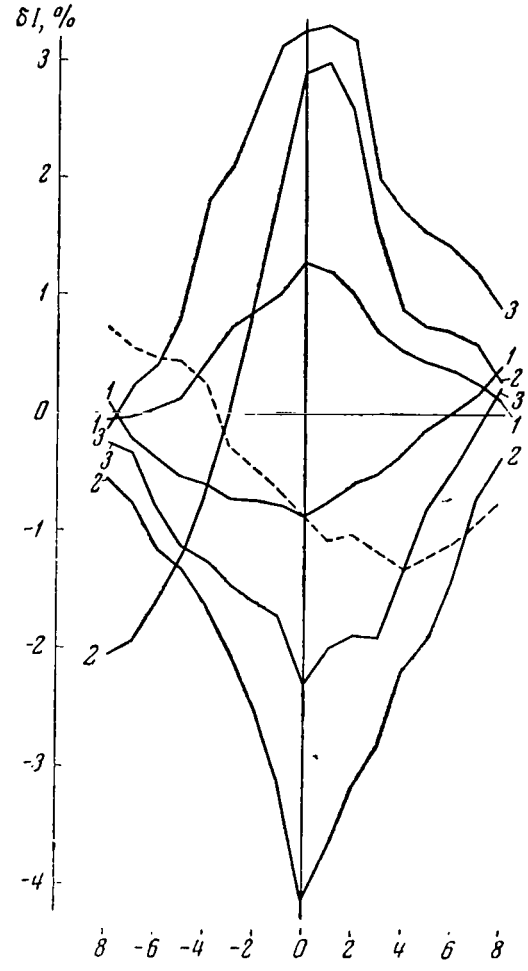

Fig. 2. Variation of cosmic ray intensity as a function of the largest spots.
Zero days: above -- spots causing an increase; below -- spots causing a decrease in the intensity. 1 -- Moscow (I); 2 -- Zugspitze (N); 3 -- Berkeley (N). Dashed curve -- according to data of Moscow Station (I).

are observed on the same day, without a lag. As is well known, such a lag (from 1 to 5 days) of the moment of maximum decrease in the cosmic ray intensity from the moment of passage of the spots through the central zone of the Sun is always detected according to the method of superposition of periods when the data are averaged over all days for a long period of time. This can be seen, for example, from Fig. 2, where the dotted curve, obtained according to the method of superposition of periods, represents the variation of the intensity of the hard compo-

nent of cosmic rays in Moscow during the period from July 1957 to June 1958 as a function of the area of sun spots.

The aforementioned increase in the cosmic ray intensity during the passage of the largest group of spots through the central zone of the Sun (18-21 September 1957) was not observed only at the three stations indicated above. It also occurred in Yakutsk, Weisenau, Climax, Leeds, Ottawa, Göttingen, Churchill, Deep River, Resolute Bay, and other sites. We should note that at the equatorial station of Juancaio this increase was practically not observed. Let us note also that during the first three days of those indicated above, when a planetary increase in the cosmic ray intensity was observed, i.e. 18, 19, and 20 September, the geomagnetic field was almost quiet. Only on 21 September did a very great magnetic storm with a sudden commencement occur, lasting for three to four days, with a subsequent decrease in the cosmic ray intensity.

In considering possible causes of the planetary increase in the cosmic ray intensity noted on 18-21 September 1957, we must remark at once that this increase apparently was not related to large solar flares, inasmuch as such flares, just as flashes of solar radio emission, were not observed during these days. In addition, the ratio of the effects on the neutron intensity to that on the hard intensity during this increase (equal to approximately 2.5) indicates the comparatively hard energy spectrum of the primary cosmic rays responsible for the observed increase, while, according to numerous investigations [8], the energy spectrum of cosmic rays of solar origin, measured during large solar flares, is far softer. On the other hand, it is known that no modulation mechanisms can create variations of the type of the observed planetary increase in the intensity.

Similar increases, in addition to that discussed in this article (18-21 September 1957), were also observed in other periods of the IGY. For example, two such planetary increases in the cosmic ray intensity, which occurred during the IGY period, were reported on by a group of Japanese scientists at the International Conference on Cosmic Rays in Moscow in July 1959 [9]. The authors proposed that such planetary increases in the cosmic ray intensity, inasmuch as they are related to magnetic storms, originate from a decrease in the cut-off energy, arising as a result of a decrease in the intensity of the Earth's magnetic field. The indicated mechanism might apparently have served as one of the possible causes of the planetary increase in the cosmic ray intensity discussed here, if it had been accompanied by a magnetic storm from the very beginning, but, as has already been indicated, the magnetic storm did not begin until 21 September. The existence on the Sun of some sort of unknown mechanism, unrelated to flares and providing for a prolonged (for several days) emission from the Sun of the low energy component of cosmic rays, remains to be proposed as a possible explanation of the observed effect. It is possible that this mechanism is in some way related to the unipolar magnetic regions on the Sun, detected by H. W. and H. D. Babcock.

In conclusion the author expresses his gratitude to Professor E. R. Mustel' and to the Collective of the Division of Cosmic Rays of the IZMIRAN for their participation in the discussion of the results obtained.

BIBLIOGRAPHY

1. J. W. Broxon. Phys. Rev., 1949, 75; Phys. Rev., 1950, 78.
2. K. K. Fedchenko. Tr. ANII (Works of the Arctic Scientific Research Institute), 1956, 83.
3. H. V. Neher, S. E. Forbush. Phys. Rev. Let, 1958, 1, p.5.
4. E. R. Mustel'. Astr. Zh. (Astronomical Journal), 1957, 34, p. 1.
5. Solar Data, 1957. Moscow-Leningrad, Publishing House of the Academy of Sciences USSR, 1957-1958.
6. Solar Data, 1958. Moscow-Leningrad, Publishing House of the Academy of Sciences USSR, 1958-1959.
7. Catalog of Solar Activity, 1954-1955. Publishing House of the Main Astronomical Observatory, 1957.
8. L. I. Dorman. Variations of Cosmic Rays. Moscow, State Technical Literature Publishing House, 1957.
9. I. Kondo, K. Nagashina, and S. Ioshida. Works of the International Conference on Cosmic Rays, 1959, Publishing House of the Academy of Sciences USSR, 1960, Vol. 4.

ABSTRACT

The article uses the data on the variations of the hard and neutron components obtained at Boukhta Tixie, Heiss I., and in Moscow for the 1954-1958 period with corrections for the barometric effect.

The article shows that the effect of cosmic rays connected with the solar activity during the maximum (decrease of intensity) is to a greater extent determined by spots than flocculae; during the minimum this effect is small in both cases.

The article also shows that some groups of spots of the largest type, occurring only in the years of high solar activity, while passing across the central zone of the Sun can bring about everywhere (except the equatorial latitudes) considerable increase of the intensity of cosmic rays in the neutron (~4%) and the hard (~2%) components.

The paper discusses the possible causes of the increase.

RELATIONSHIP OF THE COSMIC RAY INTENSITY TO THE MAGNETIC ACTIVITY AND RADIO EMISSION OF THE SUN

A. I. Ol', M. I. Tyasto

Many authors have shown that the passage of radio-emitting spots through the central meridian of the Sun (J. F. Denisse [1] called them type R spots) is accompanied by an intensification of the geomagnetic activity. On the other hand, passage through the central meridian of nonradio-emitting spots (type Q spots) is related to a decrease in the geomagnetic activity.

Apparently we might consider that storms of radio emission are a sign of the ejection of geoactive corpuscular streams from the Sun.

According to the theory of L. I. Dorman [2], variations of the cosmic ray intensity are caused by the influence of magnetic fields of solar corpuscular streams on the primary cosmic radiation. When charged primary cosmic particles intersect a solar corpuscular stream with a magnetic field "frozen" in it, they change their energy or are reflected from the stream. This leads to a change in the intensity of cosmic rays observed on the Earth's surface. Inasmuch as intensified radio emission is a sign of the ejection of solar corpuscular streams, we might expect that a definite relationship exists between the Sun's radio emission and the intensity (I) of cosmic rays observed on the Earth.

In the enclosed list of literature references, there are several works pertaining to the relationship of the radio emission and cosmic ray intensity [3, 4], but the conclusions of these investigations are not fully determined.

We took data on the radio emission of the Sun from references [5, 6] for 14 Soviet and foreign stations. The values of the stream of radio emission in units of 10^{-22} watt·m^{-2}·cycles^{-1} at frequencies of 169-209 megacycles were taken as the characteristic of the radio emission.

We investigated the average values of the stream (R), which were formed in the following way. First we found the average monthly values for each station. Moreover, days with sharply increased values of the intensity of the stream of radio emission were excluded from the computation of the average monthly values. Then we took the

deviations of each day's values from these average monthly values and averaged them for all stations. We might consider that a high value of the index R on any day characterizes this day as active with respect to radio emission. The intensity of the neutron component of cosmic rays (Heiss Island), corrected for pressure in 1958, was taken in the form of deviations of the average daily values from the smooth curve of δN_p. This curve was constructed through the average monthly values. In addition, we used the data of the meson component of cosmic rays, corrected for impact, pressure, and temperature in 1951-1955 for a number of stations. The data were taken in the form of deviations $\Delta\delta I_{ipt}$ [7].

To reveal the relationship between the solar radio emission, the cosmic ray intensity, and the magnetic activity, we conducted an investigation according to the method of superposition of periods, where the selection of the zero days was performed in the following way. During the period from March to September 1958, days with average values of the stream $R \geqslant 2.2$ were selected. These days usually follow one another, forming a group. If two groups proved to be separated by one day with $R < 2.2$, they were combined in a single group. In each group all the maxima of the quantity $R \geqslant 5.0$ were separated. In addition, the selected days were divided into first and second class. The first class included the maxima of radio emission related to a tendency of the neutron component of cosmic rays to decrease after the maximum of radio emission, while the second included the maxima related to a tendency of δN_p to increase after the radio emission maximum. Of 31 cases, only three did not fit in one of these classes. Fig. 1, a (upper portion) presents the average variations of the planetary index of magnetic activity ΣKp from -6 to +6 days for the first and second classes, individually and together (see curves I, II, and III, respectively). In the lower portion of Fig. 1, the average variations of the neutron component of cosmic rays at Heiss Island with respect to the zero days are presented for comparison.

The same investigation was conducted for the meson component of the cosmic radiation. Fig. 1, b, c presents curves analogous to the curves of Fig. 1, a, for 1951-1952 and 1953-1954, the only difference being that the principal maxima of the radio emission related to tendencies of the values of $\Delta\delta I_{ipt}$ to decrease (curve I) and to rise (curve II) after the radio emission maxima were taken as the zero days. The average variations of the meson component are also presented below in Fig. 1, b, c.

From the Figures mentioned we can see that in 1958 and 1951-1952, i.e. both during the period of the maximum and during a period of comparatively high solar activity from the falling branch of the 11-year cycle, intensified radio emission related to a decrease in the cosmic ray intensity gives a clearly pronounced increase in the magnetic activity. At the same time, the radio emission maxima related to an increase in the cosmic ray intensity are accompanied by a decrease in it. In 1953-1955 this effect becomes less noticeable, but the differ-

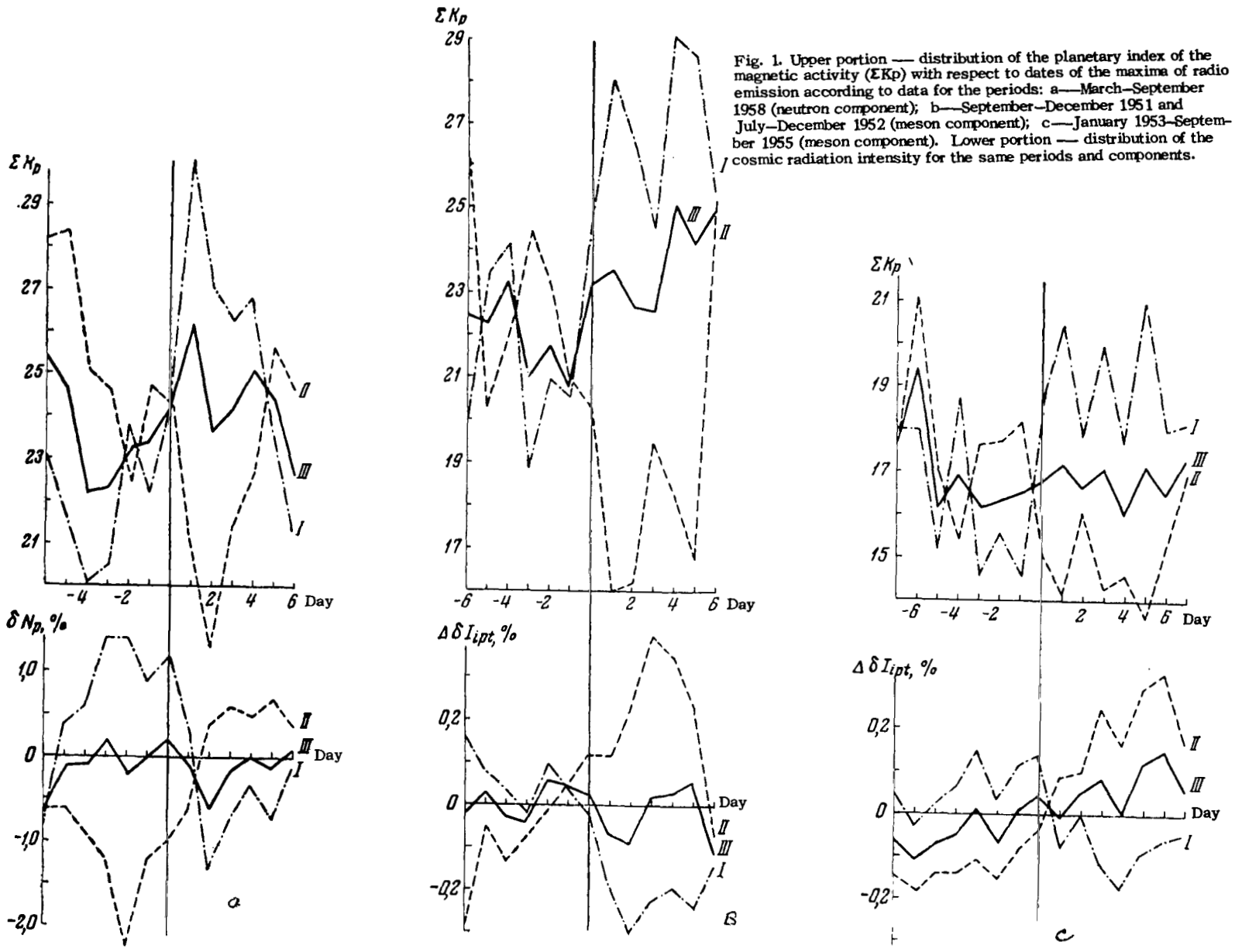

Fig. 1. Upper portion — distribution of the planetary index of the magnetic activity (ΣKp) with respect to dates of the maxima of radio emission according to data for the periods: a—March–September 1958 (neutron component); b—September–December 1951 and July–December 1952 (meson component); c—January 1953–September 1955 (meson component). Lower portion — distribution of the cosmic radiation intensity for the same periods and components.

ent curves I and II are preserved.

On the basis of the results we obtained, we cannot agree with the explanation of the relationship between the radio emission and cosmic ray intensity proposed by M. Kodama and K. Murakami [3]. They believe that during years of a minimum of the solar activity, the effect of an increase in the cosmic ray intensity, caused by emission of relativistic particles from the Sun, predominates over decreases in the cosmic ray intensity caused by the influence of the magnetic fields of solar corpuscular streams. Hence, in years of high solar activity the intensified radio emission is related to drops in I, while during the period of the minimum it is related to rises in I. As can be seen from Figs. 1, a, c, intensified radio emission can be related both to drops and to rises in the cosmic ray intensity. Moreover, this relationship does not disappear, but is only weakened during the years of the minimum solar activity.

Our conclusion that intensifications of solar radio emission that are accompanied by rises in I cause a noticeable decrease in the magnetic activity at first glance contradicts the result obtained recently by one of the authors of this article [8]. According to the data of recording of the neutron and meson components of cosmic rays in 1957-1958, it was found that magnetic storms with gradual beginnings are related to increases in the cosmic ray intensity, while in this work we conclude that decreases in the magnetic activity are related to increases in the cosmic ray intensity. However, actually this contradiction does not exist, since an investigation we conducted specially showed that magnetic storms with gradual beginnings are not related to preliminary intensifications of the radio emission. This relationship is characteristic only for storms with sudden beginnings (Fig. 2).

BIBLIOGRAPHY

1. J. F. Denisse. Ciel et Terre, 1953, 69, 3-4.
2. L. I. Dorman. Variations of Cosmic Rays. Moscow, State Technical Literature Publishing House, 1957.
3. M. Kodama, K. Murakami. J. Geomagn. Geoelectr., 1956, 8, 2.
4. E. Tanberg-Hanssen. Astrophysica Norvegica, 1956, 5, 9.
5. Quarterly Bulletin on Solar Activity, 1951-1955.
6. Solar Data, 1958. Moscow-Leningrad, Publishing House of the Academy of Sciences USSR, 1958-1959.
7. A. I. Ol'. Tr. ANII (Works of the Arctic Scientific Research Institute), 1959, 223.
8. A. I. Ol'. Solar Data, 1959. Moscow-Leningrad, Publishing House of the Academy of Sciences USSR, 1959, 2.

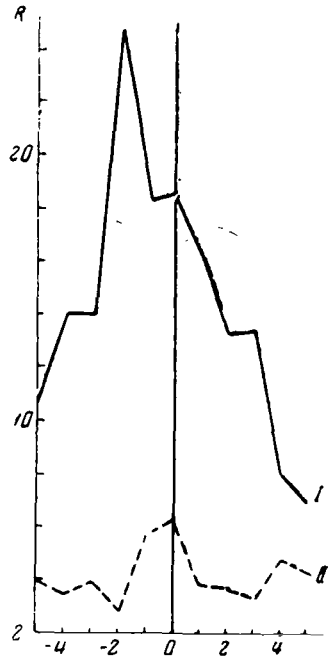

Fig. 2. Distribution of the values of the index of radio emission R with respect to magnetically disturbed days in 1957-1958.
I -- storms with gradual beginnings; II -- storms with sudden beginnings.

ABSTRACT

The paper presents results of the study of relation between the radio emission of the Sun, the intensity of cosmic rays and magnetic activity according to the registration materials of the solar radio-emission at a number of Soviet and foreign stations and the registration of the meson and neutron components of cosmic rays.

The study was carried out with the application of the method of epoch overlapping for 1951-1952, 1953-1955 and 1958 periods.

The paper shows that the increase of radio emission, connected with the decrease of the intensity of cosmic rays, brings about the increase of magnetic activity, while the increase of radio emission, connected with the increase of the intensity of cosmic rays, are followed by the decrease of magnetic activity.

The conclusions are compared with the results obtained by other authors (Tandberg-Hansen 1956, M. Kodama and K. Murakami 1956).

NASA-Langley, 1965

"The aeronautical and space activities of the United States shall be conducted so as to contribute . . . to the expansion of human knowledge of phenomena in the atmosphere and space. The Administration shall provide for the widest practicable and appropriate dissemination of information concerning its activities and the results thereof."

—NATIONAL AERONAUTICS AND SPACE ACT OF 1958

NASA SCIENTIFIC AND TECHNICAL PUBLICATIONS

TECHNICAL REPORTS: Scientific and technical information considered important, complete, and a lasting contribution to existing knowledge.

TECHNICAL NOTES: Information less broad in scope but nevertheless of importance as a contribution to existing knowledge.

TECHNICAL MEMORANDUMS: Information receiving limited distribution because of preliminary data, security classification, or other reasons.

CONTRACTOR REPORTS: Technical information generated in connection with a NASA contract or grant and released under NASA auspices.

TECHNICAL TRANSLATIONS: Information published in a foreign language considered to merit NASA distribution in English.

SPECIAL PUBLICATIONS: Information derived from or of value to NASA activities. Publications include conference proceedings, monographs, data compilations, handbooks, sourcebooks, and special bibliographies.

TECHNOLOGY UTILIZATION PUBLICATIONS: Information on technology used by NASA that may be of particular interest in commercial and other nonaerospace applications. Publications include Tech Briefs; Technology Utilization Reports and Notes; and Technology Surveys.

Details on the availability of these publications may be obtained from:

SCIENTIFIC AND TECHNICAL INFORMATION DIVISION

NATIONAL AERONAUTICS AND SPACE ADMINISTRATION

Washington, D.C. 20546